The role of IL-4Rα during acute schistosomiasis

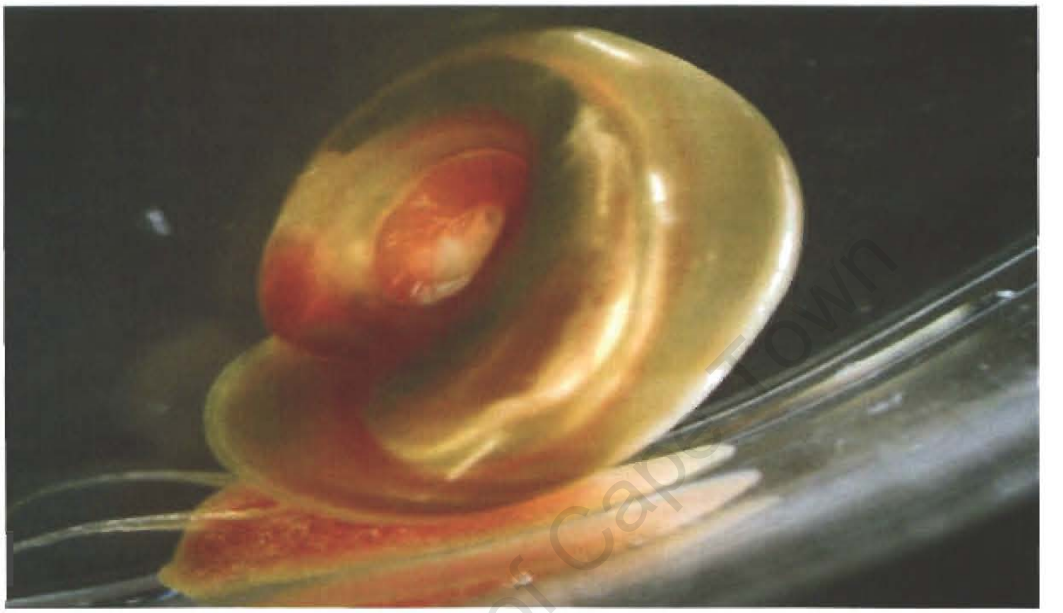

Mosiuoa Leeto

B.Sc., B.Sc.(Hons.), M.Sc.

Thesis submitted to the University of Cape Town in fulfilment of the degree

Doctor of Philosophy (Medicine)

Department of Clinical Laboratory Science & Immunology

Faculty of Health Sciences

University of Cape Town

2006

Declaration

I, Mosiuoa Leeto, hereby declare that the work on which this thesis is based, is my original work (except where acknowledgements indicate otherwise) and that neither the whole work or any part thereof is being, has been, or is to be submitted for another degree in this or any other University.

I empower the University of Cape Town to reproduce for the purpose of research either the whole or any portion of the contents in any manner whatsoever

Signed by candidate

Mosiuoa Leeto

February 2006

Dedication

This thesis is dedicated to Bataung ba Ramokgele

Acknowledgements

My sincerest gratitude goes to my supervisor, Professor Frank Brombacher, for his guidance in this work. Dr. De'Broski Herbert, an excellent teacher and an important factor in my development as a scientist, thank you for your patience and diligence in guiding and supporting me during the years. To my friends and colleagues in the Immunology department who were always willing to offer advice and encouragement both socially academically, thank you. I'm indebted to Mr. M. Simpson, Dr. M. Jacobs for many insightful discussions and support and Dr. R Guler for his critical review of this thesis. To the entire Immunology department and the UCT animal facility staff for providing an excellent service, thank you.

To my parents for their unconditional love and patience, words cannot describe my appreciation for the sacrifices you made which were not only frequent and painful, but also invisible, bringing you none of the professional satisfaction, recognition or sense of accomplishment that I feel upon completion of this projectα. To my sister, Maleshwane, you are all the sisters I need and more, I love you. To all my younger brothers and sisters, I hope my accomplishments may serve as an example of the benefits of hard work and commitment to one's cause. If I can do this, so can you. I do not have words to express my gratitude to my uncle and aunt, Mr. and Mrs. Thulo Leeto for their moral support through difficult times. Your kind words and prayers kept me going. To my son Tshepang, I'm not so naïve as to believe this dissertation to you will make up for the countless times when I wasn't there when you needed a father and a friend, but it may be a start. To my "adopted" sisters, Ivy, Boipelo and Thabang, thanks for your support. Lucas, Ernest, Hendrik & Phomolo, thank you guys for helping me to be the best man I can. And last but not least, to my angel, Ntombi, you have been the pillar of my strength, a shoulder to cry on, and a true confidant. Thank you for your unselfish sacrifices and unwavering love and for believing in me. We may have been miles apart throughout the duration of this project but you were always with me caring and supporting me all the way. I'm truly blessed to have you in my life. You are an absolute "Angel".

I give my thanks and glory to the most high, through Him anything is possible!!

Table of contents

List of figures and tables

List of Symbols and Abbreviations

AAMϕ	Alternatively activated macrophage
ANOVA	Analysis of variance
APC	Antigen presenting cell
AST	Aspartate aminotransaminase
BSA	Bovine serum albumin
CAB	Chromotrope 2R and aniline blue
CD	Cluster of differentiation
CSF	Colony stimulating factor
°C	degree Celsius
γC	Common gamma chain
DNA	Deoxyribonucleic acid
ELISA	Enzyme linked immunosorbent assay
Foxp3	Forkhead box p3
GM-CSF	Granulocyte colony stimulating factor
H&E	Haematoxylin and eosin
IFN-γ	Interferon gamma
Ig	Immunoglobulin
IL-	Interleukin
ISPF	1-phenyl-1,2-propanedione-2-oxime
LPS	Lipopolysaccharide
MHC	Major histocompatibility complex
MLN	Mesenteric/mediastinal lymph node
mRNA	Messenger ribonuncleic acid
NO	Nitric oxide
NOS	Nitric oxide synthase
PAS	Periodic acid Schiff
PBS	Phosphate buffered saline
pT_H	Precursor T helper cell
RNA	Ribonucleic acid

SD	Standard deviation
SEA	Soluble egg antigen
STAT	Signal transducer and activator of transcription
TCR	T cell receptor
Tg	Transgene
TGF-β	Tumour growth factor beta
T_H	T helper
TNF-α	Tumour necrosis factor alpha
Treg	Regulatory T cell
WT	Wild type

Publications

The following publication is based on the studies that are described in this dissertation

Herbert DR, Holscher C, Mohrs M, Arendse B, Schwegmann A, Radwanska M, **Leeto M**, Kirsch R, Hall P, Mossmann H, Claussen B, Forster I, Brombacher F. 2004 Alternative macrophage activation is essential for survival during schistosomiasis and downmodulates T helper 1 responses and immunopathology. *Immunity*. **20**(5):623-35.

Front page:

Biomphalaria glabrata snail intermediate host of *Schistosoma mansoni*

Abstract

During an infection with *Schistosoma mansoni*, immunopathology is associated with a dominant T_H-2 type cytokine expression, tissue eosinophilia and high levels of serum immunoglobulin E. It is postulated that in addition to egg-specific $CD4^+$T cells, an IL-4Rα^+ non-T cell effector population is required to prevent tissue pathology. The role of this dissertation was to examine the functional role of IL-4Rα expression on the cells of the myeloid and lymphoid lineages during [1]an acute *Schistosoma mansoni* infection and [2]its requirement for the extent of schistosome egg induced lung inflammation and pathology. Mice with myeloid IL-4Rα specific deletion were highly susceptible to acute infection. Death occurred in the presence of antigen specific T_H2 responses, eosinophil recruitment, granuloma formation, and fibrosis. It was determined that in the absence of myeloid specific IL-4Rα signalling, liver granulomas were negative for the macrophage markers, mannose receptor and arginase I and there was an impaired alternative macrophage activation which correlated with increased classical macrophage activation. This suggests that IL-4/IL-13-activated alternative macrophages are essential for surviving acute schistosomiasis. Furthermore, experiments performed in mice with a CD^+T cell specific IL-4Rα deletion showed that liver or lung granuloma development was not abrogated in the absence of $CD4^+$ T cell specific IL-4Rα signalling. This was associated with elevated levels of TGF-β in both the liver and lung tissues. Type 1 responses did not inhibit fibrosis with mutant mice being slightly more fibrotic than wild type mice. The mutant strain, which showed an impaired IL-4 promoted T_H2 development were resistant to infection. Resistance was associated with alternatively activated macrophages, $CD4^+CD25^+$ regulatory T cells and upregulated Foxp3 expression in the liver and intestine. It was also determined in mice expressing the human IL-4Rα on T and B cells that schistosome egg-induced lung granulomatous inflammation was significantly abrogated. Similarly, eosinophil infiltration, immunoglobulin E and T_H2 cytokine production, characteristics of synchronous pulmonary granuloma formation, were abrogated. Treatment of these mice with human IL-4 did not have an effect

Literature Review

LR. 1 INTRODUCTION

We live in a potentially hostile environment that contains a variety of infectious microbes- viruses, bacteria, fungi, protozoa and multicellular parasites which can cause disease and kill their hosts had we not developed a series of defence mechanisms. The immune system faces a daunting challenge in its mission of protecting the body from microbial invasion. Any immune response involves firstly, recognition of pathogen and secondly, a reaction to eliminate it. Broadly, two general systems of immunity to infectious agents have been selected during evolution: Innate or natural immunity, and acquired (adaptive) or specific immunity. Phylogenetically, innate immunity is older with some forms presumably present in all multicellular organisms, whereas adaptive immunity evolved about 400 million years ago and is found only in cartilaginous and bony fish, amphibian, reptiles, birds, mammals (Thompson, 1995). The essential difference between the two systems is the means by which they recognize micro-organisms.

Innate immune responses to many pathogens are provided by enzymes and other proteins in the blood and tissue fluids (Stites, Terr & Parslow, 1993). These proteins, whether they are cell surface receptors or soluble, usually see carbohydrate structures, for example, endocytose soluble glycoconjugates that are bound to the mannose receptor, a C-type lectin with broad carbohydrate specificity (Stahl, 1992). Macrophages also have a receptor for lipopolysaccharide (LPS), a common constituent of Gram-negative bacterial outer membranes, which signals the presence of infection by stimulating the synthesis of cytokines such as interleukin (IL)-1, IL-6, IL-12 and tumour necrosis factor (TNF) (Fearon & Locksley, 1996). These chemicals induce acute phase responses, enhance the

microbicidal functions of macrophages, and promote the development and growth of helper T cells (Ulevitch & Tobias, 1995).

An important type of innate immune response is provided by a group of serum proteins that together make up the complement pathway. The complement cascade is activated when either its alternative pathway interacts with carbohydrate-rich particles lacking sialic acid (Fearon & Locksley, 1996), or its classical pathway is triggered by the binding of collectin to certain carbohydrates (Holmskov et al., 1994).

In contrast to this relatively inflexible system is the almost infinitely adaptable acquired immune system. The adaptive immune response involves the participation of a large number of distinct cell types whose functions must be co-ordinated to ensure a response that is appropriate in quality and in magnitude to the eliciting antigenic stimulus. This coordination of function is generally believed to be regulated by the action of T lymphocytes. There are several types of T cells, each with a specialized function. One group, designated T helper (T_H)-1 cells, interacts with mononuclear phagocytes and helps destroy intracellular pathogens. The other group, T_H2 cells, interacts with B cells and helps them divide, differentiate and make antibody. The third group of T cells is responsible for the destruction of the host's cells which have become infected with viruses or intracellular pathogens (Roitt, Brostoff & Male, 2002)

Antigen-specific activation of helper T cells triggers their proliferation and initiates the programmed synthesis of secreted immunoregulatory proteins called cytokines. These small protein, signalling molecules principally act in an autocrine or paracrine way. Many cytokines act by causing aggregation of receptors at the cell surface which leads to the activation of second messenger systems. These include various colony stimulating factors (CSF), chemokines,

interleukins and interferons (IFN) (Roitt et al., 2002). However the profile of cytokines secreted is highly dependent on the particular type of T cell and in many diseases it is clear that this specific response of T cells to antigenic challenge defines the nature of the immune response (Zurawski & de Vries, 1994).

According to the new CD^+ T cell paradigm, T helper cells can be divided into two subsets based on their cytokine-producing profile and effector function (Figure A). A tenet of this paradigm is that the two subsets function in antagonism and cross-regulate one another's activity by means of secreted cytokines. The T_H1 type of cells produce interferon –gamma (IFN-γ) and tumour necrosis factor-beta (TNF-β) that participate in immune or inflammatory tissue-destructive reactions (Boros, 1999). T_H2 cytokine responses are typical of immune reactions to parasitic helminth infections, allergies, and asthma, and are characterised by the production of the cytokines interleukin (IL)-4, IL-5, IL-9, and IL-13, that can function as antiinflammatory agents and promote humoral responses by subsets of the T_H2 type cells (McKenzie, 2000).

The cytokines IL-4 and IL-13 are produced in response to antigen receptor engagement, and by mast cells and basophils upon cross-linkage of the high-affinity receptor for immunoglobulin E (IgE) (Kelly-Welch et al., 2003). Although considerable attention has been given to the roles played by IL-4 in T_H2 responses, the identification of the related cytokine IL-13 has led to the re-evaluation of how these two molecules combine in the generation of T_H2 immunity.

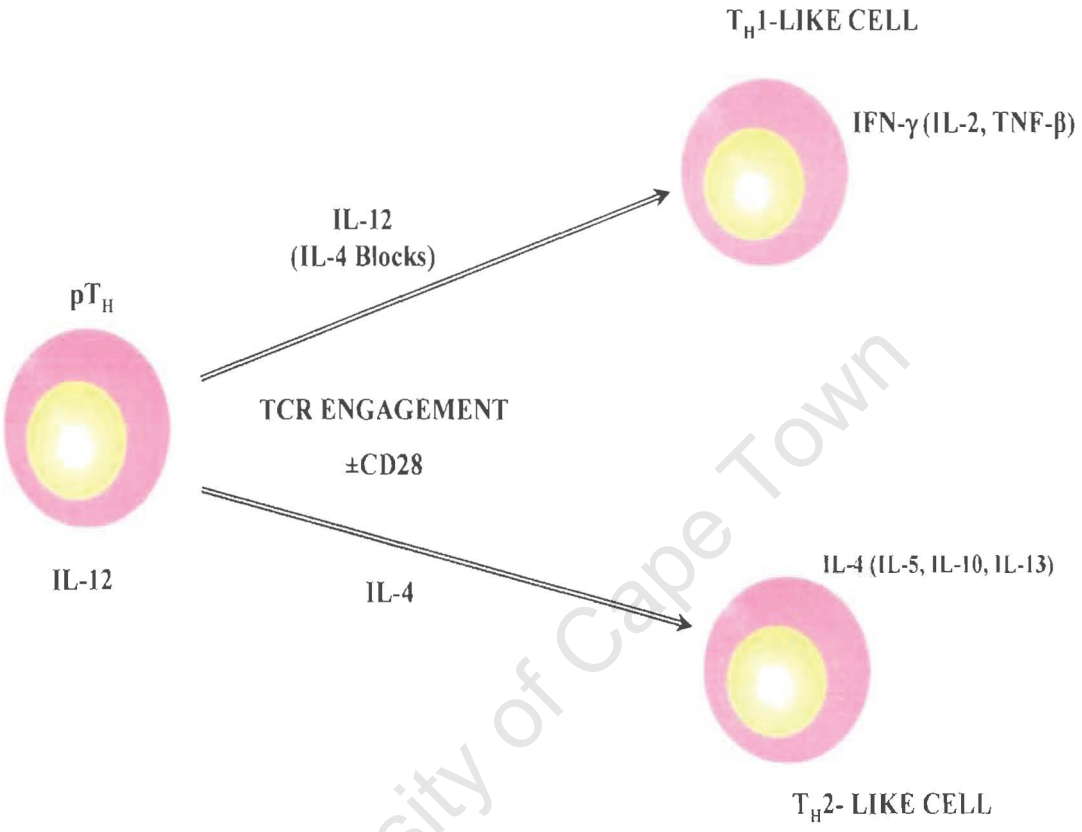

Figure A Schematic representation of the differentiation of murine T_H cells into subsets with distinctive patterns of cytokine release.

LR. 2 IL-4 and IL-13 and their receptor complexes

LR. 2.1 Interleukin 4

Interleukin-4 is a member of a subset of the immune recognition-induced lymphokines designated the "IL-4 family of lymphokines" (Boulay & Paul, 1992). This family consists of IL-4, IL-5, IL-13 and granulocyte macrophage-colony stimulating factor (GM-CSF). Murine IL-4 is a glycoprotein with an approximate molecular weight of 19kDa when purified from a T-cell source (Paul, 1991). Produced mainly by a subpopulation of activated T cells ($CD4^+$ T helper cells or T_H2 cells), it is synthesized as a precursor containing hydrophobic secretory signal sequence of 24 amino acids (Boulay & Paul, 1992). The human IL-4 gene contains four exons and has a length of approximately 10kb and maps to chromosome 5q23-3-31.2 (Arai et al., 1989), while the mouse IL-4 gene maps to chromosome 11. The murine IL-4 gene is in close proximity to other genes encoding haematopoietic growth factors like granulocyte macrophage-colony stimulating factor (GM-CSF) (Ibelgauft, 2005). IL-4 mediates its functions by binding to receptors expressed on target cells.

LR. 2.2 The IL-4 receptor

IL-4 receptors are present in haematopoietic, endothelial, epithelial, muscle, fibroblast, hepatocyte and brain tissues and are usually expressed at 100 to 5000 sites per cell (Nelms et al., 1999). IL-4 exerts it biological functions by binding to the IL-4Rα complex. The IL-4 receptor is a heterodimeric complex comprised of an IL-4Rα chain that binds IL-4 with high affinity and the common gamma chain (γC).

The IL-4Rα chain belongs to the type I cytokine receptor superfamily, characterized by four positionally conserved cysteine residues and a WSXWS motif in the extracellular region (Bazan, 1990). The cytoplasmic domain contains a short amino acid sequence termed box 1. The receptor also bears a region

(besides or in addition to conserved regions) termed insulin-IL-4 receptor (I4R) motif in the cytoplasmic domain of the human IL-4Rα (Keegan et al., 1994). This region is essential for cellular proliferation (Harada et al., 1994; Seldin & Leder, 1994). The IL-4Rα also functions as a component of the IL-13 receptor (IL-13R). The other subunit, the γC chain, initially identified as the third component of the IL-2R complex, is a component of the receptor complex for IL-2, IL-7, IL-9, and IL-15 (Brombacher, 2000). Mutations of the human γC cause X-linked SCID and are characterized by absence of T cells while the mouse phenotype is more severe, displaying the absence of B, T, and NK cells (Takeda & Kishimoto, 1997).

LR. 2.3 Biological activities of IL-4

The biological activities of IL-4 are species-specific; murine IL-4 is inactive on human cells and human IL-4 is inactive on murine cells. IL-4 was first recognized for its effects on B-cell growth (Paul & Ohara, 1987). Mouse B cells, when cultured at low densities, synthesize DNA poorly or not at all in response to anti-IgM antibody at relatively low concentrations. Although it does not itself stimulate resting B-cells to undergo DNA synthesis, IL-4 increases or induces their expression of class II MHC antigens (Noelle et al., 1984), and of the low affinity receptors for IgE, as well as increasing the number of IL-4 receptors found on the surface of the cell (Noelle et al., 1984; Ohara & Paul, 1988). In activated B-cells IL-4 stimulates the synthesis of IgG1 and IgE and inhibits the synthesis of IgM, IgG2a and IgG2b. This isotype switching induced by IL-4 in B-cells is antagonized by IFN-γ (Paul & Ohara, 1987).

The effects of IL-4 are not only restricted to B-cells, but it also has potent effects on T lymphocytes. IL-4 acts as an autocrine growth factor for a set of murine long-term T-cell lines. Resting T cells treated with IL-4 survive in culture without dividing and treatment of these cells with phorbol esters and IL-4 causes approximately 50% of the cells to enter S phase and to divide (Paul, 1991). IL-4

also acts on non-lymphoid haematopoietic cells in a variety of ways. IL-4 has been shown to suppress the growth of macrophages and to increase their cytotoxic activity for tumour cells (McInnes & Rennick, 1988). IL-4 also has activity as a stimulant of mast cell growth (Else & Finkelman, 1998).

LR. 2.4 Interleukin -13

Interleukin-13 is an immunoregulatory cytokine predominantly secreted by activated T_H2 cells and it has similar biological activities as IL-4 on human B cells and monocytes (Minty et al., 1993). Interleukin-13 belongs to the class of type I cytokines and shares the tertiary structure defined by a 4 α-helical hydrophobic bundle core (Leonard & Lin, 2000). The cDNA of mouse IL-13 (mIL-13), originally designated P600, corresponds to a relatively abundant induction-specific mRNA derived from the C1.Ly-1$^+$2$^-$9 T_H2 cell line (Brown et al., 1989). The mIL-13 cDNA encodes a 131 amino acid protein that commences at the first available ATG codon (Brown et al., 1989). The human IL-13 (hIL-13) also encodes a 131 amino acid protein although there are several variants of the cDNA. They contain either Gly or Asp at position 61 and an insertion of Gln at position 98 (Zurawski & de Vries, 1994). The gene structure for IL-13 is closely similar to that of IL-3, IL-4, IL-5 and GM-CSF, and all five genes are clustered on 5q (Ibelgauft, 2005). The IL-13 gene is located between the GM-CSF and the IL-4 gene. The hIL-13 gene is a single copy and contains four exons and shows a high degree of sequence identity with the mIL-13 gene (Ibelgauft, 2005).

LR. 2.5 IL-13 receptors

Interleukin-13 is a type I cytokine that is similar to IL-4 and it signals through the type I cytokine receptors. IL-13 receptors are expressed on human B cells, basophils, eosinophils, mast cells, endothelial cells, fibroblasts, monocytes, macrophages, respiratory epithelial cells, and smooth muscle cells. However, functional IL-13 receptors have not been demonstrated on human or mouse T cells

(Hershey, 2003). There are a total of four receptors between IL-4 and IL-13 (Figure B). Both IL-4 and IL-13 use the IL-4Rα chain as a component of their receptors. The IL-4Rα chain plays an important role in IL-13 signalling, despite the observation that it has a low affinity for IL-13. The common γ also plays a role in the IL-13R complex and although it does not specifically bind IL-13, it may participate in signalling (Jensen, 2000). Additionally, two proteins, termed IL-13Rα1 (also known as IL-13Rα′) and IL-13Rα2 (also know as IL-13Rα) (Brombacher, 2000; Kawakami et al., 2001), both members of the haemopoietin receptor superfamily, have been cloned and shown to play a role in the IL-13R complex.

Human IL-13Rα1 has a 76% homology to the corresponding mIL-13Rα chain (previously called NR4). For a functional IL-13 receptor, the IL-13Rα1 forms a productive complex with the primary IL-4 binding protein (IL-4Rα) (Kawakami et al., 2001). The second receptor chain, IL-13Rα2, originally cloned from the Caki-1 human renal carcinoma cells line (Jensen, 2000), binds IL-13 with a high affinity, but unlike the IL-13Rα1 it does not bind IL-4. IL-13Rα2 transcripts have been found in the spleen, liver, lung, thymus and brain (Donaldson et al., 1998).

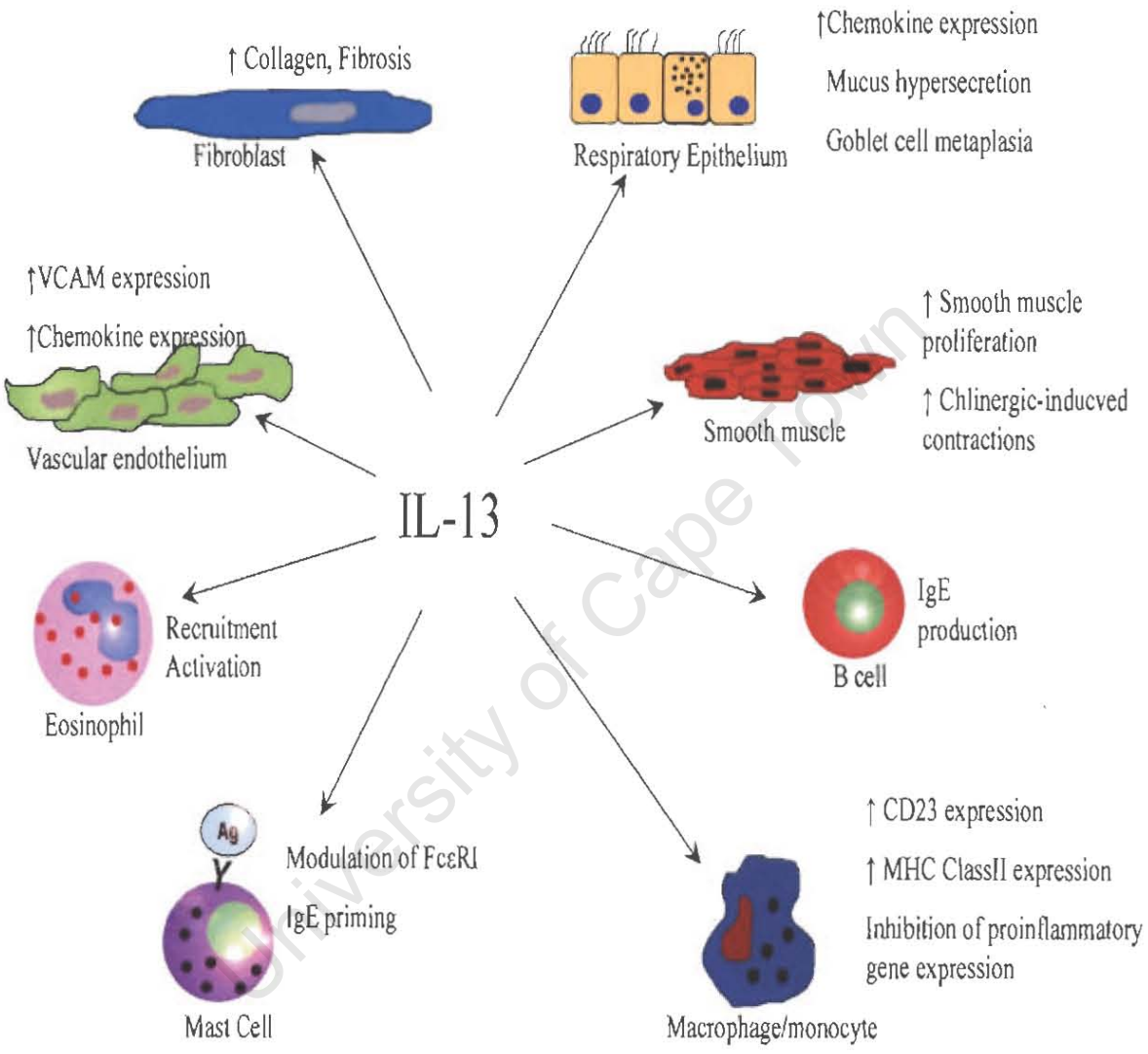

Figure B. An overview of IL-13 functions on haematopoietic and non-hematopoietic cells

Human and mouse IL-13Rα2 display a 59% amino acid sequence identity, and the cytoplasmic domains of each lack box-1 and -2 signalling motifs. IL-13Rα1, IL-13Rα2, γC, and IL-4Rα are proposed to form four types of IL-13R complexes, the type of which depends upon the cells and which of the possible receptor components are present.

LR. 2.6 Biological activities of IL-13

IL-13 has many diverse functions on a wide variety of cells types (Figure C) that are relevant to the pathogenesis of allergic disorders. In human B cells IL-13 promotes B-cell proliferation and induces class switching to IgG4 and IgE in combination with CD40/CD40 ligand stimulation. IL-13 upregulates the expression of surface antigens, including the low-affinity IgE receptor (FcεRII) and MHC classII (Chomarat & Banchereau, 1998). In monocytes and macrophages IL-13 enhances the expression of several members of the integrin superfamily including CD11b, CD11c, CD18, CD19 and CD49e (VLA-5) (Zurawski & de Vries, 1994). IL-13 also has the capacity to inhibit production of pro-inflammatory mediators including prostaglandins (Endo, Ogushi & Sone, 1996), reactive oxygen and nitrogen intermediates (Doherty et al., 1993; Endo et al., 1996), IL-6, IL-6, IL-8, TNF-α and IL-12 (de Vries, 1998). IL-13 is also involved in eosinophil survival, activation and recruitment (Luttmann et al., 1996; Pope et al., 2001).

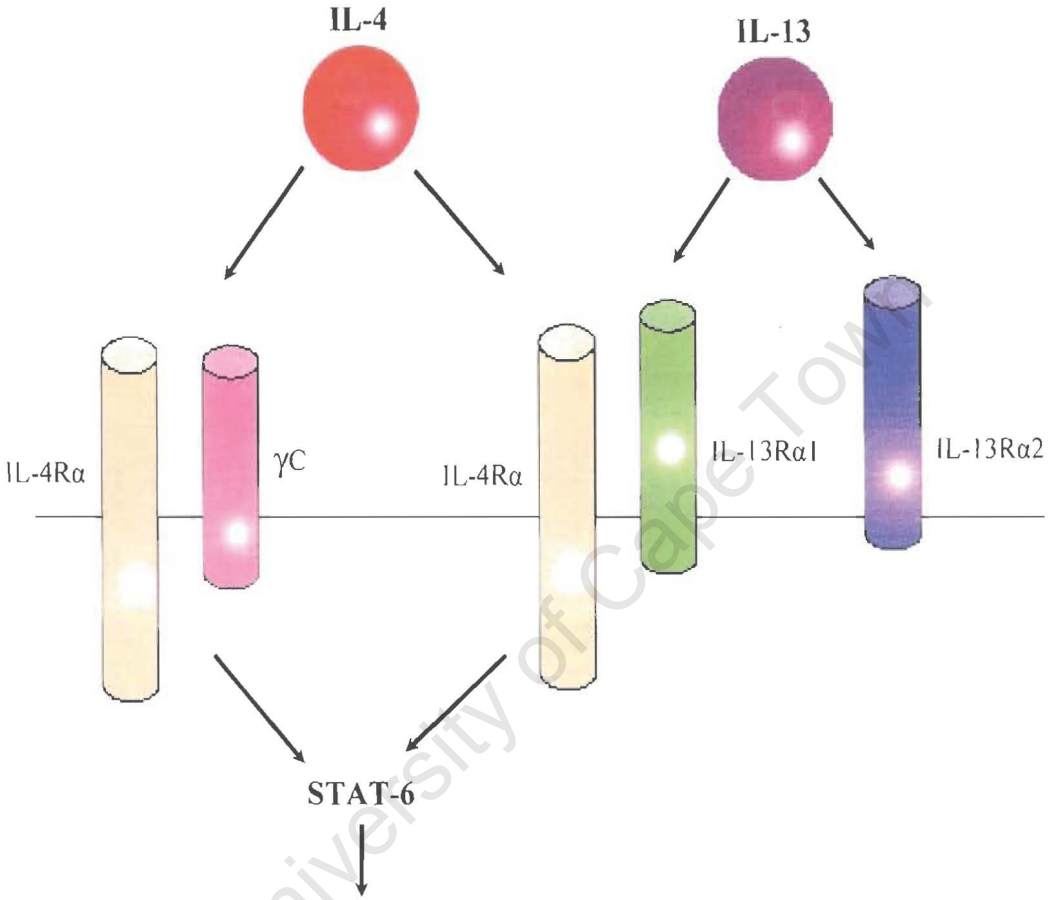

Figure C. Schematic representation of IL-4 and IL-13 receptors and signalling pathways

LR. 3. Immunity to parasitic helminth infections

Parasitic helminths, or worms, comprise a diverse group of extremely successful metazoan organisms that can parasitize all classes of vertebrates causing widespread medical and economical problems worldwide (Colley, LoVerde & Savioli, 2001). While the majority of individuals infected with parasitic worms experience relatively minor symptoms compared to those infected with organisms that typify more acute viral and bacterial infections, a small percentage suffer severe life-threatening consequences. Owing to control of insect vector populations and the availability of efficacious drugs, helminth parasites have been largely eradicated as a public health concern in many developed countries (Chitsulo et al., 2000). Unfortunately, however, in developing countries where these types of control measures are still not yet practical, helminths remain a significant biomedical problem.

Many of the parasitic worms have complex multi-stage lifecycles that involve several hosts. In their mammalian hosts, they undergo extensive growth and differentiation with the ultimate goal of producing stages, usually the larvae, intended for transmission to the next intermediate host. Many helminth parasites are long-lived and cause chronic infections. Despite the extensive organismal complexity, the immune responses of the hosts to worm infections that develop during this time often cause pathologic changes that in many cases are the primary cause of disease. (MacDonald, Araujo & Pearce, 2002)

In the majority of cases, the immune response of the hosts to worm infections are remarkably similar, being T_H2 like, with the production of IL-4, IL-5, IL-9, IL-13 and a development of strong immunoglobulin E (IgE), eosinophil and mast cell responses (Pearce et al., 2004). This inherent ability of helminths to induce T_H2 responses has led to interest in them from both the perspective of elucidation of the underlying mechanisms that lead to T_H2 response development and in terms of

understanding T_H2 response function. A well studied example of T_H2 responses is the granulomatous reaction that sequesters schistosome eggs.

LR. 4. Model of choice: *Schistosoma mansoni*

LR. 4.1 Epidemiology

Schistosoma is a genus of Digenetic Trematode flatworms (flukes) that chronically infects more than 200 million people in 74 developing countries with more than 80% of infected people living in sub-Saharan Africa (Chitsulo et al., 2000). Schistosomiasis, also known as bilharzia, after Theodore Bilharz, who first identified the parasite in Egypt in 1851, is widespread with low mortality rate but high morbidity rate. The disease is often associated with water resource development projects, such as dams and irrigation schemes, where the snail intermediate hosts of the parasite breed (Pruss et al., 2002)

LR. 4.2 Life cycle

Schistosome infection is initiated by cercariae, which burrow into the skin, transform into schistosomula and then enter the vasculature and migrate to the portal system where they mature into adults. Within the vasculature, female parasites release eggs that cross the endothelium and basement membrane of the vein and traverse the intervening tissues, basement membrane and epithelium of the intestine (*S. mansoni*) or bladder (*S. haematobium*) en route to the exterior (Figure D).

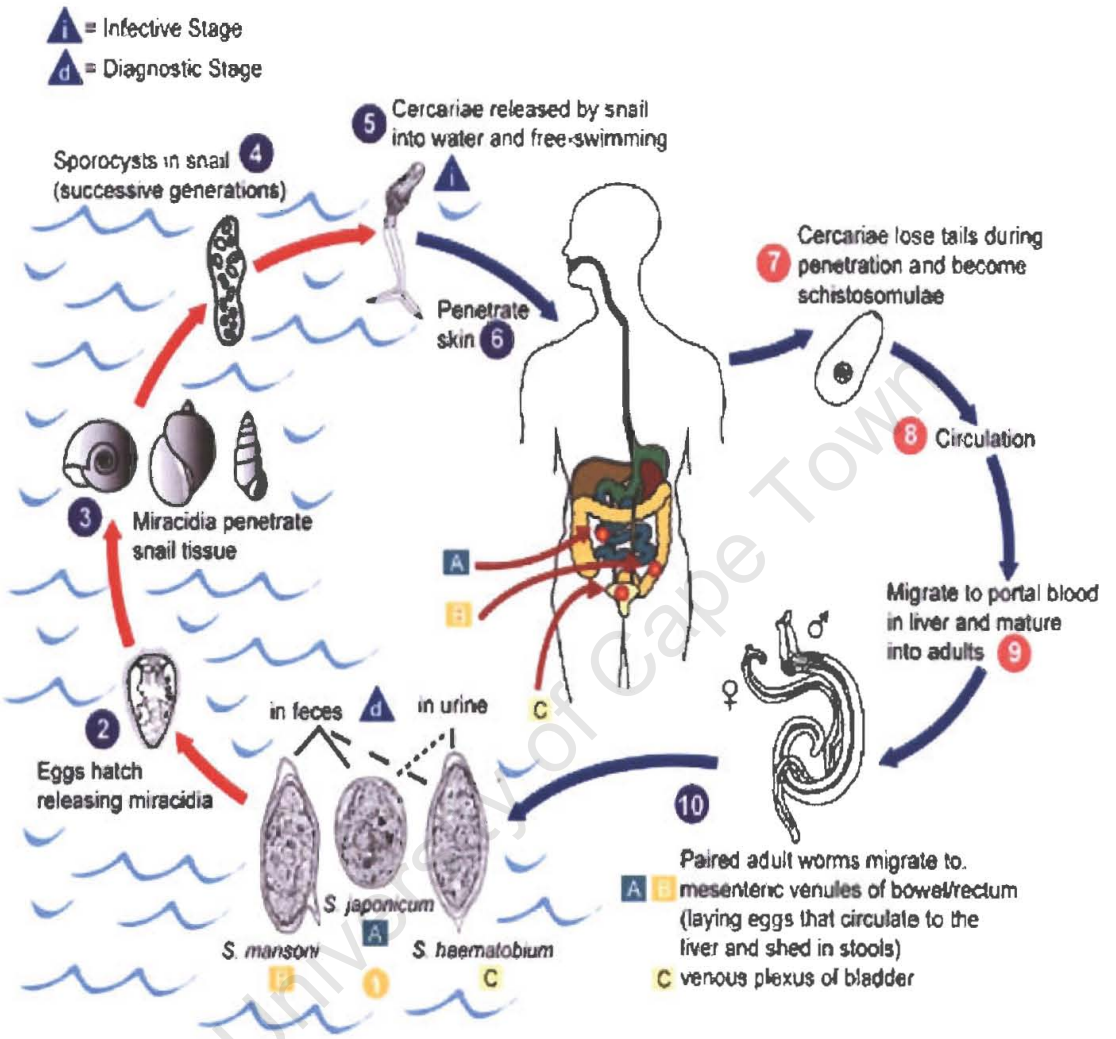

Figure D. Life cycle of the *Schistosoma* species

It is not clear yet how this process occurs. It was postulated that antigens released from the extravasated eggs induce a marked T_H2 response that orchestrates the development of granuloma around it (Grzych et al., 1991; Pearce et al., 1991). The granuloma, consisting of motile cells, then moves to the intestinal lumen, carrying the egg with it. Once in the lumen the granuloma disintegrates. However, there seems to be an immunological component involved in the process because egg expulsion is minimal in immuno-compromised mice, but can be increased by the transfer of sera or lymphocytes (Doenhoff, 1997).

In any case, about two-thirds of the eggs do not make it and large numbers build up in the gut/bladder wall particularly in chronic cases (Schmidt and Roberts, 1989). Many eggs are never expelled from the venules but are swept away by the blood, eventually to lodge in the liver or capillary beds of other organs. The response to eggs progresses through a Th0 stage to become Th2 dominant (Vella & Pearce, 1992), and is characterized by high levels of IL-4, IL-5, IL-13 and IL-10 and circulating IgE antibody (La Flamme et al., 2001). By the time the eggs reach the outside -by way of faeces or urine, they are completely embryogenated and hatch when exposed to fresh water (Schmidt & Roberts, 1989). The first indication of hatching is activation of the cilia on the miracidium. Upon hatching the miracidium swims ceaselessly until it encounters a snail host. After penetration of the snail host, it sheds its epithelium and develops into a mother sporocyst (Schmidt & Roberts, 1989). About four weeks after initial penetration by the miracidium, the infective cercariae emerge ready to infect a mammalian host (Figure 3).

LR. 5. Immunobiology of schistosomiasis

Three early findings piqued the interest of immunologists in schistosomiasis: (1) The immune response is intimately involved in the development of pathological changes that accompany infection, (2) infected individuals can have resistance to

super-infections and (3) schistosomes survive for many years in the host despite a strong immune response.

LR. 5.1 Development of the immune response in infection

In the course of infection, the immune response progresses through at least three phases. In the 3-5 weeks, during which the host is exposed to migrating parasites, the dominant response is T_H1-like. As parasites mature, mate and begin to produce eggs, at week 5-6, the T_H1 component decreases, an event associated with an emergence of a strong T_H2 response (Figure E). During the chronic phase, 10-12 weeks of infection, the T_H2 response is modulated and granulomas that form around newly-deposited eggs are smaller than during the acute phase of infection.

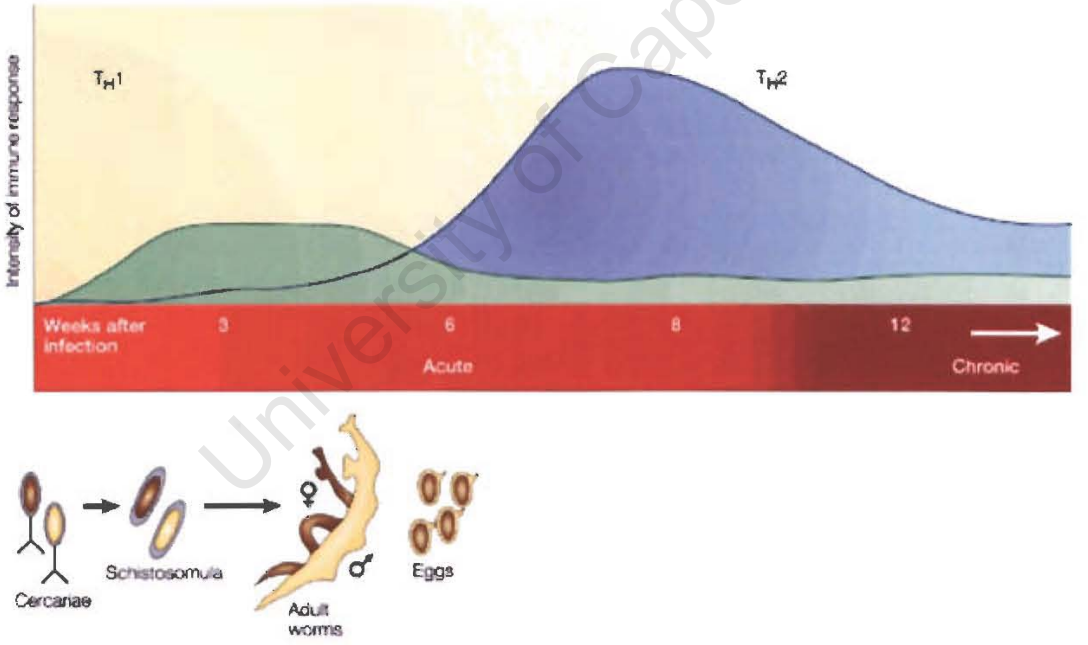

Figure E. Development of the immune response in schistosomiasis (Adapted from *Nature Reviews Immunology*, 2000)

LR. 5.2 Acute schistosomiasis

Acute schistosomiasis in humans is a debilitating febrile illness that occurs before the appearance of eggs in the stools and is thought generally to peak between 6 and 8 weeks after infection (Cheever, Hoffmann & Wynn, 2000). Symptoms associated with acute disease usually appear 4 to 10 weeks after infection and coincide with the migratory stages of the maturing schistosomula in the lungs or liver, maturation of adult worms, or early oviposition in the mesenteric veins (Boros, 1989). Acute disease is a clinical syndrome often seen in non-immune individuals (tourists, immigrants) and it rarely occurs among reinfected individuals living in an endemic area, presumably due to their pre- and postnatal exposures to schistosome antigens via placental transfer (King et al., 1998) and repeated infections in early childhood.

Schistosome egg antigens are complex host-immunogenic glycoproteins consisting of at least 30 components with molecular weights ranging from 10 to >200kDa and include those that are secreted by the egg or released following egg disintegration (Asahi & Stadecker, 2003). For many years, numerous efforts have been made to elucidate the T cell immunogens present in soluble egg antigen (SEA) preparations of *S. mansoni*. The best studied egg component is the Sm-p40 antigen.

Sm-p40 is the most abundant schistosome egg component representing approximately 10% of soluble egg antigen (SEA). First reported as a 40kDa protein from eggs and miracidia, the Sm-p40 antigen has been shown to be strikingly immuno-dominant in the large granuloma forming H-2^k mouse strains C3H and CBA (Hernandez et al., 1997a). In comparison to the mature $CD4^+$ Th cell response to unfractionated SEA, which is polarized towards the Th-2 type (Pearce et al., 1991), the Sm-p40 antigen elicits a response Th-1 biased response (Cai et al., 1996). Sm-p40 has also been shown to be an immunogen in humans

(Stadecker, 1999). In addition to Sm-p40, two additional T cell sensitizing egg antigens have been described, namely, *S. mansoni* phosphoenolpyruvate carboxykinase (Sm-PEPCK) and thioredoxin peroxidase-1 (Sm-TPx-1) (Asahi et al., 2000; Tielens et al., 1991). In contrast to Sm-p40, both of these molecules induce a more balanced T_H-1/T_H-2 response and are relatively stronger antigens in C57/Bl6 mice (Asahi, Hernandez & Stadecker, 1999a; Asahi et al., 1999b; Williams et al., 2001).

The exact mechanism(s) responsible for the pathogenesis of acute schistosomiasis remain unclear but both nonimmune and immune mechanisms may participate in the pathogenetic process (Boros, 1989). In humans, acute disease is presumably unrelated to toxins secreted by the eggs of *S. mansoni* because disease often precedes egg deposition (Wynn et al., 2004). In the murine model, at the immune level, there are increased levels of tumour necrosis factor (TNF) in the plasma and large quantities of IL-1, IL-6 as well as TNF produced by peripheral blood mononuclear cells (PBMCs) (de Jesus et al., 2002). Consequently, in the natural progression of the disease, the production and functions of these pro-inflammatory mediators is downregulated by the developing egg-induced T_H2 response with IL-10 playing a crucial role in the process (Montenegro et al., 1999). Overall, the available data indicates that the symptoms of acute schistosomiasis in humans are related to levels of circulating immune complexes, occur in response to a variety of schistosome species, and are compatible with immune complex disease (de Jesus et al., 2002).

LR. 5.3 Chronic schistosomiasis

Granuloma formation to parasite eggs signals the beginning of a chronic disease which may result in fibrosis, scarring, portal hypertension, haemorrhage and death. Granuloma formation is dependent on and mediated by MHC II restricted $CD4^+$ T helper lymphocytes with specificities directed against egg antigens (Hernandez et

al., 1997b; Mathew & Boros, 1986), and can occur in environments dominated by either T_H1 or T_H2 type cytokines (Pearce et al., 1991; Wynn et al., 1993). A dominant theme with chronic schistosomiasis is the necessity of the host to modulate its immune response appropriately (Boros, 1989). Although T_H2 responses seem crucial in modulating potentially life-threatening disease during acute stages of infection, prolonged responses contribute to the development of hepatic fibrosis and chronic morbidity (Wynn et al., 2004).

Studies of *Schistosoma mansoni* in the murine model have shown that IL-13 plays a central role in the development of fibrosis, while the absence of IL-4 allows the development of a severe, lethal inflammatory condition (Brunet et al., 1997; Fallon et al., 2000) with IL-10 exacerbating this condition (Hoffmann et al., 1999). It is, however, not yet clear whether IL-13 is important for hepatic fibrosis in humans. Most individuals who are infected develop T_H2 responses (Araujo et al., 1996; Williams et al., 1994), but the intensity of the response differs between individuals. It has been suggested that infection intensity, but more importantly the individuals genetic predisposition to the disease can affect the severity of chronic disease (Dessein et al., 1999; Mohamed-Ali et al., 1999). A segregation study by Dessein and colleagues showed that a codominant major gene, known as *SM2*, is responsible for the observed familial distribution of hepatic fibrosis (Dessein et al., 1999). The *SM2* gene was mapped to 6q22-q23- a region that contains the gene that encodes IFN-γ receptor 1(IFN-γR1) (Mohamed-Ali et al., 1999). These data suggest that mutations in IFN-γR1 that lead to loss of function of the receptor are associated with a lack of effectiveness of IFN-γ in suppressing fibrogenesis (MacDonald et al., 2002).

An additional facet of immune-regulation during helminthiases is that the marked T cell response that follows initial infection is, in the majority of patients, dampened as the infections becomes chronic (King, 2001). Down-regulation of

cellular proliferative responses during helminth infection is believed to be in the best interest of the host as it is not apparent in infected individuals exhibiting the most severe forms of the disease (Maizels et al., 1993). The underlying mechanisms behind down-regulation of cellular proliferative responses during helminth infections remain fairly unknown. Recent studies have, however, suggested that host macrophages may be alternatively activated by the parasite to effect suppression via a contact-dependent mechanism (Falcone et al., 2001; Loke et al., 2000), via NO production (Atochina et al., 2001) or through IL-10 production (Mahanty et al., 1997).

A pervasive theme of resistance to helminths is that of premonition or concomitant immunity, a state wherein the hosts is protected from further infection with a given species by ongoing persistent infection with the same organism (Butterworth et al., 1994a; Clegg, Smithers & Terry, 1971; Hagan, 1996; Hagan P et al., 2004; Hagan et al., 2004). There are at least two explanations for this type of immune response. In the first instance, parasites of the primary infection induce an immune response that, while incapable of killing them, is nevertheless able to kill incoming parasites that may cause a super-infection. This would require that adult parasites, express immune evasion mechanisms and that common antigens be shared between the different stages (MacDonald et al., 2002). A second explanation is that the primary infection alters the anatomy or physiology of the host is such a way that it becomes more difficult for incoming larval organisms to establish infection in the appropriate niche (Harrison, Bickle & Doenhoff, 1982).

These two themes are well illustrated by findings from immuno-epidemiological studies of individuals in areas of endemicity for *Schistosoma* species. In such areas, individuals who have passed their mid-teens years generally have significantly less-intensive infections than younger children, despite similar

exposure to infectious parasites, suggesting that concomitant immunity develops with age in this case (Butterworth et al., 1994b). The immunological basis of resistance to re-infection to schistosomiasis has been examined by comparing the parasite-specific immune response of older (resistant) versus younger (susceptible) individuals following treatment. Such studies indicate that anti-parasite IgE levels closely correlate with resistance (Dunne et al., 1992a; Dunne et al., 1992b; Rihet et al., 1991).

In successful infections, the robust granuloma response that peaks during acute infection, is gradually down-modulated as the infection progresses to the chronic stage (Phillips & Colley, 1978; Wynn et al., 2004). Although it is generally thought that immunopathology and immunoregulation are under the control of egg-antigen-specific T_H cells, thus far it has been difficult to unite all of the published findings into one general mechanism or pathway. Nevertheless, there is a large body of data that indicate the importance of regulatory T cells, IL-10, cross-reactive idiotypes, and anergy in these processes. Stadecker *et al.* hypothesized that immunomodulation might represent a state of anrergy in the responding T_H1 cell (Stadecker et al., 1990). Support for this hypothesis came from studies which showed that macrophages derived from hepatic granulomas induced 'anergy' in cultured T_H1-cell clones and downregulated pulmonary granuloma formation *in vivo* (Flores Villanueva et al., 1994a) with IL-10 serving as the alleged mediator (Flores Villanueva et al., 1994b). In a study by Montesano *et al.* cross-reactive idiotypic antibodies produced during schistosome infection were shown to modulate egg-induced pathology, and this modulation correlated with the production of high levels of IL-10 (Montesano et al., 2002). On the other hand, studies in related asthma/allergy models have suggested that regulatory T cells producing IL-10 and / or TGF-β might also play a role during type-2 dominant immune responses. In one of the studies, DCs exposed to a defined respiratory antigen (ovalbumin (OVA)) were shown to transiently produce IL-10,

which in turn stimulated the development of IL-10-producing $CD4^+$ T regulatory cells (Akbari, DeKruyff & Umetsu, 2001). Similarly, the importance of IL-10-producing DCs, macrophages and regulatory T cells in the induction, maintenance, and resolution of murine schistosomiasis has been established (Hesse et al., 2004).

LR. 6. Schistosomiasis in the murine model

Together studies on mouse and human schistosomiasis raise questions whether severe morbidity and mortality due to infection are attributable to the development of polarized T_H2 or T_H1-type immune responses. Data obtained from IL-10/IL-4-deficient mice show that these mice developed a highly polarized T_H1 response, lost weight rapidly at the onset of egg deposition and were all dead by 5 weeks after infection (Hoffmann, Cheever & Wynn, 2000). Acute mortality in these mice was associated with the over-expression of pro-inflammatory mediators (interferon (IFN)-γ and tumor necrosis factor (TNF)-α, nitric oxide (NO) and formation of non-fibrotic granulomas. On the contrary, IL-10-/IL-12-deficient mice developed a progressive wasting disease that correlated with increased hepatic fibrosis, formation of large eosinophil-rich granulomas, a 10-fold increase in T_H2 cytokines and significant mortality during the chronic stages of infection. These findings revealed the central regulatory role of IL-10 in the pathogenesis of schistosomiasis, and illustrate that excessive type 1 or type 2 cytokine responses trigger distinct, but equally detrimental forms of pathology following infection.

Experiments with cytokine and gene-knockout mice have shown that schistosome egg-induced granulomatous pathology is dependent on type 2-associated cytokines, with IL-4 and IL-13 playing prominent roles. The individual roles of IL-4 and IL-13 in granuloma formation were shown in earlier studies utilizing the pulmonary granuloma model. In this model live eggs are purified from the livers of *Schistosoma mansoni*-infected mice and then injected intravenously into naive, infected or egg-sensitized mice, (Wynn et al., 1993; Wynn et al., 1994) or in some

cases antigen-coated beads have been used (Ruth et al., 2000). In one of the pioneering studies, the individual roles of IL-4 and IL-13 in pulmonary granulomas were dissected by comparing IL-4$^{-/-}$ mice with IL-4$^{-/-}$ and wildtype mice treated with a soluble IL-13Rα2-Fc (sIL-13Rα2-Fc) fusion protein to block endogenous IL-13 (Chiaramonte et al., 1999b). In their study, Chiaramonte *et al.* were able to show that in WT mice, lung granulomas that peak in size at 2 weeks, were reduced by more than 50% following treatment with sIL-13Rα2-Fc, whereas in IL-4$^{-/-}$ mice, which have reduced granuloma sizes, treatment with the IL-13 blocker resulted in complete abrogation of lung granulomas (Chiaramonte et al., 1999b). This was the first study to demonstrate the non-redundant roles of IL-4 and IL-13 in lung granuloma formation and were subsequently confirmed by studies in IL-13$^{-/-}$ and IL-4/IL-13$^{-/-}$ double-knockout mice (Hesse et al., 2001; McKenzie, 2000).

As the pulmonary model showed that IL-4 and IL-13 both contribute to the inflammatory response, it became interesting to know if similar mechanisms were involved in hepatic granulomatous responses. Studies showed that liver granuloma development in IL-4$^{-/-}$ mice was similar to that observed in wild type mice (Metwali et al., 1996; Pearce et al., 1996). This was an unexpected finding as IL-4$^{-/-}$ mice generated a reduced type-2 response in the liver and draining lymph nodes (Chiaramonte et al., 1999a). Other analyses of the role of T_H2 cytokines during *Schistosoma mansoni* infection revealed that IL-4 is central effector cytokine in T_H2 cell differentiation and type 2 cytokine responses. In the absence of IL-4, T_H2 cytokine production is severely impaired but not abolished (Jankovic et al., 1999) and there are concurrent increases in the production of pro-inflammatory mediators (i.e. NO, TNF-α, IFN-γ), morbidity and mortality (Brombacher, 2000; Fallon et al., 2000).

Although IL-4 and IL-13 contribute to the induction of granulomatous responses during infection, studies employing IL-4, STAT-6 or IL-4Rα deficient mice have suggested that IL-13 may have a role in IL-4-independent responses during helminth infection. The potential role for IL-13 in granuloma formation and fibrosis was implied by studies in IL-4Rα$^{-/-}$ mice (Jankovic et al., 1999). In their studies, Jankovic and colleagues found that *S. mansoni* infected IL-4Rα$^{-/-}$ mice are distinct from both IL-4$^{-/-}$ and wildtype animals in showing a near complete ablation of egg pathology while retaining the same lymphokine profile as IL-4$^{-/-}$ mice. A direct role of IL-13 in type 2 cytokine-mediated infections has been shown by blocking IL-13 activity (Chiaramonte et al., 1999a), whilst other studies have shown that the removal of IL-13 from the T_H2 cytokine response to *S. mansoni* infection is beneficial to host survival (Fallon et al., 2000). By contrast the removal of IL-4 resulted in very high mortality characterized by a breakdown in intestinal integrity and the development of endotoxemia, implicating IL-4 as a protective cytokine in schistosomias is infection. In the absence of IL-4 during live infections, parasite eggs are not excreted efficiently and are trapped in the intestine causing intestinal inflammation leading to systemic LPS. As livers of schistosome-infected mice are more susceptible to endotoxin, LPS leakage will exacerbate liver damage and ultimately result in death of the animal (Fallon et al., 2000).

It is clear from literature that IL-4 and IL-13 have distinct biological roles. IL-4 directly induces T cell proliferation and differentiation (Kopf et al., 1993), whilst IL-13 mediates its functions on T cells indirectly (McKenzie et al., 1998a; McKenzie et al., 1998b). However, IL-13 shares homology with IL-4 and appears to have overlapping biological activities. This overlap in activity is due to IL-4 ad IL-13 using the IL-4Rα chain as a component of their receptor complexes and signalling through a shared signal transducer and activator of transcription-(STAT)6- dependent pathway (Brombacher, 2000). Both cytokines modulate IgE

expression (Emson et al., 1998), development of T_H2 cytokine responses (Chiaramonte et al., 1999b; Kaplan et al., 1998) and suppression of inflammatory cytokine production from monocytes (Fallon et al., 2000). Although it has previously been shown that tissue pathology in schistosomiasis requires, in addition to egg-specific $CD4^+$ lymphocytes, a previously unrecognized IL-4Rα non-T cell population (Jankovic et al., 1999), this postulate has not been investigated. In the present study we directly addressed the role of cell-specific expression of IL-4Rα in egg pathology in *S. mansoni*-infected mice with a specific deletion of IL-4Rα on myeloid and lymphoid cell populations.

Objectives of the project

- To determine the role of IL-4/IL-13 myeloid responsive cells during infection with *S. mansoni*
- To determine the role of IL-4/IL-13 responsive T cells during infection with *S. mansoni*
- To determine the if T cell specific IL-4Rα signalling is required for lung granuloma development and egg-induced fibrosis

Materials and Methods

MM.1 Mice

All mice were housed under specific pathogen-free barrier conditions in the animal facility of the University of Cape Town and given food and water *ad libitum*. Both male and female mice between 8-12 weeks were used in experiments. The Animal Ethics Committee of the University of Cape Town approved all experiments.

MM. 1.1 Generation and genotyping of conditional IL-4Rα-deficient mice

Conditional IL-4Rα-deficient (IL-4Rα$^{flox/flox}$) mice were generated using gene targeting in BALB/c embryonic stem cells with an isogenic target vector and Cre/loxP-mediated site-specific recombination as previously described (Mohrs et al., 1999). LysM^{Cre} (Clausen et al., 1999) and Lck^{Cre} mice were first backcrossed to BALB/c for nine generations and intercrossed with IL-4Rα$^{flox/flox}$ mice. These mice were further mated with IL-4Rα-deficient (IL-4Rα$^{-/-}$) mice to generate LysM^{Cre}IL-4Rα$^{-/flox}$ and Lck^{Cre}IL-4Rα$^{-/flox}$ mice respectively. In all experiments transgenic negative littermates (IL-4Rα$^{-/flox}$ referred to as wildtype (WT) were used as controls.

Genotypes of mice were confirmed by PCR analysis of tail biopsies under the following conditions: 94°C/1 minute, 94°C/30 seconds, 57°C/30 seconds, and 72°C/1 minute for 40 cycles on an MJ thermocycler (Biozym, Hessissch Oldendorf, Germany). Specific PCR primer pairs for the

IL-4Rα: 5′-GTACAGCGCACATTGTTTTT-3′

Deletion: 5′-GGCTGCCCTGGAATAACC-3′ and

5′-CCTTTGAGAACTGCGGGCT-3′

LoxP: 5′-CCCTTCCTGGCCCTGAATTT-3′ and

5′-GTTTCCTCCTACCGCTGATT-3′

Cre: 5′-ATGCCCAAGAAGAAGAGGAAGGT-3′ and

5′-GAAATCAGRGCGTTCGAACGCTAGA-3′

Conditional human IL-4Rα transgenic (hIL-4RαTg) mice were obtained from Dr. Masato Kubo. This transgenic mouse expresses the human IL-4Rα under the control of an intronic enhancer from the Ig H chain Eμ locus to allow specific expression of the receptor only in lymphocytes (Seki et al., 2004). The chimeric receptor composed of the human IL-4Rα (hIL-4Rα) chain and mouse γ-chain is responsive to hIL-4.

MM. 2 *Schistosoma mansoni* parasites and snail hosts

Schistosoma mansoni, Puerto Rican strain, and *Biomphalaria glabrata* snails used for the maintenance of the parasites were provided by Adrian Mountford, York, UK). The snails were maintained in the laboratory at 25°C under a regulated light/dark cycle in conditioned water and fed on commercial fish flakes and/ or Romaine lettuce.

MM. 3 Animals Infections

MM. 3.1 Live infections

Mice were infected with live *S. mansoni* cercariae using described protocols (Coligan et al., 1991). Briefly: Mice were anaesthetized with Anaket-V (Centaur Labs, RSA) and 2% Rompun (Bayer, Germany) at recommended concentrations and the abdomen cleanly shaved. The abdomen was then wiped with gauze moistened in conditioned water. Animals were placed on their backs in a slotted restraining device to prevent involuntary movement.

Cercariae were shed from snails (Coligan et al., 1991) and their numbers adjusted to the required concentrations. Stainless steel rings were placed on the abdomens of shaved mice and the cercarial suspension pipetted into the rings with a Pasteur pipette. Animals were exposed to cercariae for ~1hour, and the cercarial suspension and the rings were removed. Mice were then moved back into their cages without washing or wiping the exposure site.

MM. 3.2 Collection of schistosome eggs from mouse tissues

Infected mice were euthanized by intraperitoneal injection of 0.3 ml Anaket-V (Centaur Labs, RSA) and 2% Rompun (Bayer, Germany) at recommended concentrations. The tissues (liver and/or intestine) were dissected out and rinsed thoroughly in 4°C 1.2% NaCl. Tissues were minced with scissors and suspended in 1.2% NaCl and homogenized for 30 seconds at low speed with X620 CAT homogenizer (Staufen, Germany). A pinch of collagenase-V was added to the homogenate followed by 1hour incubation at 37°C. The suspension was then passed through a crude sieve (420µm pore size). The filtrate was then passed though a series of stainless steel sieves with decreasing pore sizes using a plastic spray bottle filled with 1.2% NaCl and collected into 450mm petri-dishes (Bibby Sterilin, Staffordshire, England). With gentle swirling, eggs were concentrated in the middle of the Petri dish and collected with a Pasteur pipette. Collected eggs were suspended in 1.2% NaCl and placed on ice until used.

MM. 3.3 Synchronized pulmonary granuloma induction

For the induction of pulmonary granulomas, purified eggs were counted and their numbers adjusted to the required concentrations. Using a 25G needle (B. Braun, Melsungen, Germany) 5000 eggs were then injected intraperitoneally into mice. After a period of 14 days, sensitized mice were challenged intravenously via the tail vein with a further 5000 eggs.

MM. 3.4 Enumeration of schistosome eggs from mouse tissues

Liver or intestinal tissues were removed from infected and euthanized mice, weighed and digested in 200ml of 5% KOH solution at 37°C for 16hr. The digest was then mixed thoroughly and the eggs counted in several aliquots using a compound microscope at 40x.

MM. 3.5 Enumeration of schistosome eggs from faecal material

Analysis of feacal samples for the presence of parasite eggs was performed using the modified Kato-Katz technique as described elsewhere (Eberl et al., 2002). Briefly: ±250mg fresh faecal samples were suspended in 3ml PBS overnight at 4°C and layered out on top of 3ml of 0.9%NaCl/60% Percoll (Sigma) solution. After centrifugation at 330 x g for 15 minutes, the supernatant was discarded and the pellet resuspended in PBS. The suspension was then passed through a 150µm mesh sieve into a collecting tube to exclude larger particles. The eggs in the flow-through were pelleted and transferred onto a glass slide marked with parallel tramlines 1.5m apart, and counted at 40x magnification in the presence of 1:10 volume of malachite green (Calbiochem, Darmstradt, Germany).

MM. 4 Enzyme Linked Immunosorbent Assay and *ex vivo* analyses

Nunc Maxisorp 96 well plates (Nalge Nunc International, Naperville, IL, USA) were coated with 10µg/ml of "capturing antibody" or 10µg/ml of *S. mansoni* soluble egg antigen (SEA) overnight at 4°C. Plates were washed with washing buffer using a SkanWasher 300 microplate washer (Skatron Instruments, Norway) and blocked with 200µl of blocking buffer overnight. Wells were washed and recombinant mouse cytokine or isotype specific antibody standards were added in serial dilutions at recommended concentrations. Samples were diluted in dilution buffer and added in serial dilutions and the plates were incubated overnight at 4°C. Plates were washed and incubated overnight at 4°C or 2 hours at 37°C with a biotinylated antibody. Plates were then washed and

incubated with streptavidin-alkaline phosphatase (BD Pharmingen) (1:1000 dilution) for 1 hour at 37°C. The plates were subsequently washed, incubated with p-nitrophenyl phosphate (1mg/ml) (Boehringer Mannheim, Germany) and the enzymatic reaction was read at 405 using a Versamax microplate reader (Molecular Devices, Sunnyvale, CA, USA).

MM. 4.1 Single cell suspensions

Splenocyte or lymph node single cell suspensions were obtained as previously described (Coligan et al., 1991) and stimulated with anti-CD3 in Iscove's Modified Dulbecco Medium (IMDM) supplemented with 10% Foetal Calf Serum (FCS), penicillin/streptomycin

MM. 4.2 Granuloma tissue homogenates for cytokine analysis

5% (wt/vol) liver or intestinal tissue suspensions (ileum and colon) from infected mice were homogenized in a lysis buffer containing 50mM Tris-HCL (pH 8.0)-0.5% NP-40, 1mM EDTA, 150mM NaCl, 10% glycerol, 1mM aprotinin, 1mM phenylmethylsulfonyl fluoride with a protease inhibitor cocktail (Sigma). The extracts were frozen immediately in liquid nitrogen and stored at -80°C until use. Before use, extracts were homogenized in a Warring blender and sonicated for 5 min. The extracts were cleared by spinning at 12000 rpm at 4°C. Protein content was assayed in all liver and intestinal homogenates using a BCA protein assay kit (Pierce, Rockford, Illinois, USA).

MM. 4.3 Granuloma cell purification

Livers of 7.5 week-infected mice were homogenized and granulomas collected by 1-G sedimentation and washed in Iscoves modified Dulbecco's medium (IMDM). Cell suspensions were incubated at 37° C with shaking in IMDM containing 0.5% collagenase. The dispersed granulomas were further disrupted by repeated suction and expulsion through 20 ml syringe. Cells were passed

through sterile gauze, washed and viability determined by Trypan blue exclusion. Granuloma cells were cultured for 48-72 hrs in 96 well cell culture plates (Nunclone surface, Nalge Laboratories, Denmark) in IMDM containing 10% foetal calf serum, 10mM HEPES, 0.2mM L-glutamine, penicillin/streptomycin. Cells were cultured with anti CD3 monoclonal antibody at 20 µg/ml.

Intestinal granulomas were prepared from 4cm sections of ileum from infected mice, flushed of faecal contents with PBS, treated with 5mM EDTA for 30 min to remove epithelial cells, then minced and digested with collagenase for 1 hour. Cells were passed through sterile gauze and layered onto Percoll (Sigma) gradient (40/60%) and spun at 2200 rpm for 1 hour in a Jouan ISO 9001 centrifuge (France) and cells collected at the interface.

MM. 5 Arginase assay

Arginase activity in macrophages was evaluated as previously described (Corraliza et al., 1994). Briefly: bone marrow-derived macrophages were washed with PBS and stimulated with LPS. To the activated cells, 50µl of 0.1% Triton X-100 containing protease inhibitors (Sigma) was added and the cells shaken at room temperature for 30 minutes. After lysis, 50µl of 10mM $MnCl_2$, 50mM Tris-HCl, pH 7.5 were added and incubated at 55°C for 10 minutes. 25µl aliquots of the previously-activated lysates were transferred to Eppendorf tubes and arginine hydrolysis initiated by addition of an equal amount of 0.5M arginine, pH 9.7, followed by incubation at 37°C for 60 minutes. The reaction was stopped by addition of 400µl of an acid mixture containing H_2SO_4, H_3PO_4, and H_2O (1:3:7). 25µl of ISPF diluted in 100% ethanol was added and mixture heated at 100°C for 45 minutes followed by incubation for 10 minutes in the dark. 200µl aliquots were transferred to microtitre plates and read at 540nm in a Versamax microplate reader

(Molecular Devices, Sunnyvale, CA, USA). A calibration curve was prepared with increasing amounts of urea between 1.5µg and 30µg.

MM. 6 Hepatocellular damage

Hepatocellular damage was indicated by elevated levels of serum aspartate transaminase as determined by AST/GOT kit (Sigma). Levels of serum LPS were determined by using a E toxate kit for endotoxin determination (Sigma) in combination with an endotoxin colorometric susbtrate (Calbiochem, Darmstadt, Germany) in endotoxin-free water and read at 405nm.

MM. 6.1 Hydroxyproline assay

Hydroxyproline content as a measure of collagen production was assayed in acid-hydrolyzed samples as previously described (Bergman & Loxley, 1963; Bergman & Loxley, 1969) Briefly, tissue (lung or liver) samples (±1g) were placed into 16 x 125 mm Kimble (Scientific Laboratories, NY, USA) screw cap glass tubes and 5ml of 6N HCl added to each tube. The samples were hydrolysed at 110° C for 18-24 hours and after cooling 40mg Dowex (Sigma)/Norit (Merck) mixture in 5ml distilled water was added to each tube and vortex mixed on a Vortex-2 Genie (Scientific Industries, NY, USA). Samples were then centrifuged at 2000rpm at 4°C for 15minutes in a cooled Beckman Model TJ-6 centrifuge (UK). Samples were then filtred into new glass tubes using number 1 Whatman 9cm filter paper. 2ml of the filtrate was neutralized with 1% phenolphthalein and titrated against 10M NaOH. 200µl aliquots were transferred to clean tubes and the final volume brought to 4ml with distilled water. The aliquots were mixed with 400ul of isopropanol (Sigma) and 200µl of chloramines-T/citrate buffer solution (pH 6.0) (Sigma) was added. Ehrlich's reagent solution (Sigma) was added to each tube and the tubes were incubated in a 60°C water bath for 25 minutes. The tubes were allowed to cool under cold running water for 3min. Aliquots of 200µl were transferred into flat bottomed 96-well microtiter plate (Bibby Sterilin, Staffordshire, UK) and the absorbance read at 558-570nm using a Versamax

microplate reader (Molecular Devices, Sunnyvale, CA, USA). Hydroxyproline levels were calculated by using 4-hydroxy-L-proline (Calbiochem, Darmstadt, Germany) as standard and results were expressed as µmoles hydroxyproline per weight of liver tissue that contained 10^4 eggs or as µg/g lung tissue.

MM. 7 FACS analysis

Peripheral blood was collected in heparinized tubes; mesenteric lymph nodes were obtained as previously described (Coligan et al., 1991). Granuloma cells were stained for surface markers by flow cytometry. After blocking in FACS buffer containing 2.4G2 mAb (Fc-block) cells were stained with 1µg of each conjugated mAbCD3-biotin, streptavidin APC, CD4-FITC, and CD25-PE (Pharmingen) Cells were washed and re-suspended in 500ml of FACS buffer and analyzed with a FACSSCAN flow cytometer (Becton Dickinson, Mountain View, California, USA)

MM. 8 Real-time RT-PCR

RNA from liver or intestinal tissue was extracted and the presence of contaminating genomic DNA was tested before cDNA synthesis by real-time PCR using β-actin primers that bind to genomic DNA (5'-TGGAATC CTGTG GCAT CCA GAAAC-3' and 5'-TAAAACGCAGCTCAGTAACAGTCCG-3'). Data were analyzed using the "Fit Points" and "Standard Curve Method" using β-2-microglubulin as the housekeeping gene.

β2MG Forward: 5'-TGA CCG GCT TGT ATG CTA TC-3'

β2MG Reverse: 5'-CAG TGT GAG CCA GGA TAT AG-3'

NOS-2 Forward: 5'-AGC TCC TCC CAG GAC CAC AC -3'

NOS-2 Reverse: 5'-ACG CTG AGT ACC TCA TTG GC -3'

Arg-1 Forward: 5'-CAG AAG AAT GGA AGA GTC AG-3'

Arg-1 Reverse: 5'-CAG ATA TGC AGG GAG TCA CC-3'

Foxp3 Forward: 5'-CAT GAT CAG CCT CCC ACC AC-3'

Foxp3 Reverse: 5'-TTG CAG ACT CCA TTT GCC AG-3'

MM. 9 Histology

Tissue samples (liver or lungs) for staining were rehydrated, fixed in neutral-buffered formalin and processed for histology. 5-7μm sections were stained with haematoxylin and eosin (H&E), periodic acid Schiff reagent (PAS), or with chromotrope 2R and aniline blue solution (CAB) and counterstained with Wegert's hematoxylin for collagen staining.

For immunohistochemistry, OCT embedded liver tissue was cut into 7 μm frozen sections. After acetone fixation, macrophages were detected using peroxidase anti F4/80 mAb (Caltag, Burlingame, California, USA). A rabbit anti-NOS-2 mAb (gift from J. Pfeilschifter, Frankfurt, Germany) was used to analyze macrophage function

MM. 9.1 Histopathology and imaging

Hepatic and pulmonary granulomas were measured in 5-μm-thick hematoxylin and eosin (H & E) sections. The diameters of each granuloma containing a single egg were measured by means of a computerized morphometry using the Scion Image Analysis Program (Scion Image, Frederick, Maryland,USA) by subtracting the egg diameter from the diameter of the whole granuloma (Cheever et al., 1992). An average of 50 granulomas per mouse was included in the analysis. All histologic examinations were scored by the same individual in a blinded fashion to obtain consistency.

Numbers of eosinophils in granulomas were also evaluated in the same sections used for granuloma measurements, whilst PAS positive cells were evaluated from sections stained with periodic acid Schiff reagent (PAS). Granuloma

cosinophils were counted under immersion oil at x1000 magnification using a Nikon Eclipse E400 microscope. Eosinophils were counted in four fields from each granuloma, and 50 granulomas were examined for each mouse.

Images of stained sections were captured using a Nikon DXM 1200 digital camera attached to a Nikon Eclipse E400 microscope and the ACT-1 software application program.

MM. 10 Statistics

Values are given as mean ± SD and significant differences were determined using the unpaired two-tailed Student's t-test or ANOVA. In all tests a p value of <0.05 was considered significant

Reagents

All chemical reagents used in these studies were of analytical grade and purchased from the following companies unless otherwise stated:

Sigma-Aldrich, South Africa

BDH Chemicals Ltd. Poole, England

Merck Laboratory Supplies, South Africa

General reagents

Phosphate Buffered Saline

- 8g NaCl
- 0.2g KCl
- 1.44g Na_2HPO_4
- 0.24g KH_2PO_4.

Dissolve reagents in 900ml distilled H_2O. Adjust to pH 7.4 HCl. Adjust volume to 1000ml. Filter through a 0.22µm filter (Millipore Corporation, Bedford, USA).

Hydroxyproline Assay reagents

Dowex/Norit mixture

Mix 40g Dowex (AG1-X8-200-400 mesh) with 20g of Norit (decolorizing carbon) in a larger beaker. Add 6N HCl and mix well. Transfer mixture to a 800ml Buchner funnel and apply suction. Wash 2 or 3 times with 6N HCl. Add 95% ethanol, mix and apply suction. Add 100% ethanol, mix and apply suction and repeat the step twice. Dry in a larger dish under the hood

Citrate-Acetate buffer

Weigh out 57g of Sodium Acetate (x $3H_2O$), 37.5g trisodium citrate (x $2H_2O$), and 5.5 g of citric acid. Mix with 385ml isopropanol (2-propanol) in a 1L-graduated cylinder. Bring volume to 1L with distilled water. Stable indefinitely at room temperature.

Chloramine T

Weigh out 7g of Chloramine T. Add distilled water to a final volume of 100ml. Store dark and refrigerated at 4°C. For the assay, mix 1 part chloramine T with 4 parts citrate acetate buffer.

Ehrlich's reagent

Add 25g of p-dimethylaminobenzaldehyde to 37.5ml of 60% perchloric acid made from a 70% stock, by adding 32.1ml perchloric acid to 5.4ml. Store in the dark at 4°C. For the assay, mix 3 parts of Ehrlich's reagent with 23 parts isopropanol.

ELISA reagents

Table A. Antibodies used in cytokine ELISA

Cytokine	Capturing antibody Clone number	Detecting Antibody Clone number (biotinylated)	Source
IL-4	BVD4-1D11	BVD6-24G2	Pharmingen
IL-5	TRFK5	TRFK4	Pharmingen
IL-10	JES5-2A5	SXC-1	Pharmingen
IL-13	38213	Matched to capturing Ab.	R & D
IFN-γ	R4-6A2	XMG1.2	Pharmingen
TGF-β	A75-2.1	A75-3.1	Pharmingen
TNF-	G281-2626	MP6-XT3	Pharmingen

Blocking buffer

- 40g Bovine Serum Albumin (Boehringer Mannheim, Germany)
- 0.2g NaN_3

Dissolve BSA and NaN_3 in 800ml PBS (pH 7.2), bring the final volume to 1000ml and store at 4°C.

Dilution Buffer

- 10g BSA
- 0.2g NaN_3

Dissolve BSA and NaN_3 in 800ml PBS (pH 7.2). Bring final volume to 1000ml and store at 4°C.

20x Washing Buffer

- 20g KCl
- 20g KH_2PO_4
- 144g NaH_2PO_4
- 800g NaCl

Dissolve reagents in 4500ml distilled H_2O. Add 50ml Tween 20 and 100ml 10% NaN_3. Bring final volume to 5000ml and store at room temperature.

Substrate Buffer

- 0.2g NaN_3
- 08g $MgCl_2$

Dissolve NaN_3 and $MgCl_2$ in 700ml distilled H_2O. Add liquefied diethanolamine and adjust the pH to 9.8. Bring final volume to 1000ml with distilled H_2). Sterilize and store in the dark at 4°C.

Iscove's Modified Dulbecco's Medium (IMDM)

Dissolve 1 tube (3.024g/L) of IMDM in 750ml distilled H_2O. Add 81.7ml 10x $NaHCO_3$ and 2ml of 500x penicillin/streptomycin. Using 1NaOH, adjust the pH to between 7.2-7.4. Bring final volume to 1000ml with distilled H_2O. Sterilize through a 0.22µm filter (Millipore Corporation, Bedford, USA) and store at 4°C.

Red cell lysis buffer

- 8.34g NH_4Cl
- 0.037g EDTA
- 1g $NaHCO_3$

Dissolve reagents in 1000ml distilled H_2O. Sterilize and store at 4°C.

Experimental Studies

CHAPTER 1

Schistosoma mansoni infection in macrophage/neutrophil-specific IL-4Rα-deficient mice

SUMMARY

Macrophage/neutrophil-specific IL-4Rα-deficient mice ($LysM^{Cre}IL\text{-}4R\alpha^{-/flox}$) were generated to understand the role of IL-4/IL-13 responsive myeloid cells during Th2 immune responses. In these studies three groups of mice were used, $IL\text{-}4R\alpha^{-/flox}$ (WT), $IL\text{-}4R\alpha^{-/-}$ and $LysM^{Cre}IL\text{-}4R\alpha^{-/flox}$ mice. A group of 6-8 mice per group were percutaneously infected with 100 *S. mansoni* cercariae and the immune response analyzed. $LysM^{Cre}IL\text{-}4R\alpha^{-/flox}$ as well as $IL\text{-}4R\alpha^{-/-}$ mice were extremely susceptible to *S. mansoni* infection with 100% mortality during infection. In $LysM^{Cre}IL\text{-}4R\alpha^{-/flox}$ mice, mortality was not dependent on neutrophils and occurred in the presence of T_H2/Type 2 responses, granuloma formation and egg-induced fibrosis. In contrast, T_H2/type 2 and granuloma formation were significantly abrogated but not completely abolished in $IL\text{-}4R\alpha^{-/-}$ mice. Death was associated with increased T_H1 cytokines, hepatic and intestinal histopathology, increased NOS-2 activity, impaired egg expulsion, and sepsis. The immunosuppressive cytokine, IL-10 was not able to compensate for the absence of IL-4/IL-13-activated alternative macrophages.

RESULTS

1.1 Generation of macrophage/neutrophil-specific IL-4Rα$^{-/-}$ mice[1]

Conditional IL-4Rα-deficient (IL-4Rα$^{flox/flox}$) mice were generated by gene targeting using isogenic targeting vector and Cre-mediated site-specific recombination in BALB/c embryonic stem cells. The neomycin resistance/ thymidine kinase (neo/tk) cassette flanked by loxP sites was introduced into intron sequences 5′ of exon 7 and an additional loxP site was inserted into the intron 5′ of exon 10 (Figure 1.1A). Transient Cre expression in successfully target embryonic stem cells resulted in removal of the selection cassette and retention of two loxP sites flanking exons 7-9. Cell-specific gene disruption in macrophage and neutrophils was achieved through an intereross between hemizygous IL-4Rα$^{-/flox}$ mice, bearing one floxed and one disrupted IL-4Rα allele, and transgenic LysM^{Cre} mice on and IL-4Rα$^{-/-}$ background. Transgene-bearing hemizygous mice, IL-4Rα$^{-/flox}$ mice were identified by PCR genotyping (Figure 1.1B). Cre-mediated disruption in bone marrow-derived macrophages from LysM^{Cre}IL-4Rα$^{-/flox}$ was confirmed by southern blotting (data not shown). A dose-dependent proliferation of IL-4 stimulated lymphocytes demonstrated that the insertion of loxP sites had no influence on IL-4 receptor function (Figure 1.1C). These results suggest a silent floxed mutation of the IL-4Rα gene.

1.2 Selective impairment of IL-4Rα function in macrophages and neutrophils[1]

IL-4Rα cell surface expression was analyzed in neutrophil (I-a^{D-}/GR1^{+}), macrophage (F4/80^{+}), lymphocyte (CD3^{+} and B220^{+}), and dendritic cell (CD11c^{+}CD8^{+} and CD11c^{+}CD8^{-}) populations from *S. mansoni*-infected mice.

In the LysM^{Cre}IL-4Rα$^{-/flox}$ strain, abrogation of IL-4Rα expression was observed only in the neutrophil and macrophage populations (Figure 1.2),

[1] Generation and cellular characterization studies were performed by C. Holscher and D. Herbert.

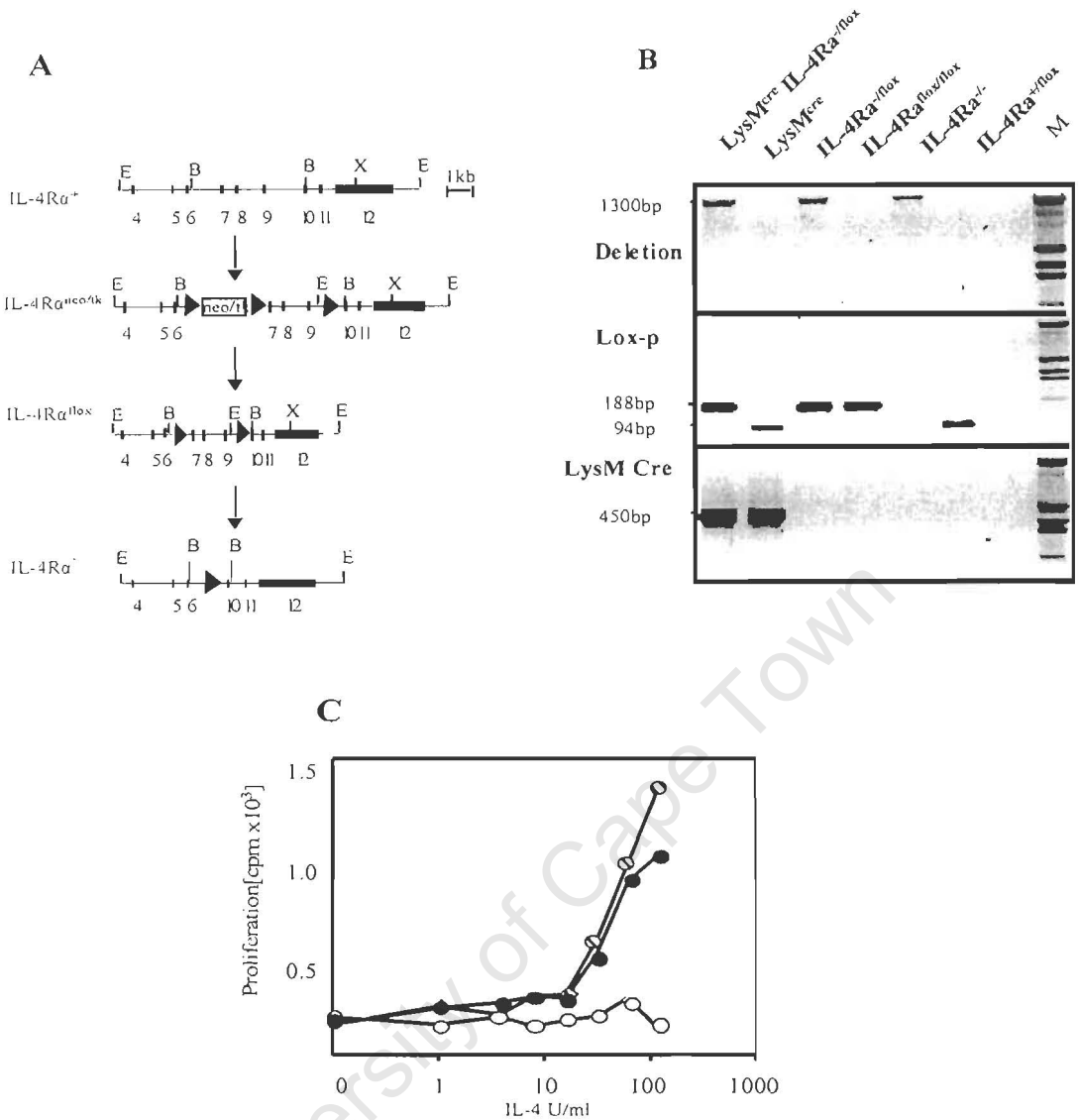

Figure 1.1

Cell specific deletion of the IL-4Rα gene in macrophages and neutrophils

A) IL-4Rα gene locus and targeted deletion. Numbers indicate exons of the IL-4Rα gene; B,E, and X, restriction sites for BamHI, EcoRI and XhoI

B) Identification of different IL-4Rα alleles and the $LysM^{Cre}$ transgene. Three specific PCR reactions were used to identify $LysM^{Cre}IL\text{-}4R\alpha^{-/flox}$ mice

C) Lymph node cells from WT (black symbol), $IL\text{-}4R\alpha^{-/-}$ (white symbol), and $IL\text{-}R\alpha^{flox/flox}$ (hatched symbol) were stimulated with IL-4 and DNA synthesis measured by thymidine incorporation. Data are mean ± SD from triplicate cultures.

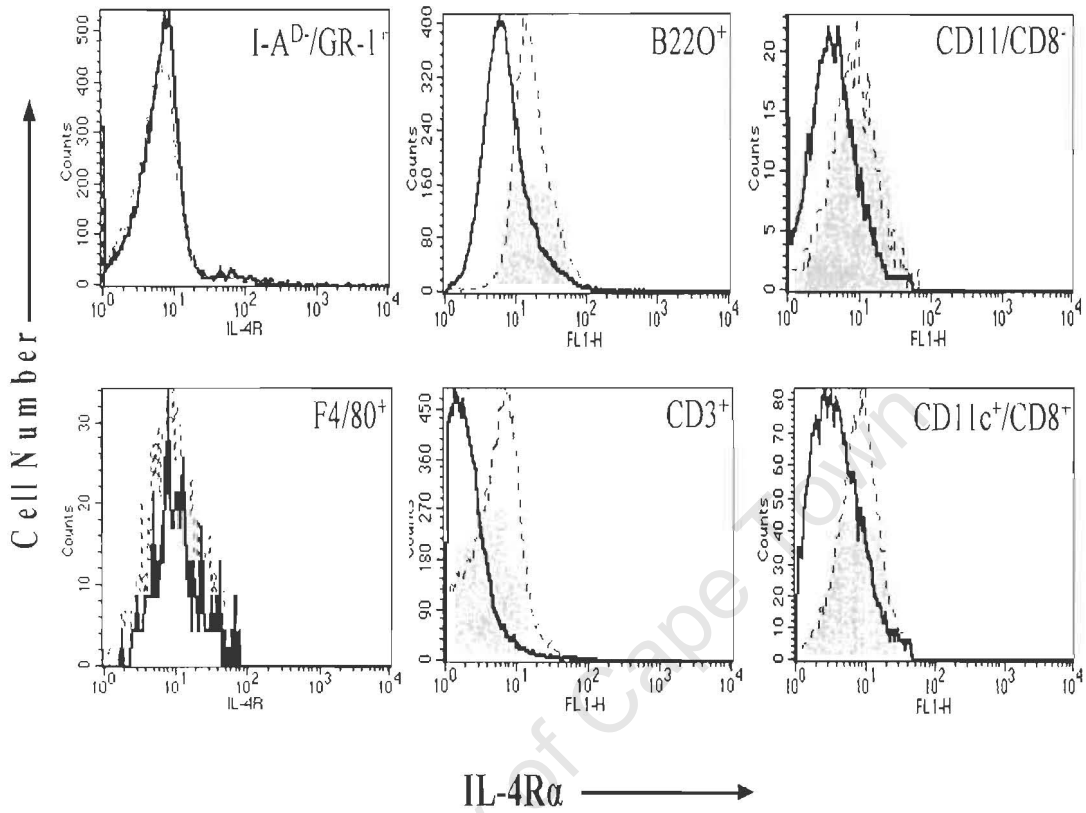

Figure 1.2

Cell type–specific IL-4Rα expression

Mesenteric lymph node cells from *S. mansoni* infected mice were costained using IL-4Rα together with GR-1^{+}/I-a^{d-} or F4/80^{+} for neutrophils or macrophages, B220^{+} or CD3^{+} for B or T cells, CD11c^{+}CD8^{-} and CD11c^{+}CD8^{+} for dendritic cell subpopulations. IL-4Rα$^{-/flox}$ (grey shade), IL-4Rα$^{-/-}$ (black line), LysM^{Cre}IL-4Rα$^{-/flox}$ (grey dotted line). Data are from pooled samples of 5 mice and are representative from four experiments.

showing efficient Cre-mediated deletion of the IL-4Rα gene. Indeed, LPS stimulated peritoneal macrophages treated with IL-4 showed a significant reduction of TNF secretion only in WT and not in IL-4Rα$^{-/-}$ or LysM^{Cre}IL-4Rα$^{-/flox}$ mice (Figure 1.3A).

Cytokine specificity was demonstrated by co-treatment with IL-10, which globally suppressed TNF production in all macrophage populations. Similarly, IL-13-mediated suppression of NO production was absent in LPS/IFN-γ-stimulated peritoneal macrophages form IL-4R$^{-/-}$ and LysM^{Cre}IL-4Rα$^{-/flox}$ mice but present in WT mice (Figure 1.3B). In addition, F4/80^{+} macrophages from LysM^{Cre}IL-4Rα$^{-/flox}$ mice also showed impaired IL-4-mediated MHC-II (I-a^{D}) upregulation and STAT6 phosphorylation (data not shown).

Granulocytes were isolated to determine the ability of IL-4 to suppress O_2^- production. Pre-treatment with IL-4 (Figure 1.3C) or IL-13 (data not shown) could effectively suppress up to 40% of O_2^- release in PMA-stimulated WT but not in IL-4Rα$^{-/-}$ or LysM^{Cre}IL-4Rα$^{-/flox}$ granulocytes. Impairment was IL-4Rα-specific since IL-10 could effectively suppress O_2^- production in all strains.

To further characterise the function of IL-4Rα expression, CD4^{+}T cells were isolated from lymph nodes of naïve mice, stimulated with anti-CD3/CD28, and given either IL-12/anti-IL-4 or IL-4/anti-IFN-γ. Results demonstrate that T_H1 polarization was achieved in all three strains following IL-12/anti-IL-4 treatment, while IL-4 was able to drive T_H2 polarization from CD4^{+}T cells of LysM^{Cre}IL-4Rα$^{-/flox}$ and WT, but not IL-4Rα$^{-/-}$ mice (Figure 1.3D). In vitro proliferation of B cells, which is IL-4 promoted was comparable between WT and LysM^{Cre}IL-4Rα$^{-/flox}$ lymphocytes in a dose-responsive manner, but completely absent in IL-4Rα$^{-/-}$ lymphocytes (Figure 1.3E). IL-4 treatment of CpG-stimulated bone marrow derived dendritic cells enhanced IL-12p70 production in LysM^{Cre}IL-4Rα$^{-/flox}$ and WT but not the IL-4Rα$^{-/-}$ strain (Figure 1.3F). Together these data provide evidence for efficient impairment of IL-4Rα

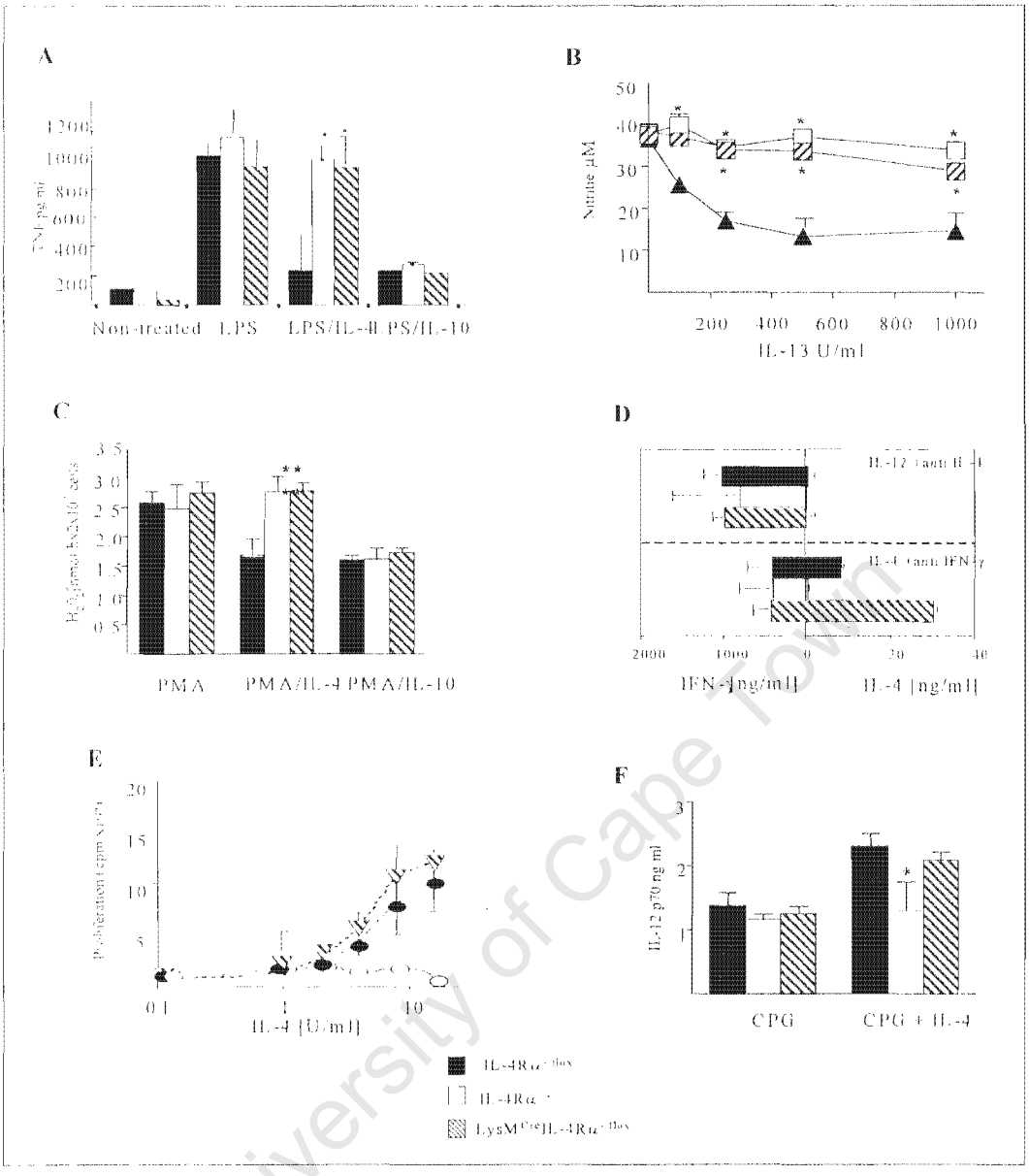

Figure 1.3

Cellular characterisation of IL-4 and IL-13-mediated functions in $LysM^{Cre}IL\text{-}4R\alpha^{flox}$ *mice*

Five mice per group were used for cellular characterisation with a representative from two or four experiments. TNF (Panel A), Nitrite (panel B) and suppression of oxidative burst were measured in treated peritoneal macrophages. T helper polarization (panel D) and proliferation (panel E) were determined in stimulated lymph node cells. IL-4 instructed IL-12p70 production by dendritic cell (panel F). Data are mean ± SD of triplicate cultures with **p<0.01 by ANOVA compared to WT

mediated functions in LysM^{Cre}IL-4Rα$^{-/flox}$ macrophages and neutrophils but not in lymphocytes or dendritic cells.

1.3 Susceptibility of LysM^{Cre}IL-4Rα$^{-/flox}$ mice to *S. mansoni* infection[2]

To determine the role of macrophage-specific IL-4Rα expression, IL-4Rα$^{-/flox}$ (WT), IL-4Rα$^{-/-}$, and LysM^{Cre}IL-4Rα$^{-/flox}$ mice were infected with the Puerto Rican strain of *S. mansoni* parasites. Groups of 6 mice per strain were percutaneously infected with 100 cercariae and monitored for disease outcome. LysM^{Cre}IL-4Rα$^{-/flox}$ and IL-4Rα$^{-/-}$ mice succumbed to *S. mansoni* infection with the mean survival times of 54±2 and 59±3 days, respectively, in contrast to their WT littermates that survived the monitored 80 days with little mortality (Figure 1.4A).

Rapid weight loss is a well-documented symptom of patients with chronic schistosomiasis. The effect of *S. mansoni* infection on body weight was therefore investigated. Results show that the observed mortality was associated with progressive weight loss in both mutant strains that began late in the 6th week of infection, and some animals had lost up to 20% of their original body weight at the time of death (data not shown).

To determine if granulocytes were involved in the early mortality after *S. mansoni* infection, neutrophils were depleted in infected mice. Despite the weekly injections of RB6-8C5 starting at week 5 post-infection, no influence on survival kinetics was observed (Figure 1.4B). Together, this strongly suggests that IL-4/IL-13-activated macrophages, but not eosinophils are essential for survival during acute schistosomiasis.

[2] Infection studies performed by M. Leeto and D. Herbert

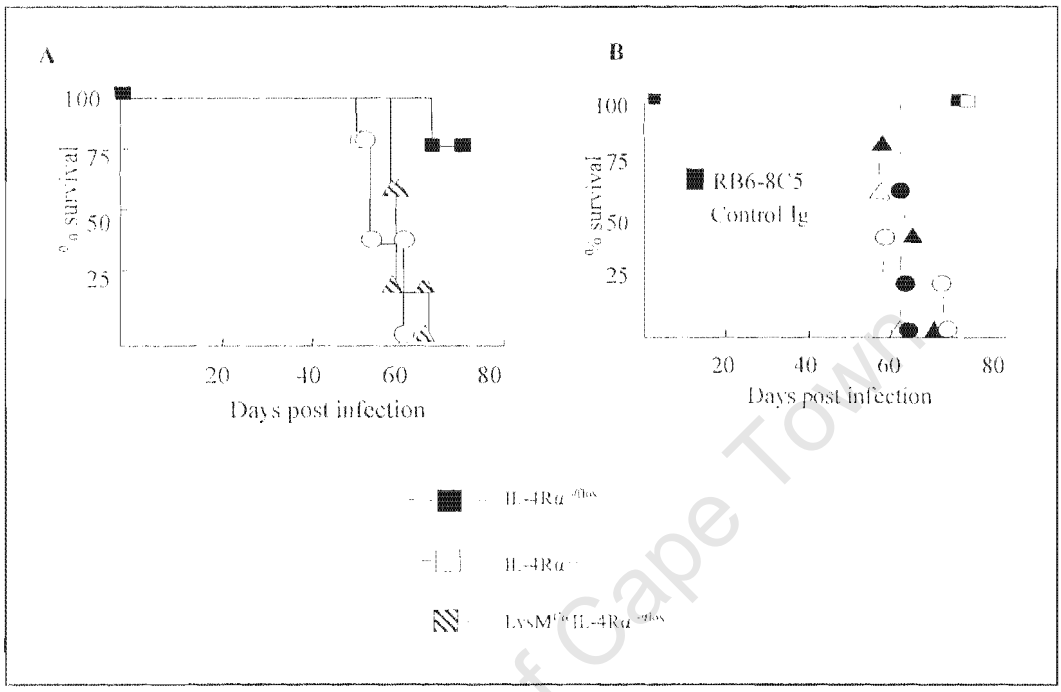

Figure 1.4

Survival kinetics in S. mansoni infected mice.

Four to six mice were infected percutaneously with 100 cercariae of *S. mansoni* and analyzed 7 weeks post-infection. Mice were monitored on a weekly basis for survival (Panel A). Panel B - survival kinetics after depletion of granulocytes. RB6-8C5 (black symbols) or an isotype control GL113 mAb (white symbols) were injected weekly, starting at 5 weeks post-infection.

1.4 Alternative macrophage activation is not required for granuloma formation or hepatic fibrosis

The effects of *S. mansoni* infection on the pathology of the livers in LysM^{Cre}IL-4Rα$^{-/flox}$ mice were investigated due to the strain's susceptibility to infection. Histological examination of egg-induced granulomas in liver sections of acutely infected mice revealed a clear importance for IL-4Rα expression in liver pathology. In contrast to the eosinophilic, circumoval appearance of the WT granulomas, a significant decrease in the eosinophil content and overall size of IL-4Rα$^{-/-}$ liver granuloma tissue was observed (Table I and Figure 1.5A). LysM^{Cre}IL-4Rα$^{-/flox}$ liver granulomas, however, were similar to the WT strain but larger and less compact. Although there were half as many eosinophils per μm^2 in LysM^{Cre}IL-4Rα$^{-/flox}$ tissue (Table I), the absolute number were comparable to WT due to the increased granuloma size in the former. In contrast granulomas that formed in IL-4Rα$^{-/-}$ mice were impaired but not completely abolished with significantly abrogated number of eosinophils (Table I and Figure 1.5A).

IL-4/IL-13-mediated activation of macrophages is thought to induce collagen by enhanced proline production, thus leading to fibrosis. However, only IL-4Rα$^{-/-}$ mice but not LysM^{Cre}IL-4Rα$^{-/flox}$ mice showed impaired collagen production as determined by CAB staining and quantitation of liver hydroxyproline (Table I and Figure 1.5B). Examination of fibrosis in mice 20 weeks after-infection with 25 cercariae also revealed that WT and LysM^{Cre}IL-4Rα$^{-/flox}$ mice had similar levels of fibrosis with mean values of 1.5μmoles/10^4 eggs, versus 1.9μmoles/10^4 eggs, respectively.

Table 1

Liver pathology during acute schistosomiasis

Liver pathology was analyzed in mice infected with 100 S. mansoni cercariae 7 weeks post-infection

	IL-4Rα$^{-/flox}$	IL-4Rα$^{-/-}$	LysM^{Cre}IL-4Rα$^{-/flox}$
Liver granuloma area [(μm^2) x 10^{-3}][a]	78 ± 36	13.7 ± 9*	130 ± 47
Granuloma eosinophils (1000x)[b]	200 ± 72	9 ± 6*	109 ± 27
Hydroxyproline ($\mu M/10^4$ eggs)	7.2 ± 2.3	2.2 ± 1*	8.1 ± 1.5
Parasite burden [(eggs/liver) x 10^3]	21.5 ± 5	18 ± 7	17 ± 9

[a]Data shown represent the mean of 50 granulomas measured per mouse in a group of five animals

[b]Data shown represent the mean number of eosinophils per high-powered field in each granuloma, measured as above *$p<0.05$ by ANOVA in comparison to WT.

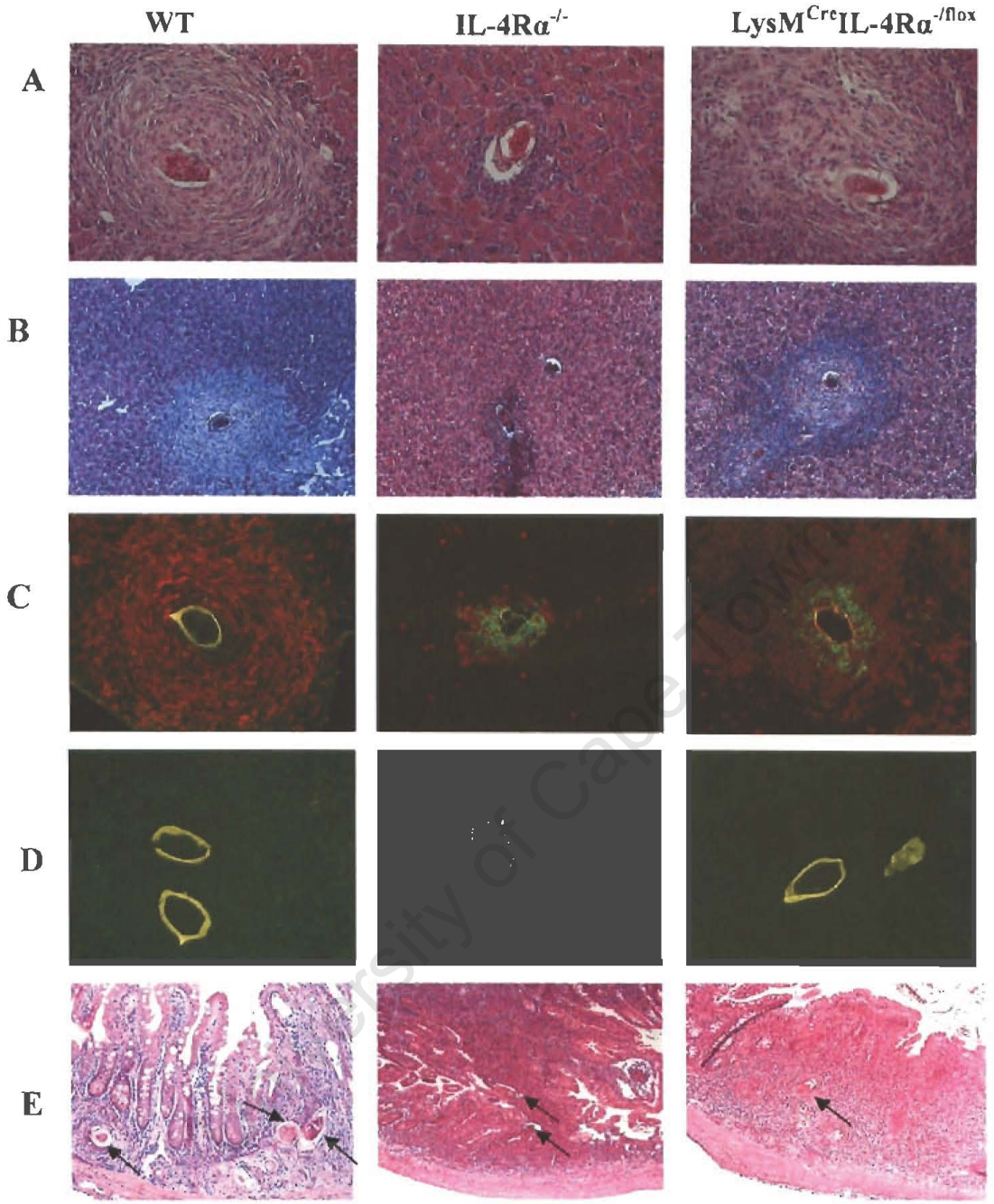

Figure 5

Histopathology of S. mansoni infected IL-4Rα$^{-/-}$ and LysM^{Cre}IL-4Rα$^{-/flox}$ mice

Five mice per group were infected with 100 cercariae of *S. mansoni* and analyzed 7 weeks later. Liver sections were removed and stained as described in Materials and Methods. Shown are representative of a total of 250 analyzed sections from three independent experiments. Magnification =200x (A &C), 100x (B & E)

To determine macrophage recruitment and classical activation, liver sections were stained with F4/80 and NOS-2 staining, respectively. Results show that impaired granuloma formation in IL-4Rα$^{-/-}$ corresponded to reduced F4/80 staining (Figure 1.5C), while both IL-4Rα$^{-/-}$ and LysM^{Cre}IL-4Rα$^{-/flox}$ liver granulomas contained many NOS-2 positive cells mostly co-stained with F4/80 macrophage marker (Figure 1.5C). A marker for alternatively activated macrophages, mannose receptor, was absent in IL-4Rα$^{-/-}$ and LysM^{Cre}IL-4Rα$^{-/flox}$ liver granuloma tissue but present in the WT (Figure 1.5D). These results show that *S. mansoni* infected LysM^{Cre}IL-4Rα$^{-/flox}$ mice have impaired alternative macrophage activation and enhanced NOS-2 production, together with a larger granuloma size, and unaltered eosinophil recruitment and egg-induced collagen production.

To further characterize pathology in infected mice, sera from *S. mansoni* infected mice were analyzed for levels of aspartate aminotransaminase (AST) and endotoxin (LPS) as an indicator of hepatocellular and intestinal damage, respectively. Both LysM^{Cre}IL-4Rα$^{-/flox}$ and IL-4Rα$^{-/-}$ strains had significantly increased levels of AST and LPS, as compared to WT (Figures 1.6A &B). These results demonstrate that mortality in IL-4Rα$^{-/-}$ mutant strains was associated with increased hepatocellular damage (Figure 1.7) and endotoxemia.

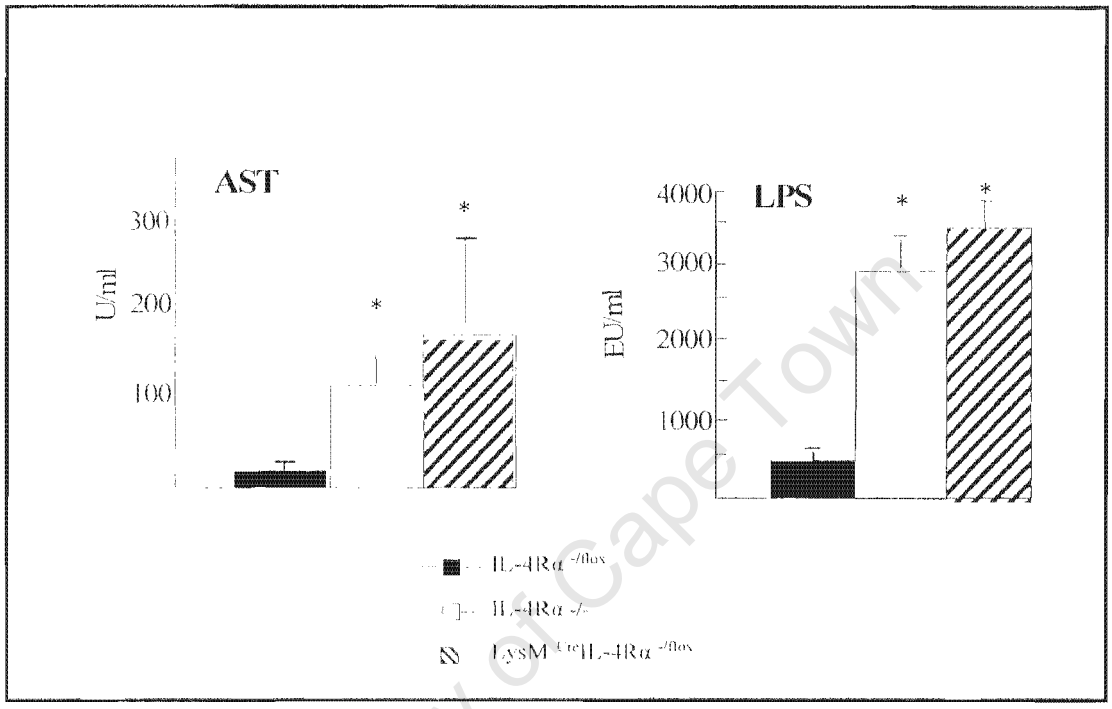

Figure 1.6

Hepatocellular damage and sepsis in acutely-infected mice

Four to six mice were percutaneously infected with 100 cercariae of *S. mansoni and* analyzed 7 weeks after-infection. Aspartate aminotransaminase (AST) and LPS levels were determined in the sera of infected mice as indicators of hepatocellular damage and sepsis respectively. *$p<0.05$ by ANOVA

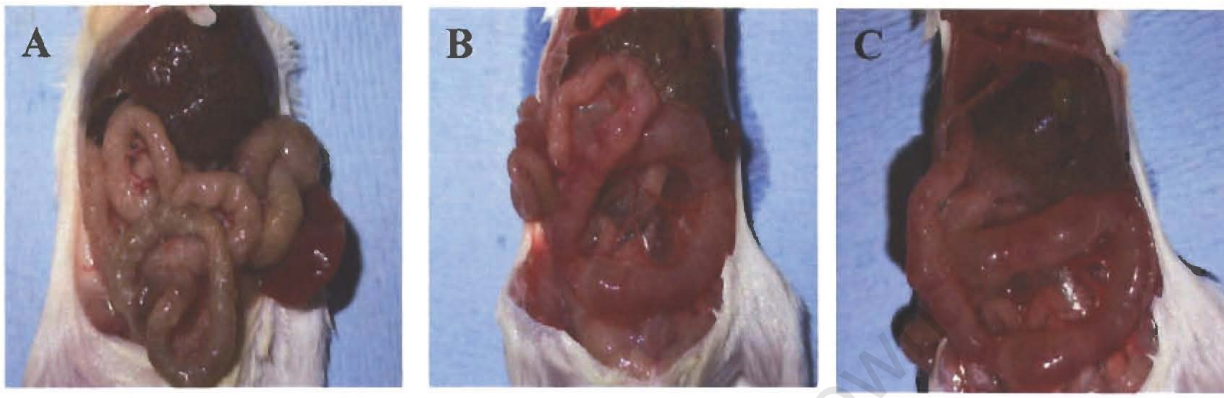

Figure 7

Pathology in schistosome infected mice

Mice were percutaneoulsy infected with 100 *S. mansoni* cercariae and analyzed for pathology at week 7 post-infection. A representative image from four to six mice per strain is shown.

A) IL-4Rα$^{-/flox}$ (WT)

B) IL-4Rα$^{-/-}$

C) LysM^{Cre}IL-4Rα$^{-/flox}$

The two mutant strains also showed massive inflammatory cell infiltrates in intestinal granulomas (Figure 1.7) associated with the enhanced production of both anti-inflammatory (IL-10) and pro-inflammatory (IFN-γ) cytokines in gut tissue (Figure 1.8A&B)

Furthermore, the faecal egg output of IL-4Rα$^{-/-}$ and LysM^{Cre}IL-4Rα$^{/-flox}$ mice was significantly reduced compared to WT animals (Figure 1.9). To determine if septic shock was the cause of mortality in infected LysM^{Cre}IL-4Rα$^{/-flox}$ and IL-4Rα$^{-/-}$ mice, infected mice were given 50mg/ml of enrofloxacin antibody in drinking water starting at week 5 post-infection. Systemic antibiotic treatment resulted in extension of survival time in LysM^{Cre}IL-4Rα$^{/-flox}$ and IL-4Rα$^{-/-}$ mice, as compared to the untreated counterparts (Figure 1.10) suggesting that sepsis was a factor causing death of the mutant mouse strains.

1.5 T_H1 and T_H2 responses are present in LysM^{Cre}IL-4Rα$^{/-flox}$ mice

The kinetics of cytokine production was determined from splenocyte cell culture supernatants of infected mice. Stimulation of cells with antigen (SEA) revealed increased IFN-γ responses but reduced IL-4, IL-5 and IL-10 production in IL-4Rα$^{-/-}$ mice (Figure 1.11), as compared to WT mice at day 49 post-infection. LysM^{Cre}IL-4Rα$^{/-flox}$ showed a differential profile with increased levels of IL-4, IL-5 and IL-10, but also high levels IFN-γ.

Accordingly, measurement of SEA-specific antibody responses showed high levels of IgG1 and IgE antibody production in LysM^{Cre}IL-4Rα$^{/-flox}$ mice. Similarly, SEA-specific IgG2a levels were also elevated compared to WT (Figure 1.12). A similar cytokine profile was also observed in hepatic mRNA transcripts, as determined by real-time PCR (Figure 1.13). The presence of IL10 in infected LysM^{Cre}IL-4Rα$^{/-flox}$ mice (Figures 1.8 & 1.13) indicated that IL-10 might not influence alternative macrophage activation. This was confirmed as only IL-4 and IL-13, but not IL-10 or IFN-γ were able to promote

Arginase I upregulation in LPS-stimulated thioglycollate-elicited WT macrophages (Figure 1.14). In summary, these results suggest that IL-10 is not involved in alternative macrophage activation and the presence of a T_H2 response is not able to prevent death from schistosomiasis in $LysM^{Cre}IL\text{-}4R\alpha^{-/-flox}$ mice.

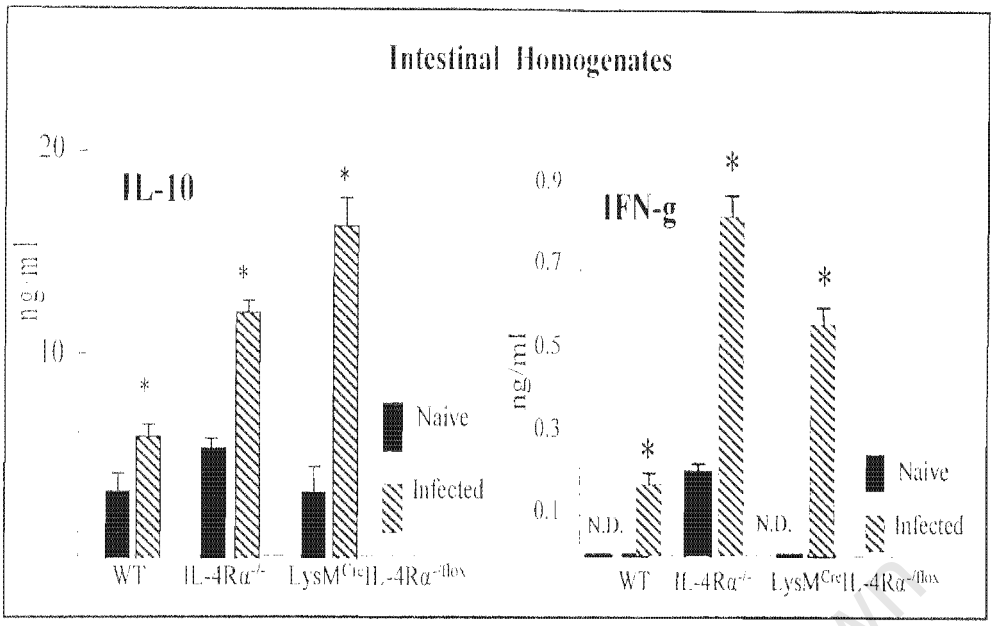

Figure 1.8

Intestinal cytokine production

IL-10 and IFN-γ concentrations were measured in ileum homogenates from non-infected and infected mice by ELISA. *p<0.05 by ANOVA compared to WT

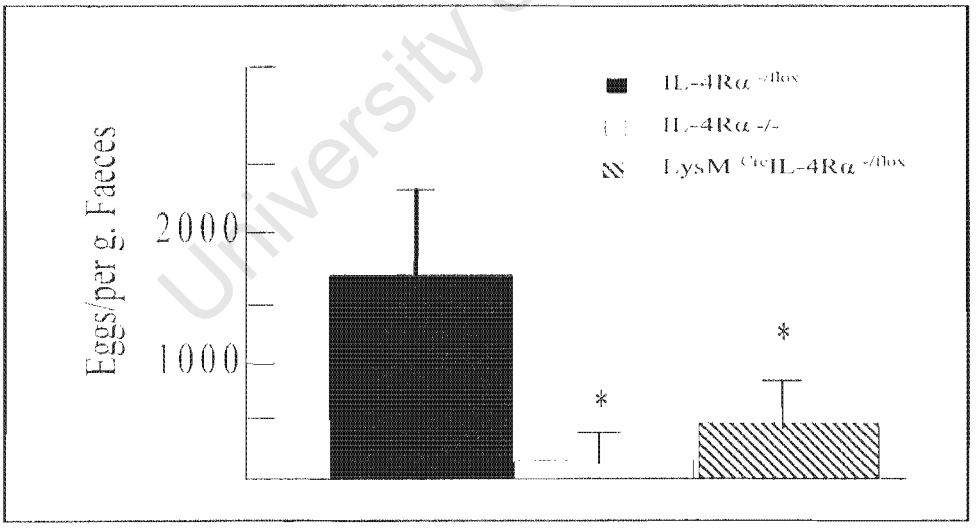

Figure 1.9

Faecal egg output

Egg counts were enumerated from faecal pellets as described in Materials and Methods. Data are mean ± SD and are representative of one of three independent experiments. *p<0.05 by ANOVA compared to WT

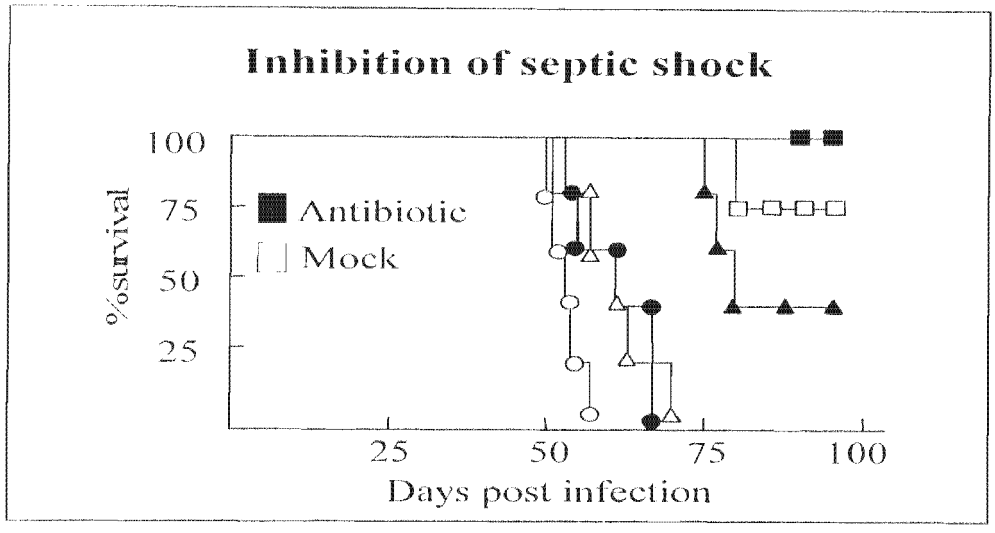

Figure 1.10

Inhibition of septic shock

Survival after treatment with broad spectrum antibiotics. WT (squares), IL-4Rα$^{-/-}$ (circles), and LysM^{Cre}IL-4Rα$^{-/flox}$ (triangles) were given 50mg/ml of enrofloxacin-treated water (black symbols) or left untreated (white symbols) starting at 5 weeks post-infection with 75 cercariae of *S. mansoni*

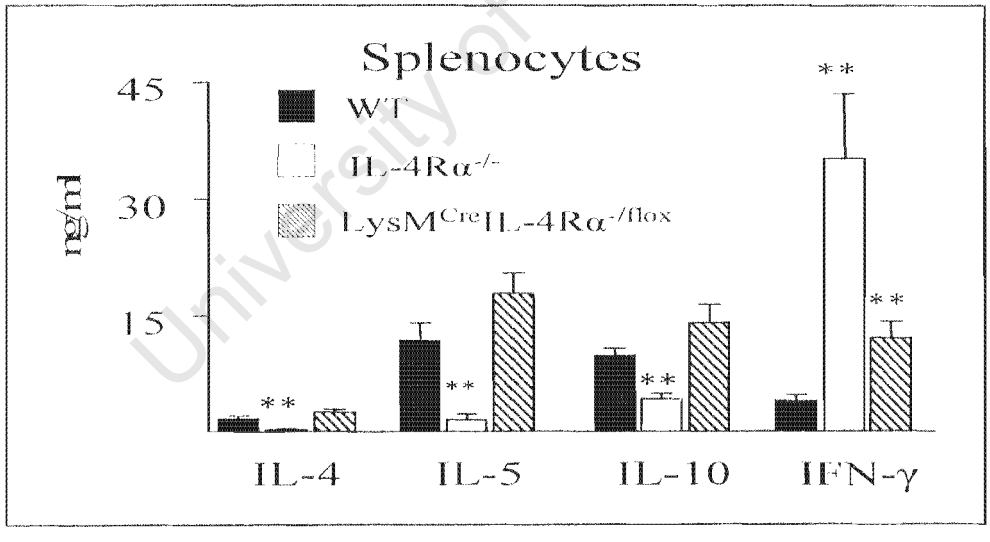

Figure 1.11

Antigen specific T cell responses

Splenocytes from acutely infected mice were restimulated with SEA and supernatants analyzed for cytokine production. **p<0.01 compared to WT. Each data point represents the average ± SD of triplicate samples. A representative from two of five independent experiments is shown.

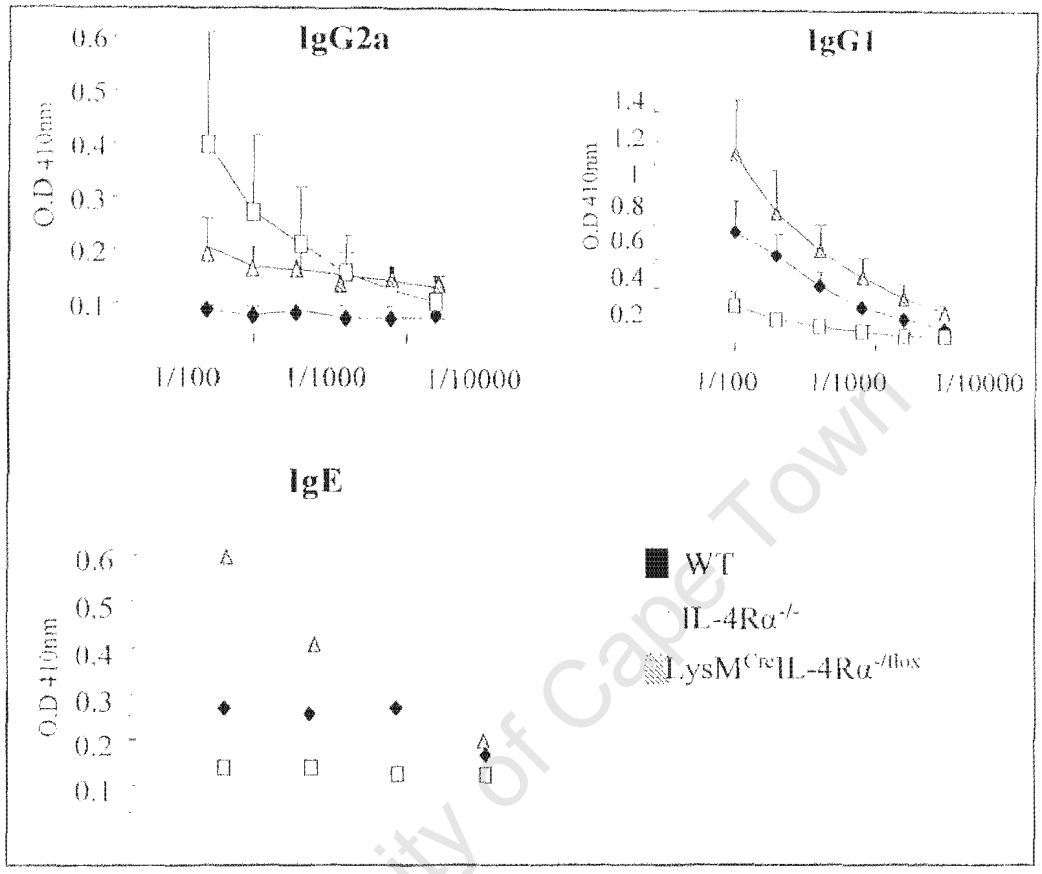

Figure 1.12

Antigen-specific B cell responses

SEA-specific antibody production was determined in sera of individual mice (pooled for total IgE). Data are mean ± SD of five mice per group.

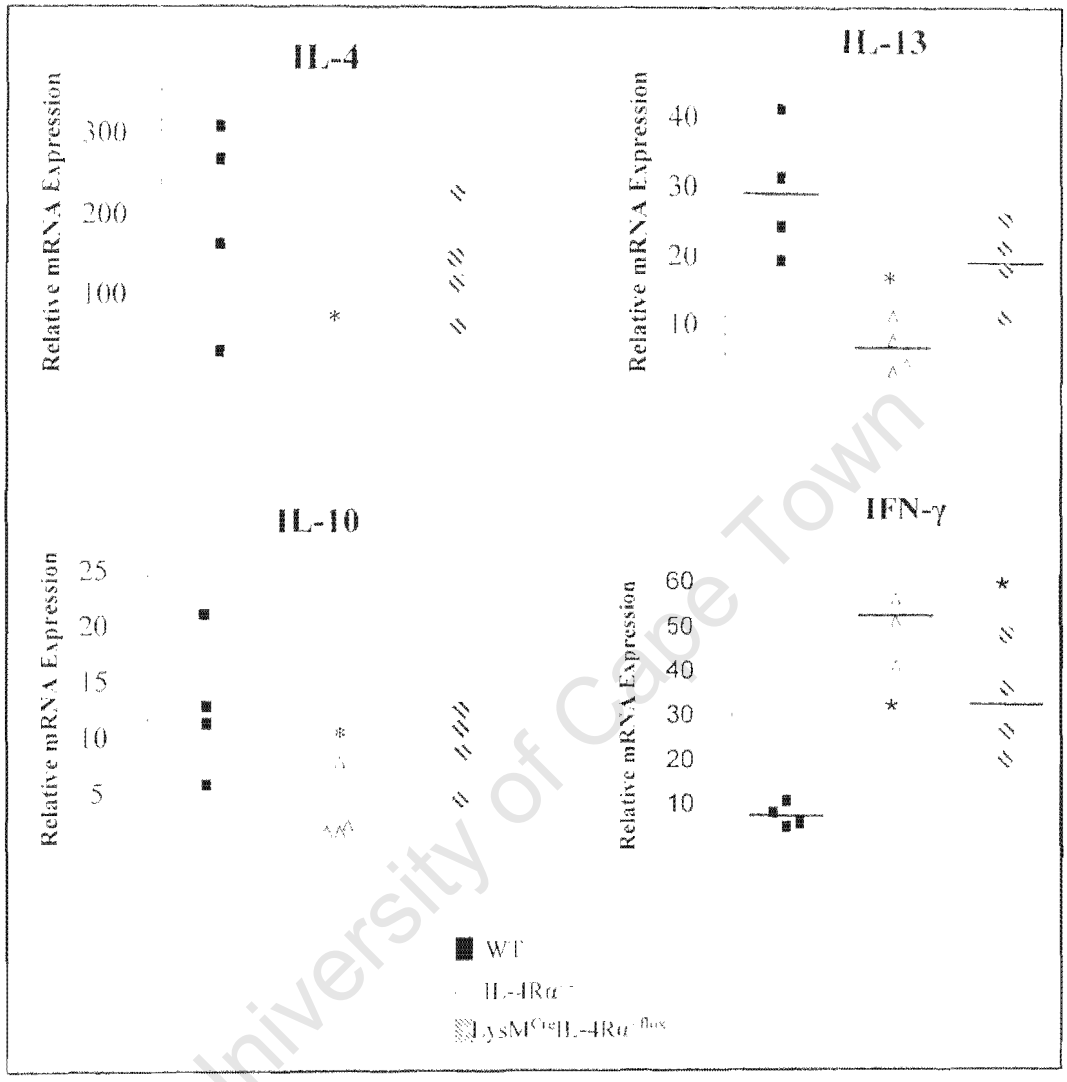

Figure 1.13

Cytokine transcripts in liver tissue of infected mice

Cytokine transcripts were determined in liver tissue from infected mice by real-time PCR. Data are shown as relative expression compared to WT non-infected tissue with *p < 0.05 ANOVA compared to infected WT.

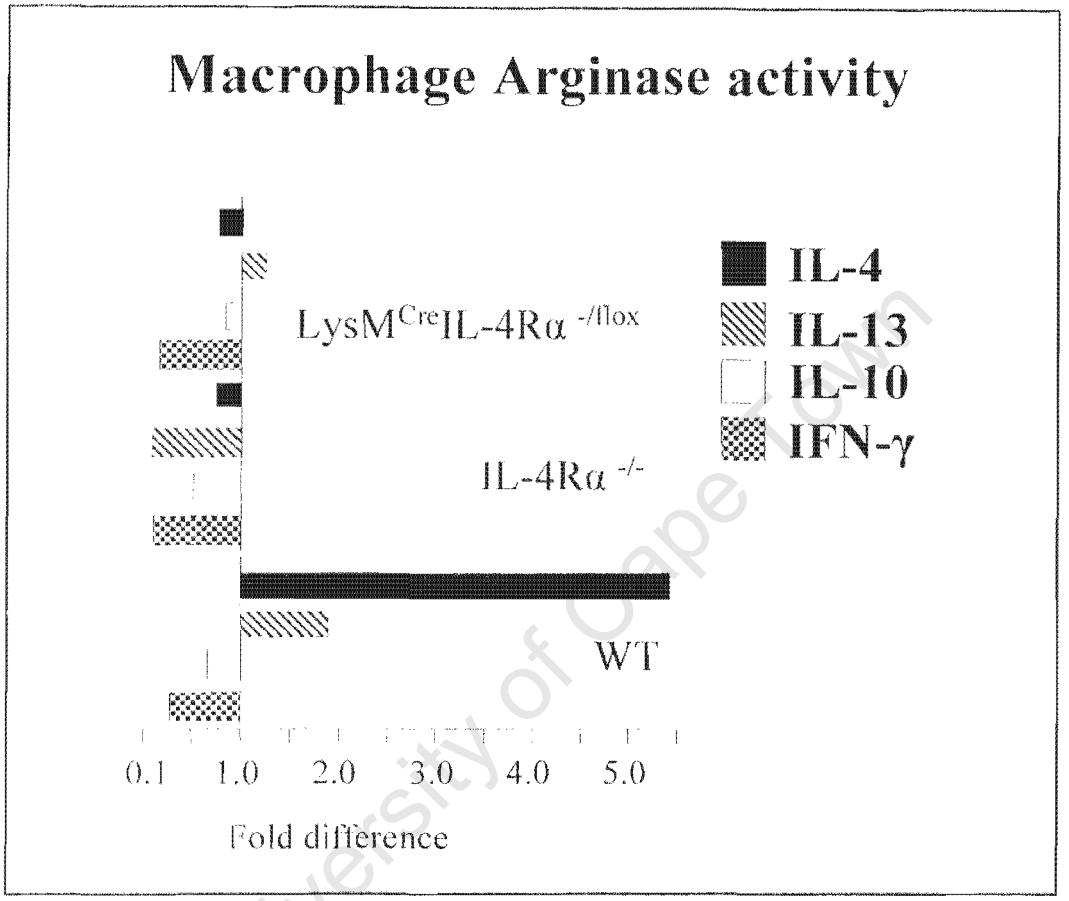

Figure 1.14

Arginase activity in peritoneal macrophages

LPS-stimulated peritoneal macrophages were co-stimulated with IL-4, IL-13, IL-10 and IFN-γand analysed for arginase activity. Data are expressed as fold increase of urea compared to LPS treatment only.

Discussion

The present work describes the generation, characterization, and functional analysis of mice lacking the IL-4Rα chain selectively in macrophages and neutrophils. An infectious disease model was employed in which host protection or pathology was dependent upon Type 2 immune responses. Here, we provide evidence that IL-4/IL-13-activated alternative macrophages are essential for surviving acute schistosomiasis. $LysM^{Cre}IL\text{-}4R\alpha^{-/flox}$ mice were established after generating conditional knockout $IL\text{-}4R\alpha^{flox/flox}$ mice by gene targeting in BALB/c ES cells and subsequent interbreeding with $LysM^{Cre}$ knock-in mice. FACS analysis and subsequent functional studies revealed cell type-specific disruption of the IL-4Rα gene in macrophages and neutrophils only, with normal IL-4/IL-13 responsiveness in B and T lymphocytes, as well as dendritic cells. This was confirmed in an experimental helminth infection (*S. mansoni*) with impaired IL-4/IL-13-activated alternative macrophage activation in $LysM^{Cre}IL\text{-}4R\alpha^{-/flox}$ mice but normal T_H2/Type 2 responses compared to WT littermate controls.

Infection with *S. mansoni* leads to $CD4^+$ T cell-dependent granulomatous pathology that occurs in response to parasite eggs deposited in liver and intestinal tissue (Phillips and Colley, 1978; Stadecker and Hernandez, 1998). A comparative analysis of granuloma size and composition was performed in order to explore a possible role for alternative macrophage activation in this process. In comparison to the WT liver granulomas, there was much less cell recruitment in the $IL\text{-}4R\alpha^{-/-}$ strain (Figure 1.6). This contrasted with $LysM^{Cre}IL\text{-}4R\alpha^{-/flox}$ mice that had slightly larger and somewhat less compact granulomas, as compared to the WT, but still contained significant numbers of eosinophils (Figure 1.6A). Detection of $F4/80^+$ and CD11b -positive cells by immunostaining demonstrated that macrophage recruitment was not inhibited by the myeloid-specific IL-4Rα deletion (data not shown). More importantly, the activation status of granuloma macrophages was profoundly altered in the

absence of IL-4Rα expression. Whereas WT liver granulomas were strongly positive for mannose receptor (Figure 1.6D) or Arginase I (Hesse et al., 2001; Linehan et al., 2003), there was no staining for these markers in $LysM^{Cre}IL\text{-}4R\alpha^{-/flox}$ or $IL\text{-}4R\alpha^{-/-}$ granuloma tissue. Impaired alternative macrophage activation correlated with increased classical macrophage activation, as indicated by increased nitric oxide synthase (NOS-2)-positive cells in liver granuloma tissue of both IL-4Rα mutant strains (Figure 1.6C).

Competition between NOS-2 and Arginase I for the common substrate L arginine results in the production of nitric oxide or polyamines, proline, and urea, respectively (Munder et al., 1998; Murata et al., 1998). Arginase I is an essential enzyme of the urea cycle that hydrolyzes L arginine to urea and L ornithine; ammonia detoxification is thus its primary function in the liver. L-ornithine is also a necessary metabolite for the production of proline (a critical amino acid for the synthesis of collagen), which links arginase activity to hepatic fibrosis during *S. mansoni* infection. Blocking ornithine-carbamoyltransferase (ODC)-dependent polyamine production showed a direct role for the arginase biosynthetic pathway in pathological fibrosis (Hesse et al., 2001). Since IL-4/IL-13-activated macrophages are an important source of proline, they were hypothesized to serve as important controllers of fibrosis (Hesse et al., 2001). Our results do not support this hypothesis, since there was no decrease in the hydroxyproline content of *S. mansoni* liver tissue in $LysM^{Cre}IL\text{-}4R\alpha^{-/flox}$ mice, as compared to the WT. However, there was abrogation of collagen production in the granulomas of $IL\text{-}4R\alpha^{-/-}$ mice, which agrees with a previous study of impaired granulomatous pathology in absence of IL-4Rα (Jankovic et al., 1999). Thus, although IL-13 is essential for collagen production (Chiaramonte et al., 1999), alternatively-activated macrophages are not the only proline source. A more likely cause of fibrosis during schistosomiasis are IL-13-activated fibroblasts termed stellate cells in the liver, which are well-known to be producers of collagen (Murata et al., 1998). This may explain why collagen deposition, an important component of

wound healing, was not significantly impaired in the absence of alternative macrophages and suggests that other IL-4Rα-responsive cell types compensate for Type 2-dependent egg-induced granulomatous pathology.

The presence of normal T_H2/type 2 responses in *S. mansoni*-infected $LysM^{Cre}IL\text{-}4R\alpha^{-/flox}$ mice also rules out an important role for IL-4/IL-13-activated macrophages in T_H2 cell development. This is a significant observation, as there are to reports that alternative macrophage-activation promotes Type 2 responses (Goerdt and Orfanos, 1999; Mantovani et al., 2002). Even though less pronounced than in $IL\text{-}4R\alpha^{-/-}$ mice, antigen-specific T_H1/type1 responses were present in $LysM^{Cre}IL\text{-}4R\alpha^{-/flox}$ mice, as observed in peripheral lymphoid organs and blood, indicating that proinflammatory macrophages may promote T_H1 responses (Brombacher et al., 2003). Moreover, IFN-γ and IL-6 were significantly increased in hepatic and intestinal tissue, as compared to WT controls (data not shown). These inflammatory cytokines at the site of antigen deposition correlated with enhanced NOS-2-positive cells that were in close proximity to parasite eggs (Figure 1.5C). The finding that hepatic mRNA expression of IL-10 was equivalent between WT and $LysM^{Cre}IL\text{-}4R\alpha^{-/flox}$ *S. mansoni* infected mice despite elevated proinflammatory cytokines and NOS-2 production in the latter supports the contention that IL-10 is not able to compensate for alternative macrophage activation in the absence of IL-4/IL-13 (Gordon, 2003). This was confirmed *in vitro* by the ability of IL-4 and IL-13 but not IL-10 to stimulate macrophages for Arginase activity (Figure 1.6D). These results support a recent study demonstrating that IL-10 and IL-4 induce distinct and non-overlapping gene expression patterns in macrophages (Stumpo et al., 2003).

$LysM^{Cre}IL\text{-}4R\alpha^{-/flox}$ mice were unable to survive acute schistosomiasis, and the severity of disease progression was strikingly similar to $IL\text{-}4R\alpha^{-/-}$ mice, with 100% mortality within the first two months, whereas WT littermate controls

survived the acute phase with few losses. Neutrophils served no essential role, as *in vivo* depletion did not alter the kinetics of mortality observed in IL-4Rα$^{-/-}$ and LysM^{Cre}IL-4Rα$^{-/flox}$ strains (Figure 1.4B). Thus, IL-4/IL-13-activated alternative macrophages were essential to survive acute schistosomiasis.

The observation that the presence of antigen-specific T_H2 responses, eosinophil recruitment, granuloma formation, and fibrosis (all of which were absent in IL-4Rα$^{-/-}$ mice) were not sufficient for survival of LysM^{Cre}IL-4Rα$^{-/flox}$ mice further highlights IL-4/IL-13-activated macrophages as the pivotal downstream effector cells responsible for protection conferred by T_H2 cytokines during schistosomiasis. This is an important finding, as it provides a cellular model to explain the large body of evidence for a beneficial role of T_H2 cytokines during this disease (Brunet et al., 1999; Dunne and Pearce, 1999; Fallon and Dunne, 1999; Patton et al., 2002; Pearce and MacDonald, 2002).

Since the major target organs of egg deposition during *S. mansoni* infection are the liver and intestine, experiments were conducted in order to identify factors that could be correlated with the mortality observed in both IL-4Rα$^{-/-}$ and LysM^{Cre}IL-4Rα$^{-/flox}$ mice. Examination of intestinal granuloma tissue revealed a massive infiltration in both IL-4Rα$^{-/-}$ and LysM^{Cre}IL-4Rα$^{-/flox}$ strains that was closely associated with a reduced faecal egg output (Figure 1.9). Furthermore, the significantly increased serum LPS levels in IL-4Rα$^{-/-}$ and LysM^{Cre}IL-4Rα$^{-/flox}$ mice suggested that excessive inflammation in the gut was contributing to mortality via septic shock. Indeed, there was dissemination of non-fermentative gram-negative bacilli (gut flora) in the spleen and liver of infected IL-4Rα$^{-/-}$ and LysM^{Cre}IL-4Rα$^{-/flox}$ mice (data not shown), and treatment with an antibiotic resulted in a transient extension of survival in both strains (Figure 1.10). However, anti-biotic-treated IL-4Rα$^{-/-}$ mice only showed a slight extension in survival time, most likely due to multiple organ defects, indicated by a severe atrophy of spleen and liver by 7 to 8 weeks post-infection. Extension of

survival time in IL-4Rα$^{-/-}$ and LysM^{Cre}IL-4Rα$^{-/flox}$ infected mice suggests that mortality is at least partially attributed to septic shock due to the gut pathology, a finding also seen in other helminth infections (Nakagawa et al., 2002; Schopf et al., 2002).

As SOCS-1 is upregulated in macrophages in response to LPS for regulation of NFK-β activation and proinflammatory cytokine production (Nakagawa et al., 2002), we explored the possibility that suppressors of cytokine signalling proteins (SOCS) were impaired in LysM^{Cre}IL-4Rα$^{-/flox}$ and IL-4Rα$^{-/-}$ mice. This was not the case, as similar expression levels of SOCS-1 (or SOCS-3) in intestinal homogenates from the infected mouse strains were observed (data not shown).

Traversal of eggs across the gut lining during *S. mansoni* infection is thought to contribute to the intestinal bleeding seen in schistosomiasis patients (Chatterjee et al., 2001) and *S. mansoni*-infected IL-4$^{-/-}$ mice present with hemorrhagic lesions of the gut (Brunet et al., 1997). Excretion of parasite eggs is an immune-mediated process abrogated by T cell tolerance to egg antigens (Fallon and Dunne, 1999), HIV/*S. mansoni* co-infection (Karanja et al., 1997), or experimental infection of IL-4$^{-/-}$ or IL-4/ IL-13$^{-/-}$ mice (Fallon et al., 2000). Our results extend these findings and suggest that IL-4/IL-13-responsive macrophages serve a unique role in promoting the successful passage of eggs into the faecal stream by controlling inflammation, a process that seems not to be substituted by IL-10. This was demonstrated by the presence of substantial IFN-γ and IL-10 in gut homogenates (Figure 1.8). The amounts of IL-10 in the intestine seemed to correlate with inflammation, as there were much higher levels of IL-10 in IL-4Rα mutant strains, as compared to the WT. In addition to gut pathology, enhanced hepatocellular damage was also detected in both IL-4Rα$^{-/-}$ and LysM^{Cre}IL-4Rα$^{-/flox}$ strains (Figure 1.6A).

Hepatocellular damage and endotoxemia are two morbidity factors in schistosomiasis that are more pronounced in IL-4$^{-/-}$ and IL-4/IL-13$^{-/-}$ mice (Fallon et al., 2000; La Flamme et al., 2001). Hepatocellular damage in schistosomiasis is due to dysregulated nitric oxide production and oxidative damage to liver tissue is inhibited by IL-4 (La Flamme et al., 2001). From the present work it can be concluded that in WT mice the destructive potential of *S. mansoni* egg-induced inflammation is counterbalanced by alternative macrophage activation. This allows preservation of intestinal and liver functions during acute schistosomiasis.

In summary, the comparative analysis of LysM^{Cre}IL-4R$\alpha^{-/flox}$ and IL-4R$\alpha^{-/-}$ mice provides a cell specific explanation of how IL-4/IL-13 activated alternative macrophages prevent overt pathogenesis during *S. mansoni* infection.

CHAPTER 2

Schistosoma mansoni infection in the absence of $CD4^+$-specific-IL-4Rα signalling[1]

[1]All live infection experiments conducted by M. Leeto and D. Herbert

SUMMARY

$CD4^+$ T_H2 cells are thought to be responsible for the extensive granulomatous pathology that develops around *S. mansoni* eggs lodged in host tissue. T cell-specific IL-4Rα-deficient mice (Lck^{Cre}IL-$4R\alpha^{-/flox}$) were generated to (i) study the role of IL-4 responsive T cells during infection with *S. mansoni*, and to (ii) determine the requirement of $CD4^+$ T cell specific IL-4Rα signalling for the extent of granuloma development or egg-induced fibrosis. In these studies, three groups of mice were used: IL-$4R\alpha^{-/flox}$ (WT), IL-$4R\alpha^{-/-}$, and Lck^{Cre}IL-$4R\alpha^{-/flox}$ ($CD4^+$ T cell specific IL-$4R\alpha^{-/-}$) mice. In the first set of experiments, we percutaneously infected mice with 75 *S. mansoni* cercariae and analyzed the immune response. In the second set of experiments, synchronized lung granulomas were induced by injecting 5000 live eggs into mice that were sensitized to *S. mansoni* eggs. These studies demonstrate that Lck^{Cre}IL-$4R\alpha^{-/flox}$ mice survived acute schistosomiasis despite excessive granuloma IFN-γ/NOS-2 production and severe liver pathology. Resistance was associated with alternatively activated macrophages (AAMϕ), $CD4^+CD25^+$ cells, increased TGF-β and up-regulated Foxp3 expression in the liver and intestine. Paradoxically, IL-$4R\alpha^{-/-}$ granulomas were devoid of these components and mice experienced 100% mortality despite significantly elevated IL-10 levels in ova-containing organs. Examination of mice following egg embolization showed that liver granulomas were slightly exacerbated by the $CD4^+$ T cell specific IL-4Rα deletion in comparison to WT. Similarly, lung granulomas in Lck^{Cre}IL-$4R\alpha^{-/flox}$ mice were significantly exacerbated 21 days after-infection compared to WT controls. Interestingly, Type 1 responses did not inhibit fibrosis in liver or lung granulomas, with CD^+ T cell specific IL-4Rα-deficient mice being slightly more fibrotic than wild-type mice. IL-13 and TGF-β secretion were both significantly elevated in WT and $CD4^+$ T cell specific IL-4Rα-deficient liver granuloma cells. In the lung, a strong increase of TGF-β production was also observed in T cell specific IL-4Rα-deficient mice. Overall, these studies demonstrate that CD4 specific IL-4Rα signalling during natural *S.*

mansoni infection is protective for the liver during acute disease and controls the extent of granulomatous pathology in different tissue compartments.

RESULTS

2.1 Alternative macrophage activation is maintained despite an impaired T_H2/elevated T_H1 phenotype in Lck^{Cre}IL-4R$\alpha^{-/flox}$ mice

The *S. mansoni* egg-specific response in mice harbouring a natural infection is characterized by a profound induction of T_H2 cytokines after 7-8 weeks. Splenocyte responses in IL-4R$\alpha^{-/flox}$, IL-4R$\alpha^{-/-}$, and Lck^{Cre}IL-4R$\alpha^{-/flox}$ mice were analyzed 7.5 weeks post-infection to determine if $CD4^+$ T cell-specific deletion of IL-4Rα signalling would impair T_H2 cytokine production. Stimulation of cells with the T cell mitogen anti-CD3 revealed severely impaired IL-4 and IL-13 responses from both IL-4Rα mutant strains that were highly significant when compared to WT mice (Figure 2.1A&C). Also, significantly higher IFN-γ production was detected in both IL-4Rα mutant strains, as compared to the WT.

WT splenocytes secreted high levels of the immunosuppressive cytokine IL-10, which is an essential component for survival of mice during *S. mansoni* infection. Conversely, IL-10 production was severely abrogated in IL-4R$\alpha^{-/-}$ and Lck^{Cre}IL-4R$\alpha^{-/flox}$ cultures, with the lowest amounts produced in the latter strain (Figure 2.1D). Experiments that analyzed cytokine production from anti-CD3 stimulated mesenteric lymph nodes revealed a nearly identical cytokine secretion profile as shown here for splenocytes (data not shown). These data demonstrate that T cell-specific deletion of IL-4Rα signalling led to an impaired T_H2 response, reduced IL-10, and an enhanced IFN-γ response upon polyclonal stimulation of peripheral lymphoid cells.

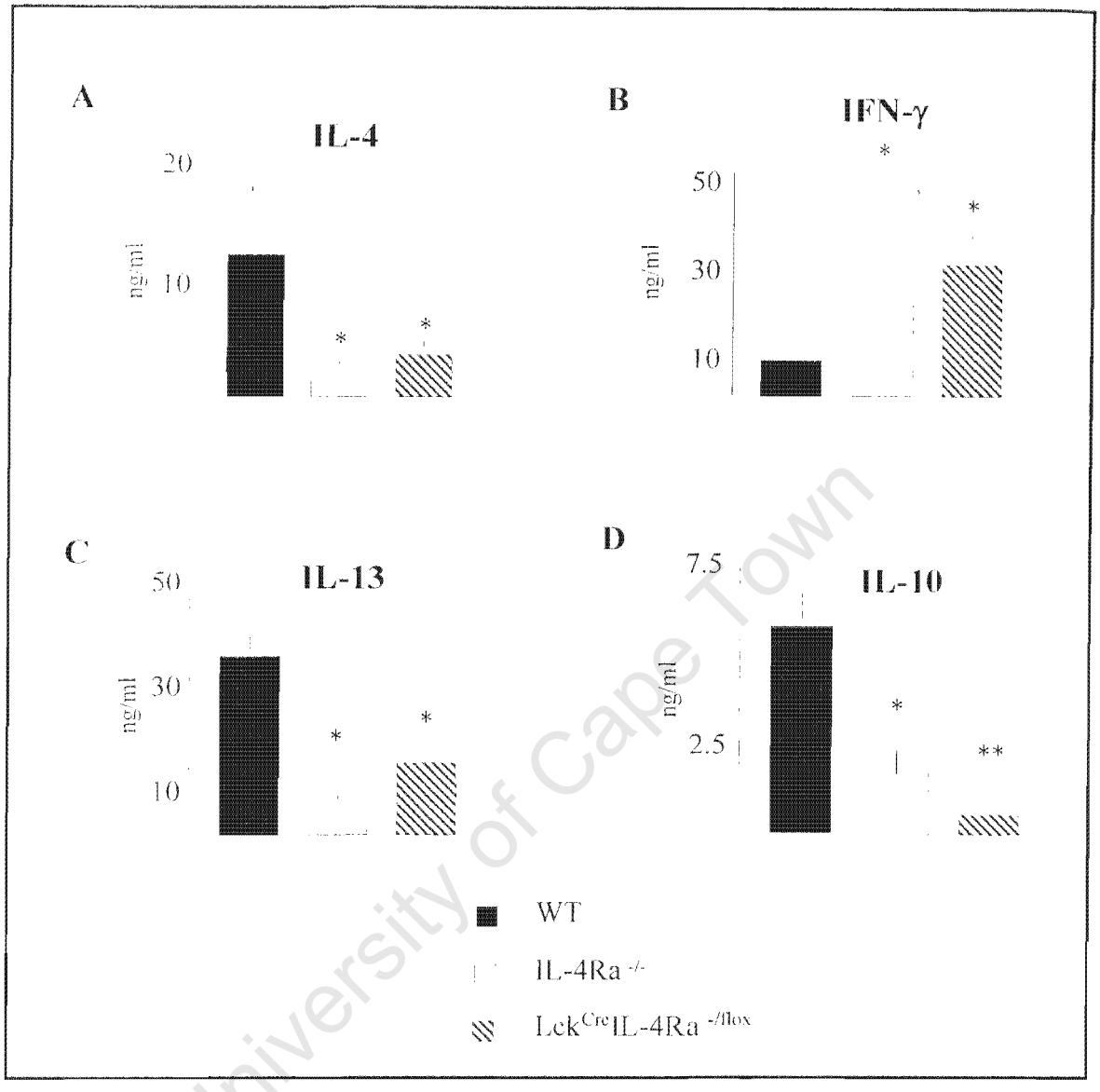

Figure 2.1

Cytokine production in spleens cells of infected mice

Splenocytes from acutely infected mice were stimulated with anti-CD3 mAb (20μg/ml) for 72 hours and measurement of IL-4, IL-13, IL-10 and IFN-γ levels in supernatants determined by ELISA. Data shown are mean ± SD from five individual mice and are representative of three independent experiments. Statistical significance was determined by one way ANOVA with (*) =$p<0.05$ and (**) =$p<0.01$, as compared to WT value.

In order to determine whether T cell-specific IL-4Rα deletion skewed the phenotype of macrophages towards classical or alternative activation, respectively; NOS-2 and arginase activity was quantified by utilizing anti-CD3 stimulated splenocytes. The elevated nitrite levels in the supernatants of IL-4Rα$^{-/-}$ and Lck^{Cre}IL-4Rα$^{-/flox}$ splenocytes was an expected result since NOS-2 is an IFN-γ-activated gene (Figure 2.2A). However, Figure 2.2B reveals that Lck^{Cre}IL-4Rα$^{-/flox}$ splenocytes also contained significant arginase activity, indicating that although significantly decreased amounts of IL-4 and IL-13 were present in these cultures, they were sufficient to drive alternative macrophage activation. On the contrary IL-4Rα$^{-/-}$ splenocytes were completely devoid of Arginase activity (Figure 2.2B).

Profiles of antibody production were assessed in sera of infected mice using SEA-specific ELISA. Measurement of the SEA-specific antibody response revealed a significant rise of IgG2b in Lck^{Cre}IL-4Rα$^{-/flox}$ sera, whereas levels of IgG1 were not different when compared to the WT (Figure 2.3A&B). Increased levels of antigen-specific IgG2b, most likely due to IFN-γ driven T cell help, since polyclonal IgE production was equivalent between Lck^{Cre}IL-4Rα$^{-/flox}$ and WT mice (Figure 2.3C), thus confirming intact B cell IL-4Rα signaling. These data indicate that T cell-specific deletion of IL-4Rα skews antigen-specific antibody responses towards Type 1, but sufficient levels of IL-4/IL-13 remain that are capable of inducing IgE production and arginase activity in peripheral lymphoid tissue.

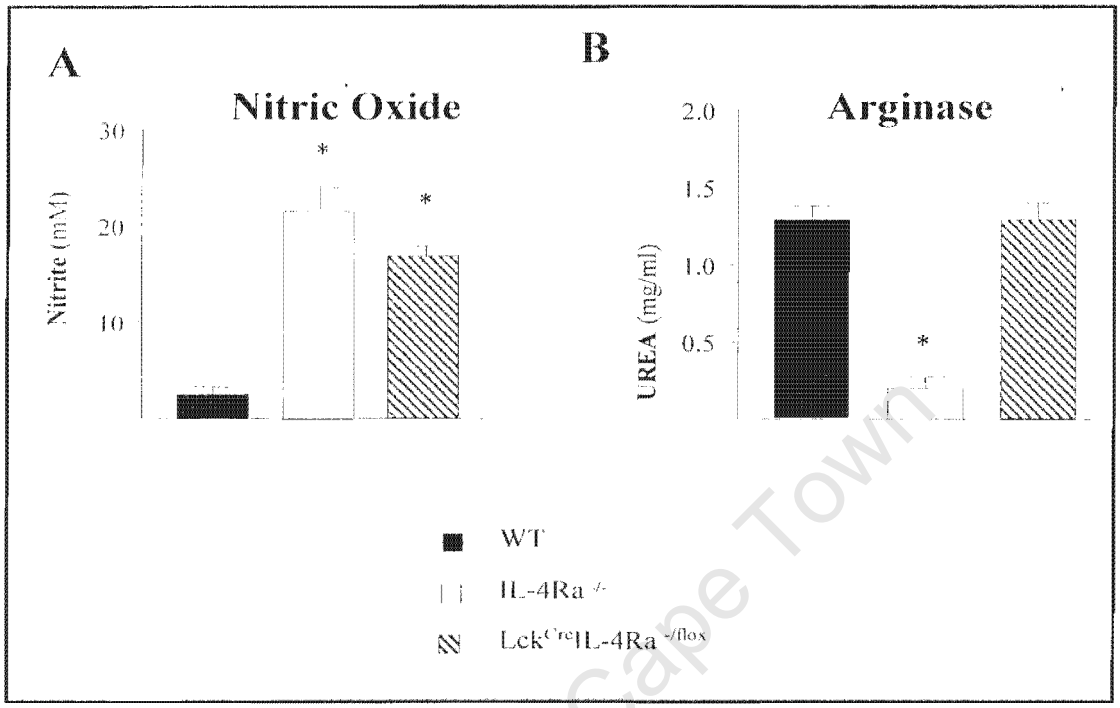

Figure 2.2

Nitric oxide and arginase production

Supernatants from anti-CD3-stimulated splenocytes were subjected to the Griess reaction to measure nitrite levels (Panel A). Spleen cell lysates from infected mice were analyzed for arginase activity as expressed by levels of Urea (Panel B). Experiments were performed twice with similar results. (*) =$p<0.05$ by ANOVA compared to WT.

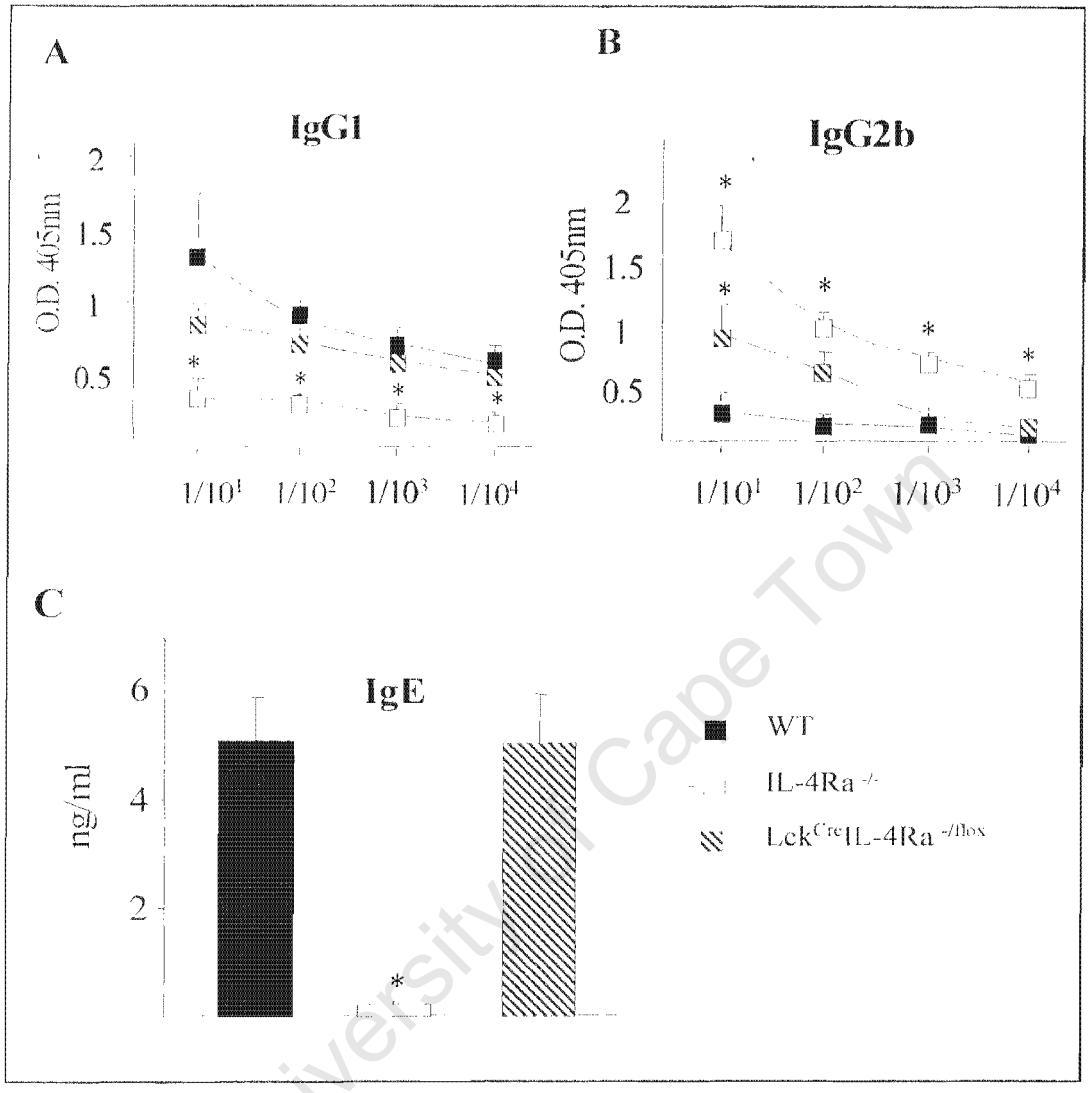

Figure 2.3

SEA-specific antibody production in S. mansoni infected mice

SEA-specific IgG1 and IgG2b levels in pooled serum from acutely-infected mice were measured by ELISA (Panel A and B). Panel C shows serum levels of total IgE in pooled serum from infected mice as determined by ELISA. Data shown are mean ± SD from triplicate wells and are representative of three independent experiments. Statistical significance was determined by one way ANOVA with (*) =$p<0.05$, as compared to WT value.

2.2 *S. mansoni*-infected $Lck^{Cre}IL\text{-}4R\alpha^{-/flox}$ mice develop augmented granulomatous pathology, elevated NOS-2, and severe liver damage

Schistosoma mansoni egg accumulation in hepatic tissue during human infections has been reported as a causative agent of portal hypertension, venous shunting, and potentially liver failure. To assess the extent of hepatocellular damage, serum levels of aspartate transaminase (AST) were measured as an indication of overall morbidity. Mice infected with 70 cercariae were bled at 7.5 weeks post-infection and measurement of AST performed. $Lck^{Cre}IL\text{-}4R\alpha^{-/flox}$ mice produced 8-fold higher amounts of this enzyme than littermate controls ($p \leq 0.001$) and 2-fold more than $IL\text{-}4R\alpha^{-/-}$ mice ($p \leq 0.05$) (Figure 2.4A). NOS-2 expression followed the same trend, with hepatic mRNA transcripts in $Lck^{Cre}IL\text{-}4R\alpha^{-/flox}$ mice yielding the most pronounced response, as compared to $IL\text{-}4R\alpha^{-/-}$ ($P<0.05$) and WT ($P<0.001$) liver tissue (Figure 2.4B). These data support the conclusion that a causal link exists between NOS-2 activity and hepatocellular damage during acute schistosomiasis.

Liver granuloma size and cellular composition was compared among groups in order to further characterize enhanced liver damage in T cell specific IL-4Rα deficient mice. Hepatic granulomas that developed in $Lck^{Cre}IL\text{-}4R\alpha^{-/flox}$ mice ($127 \pm 23\mu m^2 \times 10^{-3}$) were significantly larger than WT ($54 \pm 19\mu m^2 \times 10^{-3}$) ($p<0.05$) and $IL\text{-}4R\alpha^{-/-}$ ($11 \pm 14\mu m^2 \times 10^{-3}$) lesions ($p<0.001$) (Figure 2.5A and Table 1). Macrophage composition, as determined by immunofluorescence staining for $F4/80^+$ cells, did not reveal any obvious differences between WT and $Lck^{Cre}IL\text{-}4R\alpha^{-/flox}$ granuloma tissue and although $IL\text{-}4R\alpha^{-/-}$ granulomas were significantly smaller, there was an equivalent proportion of F4/80+ cells present (Figure 2.5B). There was also no difference in the mean number of eosinophils per granuloma of WT and $Lck^{Cre}IL\text{-}4R\alpha^{-/flox}$ tissue, whereas significantly fewer eosinophils were found in $IL\text{-}4R\alpha^{-/-}$ hepatic granulomas (Table 1).

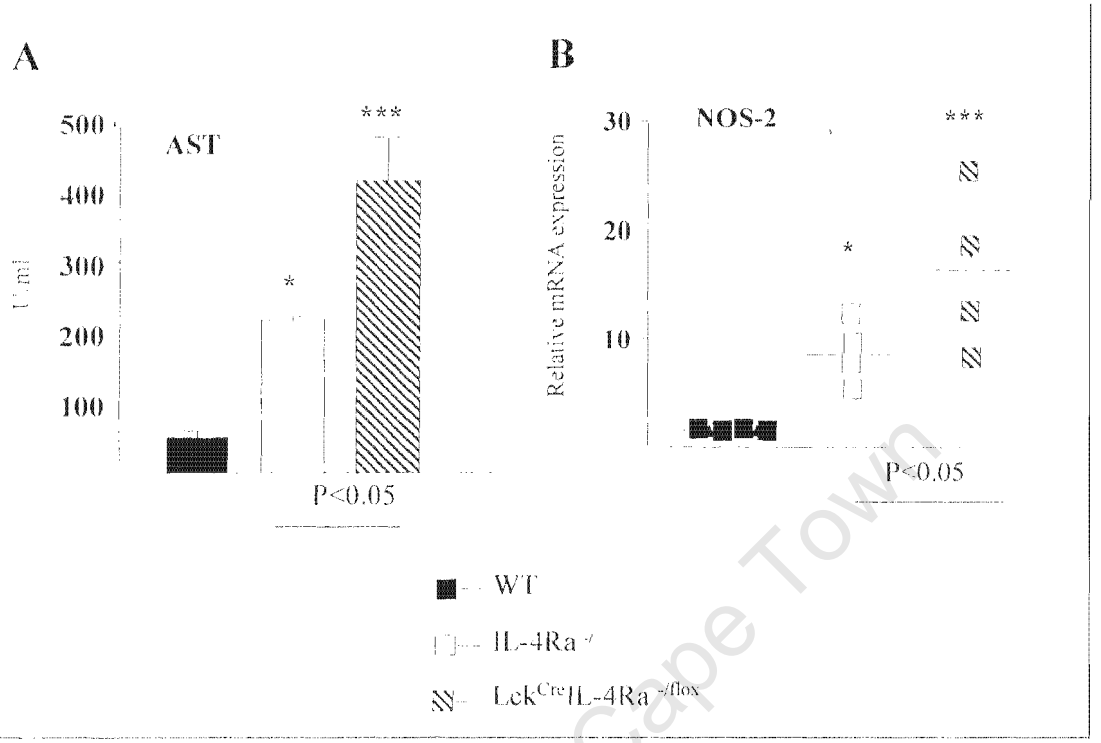

Figure 2.4

Hepatocellular damage in schistosome- infected mice

Mice were acutely infected with 75 *S. mansoni* cercariae and serum levels of aspartate transaminase, an indicator of hepatocellular damage determined. Data expressed as mean ± SD of five individual samples per group. Data are representative of three independent experiments. (*) =p<0.05, (***) = p<0.001 by ANOVA compared to WT

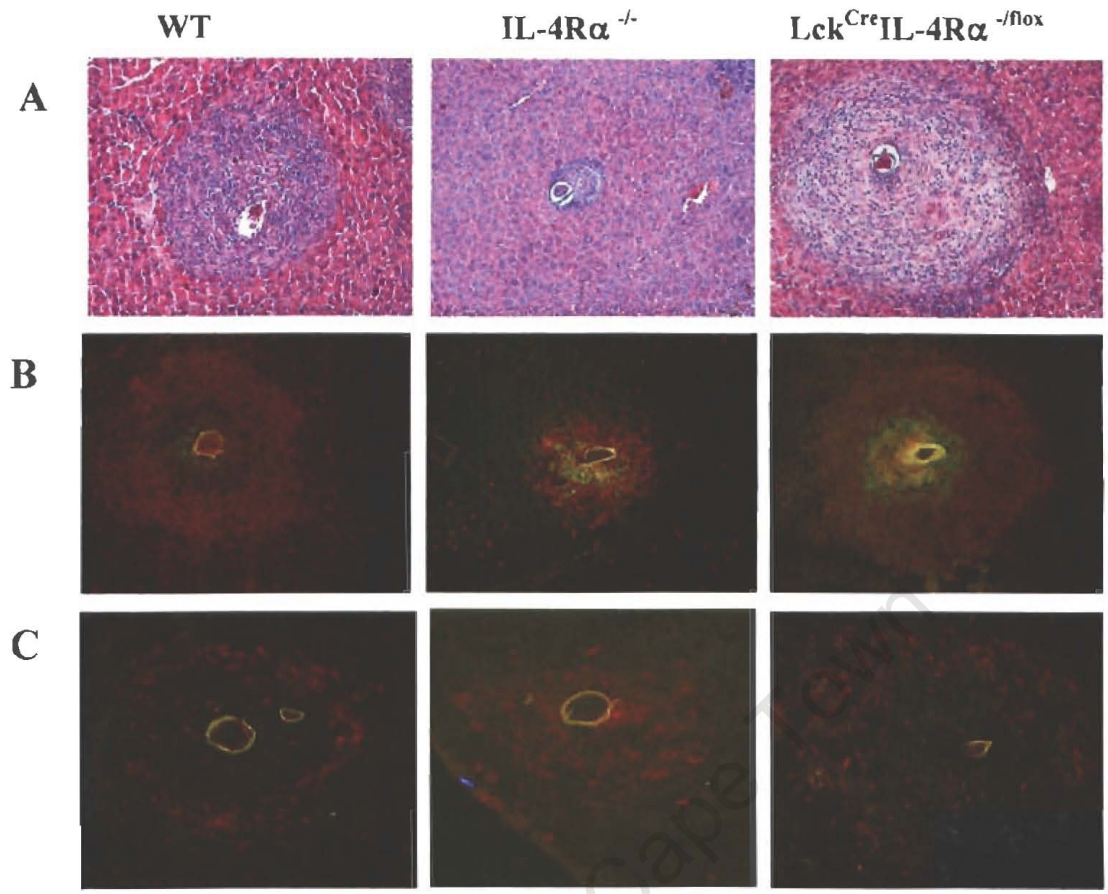

Figure 5
Immunohistochemical staining of liver tissue samples from infected mice.

A) Hematoxylin and eosin staining of formalin fixed liver tissue showing granulomas of the indicated strains. (Magnification 200x)

B) Immunoflorescence staining was performed on frozen sections of liver granulomas from the indicated strains. F4/80 (red) and NOS-2 (green) (Magnification 200x)

C) Immunoflorescence staining for $CD3^+$ cells on frozen sections of liver granulomas from the indicated strains. (Magnification 200x)

Table I

Comparison of granuloma sizes, hydroxyproline, granuloma eosinophils and liver egg burden in acutely infected *S. mansoni* mice at week 7.5 post-infection. Data shown represent the mean ± SD. Statistical significance was determined by one way ANOVA with (*) =$p<0.05$ and (***) = $p<0.001$, as compared to the WT value

	IL-4Rα$^{-/flox}$	IL-4Rα$^{-/-}$	Lck^{Cre}IL-4Rα$^{-/flox}$
Granuloma area (μm^{2}x10^{-3})	54 ± 19	21 ± 11*	127 ± 23
Hydroxyproline (μM/10^4 eggs)	6.18 ± 0.31	1.9 ± 0.72 *	8.95 ± 0.49
Eosinophils	172 ± 25	16 ± 11***	146 ± 21
Eggs/liver (x10^3)	20 ± 4	16 ± 8	21 ± 5

Immunofluorescence staining for $CD3^+$ cells revealed a clear circumoval distribution of T cells around the periphery of eggs in WT liver tissue, whereas IL-4Rα$^{-/-}$ granulomas contained seemingly more T cells closely apposed to parasite ova (Figure 2.5C). Curiously, there was a dramatic increase of $CD3^+$ cells present throughout liver granuloma tissue of Lck^{Cre}IL-4Rα$^{-/flox}$ mice.

Ex vivo analysis of dispersed liver granuloma cells was performed to determine whether the impaired T_H2/enhanced T_H1 cytokine profile observed for spleen and mesenteric lymph nodes was the same as within the local antigenic microenvironment. In contrast to peripheral responses, Lck^{Cre}IL-4Rα$^{-/flox}$ granuloma cells produced significant amounts of IL-4, IL-13, and IL-10 that were equivalent to WT levels and significantly higher than IL-4Rα$^{-/-}$ (Figures 2.6A-C). Interestingly, IFN-γ production by Lck^{Cre}IL-4Rα$^{-/flox}$ granuloma cells was more similar to IL-4Rα$^{-/-}$ cultures, both of which were significantly elevated over amounts produced by the WT ($p<0.01$) (Figure 2.6D). These data demonstrate that IFN-γ producers expand *in vivo* when IL-4Rα is deleted T cell-specifically, or as a null mutation, whereas secretion of IL-4, IL-13, and IL-10 is up-regulated in the parasite egg microenvironment independently of T cell specific IL-4Rα expression.

2.3 Asymptomatic gut pathology and alternative macrophage activation are predictors of survival during acute schistosomiasis

Naïve WT, IL-4Rα$^{-/-}$, and Lck^{Cre}IL-4Rα$^{-/-}$ mice were infected percutaneously with 70-80 cercariae (high dose) and monitored weekly for weight loss and mortality to determine if T cell-specific expression of IL-4Rα was critical for survival during acute disease. Remarkably, 4 independent experiments showed that greater than 95% of Lck^{Cre}IL-4Rα$^{-/flox}$ mice infected with a high dose (75 cercariae) survived beyond 11 weeks post infection (Figure 2.7), whereas WT littermates showed only a 60-50% survival rate at this dose.

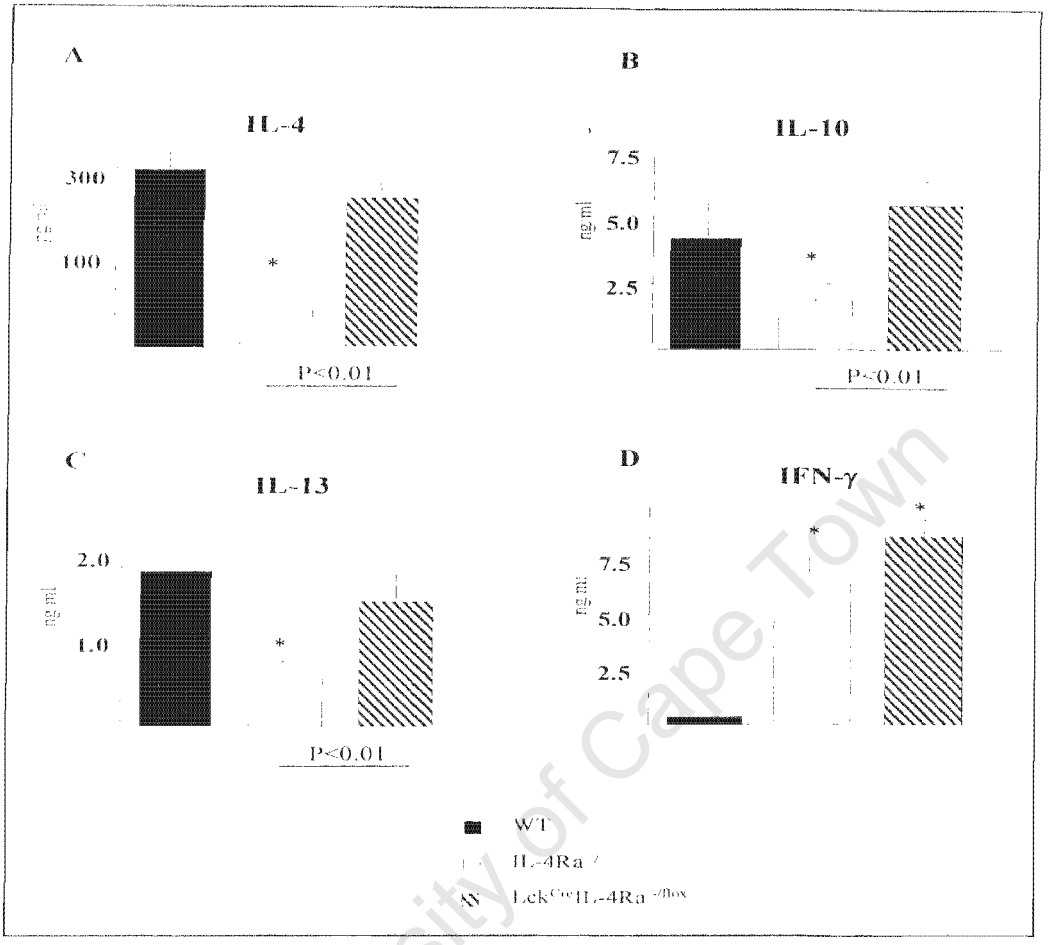

Figure 2.6

Cytokine production in liver granuloma cells

Isolated liver granuloma cells of WT, IL-4Rα$^{-/-}$, and Lck^{Cre}IL-4Rα$^{-/flox}$ mice at 7.5 weeks post-infection were analyzed for cytokine production. Levels of IL-4, IL-10, IL-13, and IFN-γ measured in supernatants after stimulation with anti-CD3 (20μg/ml) for 48 hrs. Data shown are the mean ±SD of five mice per group. Significance in all panels was determined by one way ANOVA with (*) =$p<0.05$ compared to the WT value. Any significant differences between IL-4Rα$^{-/-}$ and Lck^{Cre}IL-4Rα$^{-/flox}$ mice are shown on the figure. Experiment performed three times with similar results.

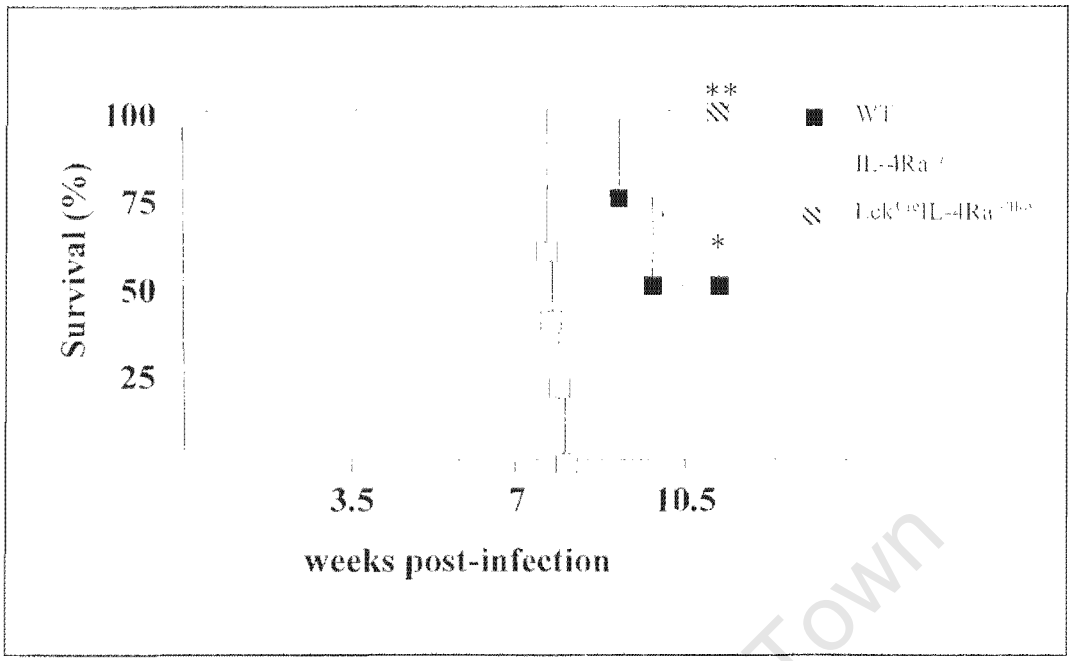

Figure 2.7

Survival of S. mansoni- infected mice

WT, IL-4Rα$^{-/-}$, and Lek^{Cre}IL-4Rα$^{-/flox}$ mice were infected with 70 cercariae and monitored for survival over eleven weeks. Significance was determined by one way ANOVA with * =$p<0.05$ and ** =$p<0.01$, as compared to the IL-4Rα$^{-/-}$ group. (n=5)

Strikingly, IL-4Rα$^{-/-}$ mice were highly susceptible to high dose *S. mansoni* infection, showing 100% mortality by 8 weeks post-infection (Figure 2.7).

Accordingly, WT and T cell-specific IL-4Rα$^{-/-}$ strains lost little weight over the course of infection (data not shown), whereas IL-4Rα$^{-/-}$ animals experienced severe cachexia, peri-orbital oedema, hunched postures, and ruffled coats. Macroscopic examination of IL-4Rα$^{-/-}$ mice revealed severe multi-organ pathology that involved liver degeneration, spleen atrophy, and markedly swollen small intestine that was hemorrhagic and oedematous, affecting the distal jejunum and entire ileum (Figure 2.8). This type of pathology was never observed in WT or Lck^{Cre}IL-4Rα$^{-/flox}$ infected mice and even post-mortem analysis of WT animals that died during the acute phase revealed more of a colitis-type pathology and bloody stool (unpublished observations). Hepatosplenomegaly was a consistent observation of acutely-infected WT and Lck^{Cre}IL-4Rα$^{-/flox}$ mice, with little obvious gut pathology (Figure 2.8).

There was a high rate of egg excretion in both WT and Lck^{Cre}IL-4Rα$^{-/flox}$ strains, with a slightly higher number of eggs excreted in the latter strain. In contrast, IL-4Rα$^{-/-}$ mice showed a severe abrogation of faecal egg numbers six weeks (data not shown) and 7 weeks post-infection (Figure 2.9A). Indeed, the significant increase of serum endotoxin levels in IL-4Rα$^{-/-}$ mice (Figure 2.4), supports a working hypothesis that egg accumulation in gut tissue leads to intestinal barrier dysfunction. Moreover, quantitation of intestinal mRNA transcripts for Arginase 1, an IL-4/IL-13 dependent gene specific for macrophages and dendritic cells, showed up-regulated expression in both WT and Lck^{Cre}IL-4Rα$^{-/flox}$ mice, but virtually undetectable levels in IL-4Rα$^{-/-}$ gut tissue (Figure 2.9B). Together, these data indicate that an absence of AAMϕ is associated with defective parasite egg excretion and lethal intestinal inflammation.

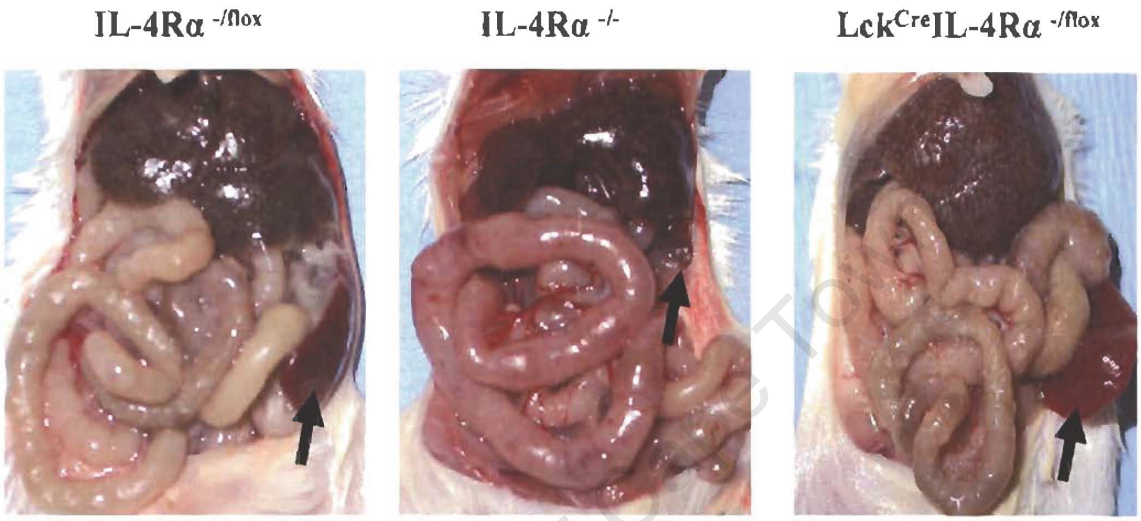

Figure 8

Post-mortem photographs of mice sacrificed at 7.5 weeks post-infection.

Note marked hepatosplenic atrophy in the IL-4Rα$^{-/-}$ group as compared to the other strains (arrowheads), in addition to the marked hemorrhagic distension of the small intestine. A representative image from each group is shown.

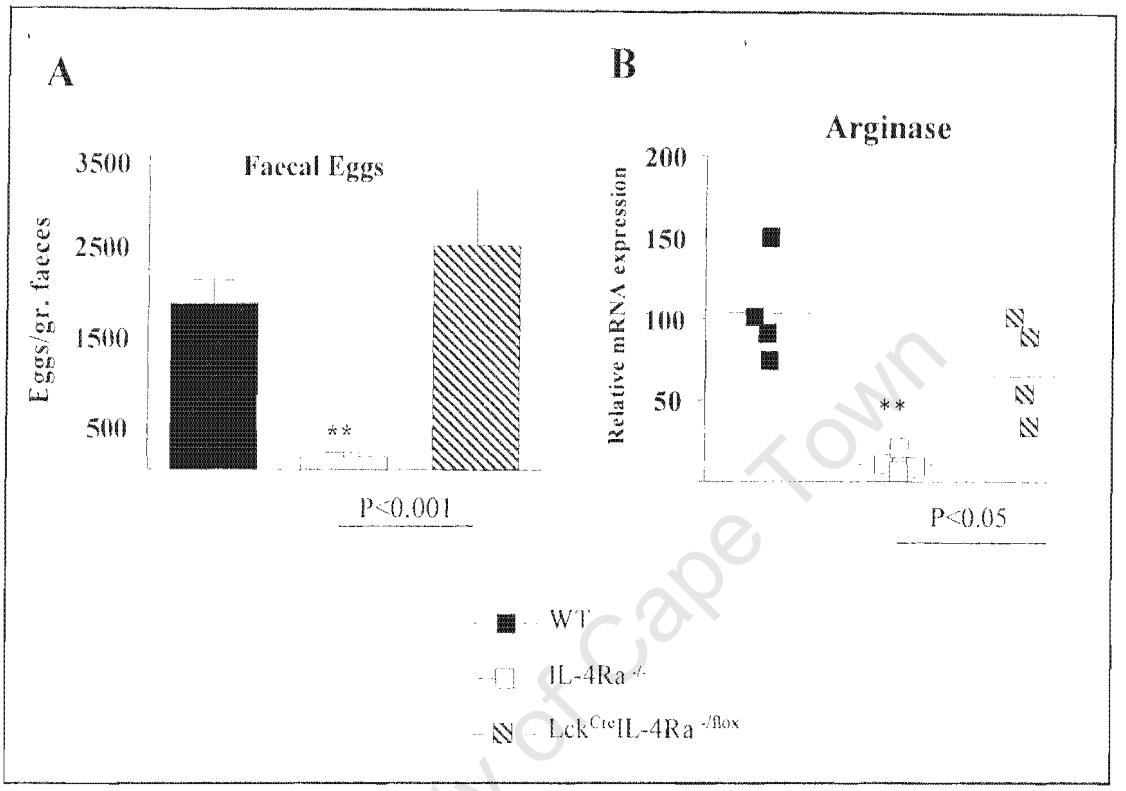

Figure 2.9
Faecal egg output and arginase activity

A) Quantitation of *S. mansoni* egg excretion at 7 weeks post-infection. Data are expressed as the mean ± SD of ova counted per gram of faecal matter. Data represent three experiments performed with similar results.

B) mRNA levels of Arginase-1 in gut tissue at 7 weeks post-infection, determined by real-time PCR, normalized to beta-2 microglobulin and expressed as fold increase over non-infected WT mice. Each symbol represents an individual mouse liver sample. Data represent two independent experiments with similar results.

2.4 Selective deficit of the $CD4^+CD25^+$ cell population in granuloma tissue of IL-4Rα$^{-/-}$ mice leads to increased inflammation in the presence of IL-10

IL-4 and IL-10 both promote host survival during murine schistosomiasis through antagonism of egg-driven TNF-α and IFN-γ production. Experiments were performed to ascertain whether the differences in organ immunopathology between IL-4Rα$^{-/-}$ vs. WT and Lck^{Cre}IL-4Rα$^{-/flox}$ mice reflected distinctive patterns of cytokine secretion. At 7.5 weeks post-infection, crude organ homogenates of liver and intestinal tissue were prepared, adjusted for equal total protein content, and analyzed for cytokine levels by ELISA. Profoundly elevated amounts of TNF and IFN-γ were detected in IL-4Rα$^{-/-}$ liver and intestinal tissue, as compared to levels in WT and Lck^{Cre}IL-4Rα$^{-/flox}$ samples (Fig. 2.10A-B). Although IFN-γ levels within Lck^{Cre}IL-4Rα$^{-/flox}$ intestinal tissue were higher than the WT ($p<0.05$), this amount was always significantly lower than the IL-4Rα$^{-/-}$ strain ($p<0.01$). Surprisingly, analysis of the same organ homogenates revealed significantly increased IL-10 levels in both liver and intestinal tissue of IL-4Rα$^{-/-}$ mice, as compared to the other two strains (Figure 2.10C).

These results prompted a closer investigation into the cellular composition of ova-containing tissues with a particular interest placed upon regulatory T cells, as identified by $CD4^+CD25^+$ expression. Comparison of the $CD4^+CD25^+$ populations in various organ compartments among the three strains at 7 weeks post-infection revealed a striking defect of $CD4^+CD25^+$ cells in granuloma containing organs of IL-4Rα$^{-/-}$ mice. The results show that IL-4Rα null mutants had a 6-fold decrease in liver $CD4^+CD25^+$ cells and nearly 4-fold decrease in gut $CD4^+CD25^+$ cells when compared to WT mice (Figure 2.11C-D). The relative absence of $CD4^+CD25^+$ cells in IL-4Rα granuloma cell suspensions was not an overall defect in $CD4^+$ T cell numbers or the ability of

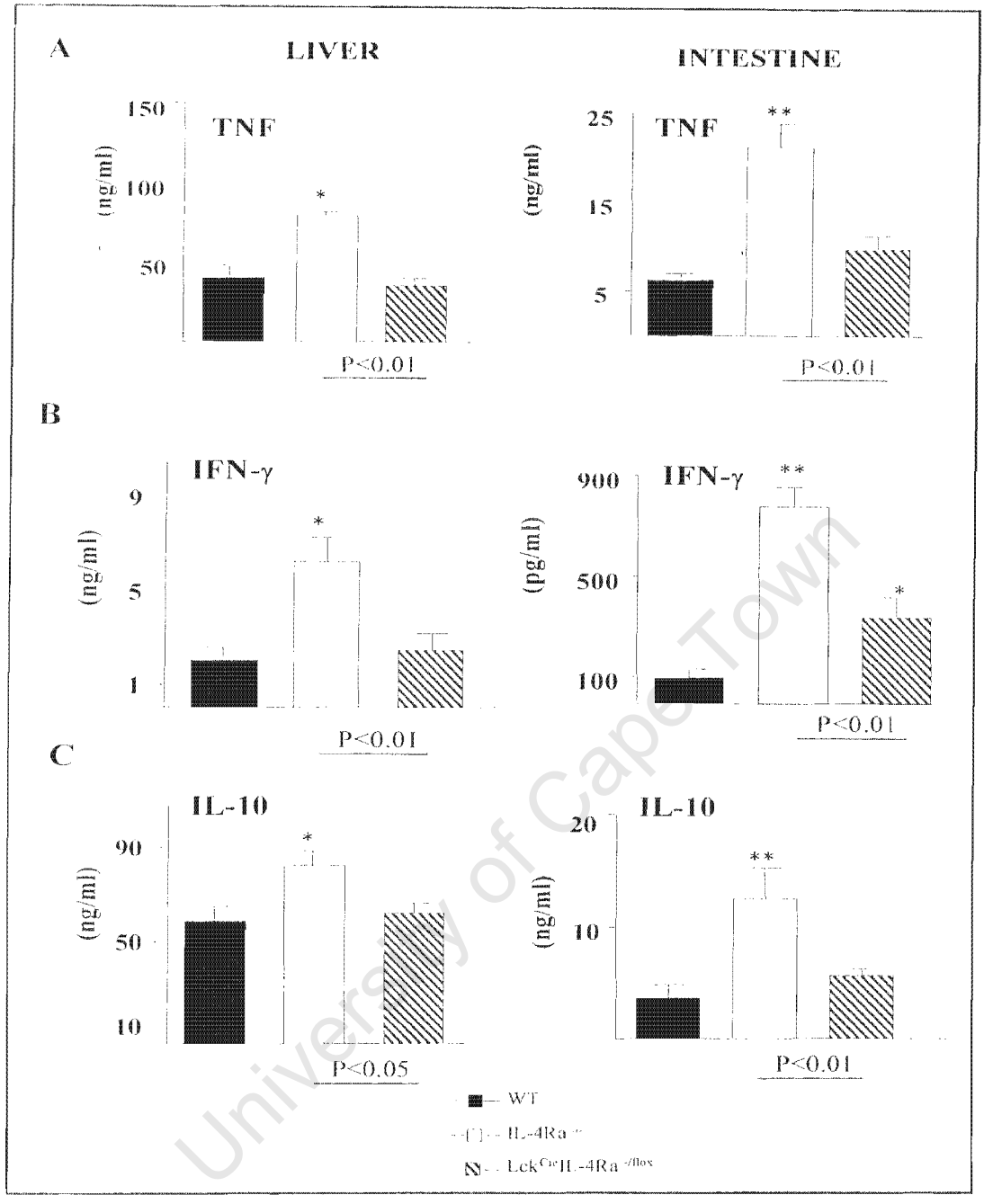

Figure 2.10

Pro-inflammatory cytokine production in mouse tissue homogenates

5% (wt/vol) suspensions of tissue homogenates from infected mice were analyzed for cytokine production. Data are from four experiments and are the mean ±SD of 5-7 individual samples per group. Significance in all panels was determined by one way ANOVA with (*) =$p<0.05$ and (**) =$p<0.01$, as compared to the WT value. Any significant differences between IL-4Rα$^{-/-}$ and Lck^{Cre}IL-4Rα$^{-/flox}$ mice are shown on the figure.

these mice to generate the $CD4^+CD25^+$ population, as there was an increased percentage of these cells within the peripheral blood and mesenteric lymph node organs (Figure 2.11A-B). Furthermore, this organ-specific defect was not dependent upon T cell-specific expression of IL-4Rα as there were equivalent percentages of $CD4^+CD25^+$ cells in the liver and intestines of Lck^{Cre}IL-$4R\alpha^{-/flox}$ mice when compared to the WT (Figure 2.11C-D).

Nonetheless, these data indicate that (1) in IL-4Rα-deficient mice there is specific abrogation of the $CD4^+CD25^+$ cell population in the antigenic microenvironment, but not in the peripheral circulation (2) increased IL-10 levels in ova-containing tissue did not reflect the presence of $CD4^+CD25^+$ cells and (3) T cell-specific IL-4Rα expression was not required for $CD4^+CD25^+$ presence in liver and intestinal organs.

2.5 Foxp3 expression and TGF-β production in granuloma tissue is controlled by T cell-independent IL-4Rα expression

Experiments were performed to determine whether lethal egg-driven inflammation evident in IL-$4R\alpha^{-/-}$ mice reflected an impaired presence of regulatory T cells, as determined by Foxp3 expression. TGF-β producing Treg have shown efficacy in protection against various inflammatory diseases and we hypothesized that a reciprocal pattern of Foxp3 expression and/or TGF-β production would exist between the periphery and microenvironment of *S. mansoni* egg deposition. Indeed, TGF-β levels in serum of mice 7.5 weeks post-infection revealed significantly elevated amounts of this cytokine in both IL-$4R\alpha^{-/-}$ and Lck^{Cre}IL-$4R\alpha^{-/flox}$ mice, as compared to the WT (Figure 2.12A). Also, anti-CD3 stimulation of splenocytes from infected animals revealed that Lck^{Cre}IL-$4R\alpha^{-/flox}$ cells secreted the most TGF-β compared to both WT and IL-$4R\alpha^{-/-}$ groups ($p<0.05$), with amounts produced by IL-$4R\alpha^{-/-}$ splenocytes slightly elevated over WT levels (Figure 2.12B).

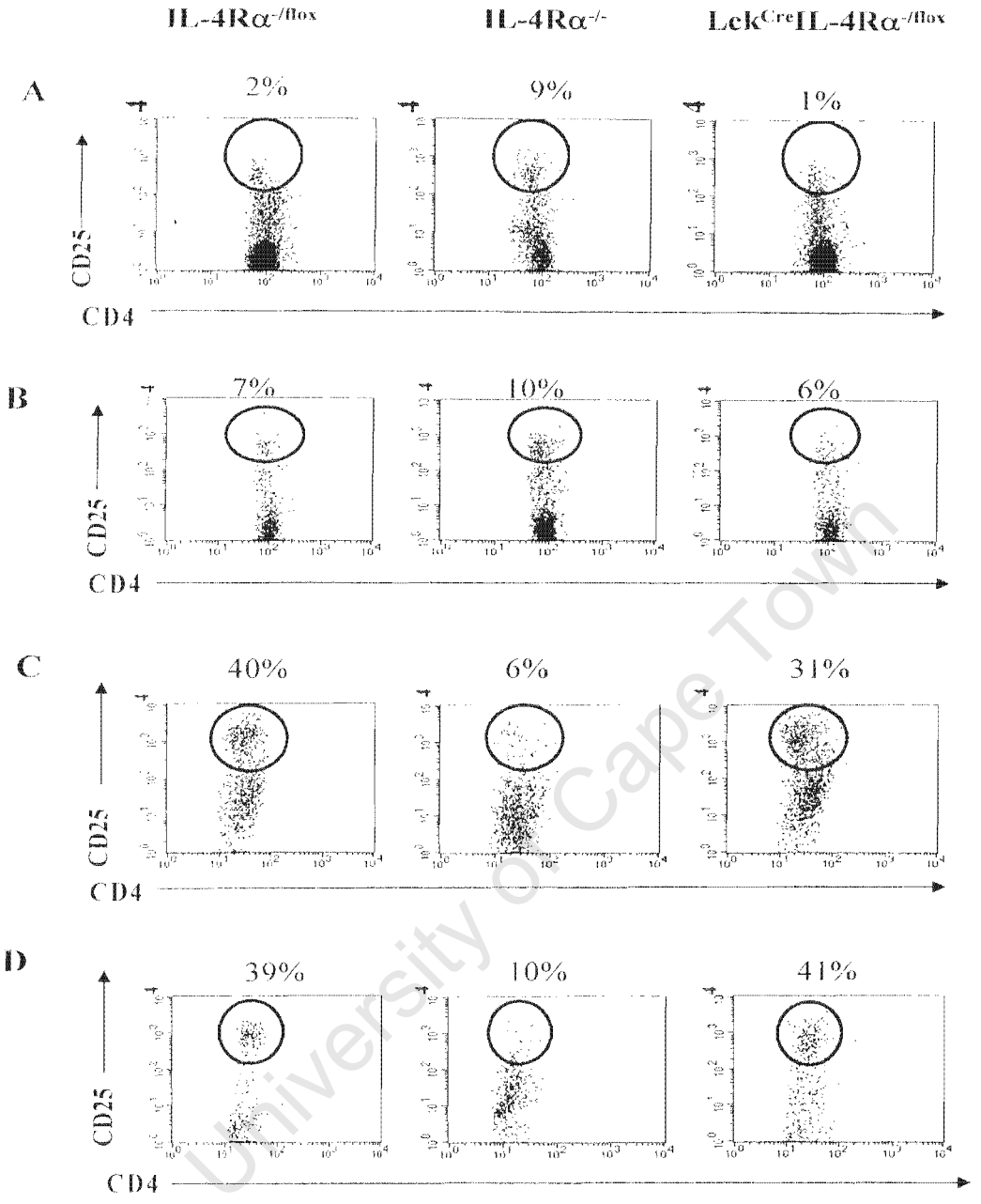

Figure 2.11

$CD4^+CD25^+$ T-cell populations in infected mice

Pooled samples from *S. mansoni*-infected mice were analyzed for the presence of $CD4^+CD25^+$ cell populations in peripheral blood (Panel A), mesenteric lymph nodes (Panel B), dispersed liver granuloma cells (Panel C) and in dispersed intestinal granuloma cells (Panel D). Numerical value represents the percentage of $CD4^+CD25^+$ cells within an initial $CD3^+CD4^+$ gate. Data are representative of two independent experiments with similar results.

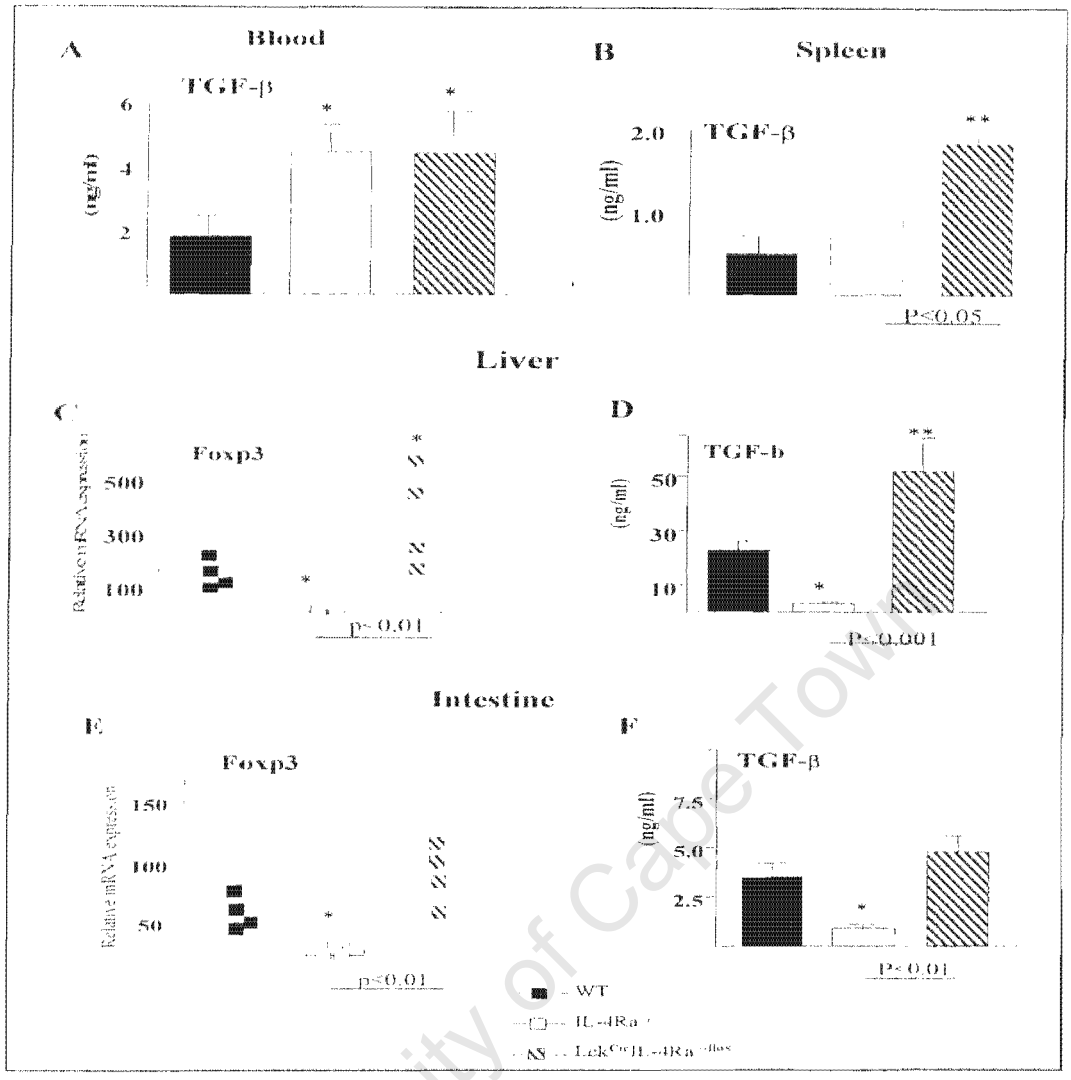

Figure 2.12

TGF-β production and Foxp-3 expression

A) Serum levels of TGF-β as determined by ELISA.

B) Splenocyte production of TGF-β upon stimulation with anti-CD3

C) mRNA levels of Foxp-3 in liver tissue analyzed at 7 weeks post-infection determined by real-time PCR

D) Levels of TGF-β in liver homogenates

E) mRNA levels of Foxp-3 in gut tissue analyzed at 7 weeks post-infection determined by real-time PCR.

F) Levels of TGF-β in intestine homogenates. Data shown are the mean ± SD of 4-5 mice per group. Experiments performed three times with similar results.

In contrast, there was a striking decrease in tissue levels of TGF-β as well as Foxp-3 expression in the liver and intestinal tissue of IL-4Rα$^{-/-}$ mice that bore a remarkably similar pattern to the CD4^{+}CD25^{+} FACS results (Figure 2.12C-D). Curiously, there was a highly significant increase in TGF-β and Foxp-3 levels in liver and intestines of Lck^{Cre}IL-4Rα$^{-/flox}$ mice compared to WT or IL-4Rα$^{-/-}$ animals. This may have reflected the necessity to counteract significantly elevated levels of IFN-γ and NOS-2 in granulomas of this strain (Figure 2.4B, 2.6D) Overall, these data strongly support a hypothesis that IL-4Rα controls the outcome of acute schistosomiasis through its control of TGF-β, Treg, and AAMϕ populations independently of T cell-specific expression and extends the current understanding of Treg behaviour *in vivo* during murine schistosomiasis.

2.6 CD4^{+} T cell independent IL-4Rα expression is required for lung granuloma development.

To address the requirement for CD4^{+} T cell IL-4Rα signalling in egg-induced lung granuloma formation and fibrosis, we compared granuloma size and cellular composition among WT, IL-4Rα$^{-/-}$, and Lck^{Cre}IL-4Rα$^{-/flox}$ mice. To induce synchronous pulmonary granulomas, 12-16 mice per group were intraperitoneally sensitized with 5000 eggs and 14 days later injected with 5000 live parasite eggs intravenously. Mice were killed on day 7, 14, 21, and 28 for analyses.

Histological examination of granuloma development showed no significant differences in granuloma sizes among the three groups during the first two weeks after egg-challenge (Figure 2.13 and Figure 2.14). On the contrary there was a significant difference in granuloma sizes at day 21 post-challenge between the IL-4Rα$^{-/-}$ ($32\mu m^2x10^{-3} \pm 12$) and the two other groups of mice with the Lck^{Cre}IL-4Rα$^{-/flox}$ mice ($122\mu m^2x10^{-3} \pm 61$) developing larger granulomas in comparison to WT ($93\mu m^2x10^{-3} \pm 38$) mice ($p<0.05$). There was, however, a

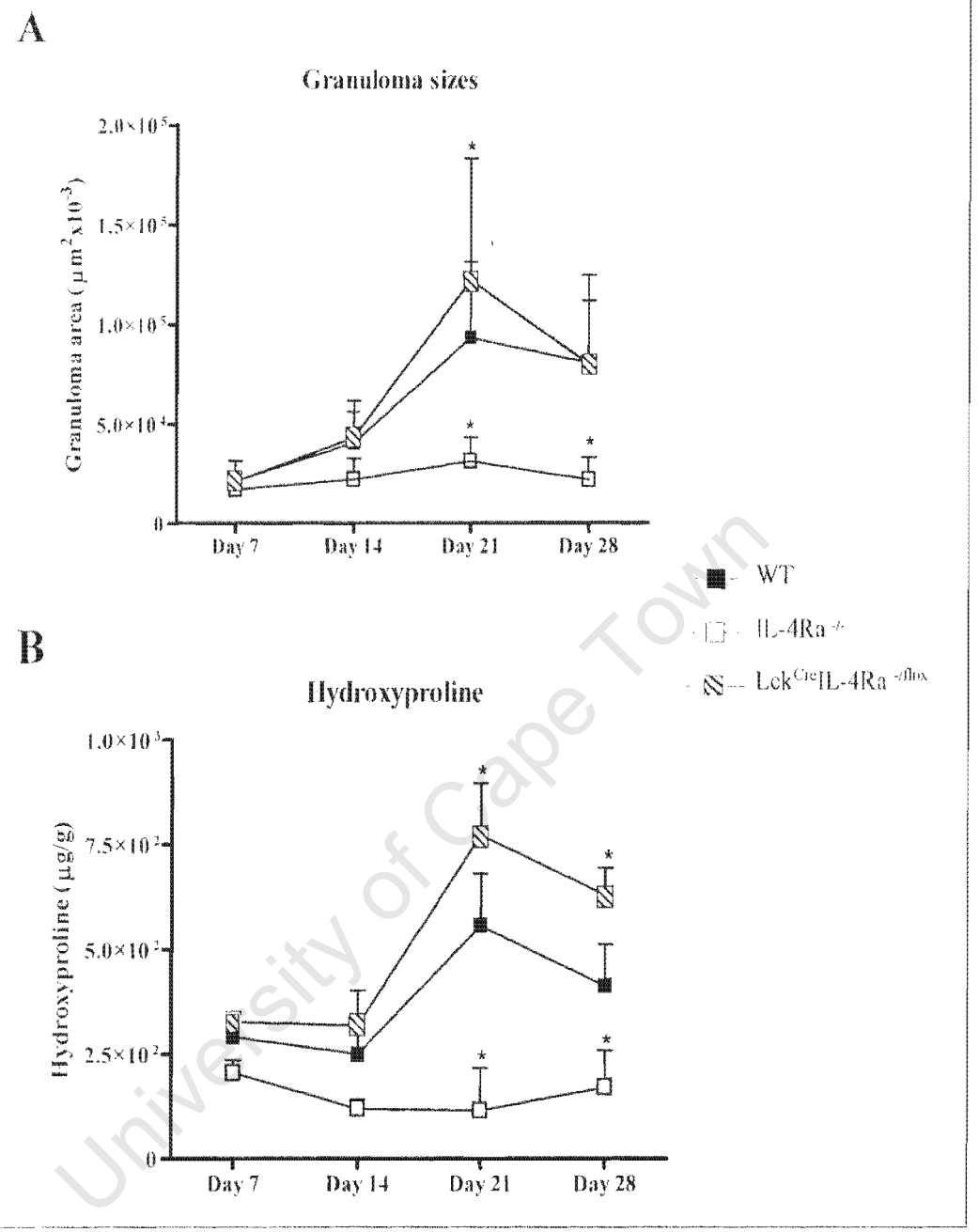

Figure 2.13

Pulmonary granuloma development and lung hydroxyproline levels in egg-injected mice

Lung tissue from egg-injected mice was processed for histology. Lung hydroxyproline levels were measured as described in Materials and Methods. Pulmonary granuloma sizes were determined from histological sections using computerized morphometry analysis program. An average of 50 granulomas per mouse was included in the analysis. (*)= $p<0.05$ by ANOVA compared to WT

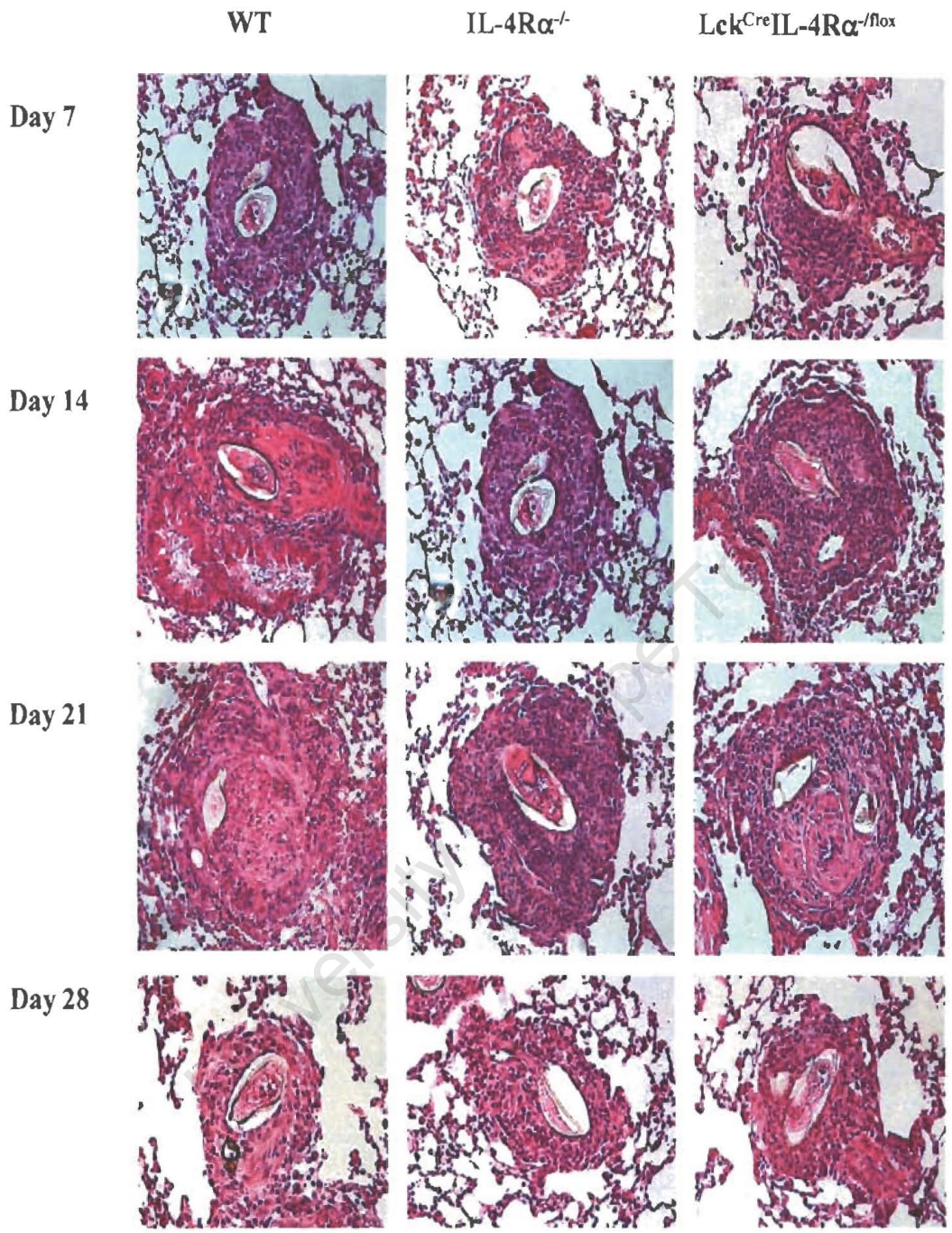

Figure 14

Pulmonary granuloma formations in egg-injected mice

Mice were sensitized with live eggs ip and late challenged with live eggs i.v. Mice were sacrificed at day 7, 14, 21 and 28 and lungs removed. Paraffin embedded tissue were sectioned at 5μm and stained with haematoxylin and eosin. Sections are representative of 4 mice per strain at each time point. (Magnification =200x)

modest granuloma sizes of $Lck^{Cre}IL\text{-}4R\alpha^{-/flox}$ mice ($80\mu m^2x10^{-3} \pm 31$) as well as WT ($80\ \mu m^2x10^{-3} \pm 44$) mice on 28 post-challenge.

Consistent with these results, the analysis of collagen deposition within the lung, from CAB stained lung sections and by measurement of hydroxyproline levels, showed a similar profile among all strains during the first two weeks after egg challenge (Figure 2.13B and Figure 2.15). In keeping with the gradual growth of granuloma in the lung, hydroxyproline levels were significantly elevated at day 21 post-challenge in the WT and $Lck^{Cre}IL\text{-}4R\alpha^{-/flox}$ mice ($p<0.001$). There was, however, a considerable decrease in hydroxyproline levels at day 28 in both the WT and the $Lck^{Cre}IL\text{-}4R\alpha^{-/flox}$ strains ($p<0.05$) (Figure 2.13B). In general these data show that $CD4^+$ T cell independent IL-4Rα expression is required for lung fibrosis and granuloma development in $Lck^{Cre}IL\text{-}4R\alpha^{-/flox}$ mice.

2.7 Cellular recruitment in the pulmonary granuloma of $Lck^{Cre}IL\text{-}4R\alpha^{-/flox}$ mice

Examination of cellular recruitment in the lung granuloma of egg-injected mice showed weak eosinophil recruitment in $Lck^{Cre}IL\text{-}4R\alpha^{-/flox}$ mice at day 7 and day 14 after egg embolization (Table II), whereas $IL\text{-}4R\alpha^{-/-}$ lung granulomas were completely devoid of eosinophils at day 7. There were slightly more eosinophils per granuloma in $Lck^{Cre}IL\text{-}4R\alpha^{-/flox}$ at day 21 post-challenge although the levels were still significantly lower compared to WT mice ($p<0.05$) (Table II). On the other hand, examination of PAS positive cells from stained lung sections showed no presence of PAS positive cells in the lungs of both $Lck^{Cre}IL\text{-}4R\alpha^{-/flox}$ and $IL\text{-}4R\alpha^{-/-}$ mice at any stage after egg challenge (Table II and Figure 2.16).

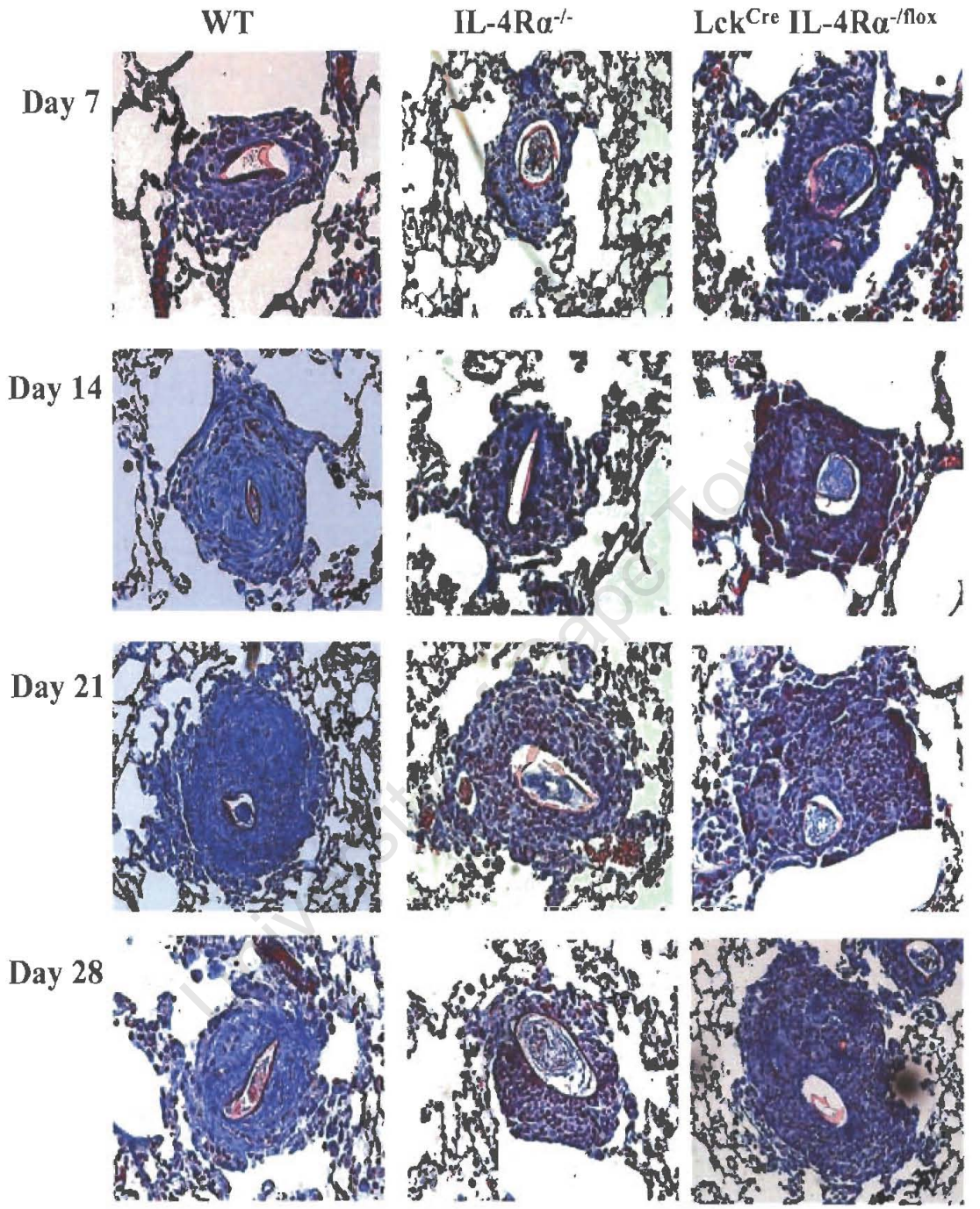

Figure 15

Collagen deposition in the lungs of egg challenged mice

Paraffin embedded tissue from sensitized, egg-challenged mice were sectioned at 5μm and stained with CAB. Sections are representative of 4 mice per strain at each time point. (Magnification =200x)

Table II

Comparison of granuloma cellular recruitment in egg challenged mice. Numbers of eosinophils and PAS positive cells were determined from histological sections. An average of 50 granulomas per mouse was included in the analysis. Data shown represent the mean ± SD. Statistical significance was determined by one way ANOVA with (*) $p<0.05$ and (***) $p = <0.001$, as compared to WT value.

		IL-4Rα$^{-/flox}$	IL-4Rα$^{-/-}$	LcK^{Cre}IL-4Rα$^{-/flox}$
Day 7	**Eosinophils**	13 ± 6.5	0.00± 0.00***	4 ± 2.46 *
	PAS+ve cells	21 ± 7.85	0.00± 0.00***	0.00± 0.00***
Day 14	**Eosinophils**	28 ± 12.3	3 ± 1.87***	6. ± 3.73 ***
	PAS+ve cells	28 ± 13.25	0.00± 0.00***	0.00± 0.00***
Day 21	**Eosinophils**	37 ± 15.6	7± 5.2***	15 ± 7.84*
	PAS+ve cells	51 ± 11.95	0.00± 0.00***	0.00± 0.00***
Day 28	**Eosinophils**	24 ± 8.4	2 ± 1.03 ***	9 ± 4.96*
	PAS+ve cells	40 ± 9.68	0.00± 0.00***	0.00± 0.00***

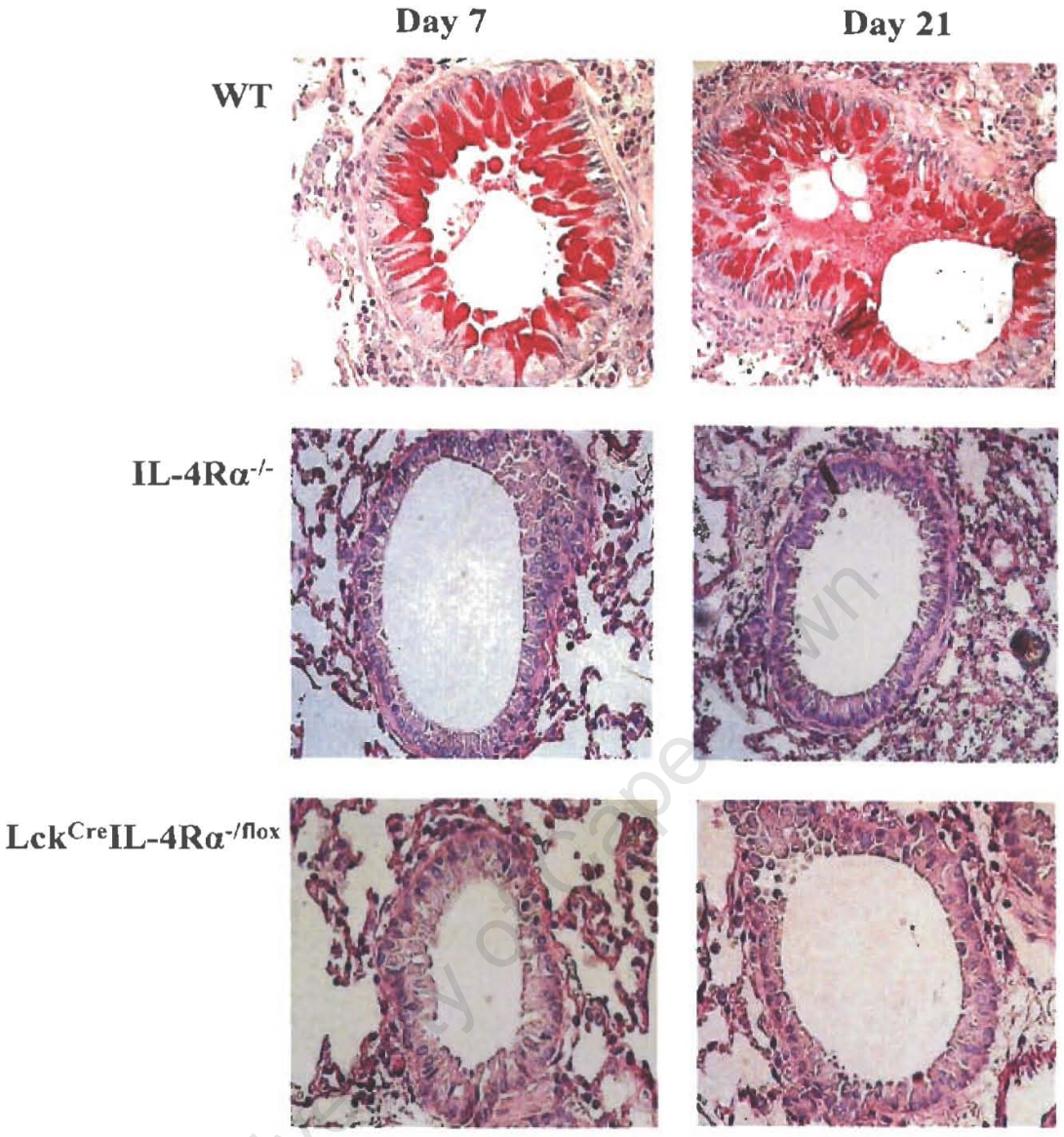

Figure 16

Absence of PAS positive cells in the lungs of egg-challenged LcK^{Cre}IL-4Rα$^{-/flox}$ mice

Paraffin embedded tissue from sensitized, egg-challenged mice were sectioned at 5μm and stained with PAS. Sections are representative of 4 mice per strain at indicated time points. (Magnification =200x)

2.8 Egg-injected Lck^{Cre}IL-4Rα$^{-/flox}$ mice develop polarized T_H1 and type1 immune response

The correlation between the development of schistosome egg-induced granulomas and the presence of T_H2 cells in the granuloma has been established. The production of T_H1 vs. T_H2 cytokines was directly compared with changes in granuloma development in pre-sensitized egg challenged Lck^{Cre}IL-4Rα$^{-/flox}$ mice. Lung homogenates, mediastinal lymph nodes as well as splenocyte supernatants were used to determine the changes in cytokine levels in the local milieu of granuloma formation.

Independent studies (n =3) analyzing cytokine production in lung showed a significantly impaired T_H2 cytokine (IL-4, IL-5 and IL-13) production in the lung homogenates after egg embolization in Lck^{Cre}IL-4Rα$^{-/flox}$ as well as IL-4Rα$^{-/-}$ mice, whereas IFN-γ levels were significantly elevated in these two strains in comparison to WT mice (Figure 2.17). In contrast, similar levels of immunosuppressive cytokine IL-10 were observed between the WT and Lck^{Cre}IL-4Rα$^{-/flox}$ mice. However, IL-10 levels were significantly elevated in Lck^{Cre}IL-4Rα$^{-/flox}$ mice at day 28 post-challenge ($p<0.05$) (Figure 2.18A). Similarly, TGF-β levels were also profoundly elevated in Lck^{Cre}IL-4Rα$^{-/flox}$ mice in comparison to WT mice, throughout the study (Figure 2. 18B).

Anti-CD3 stimulation of mediastinal lymph nodes and splenocytes also revealed a similar profile of cytokine levels as that observed in lung homogenate samples. At day 7 post-challenge, whereas IL-13 levels were similar between WT and Lck^{Cre}IL-4Rα$^{-/flox}$ mice (Figure 2.19C), IL-4 and IL-5 levels were significantly reduced in Lck^{Cre}IL-4Rα$^{-/flox}$ mice ($p<0.05$) (Figure 2.19A & B) and remained so throughout the study (Figure 2.19 and Figure 2.20). On the contrary, IFN-γ were detected from as early as day 7 following egg embolization with IL-4Rα$^{-/-}$ and Lck^{Cre}IL-4Rα$^{-/flox}$ mice producing

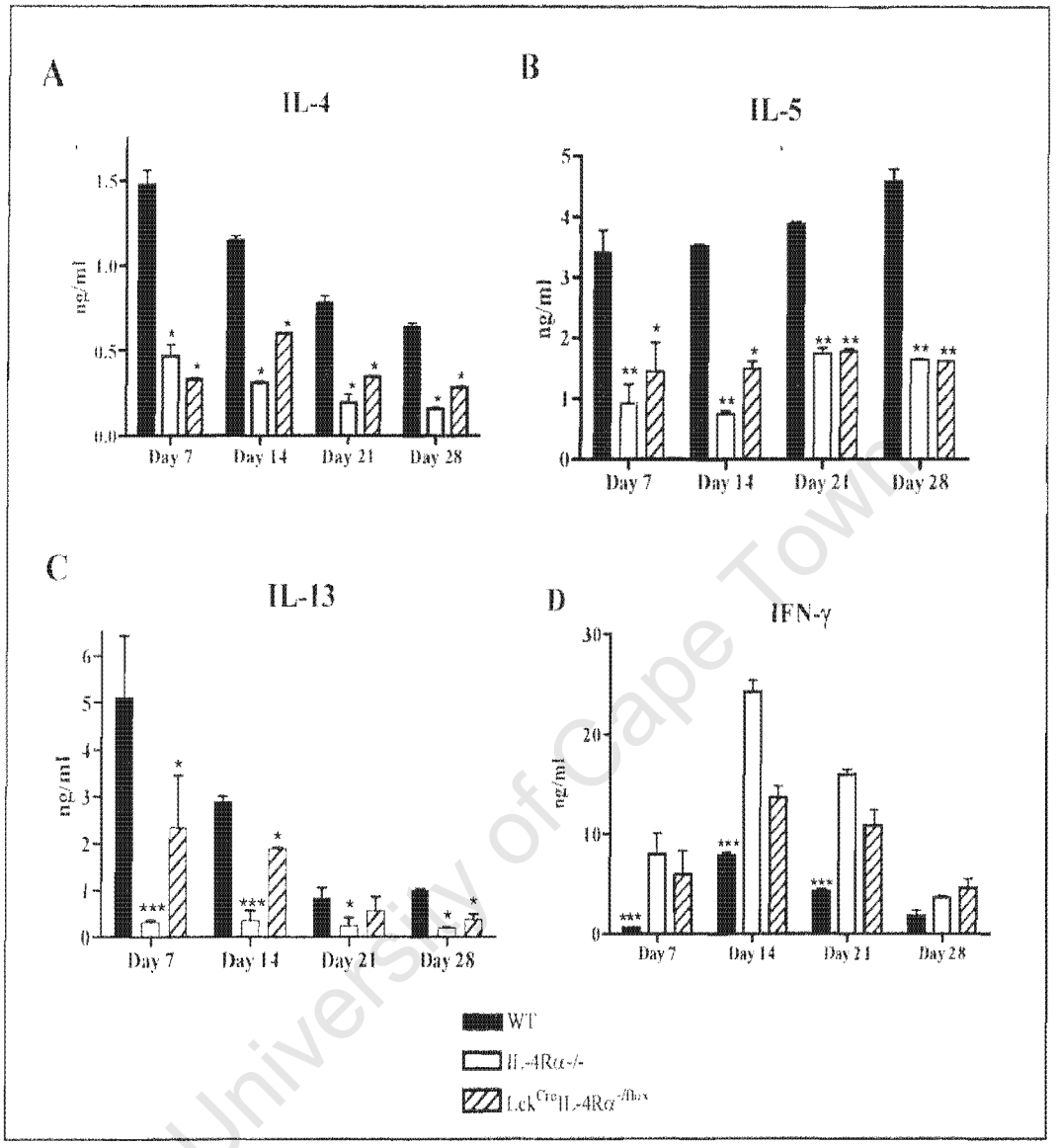

Figure 2.17

T_H1 and T_H2 cytokine levels in lung homogenates of egg-challenged mice

Lung tissue homogenates from egg-sensitized and challenged mice were analyzed for T_H1 (panel D) vs. T_H2 (Panel A-C) cytokine production. Each data point represents the mean ± SD of triplicate samples. Results are representative of one of three similar experiments.(*) = $p<0.05$, (**)=$p<0.01$ and (***) = $p<0.001$ by ANOVA.

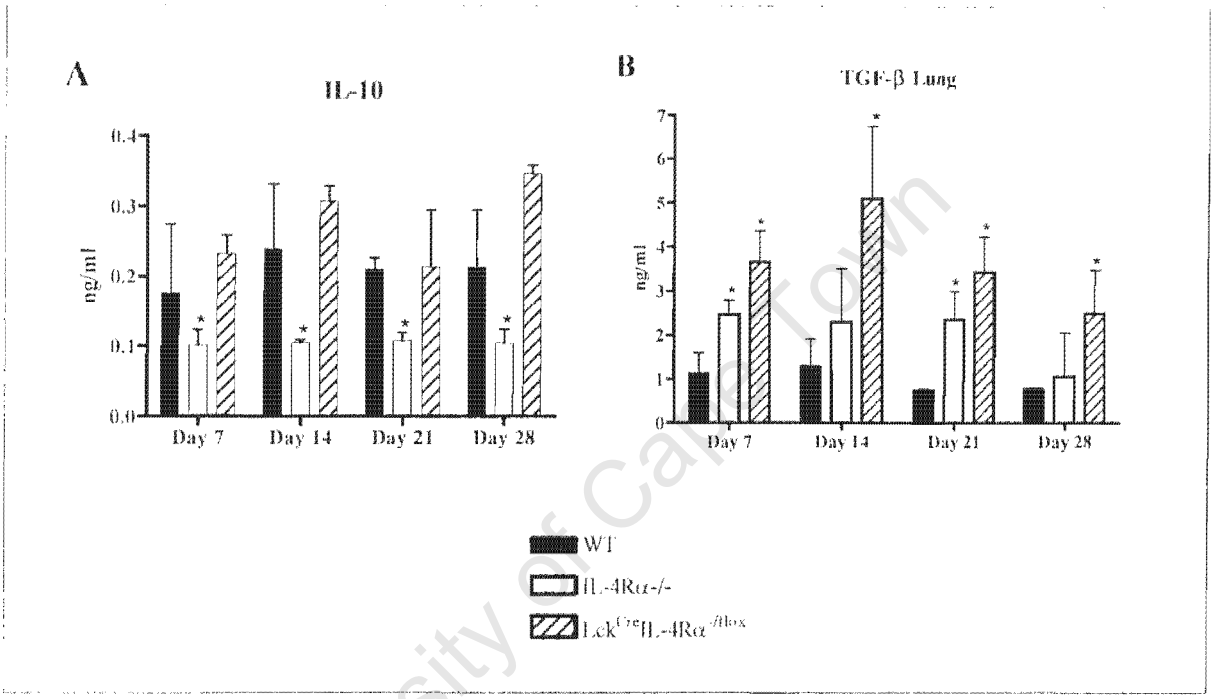

Figure 2.18

IL-10 and TGF-β levels in lung homogenates of egg-challenged mice

Lung homogenates were analysed for the levels of IL-10 and TGF-β by ELISA. Data represents mean ± SD of triplicate samples. Results are representative of three similar experiments. (*)= $p<0.05$ by ANOVA in comparison to WT

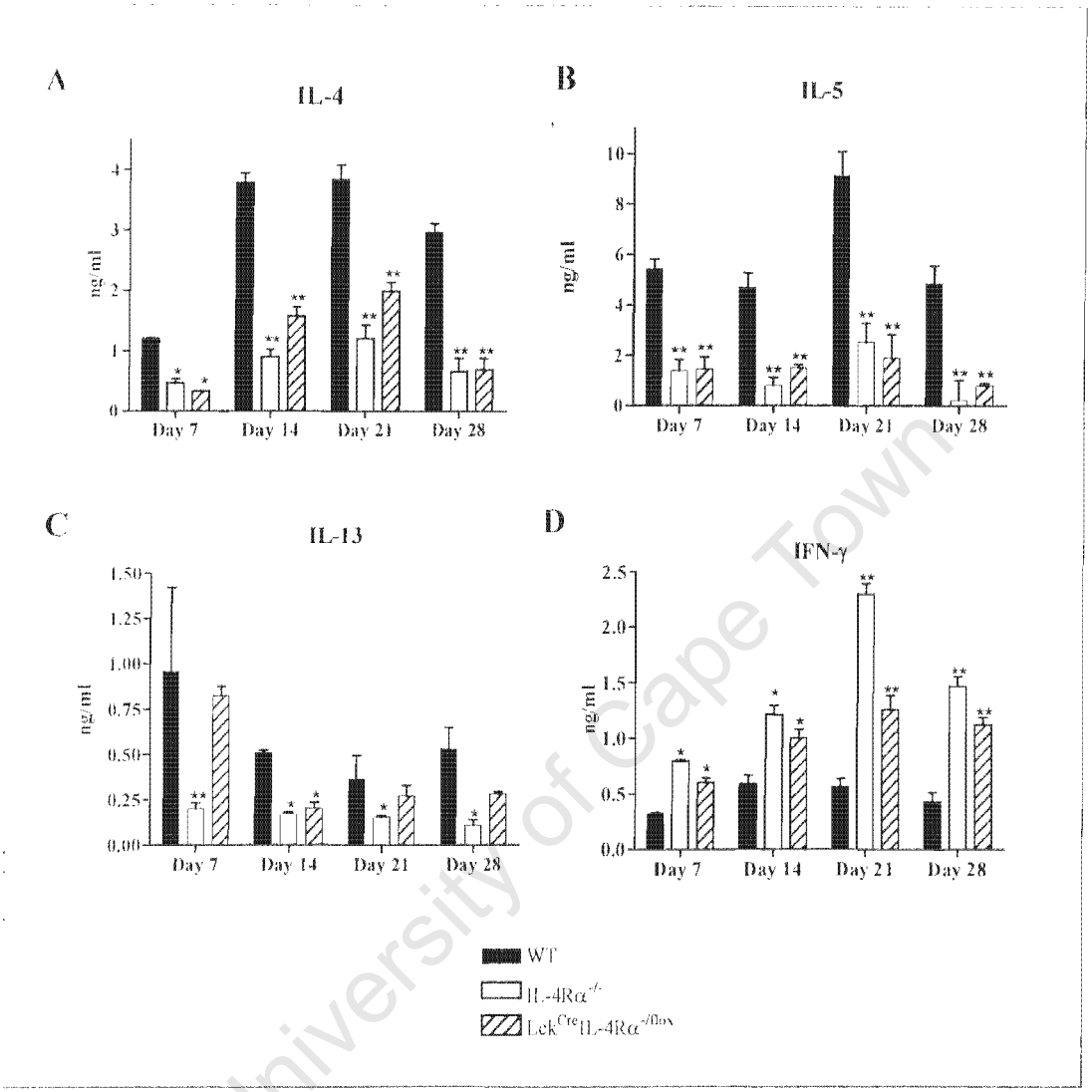

Figure 2.19

Th1 and Th2 cytokine levels in splenocyte cultures of egg-challenged mice

Anti-CD3-stimulated splenocyte cell cultures from sensitized egg-injected mice were analyzed for T_H1 (Panel D) and T_H2 (Panel A-C) cytokine levels by ELISA. Data are mean ± SD of triplicate samples. Results represent one of three similar experiments. (*) = $p<0.05$ and (**) = $p<0.01$ by ANOVA in comparison to WT

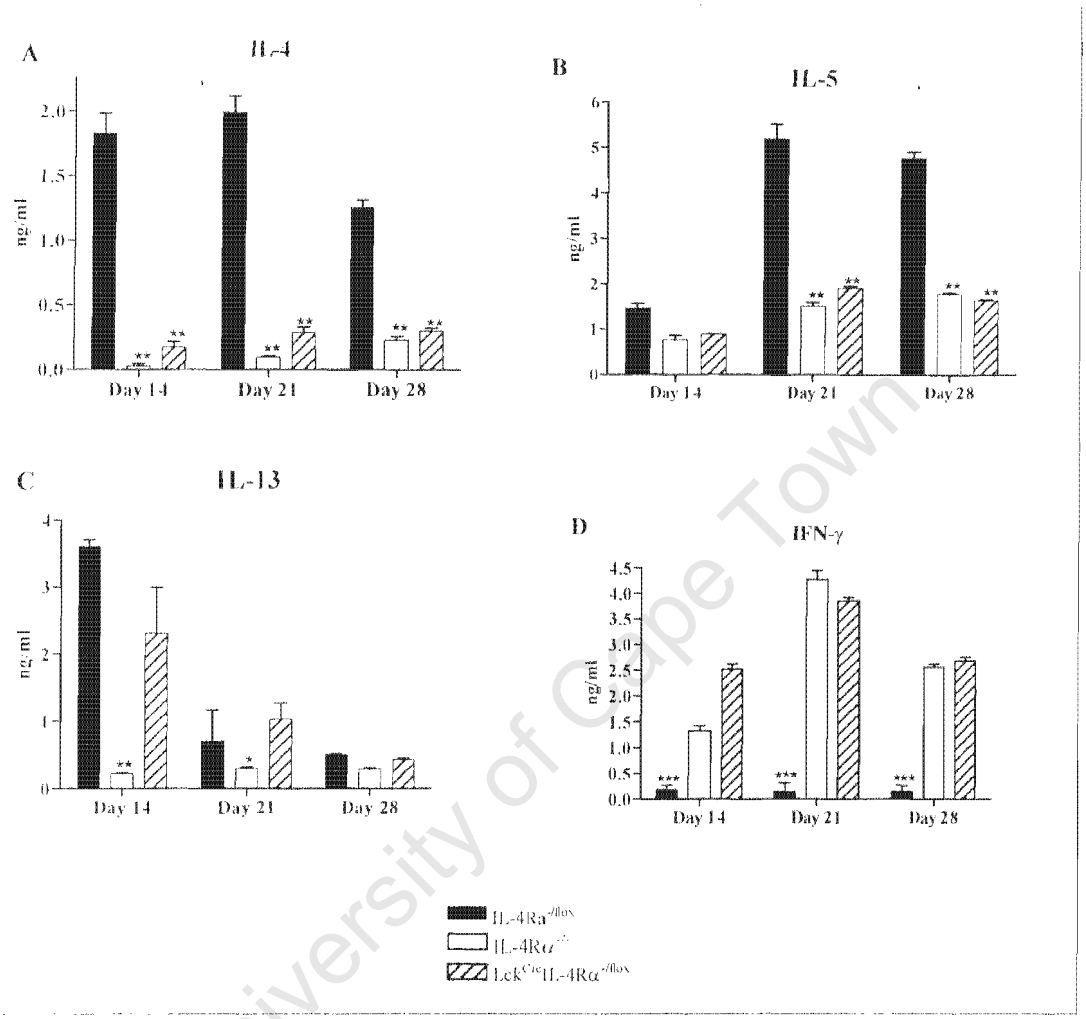

Figure 2.20

Th1 and Th2 cytokine levels in lymph node cell cultures of egg-challenged mice

Mice were sensitized with *S. mansoni* eggs 14 days prior to i.p challenge with live eggs. T_H2 (Panel A-C) and T_H1 (Panel D) cytokine levels were measured from anti-CD3 mediastinal lymph node culture supernatant by ELISA. Data shown are mean ± SD from triplicate samples and are representative of three independent experiments. (*) = $p<0.05$, (**) = $p<0.01$ and (***) = $p<0.001$ by ANOVA

significantly higher levels of IFN-γ levels compared to WT mice (Figure 2.19 and Figure 2.20).

Likewise, TGF-β levels were significantly higher in IL-4R$^{-/-}$ and LcK^{Cre}IL-4Rα$^{-/flox}$ mice throughout the study (Figure 2.21B and 2.22B), whereas IL-10 levels were similar from day 14-day to day 28 post-challenge (Figure 2.21A and Figure 2.22A). This data supports the contention that, in schistosomiasis, IL-13 induced tissue fibrosis is independent of TGF-β.

In mice, high IgG1/IgE and low IgG2 Ab isotype titers associate with T_H2 responses, while IgG2 and low IgG1/ IgE titers are observed in T_H1-type cellular immune responses. We compared antibody production in WT and LcK^{Cre}IL-4Rα$^{-/flox}$ mice to study the association between Ab production and cytokine production. Measurements of the SEA-specific antibody response revealed a significant rise in IgG2a and IgG2b in LcK^{Cre}IL-4Rα$^{-/flox}$ mice sera from day 7-day to day 28 (Figure 2.23A & B) whereas IgG1 and total IgE levels were significantly abrogated in these mice (Figure 2.23C & D). Taken together, T cell specific deletion of IL-4Rα skews antigen-specific antibody responses towards Type 1 and that polarized T_H1 vs T_H2 cytokine production does not correlate with granulomatous pathology in the lung.

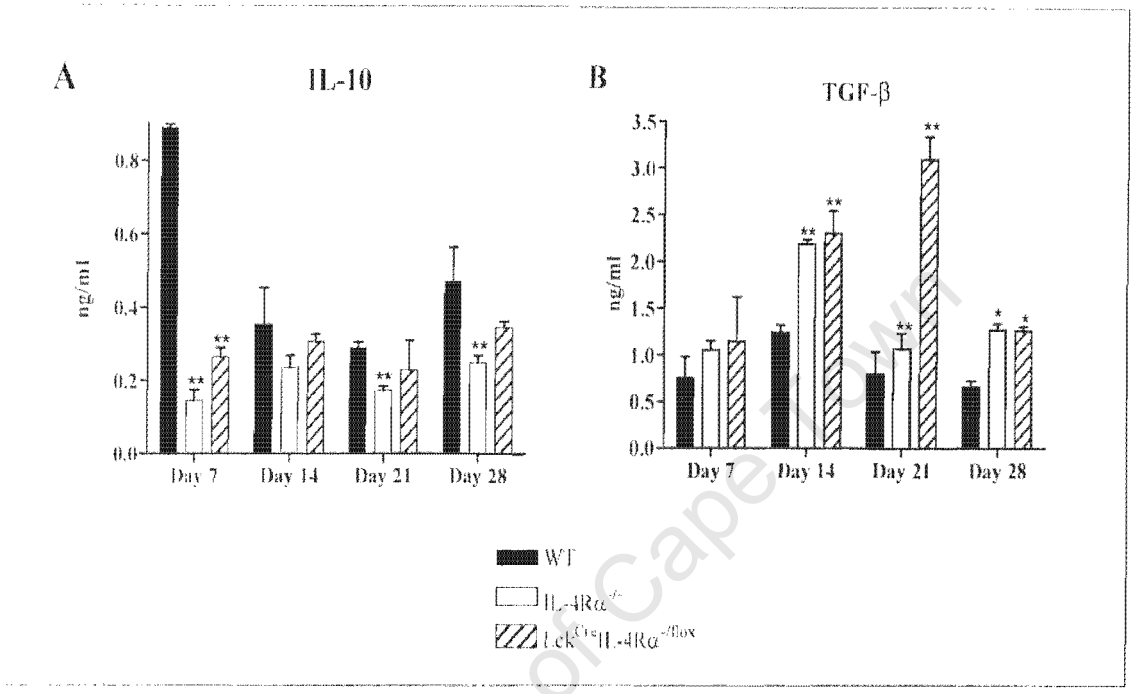

Figure 2.21

IL-10 and TGF-β levels in splenocytes of egg-challenged mice

Splenocyte cell culture supernatants from mice pre-sensitized and challenged with *S. mansoni* eggs were analyzed for IL-10 and TGF-β levels following stimulation with anti-CD3. Data are the mean ± SD of triplicate samples from three similar experiments. (*) =$p<0.05$ and (**) = $p<0.01$ by ANOVA compared to WT

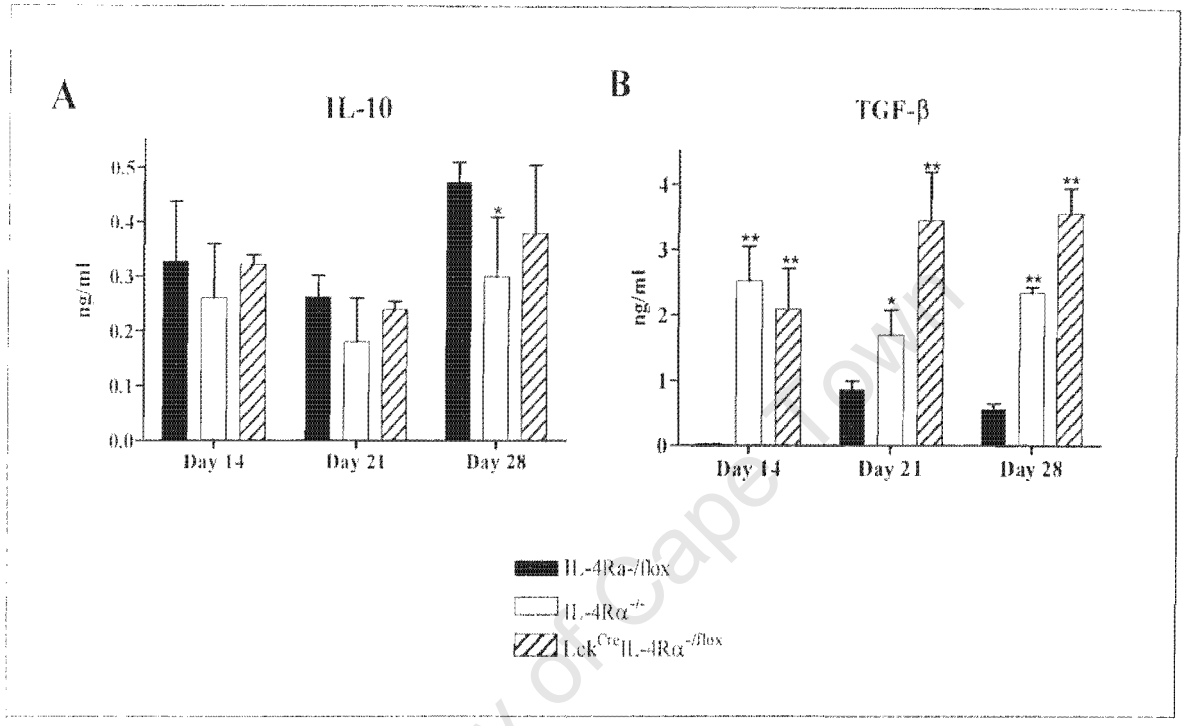

Figure 2.22

IL-10 and TGF-β levels in mediastinal lymph nodes of egg-challenged mice

Mediastinal lymph nodes from egg-injected mice were stimulated with anti-CD3 mAb (20μg/ml) or 72 hours and measurements and IL-10 and TGF-β levels in supernatants determined by ELISA. Data shown are mean ± SD from triplicate samples and are representative of three independent experiments. (*) = $p<0.05$ and (**) = $p<0.01$ by ANOVA in comparison to WT

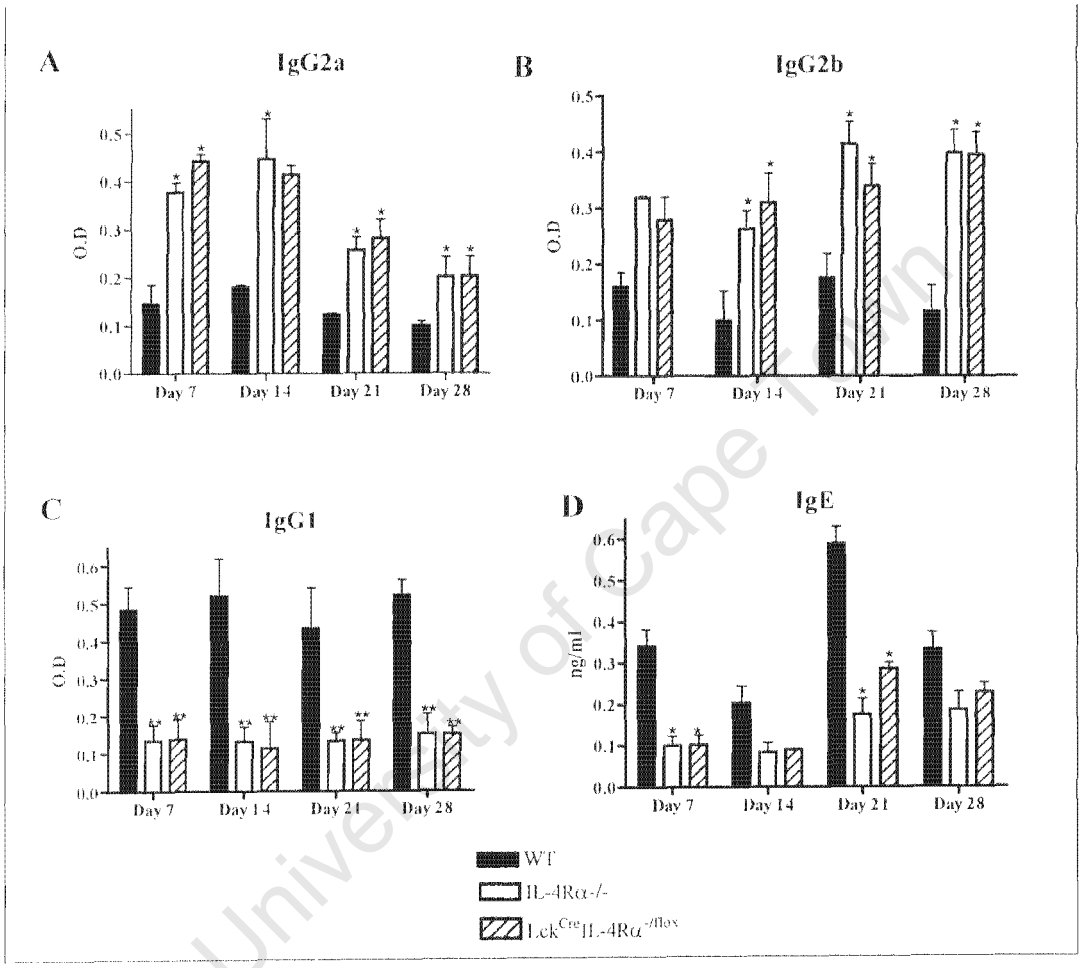

Figure 2.23

Antibody Production in sensitized egg-challenged mice

SEA-specific Type 1 (Panel A and B) and Type 2 (Panel C and D) antibodies were analyzed in the sera of mice by ELISA at indicated time points after egg-challenge. Panel D represents total serum IgE levels. Each data point represents mean ± SD triplicate serum samples. Results represent one of three similar experiments. (*)=$p<0.05$ and (**) =$p<0.01$ by ANOVA compared to WT value.

DISCUSSION

The objectives of these studies were to determine the role of IL-4 /IL-13 responsive T cells during infection with *S. mansoni* and to determine the requirement of T cell-specific IL-4Rα signalling for the extent of granuloma development or egg-induced fibrosis. A clear distinction was seen in the survival of Lck^{Cre}IL-4$R\alpha^{-/flox}$ during an infection with *S. mansoni* parasites. As compared to survival in WT and IL-4$R\alpha^{-/-}$ mice, Lck^{Cre}IL-4$R\alpha^{-/flox}$ mice had significantly increased survival, despite the excessive IFN-γ/NOS-2 production and severe liver pathology. Although IL-4, IL-10, and IL-13 each serve distinct and essential roles in liver pathology during schistosomiasis, the mechanism(s) controlling parasite egg-driven gut inflammation and faecal egg excretion are poorly understood. Comparative analysis among the three strains show that profound egg-induced gut pathology occurred in the presence of significantly elevated IL-10 levels in the intestine. Furthermore, the presence of $CD4^+CD25^+$ regulatory T cells and TGF-β in liver and intestinal granuloma tissue was IL-4Rα-dependent, but expression was required on a non-T cell population. Therefore, this indicates that IL-4/IL-13 responsiveness is a fundamental requirement for prevention of lethal T_H1 driven gut pathology during experimental schistosomiasis and that IL-4Rα is central to both of these processes through promotion of AAMϕ and control of $CD4^+CD25^+$ T regulatory cell behaviour.

IL-4 drives STAT-6 activation and T_H2 polarization (Zheng and Flavell 1997; Kurata et al. 1999; Nelms et al. 1999), but several reports have shown that STAT-6/IL-4Rα responsiveness is not essential for T_H2 differentiation (Noben-Trauth et al. 1997; Jankovic et al. 2000), suggesting that IL-4Rα serves a more important role as an antagonist for T_H1 cell differentiation (Metwali et al. 2002). Our data in the *S. mansoni* mouse model shows that IL-4Rα null mutants, macrophage/neutrophil-specific ($LysM^{Cre}$IL-4$R\alpha^{-/flox}$) (Herbert et al. 2004) and T cell specific IL-4Rα deficient mice all produce more IFN-γ during

acute disease. $Lck^{Cre}IL\text{-}4R\alpha^{-/flox}$ mice generate the highest precursor frequencies of IFN-γ effector cells as determined by ELISPOT (data not shown) and splenocyte cultures of these mice contains highly elevated NOS-2 activity (Figure 2.2A). IL-4 can instructively signal professional antigen presenting cells (APC) for increased secretion of IL-12p70, thus driving T_H1 cell expansion (Biedermann et al. 2001). Moreover, the short half-life of phosphorylated STAT-6 necessitates constant re-activation via IL-4 receptor signalling. Therefore, it is likely that *S. mansoni* egg-induced IL-4 production acting on APC combined with the T cell specific IL-4Rα deletion leads to such a prominent IFN-γ response in $Lck^{Cre}IL\text{-}4R\alpha^{-/flox}$ mice.

IFN-γ dominated responses are detrimental for both human and experimental schistosomiasis and the severity of hepatic immunopathology during *S. mansoni* infection bears a strong genetic linkage to IFN-γ, (Brunet et al. 1997; Fallon and Dunne 1999; McKenzie et al. 1999; Flamme et al. 2001; Patton et al. 2001). Indeed, studies performed with mice deficient for IL-4 (Patton et al. 2001), IL-4/IL-13 (Fallon et al. 2000), or IL-4/IL-10 (Hoffmann et al. 2000), all die rapidly during acute disease through a common mechanism involving enhanced production of IFN-γ, NOS-2, TNF, and hepatocyte destruction. $Lck^{Cre}IL\text{-}4R\alpha^{-/flox}$ dispersed granuloma cells stimulated with anti-CD3 produced significantly elevated IFN-γ levels that were indistinguishable from $IL\text{-}4R\alpha^{-/-}$ those of mice (Figure 2.6). In addition, $Lck^{Cre}IL\text{-}4R\alpha^{-/flox}$ hepatic granulomas were larger and more fibrotic than those of littermate controls, factors that could have also contributed to increased liver injury in this strain. Surprisingly, our data clearly demonstrate that $Lck^{Cre}IL\text{-}4R\alpha^{-/flox}$ mice given high infectious doses (75 cercariae) display extended survival times despite significantly elevated T_H1 responses, NOS-2 activity, and AST levels (Figure 2.4). In contrast to $IL\text{-}4Ra^{-/-}$ mice, $Lck^{Cre}IL\text{-}4R\alpha^{-/flox}$ mice produced high levels of T_H2 cytokines (IL-4, IL-5, and IL-13) in the liver whereas peripheral lymph nodes and spleen showed significantly impaired T_H2 responses. It has been

shown that antigen specific T cell responses differ in the various organs during *S. mansoni* infection which is reflected in our results. Therefore different profiles of cytokine secretion are observed depending upon the specific organ analyzed.

To this end, we decided to measure cytokine levels present in liver tissue homogenates instead of re-stimulated collagenase-digested granuloma cell suspensions to determine the cytokine content per gram of tissue. Surprisingly, there were actually significantly lower amounts of IFN-γ and TNF in Lck^{Cre}IL-$4R\alpha^{-/flox}$ liver when compared to IL-$4R\alpha^{-/-}$ tissue. TNF is a known contributor to increased mortality rates of *S. mansoni* infected IL-$4^{-/-}$ mice. Therefore, demonstration of lower tissue levels of both IFN-γ and TNF in Lck^{Cre}IL-$4R\alpha^{-/flox}$ mice provided an additional clue to explain the extended survival times of these mice. Thus, while Lck^{Cre}IL-$4R\alpha^{-/flox}$ and IL-$4R\alpha^{-/-}$ liver contained the potential for release of pathogenic T_H1 inflammatory cytokines, mechanism(s) existed restricting secretion in the former strain, but not in the latter.

IL-10 was a likely candidate for this role due to its well known immunosuppressive capabilities and recent demonstration that it is an essential hepatoprotective factor in murine schistosomiasis. Significant elevations of IL-10 were detected after anti-CD3 stimulation of WT and Lck^{Cre}IL-$4R\alpha^{-/flox}$ liver granuloma cells, as compared to IL-$4R\alpha^{-/-}$ mice. However, amounts of IL-10 in liver homogenates showed a reciprocal pattern, with significantly higher amounts of IL-10 produced by IL-$4R\alpha^{-/-}$ mice as compared to the other strains, suggesting two different cell sources of this cytokine. T cell derived IL-10 is completely independent of IL-10 produced by non-lymphocyte cell populations in the liver during experimental schistosomiasis. LPS-stimulated macrophages secrete high levels of inflammatory and anti-inflammatory cytokines (IL-6, TNF, IL-12, and IL-10) and constitute a predominant cell type of *S. mansoni* granulomas. This, combined with demonstrated sepsis in IL-$4R\alpha^{-/-}$ mice at 7.5

weeks post-infection strongly suggests that macrophages were major contributors to the high levels of both TNF and IL-10 in liver homogenates of IL-4Rα$^{-/-}$ mice. Overall however, our data do not favour a hypothesis that hepatic injury or IL-10 levels in liver tissue are determinants of mortality vs. survival during experimental schistosomiasis. Instead, our working hypothesis is that IL-4Rα expression is central for control of potentially lethal gut inflammation.

During *S. mansoni* infection of various inbred mouse strains, peak levels of IL-4Rα1 mRNA transcripts are reached during acute disease (6-8 weeks post-infection). IL-4Rα$^{-/-}$ mice consistently developed severe gut pathology by 7 weeks post infection and experienced 100% mortality by 8 weeks. Profound hemorrhagic distention of the small bowel involving the entire ileum and distal jejunum occurred in this strain, with pathology somewhat resembling toxic mega colon in humans. Microscopic analysis of this region revealed that many parasite eggs present in the muscularis propria encased by erythrocytes and very few surrounding inflammatory cells (data not shown). *S. mansoni* infected IL-4$^{-/-}$ and IL-4$^{-/-}$/IL-13$^{-/-}$ mice also experience increased intestinal damage accompanied by parasite-egg accumulation in gut tissue, decreased fecal egg excretion, endotoxemia, and premature lethality by 7-8 weeks post infection. In chapter 1 we demonstrated that IL-4Rα dependent AAMϕ were essential for control of T_H1 driven egg-inflammation that led to increased gut immunopathology and sepsis (Herbert et al. 2004). LysM^{Cre}IL-4Rα$^{-/flox}$ and IL-4Rα$^{-/-}$ mice produced high amounts of IFN-γ, TNF, and IL-10 in gut tissue accompanied by premature lethality. Of note, while premature lethality of macrophage-specific IL-4Rα deficient mice was preventable by antibiotic prophylaxis, this treatment was unable to rescue IL-4Rα$^{-/-}$ mice. Thus, even though AAMϕ are necessary for survival, it was clear that other defects were contributing to the greater sensitivity of IL-4Rα$^{-/-}$ mice to even low dose infection with *S. mansoni* (data not shown).

The selective impairment of the $CD4^+CD25^+$ population in IL-4Rα$^{-/-}$ intestinal tissue, but not in WT and Lek^{Cre}IL-4Rα$^{-/flox}$ mice provides a possible mechanistic explanation for our previous observations. $CD4^+CD25^+$ regulatory T cells have been widely described as suppressors of tissue destructive inflammatory responses and providers of host protection in models of colitis, diabetes, and arthritis. Although these markers have been widely used to isolate and study regulatory T cell populations, $CD4^+CD25^+$ also designates activated T lymphocytes. Figure 2.12 shows that hepatic and intestinal mRNA transcripts for the Treg specific transcription factor Foxp3 were barely detectable in IL-4Rα$^{-/-}$ mice, but strongly up-regulated in WT and Lek^{Cre}IL-4Rα$^{-/flox}$ strains. Curiously, Lek^{Cre}IL-4Rα$^{-/flox}$ mice expressed 10-fold higher levels of Foxp3 compared to the WT and in some of our FACS experiments there were double the percentage $CD4^+CD25^+$ cells in Lek^{Cre}IL-4Rα$^{-/flox}$ granuloma tissue when compared to littermate controls (data not shown). This impaired presence of $CD4^+CD25^+$ cells in IL-4Rα$^{-/-}$ granulomas did not reflect a defect in Treg ontogeny or an overall inability of these mice to produce suppressive cytokines because analysis of blood, spleen and mesenteric lymph nodes demonstrated slightly higher percentages of $CD4^+CD25^+$ cells accompanied by elevated TGF-β production (Figure 2.12) in these peripheral tissues. Therefore we propose that $CD4^+$ T cell populations in *S. mansoni* granuloma tissue can be divided into two populations, $CD4^+CD25^-$ whose tissue entry is IL-4Rα independent and $CD4^+CD25^+$ cells that are dependent upon IL-4Rα expression on non-T cells. STAT-6-dependent chemokines such as macrophage-derived chemokine (MDC/CCL22) and thymus activation-regulated chemokine (TARC/CCL17) have been shown to direct Treg, as well as T_H2 cell migration (Iellem et al. 2001). However, it is currently unclear whether these results reflect defects in chemotaxis or impaired expansion of Treg in granuloma tissue due to possible defects in APC function via the IL-4Rα null mutation.

Locally produced TGF-α is able to cause the rapid expansion of Foxp3 expressing regulatory T cells that suppress disease causing T_H1 effectors. TGF-β-mediated suppression of colitis in various mouse models has been extensively studied, but little is known about the role for TGF-β in suppression of intestinal inflammation during schistosomiasis. Results of experiments involving depletion of $CD25^+$ show increased pro-inflammatory cytokine levels (IFN-γ, TNF) and decreased faecal egg excretion in WT and Lck^{Cre}IL-$4R\alpha^{-/flox}$ mice during acute disease (unpublished results) Data presented herein suggest that TGF-β producing $CD4^+CD25^+$ regulatory T cells are responsible for protection against lethal gut inflammation during murine schistosomiasis in a IL-4Rα dependent manner. Although we cannot rule out a role for T cell independent TGF-β production, Figure 2.12 shows highly elevated levels of TGF-β are produced by anti-CD3-stimulated splenocytes and $CD4^+$ T cells purified from spleens of WT, IL-$4R\alpha^{-/-}$ and Lck^{Cre}IL-$4R\alpha^{-/flox}$ infected mice all produce highly elevated levels of TGF-β. The elevated production of TGF-β in the peripheral tissues of IL-$4R\alpha^{-/-}$ mice, but selective defect in granuloma tissue reflects our data for $CD4^+CD25^+$ cells, and Foxp3 expression, which together strongly supports our contention that TGF-β-producing $CD4^+CD25^+$ Treg cells balance potentially fatal T_H1- driven egg responses in the gut and promotes the passage of faecal eggs. The non-T cell IL-4Rα-expressing cell that controls Treg entry and /or expansion in granuloma tissue is currently unknown, but is likely to be a non bone marrow-derived cell. IL-4/IL-13 dependent responsive intestinal epithelial cell functions have been shown to control expulsion mechanisms against parasitic helminths. Nonetheless, these data are the first to our knowledge to demonstrate a role for IL-4Rα in the behaviour of Treg cells *in vivo* and provide additional insight for the design of therapies that limit or promote their presence during anti-tumour or anti-parasite responses, respectively.

Similar to liver pathology, analysis of granulomatous inflammation in the lung also revealed that Lck^{Cre}IL-4R$\alpha^{-/flox}$ mice developed larger and more fibrotic granulomas in comparison to their WT control littermates. In contrast, examination of cellular recruitment showed a weak eosinophil infiltration in Lck^{Cre}IL-4R$\alpha^{-/flox}$ mice as compared to WT mice. Consequently ELISA results also showed that the immune response of the animals to the eggs in the lung milieu was dominated by T_H1 cytokines. These findings are in stark contrast to previous findings which showed that a T_H2-type response is critical for normal egg-induced lesion formation (Wynn et al. 1994). Most interestingly, the current data support the hypothesis that although IL-13 is a known potent activator of collagen production by fibroblasts, there may be other mediators which are involved in collagen production, such as TGF-β, as suggested in a murine asthma model (Lee et al. 2001). Indeed we observed elevated levels of TGF-β in the lung homogenates as well as LN and spleen cultures of Lck^{Cre}IL-4R$\alpha^{-/flox}$ mice which may suggest that TGF-β is indeed another mediator for collagen deposition in the lung. Our current data, does not, however, completely rule out IL-13 as the dominant factor in mediating collagen deposition in the lung. A number of studies in other disease models have shown that that although IL-13 production is markedly decreased in the absence of IL-4, for example in IL-4 or IL-4Rα-deficient mice, the residual IL-13 response remains highly active (Urban et al. 1998; Wills-Karp et al. 1998; Chiaramonte et al. 1999; Mohrs et al. 1999; Noben-Trauth et al. 1999). Even a small amount of IL-13 is sufficient to mediate many of its *in vivo* effector functions. This may explain our findings in which IL-13 levels in Lck^{Cre}IL-4R$\alpha^{-/flox}$ mice are low, but granulomatous inflammation is highly increased and suggest that $CD4^+$ T cell-independent IL-4Rα expression is required for lung granuloma development.

CHAPTER 3

Schistosoma mansoni infection in hIL-4RαTg mice

Summary

Granuloma formation induced by schistosome eggs is a cell-mediated inflammatory response which has been shown to be associated with a dominant Th2-type 2 cytokine expression, tissue eosinophilia and high levels of serum IgE. The goal of this study was to determine the role of T-cell dependent IL-4 and IL-13 responsiveness with specific focus upon granuloma development. Two models, the live infection and induced synchronized lung granuloma models were used. In these studies, three strains of mice were used: BALB/c IL-4Rα$^{-/flox}$ (WT), IL-4Rα$^{-/-}$ and human IL-4Rα/mouse IL-4Rα$^{-/-}$ transgenic mice (hIL-4RαTg). The latter strain expresses the human IL-4R on a mouse IL-4Rα-deficient background specifically on T and B cells. Comparison of hepatic granulomas between WT and the mutant strains showed that the latter developed significantly smaller granulomas. Microscopic examination of hepatic granulomas showed an abrogation of eosinophil recruitment in IL4Rα$^{-/-}$ and hIL-4RαTg strains. Correspondingly, quantitation of liver collagen content in hepatic samples showed significantly reduced levels of hydroxyproline in IL-4Rα$^{-/-}$ mice and hIL-4RαTg mice samples. In contrast, granulomas that formed in WT mice were large with high numbers of mean eosinophils per granuloma and elevated levels of hydroxyproline. Analysis of the host's immune response to infection showed a clear default to type 1 antibody production, with elevated levels of antigen-specific IGg2a and IgG2b and low levels of IgG1 and total IgE. Similarly, cytokine analyses showed a predominantly Th1 cytokine profile with high levels of IFN-γ. Use of the induced synchronous pulmonary model to study granuloma development in the hIL-4RαTg mice showed similar results to those obtained during the live infection. Analysis of lung granulomas showed that granulomas that formed in IL-4Rα$^{-/-}$ and hIL-4 treated and non- treated hIL-4RαTg mice were equivalent to those of WT mice at day 7 post-challenge. However, they were significantly reduced at day 21 and day 28 post-challenge compared to WT controls. Similar to those in the live infection model, granulomas in the mutant strains were

devoid of eosinophils at day 7 after challenge. Although the numbers of eosinophils were slightly increased from day 14 to day 28, they were significantly few compared to controls. Correspondingly, hydroxyproline levels were similar between all groups at day 7 but were significantly increased at day 21 and day 28 with WT mice showing significantly elevated levels of hydroxyproline. In conclusion, the results of this study show that hIL-4RαTg mice have a similar immune profile as IL-4Rα$^{-/-}$ in response to *S. mansoni* infection and although granuloma development was significantly abrogated in these two strains it was not completely abolished. Likewise exogenous hIL-4 has no significant effect in driving the immune response towards T_H2/type-2 or in granuloma development of these mice. This may suggest that the dosage of hIL4 used was not adequate.

RESULTS

3.1 hIL-4RαTg mice develop T_H1/type1 immune responses against *S. mansoni* infection

The correlation between the development of schistosome egg-induced granulomas and the presence of Th2 cells in the granuloma has been established. Mice were percutaneously infected with a dose of 75 *S. mansoni* cercariae and the immune response analyzed to determine the role of T cell-dependent IL-4 and IL-13 responsiveness on granuloma development. The kinetics of T_H1 vs. T_H2 cytokine responses were determined from splenocytes and mesenteric lymph node (MLN) cell culture supernatants 7.5 weeks post-challenge. Stimulation of cells with anti-CD3 revealed a significant impairment ($p<0.01$) of Th2 cytokine responses (IL-4, IL-5, and IL-13) in both the IL-4Rα$^{-/-}$ and hIL-4RαTg mice (Figure 3.1A-C). In contrast, significantly higher levels of T_H1 cytokine IFN-γ were detected in the culture supernatants of IL-4Rα$^{-/-}$ and hIL-4RαTg mice (Figure 3.1D). WT MLN and splenocytes secreted high levels of the immunosuppressive cytokine IL-10 and significantly reduced levels of TGF-β (Figure 3.2). Conversely, IL-10 production was significantly abrogated in the mutant strains whereas TFG-β levels were increased.

The ability of hIL-4 to drive activation of TCRto Th2 differentiation has been shown (Seki, Miyazaki et al. 2004). We therefore determined the optimal dose of hIL-4 that could induce signalling through the chimeric hIL-4Rα in the mouse, and in order possibly to drive the immune response towards T_H2/type *in vivo*. Naïve hIL-4RαTg mice were treated with three injections of varying doses (10μg/ml 50μg/ml and 100μg/ml total protein) of human hIL-4 and total IgE serum levels determined at different intervals. A dose of 100μg/ml gave the highest levels of serum IgE and was subsequently used in infection studies (data not shown).

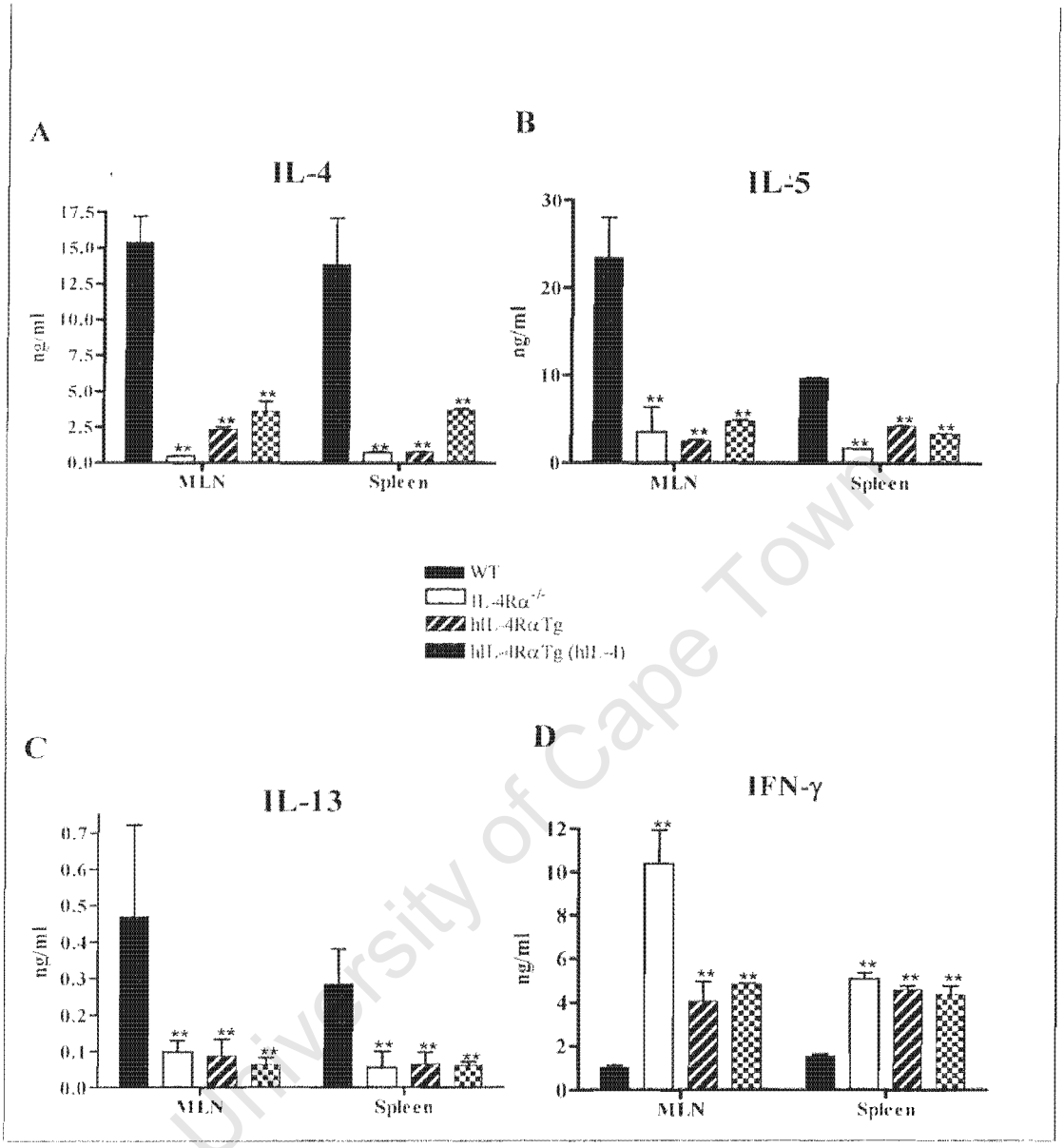

Figure 3.1

Cytokine levels in the cultures of mesenteric lymph node (MLN) and spleen cells of infected mice

Mice were acutely infected with 75 *S. mansoni* cercariae and T_H1 and T_H2 cytokine levels in MLN and spleen cells determined by ELISA. Each data point represents mean ± SD of triplicate samples. Results are representative of four similar experiments. (**) = $p<0.01$ by ANOVA compared to WT value.

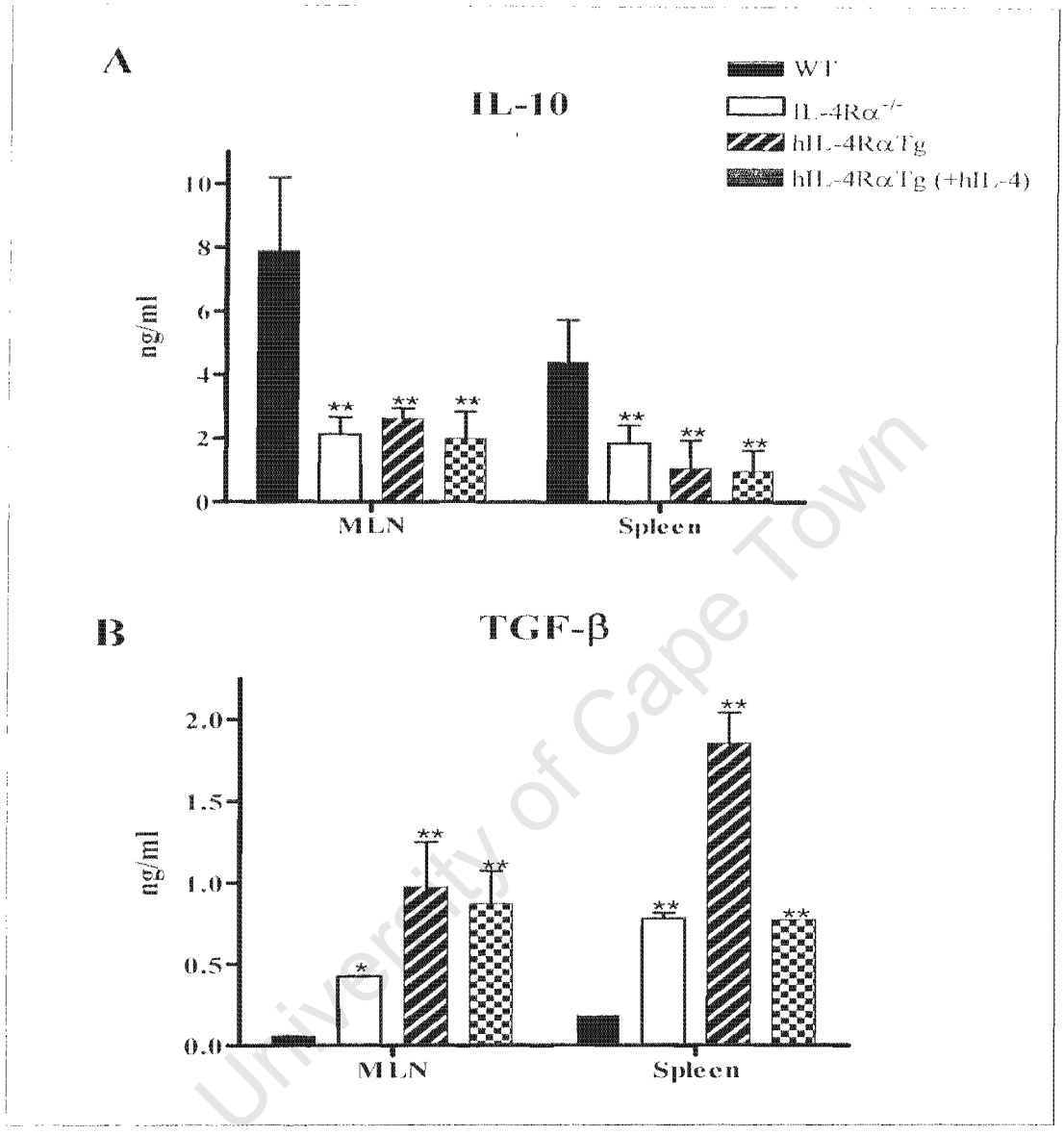

Figure 3.2

IL-10 and TGF-β levels in cultures of mesenteric lymph node (MLN) and spleen cells of infected mice

Mesenteric lymph nodes and splenocytes of acutely infected mice were stimulated with α-CD3 for 72 hours and measurement of IL-10 and TGF-β levels in supenatants determined by ELISA. Each data point represents the average ± SD of triplicate serum samples. The results are representative of four similar experiments. (*) = $p<0.05$ and (**) = $p<0.01$ by ANOVA compared to the WT value

Treatment of hIL-4RαTg mice with hIL-4 induced a slight increase production of IL-4 in MLN and splenocyte cultures, whereas there were no observable changes in other cytokine levels (Figure 3.1) Concurrently, there was a slight reduction in IL-10 levels and a significant decrease in TGF-β in the splenocyte cultures of treated animals (Figure 3.2).

Profiles of antibody production were assessed in sera of infected mice using SEA-specific ELISA. Measurement of SEA-specific antibody response showed a significant rise of type 1 (IgG2a and IgG2b) levels in both mutant strains (Figure 3.3A & B) and a significant abrogation of type 2 (IgG1 and IgE) (Figure 3C & D) antibody production. In contrast, levels of IgG1 and total IgE were significantly elevated in WT mice, whereas IgG2a and IgG2b levels were abrogated. Similar to other mutant strains, hIL-4 treated transgenics also had elevated levels of type 1 (Figure 3.3A & B) and abrogated levels of type 2 (Figure 3.3C & D) antibody production.

3.2 Hepatic granuloma formation in hIL-4RαTg mice is significantly abrogated

To assess granuloma development, liver granuloma sizes and cellular composition were compared among the groups 7.5 weeks post-infection. Hepatic granulomas that developed in hIL-4RαTg mice and IL-4Rα$^{-/-}$ mice were significantly smaller than WT lesions ($p<0.001$) (Figure 3.4 and Figure 3.5) compared to their WT littermates. Similarly, granuloma sizes in treated hIL-4RαTg mice were also significantly abrogated ($p<0.001$) although slightly larger than in their non-treated littermates. Quantitation of granuloma eosinophils showed significantly reduced numbers ($p<0.001$) of mean eosinophils per granuloma in IL-4Rα$^{-/-}$ (9 ± 6) and hIL-4RαTg (7 ± 4) mice compared to WT (200 ± 72) mice. Accordingly, quantification of hydroxyproline, as a measure of collagen deposition in the liver, showed a significant abrogation ($p<0.001$) of granuloma collagen in the mutant strains compared to controls (Figure 3.6 and Figure 3.7).

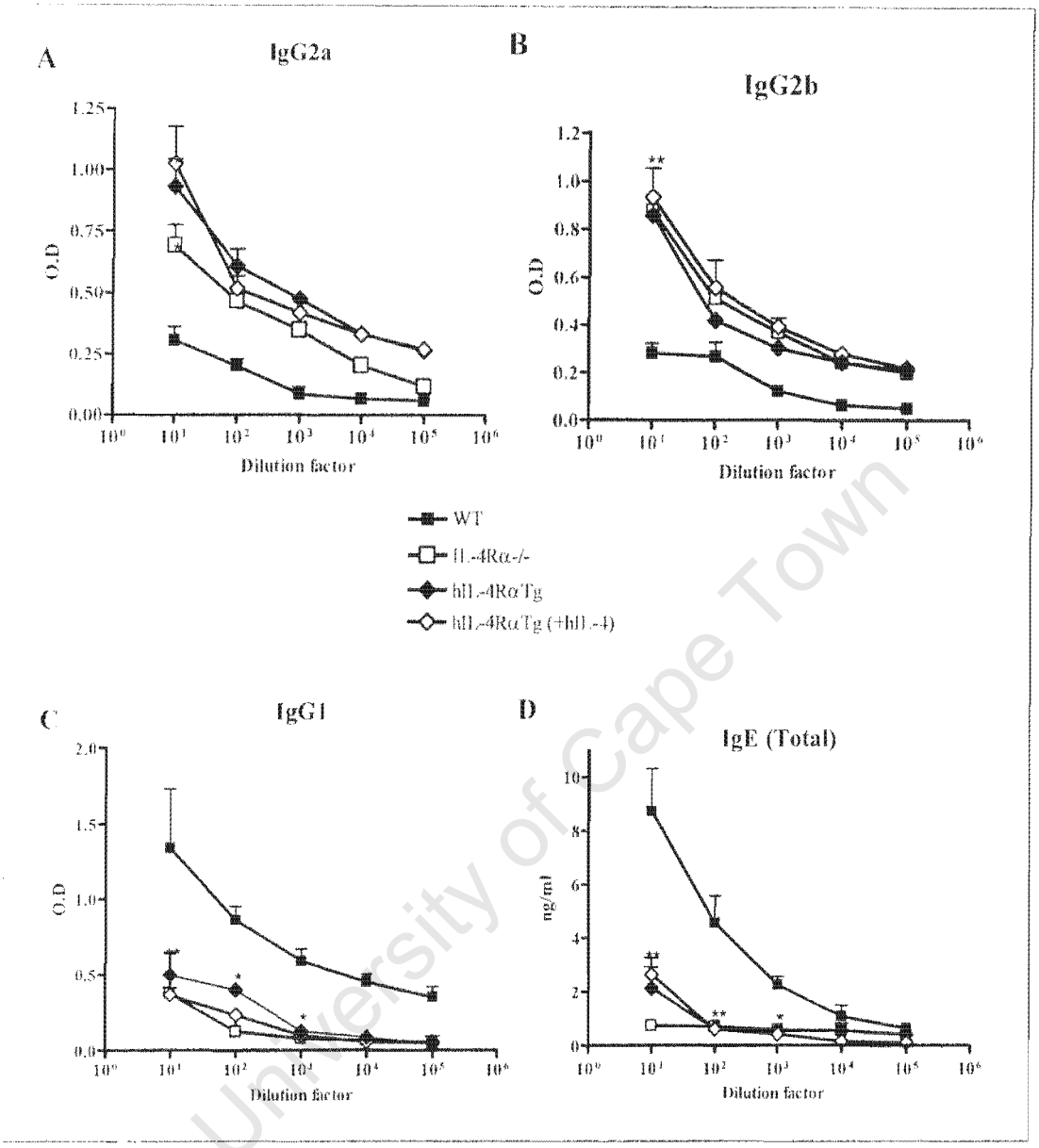

Figure 3.3

Enhanced type 1 antibody levels in acutely infected hIL-4RαTg mice

SEA-specific Type 1 (A & B) vs. type 2 (C & D) antibodies were analysed in the sera of infected mice by ELISA. Panel D represents total serum IgE levels. Each data point represents the average ± SD of triplicate serum samples. Results are representative of four similar experiments. (*) = $p<0.05$ and (**) = $p<0.01$ by ANOVA in comparison to WT value

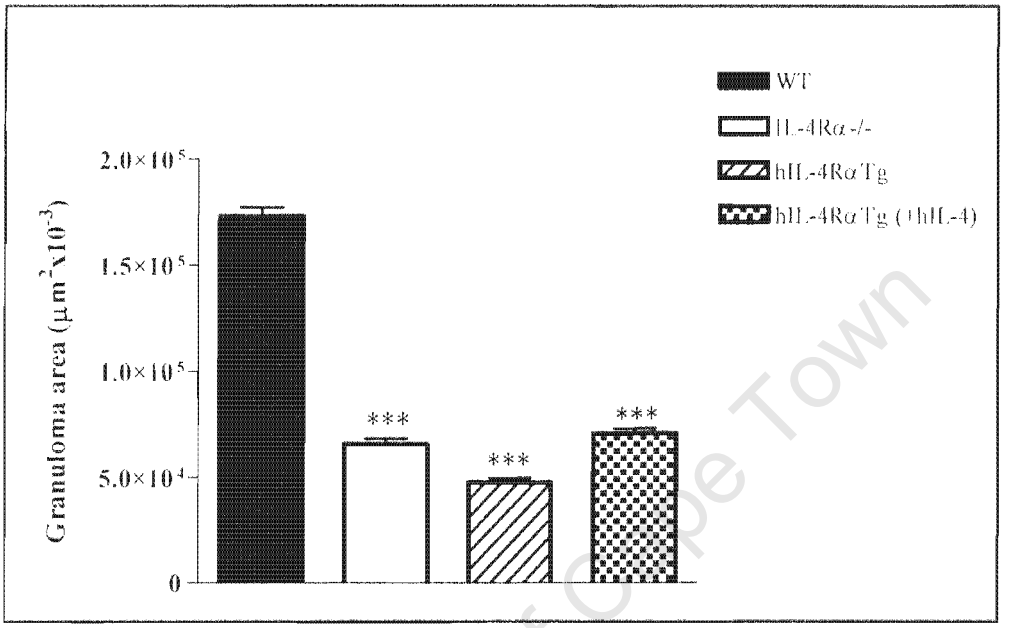

Figure 3.4

Abrogated hepatic granuloma development in S. mansoni infected hIL-4RαTg mice. Livers were obtained from acutely infected mice and processed for histology as described in Materials and Methods. Hepatic granuloma sizes were determined from histological sections using computerized morphometry analysis program. An average of 250 granulomas per strain was included in the analysis. Data are representative of four similar analyses. (**)= $p<0.001$ by ANOVA in comparison to WT

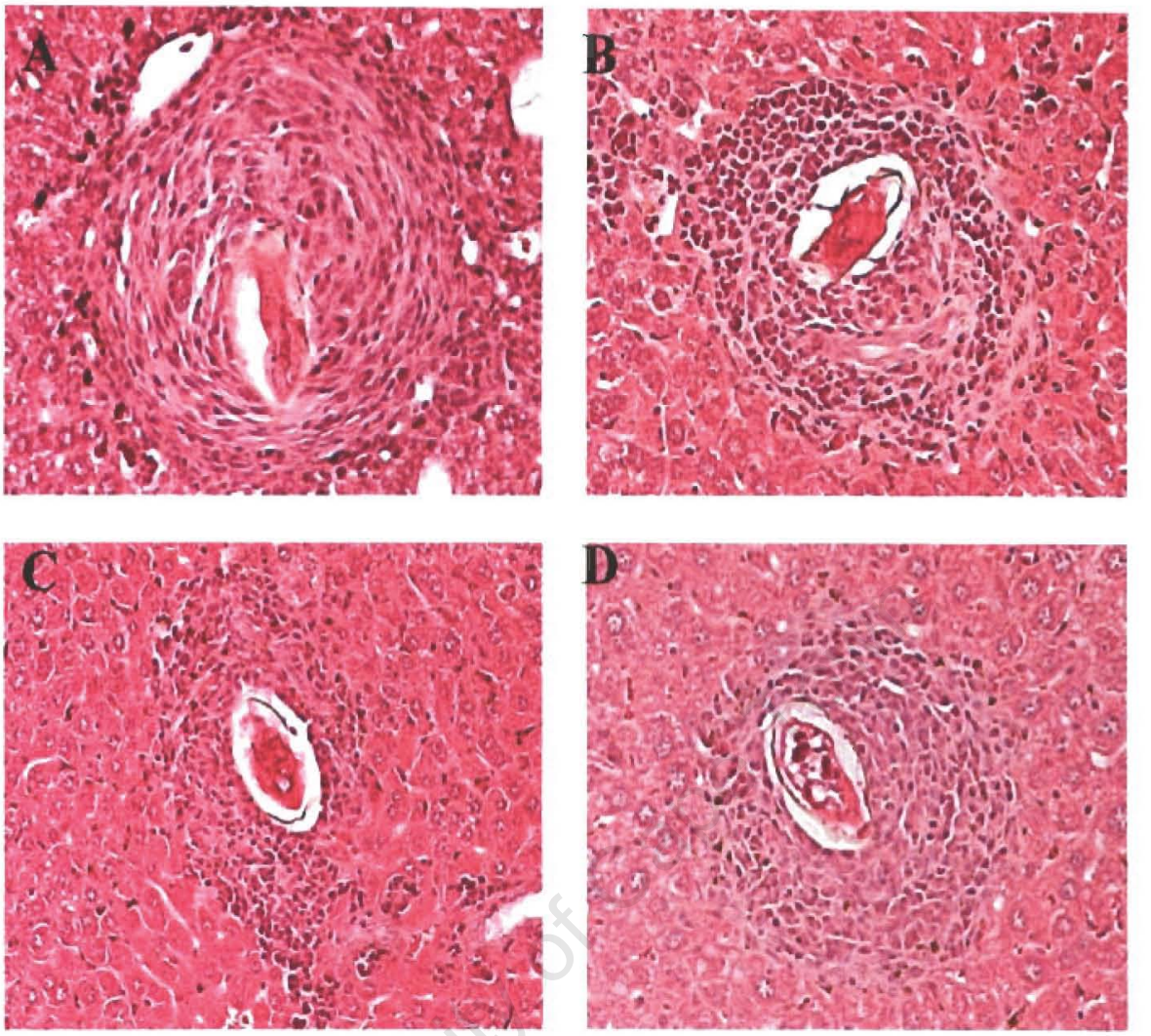

Figure 5

H&E staining of hepatic granuloma in IL-4Rα$^{-/-}$ and hIL-4RαTg mice

Livers were removed from *S. mansoni* infected mice and fixed in PBS buffered formalin. Paraffin embedded tissues were sectioned at 5μm and stained with hematoxylin and eosin.

A) IL-4Rα$^{-/flox}$ (WT)

B) IL-4Rα$^{-/-}$

C) hIL-4RαTg

D) hIL-4RαTg (+hIL-4 treatment) (Magnification = 100x)

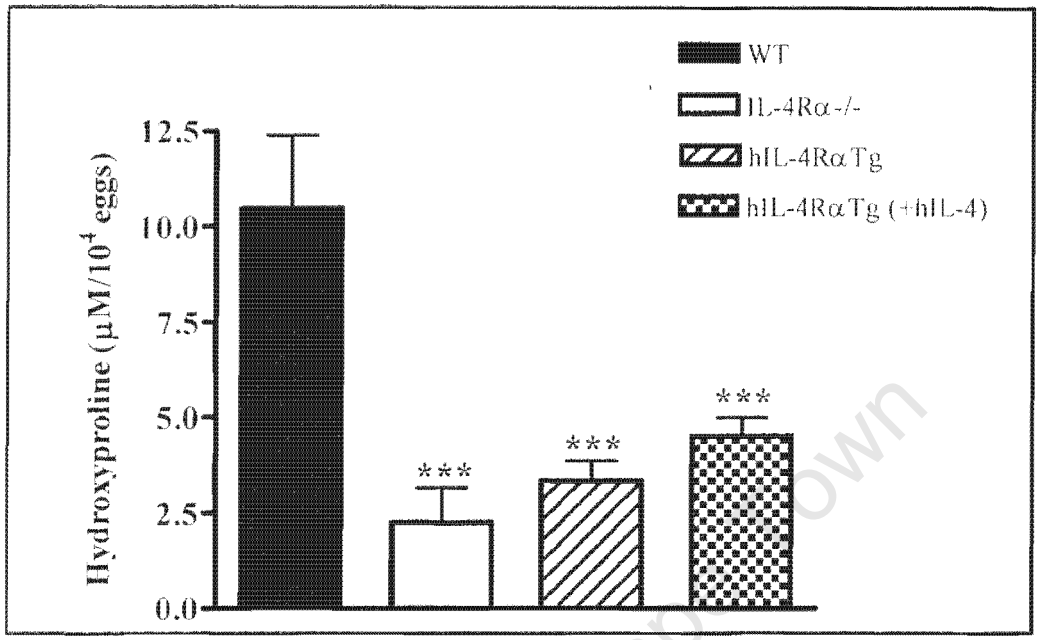

Figure 3.6

Reduced hepatic collagen deposition in the livers of infected hIL-4RαTg mice

Hydroxyproline levels, as an indicator of collagen deposition, was measured in liver tissue as described in the Materials and Methods. Data are representative of 4 similar analyses. ** $p<0.001$ by ANOVA in compared to WT

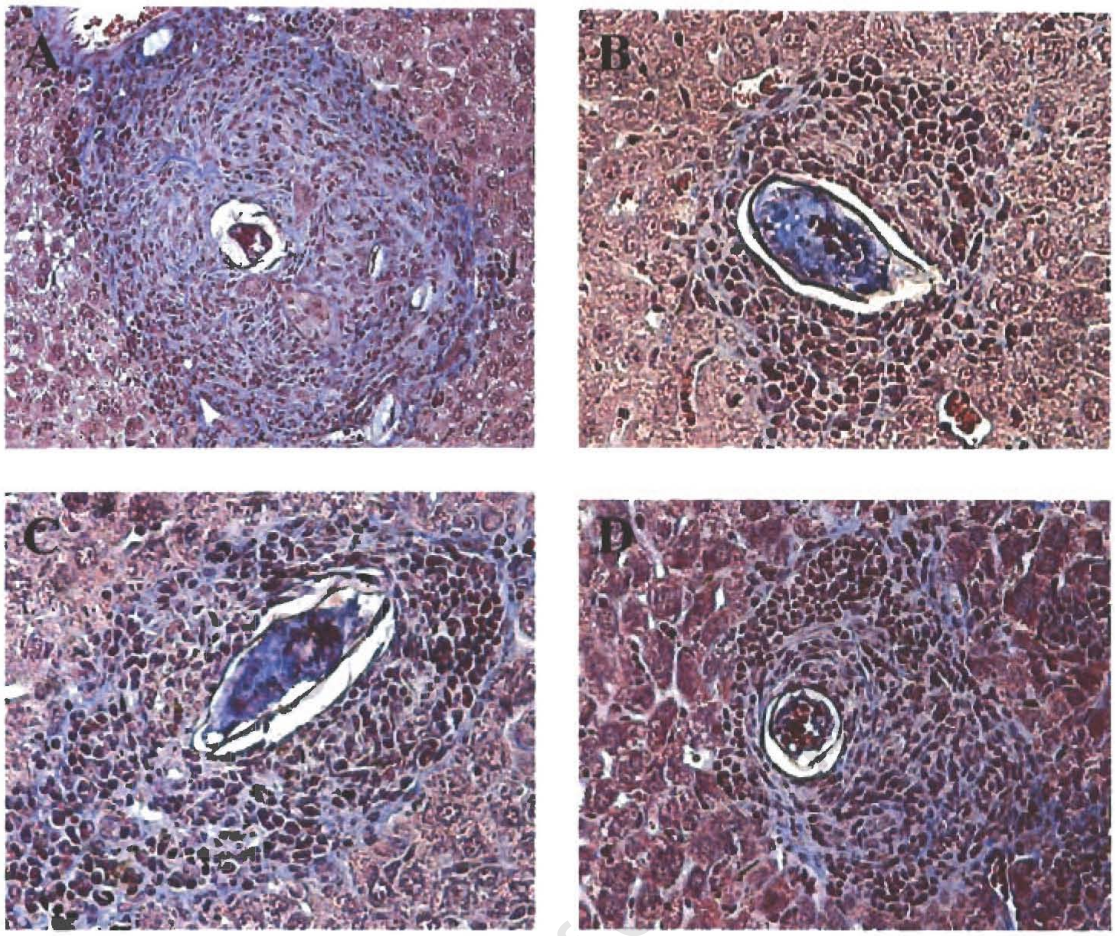

Figure 7

Reduced collagen deposition in granulomas of IL-4Rα$^{-/-}$ and hIL-4RαTg mice

Livers of acutely infected IL-4Rα$^{-/flox}$ (WT) (A), IL-4Rα$^{-/-}$ (B), hIL-4RαTg (C) and hIL-4 treated hIL-4RαTg (D) mice were processed for histology as described in materials and methods and stained with CAB. (Magnification = 100x)

3.3 hIL-4RαTg mice are highly susceptible to acute *S. mansoni* infection

The importance of type 2 immune responses in protection against *S. mansoni* infection has been shown in mouse studies and corroborated by human studies of patients of hepatosplenic schistosomiasis (Dunne and Pearce 1999; Hoffmann, James et al. 1999; de Jesus, Silva et al. 2002). We assessed the effect the observed immune response has on the survival of mice with lymphocyte reconstitution of hIL-4Rα during infection with *S. mansoni*. IL-4Rα$^{-/flox}$, IL-4Rα$^{-/-}$ and hIL-4RαTg (8 mice per strain) were percutaneously infected with 75 *S. mansoni* cercariae and their rate of mortality recorded. Results show that hIL-4RαTg mice as well as IL-4Rα$^{-/-}$ mice were highly susceptible and succumbed to *S. mansoni* infection by week 7.5 in contrast to their WT littermates that had more than 50% survival rate beyond acute infection (week 6-8 post infection) (Figure 3.8A).

Rapid weight loss is a well documented symptom of patients with chronic schistosome infections. To determine whether a correlation exists between mortality and weight loss, morbidity rates were monitored from week 5 post-infection. There was a clear correlation between mortality and weight loss in infected hIL-4RαTg mice and IL-4Rα$^{-/-}$ mice with both strains of animals showing more than 20% loss of body weight by 7 weeks post infection (Figure 3.8B).

3.4 hIL-4 treatment has no significant effect on the survival of hIL-4RαTg mice

To determine whether hIL-4 treatment has any effect on the survival rate of hIL-4RαTg mice during *S.mansoni* infection, a group of acutely infected hIL-4RαTg mice were treated with three doses of 100µg/ml hIL-4(total protein) at week 5, week 5.5 and week 6 post-infection. Human IL-4 treated mice were highly susceptible to infection and succumbed to infection with the same kinetics as their non-treated littermates (Figure 3.8A).

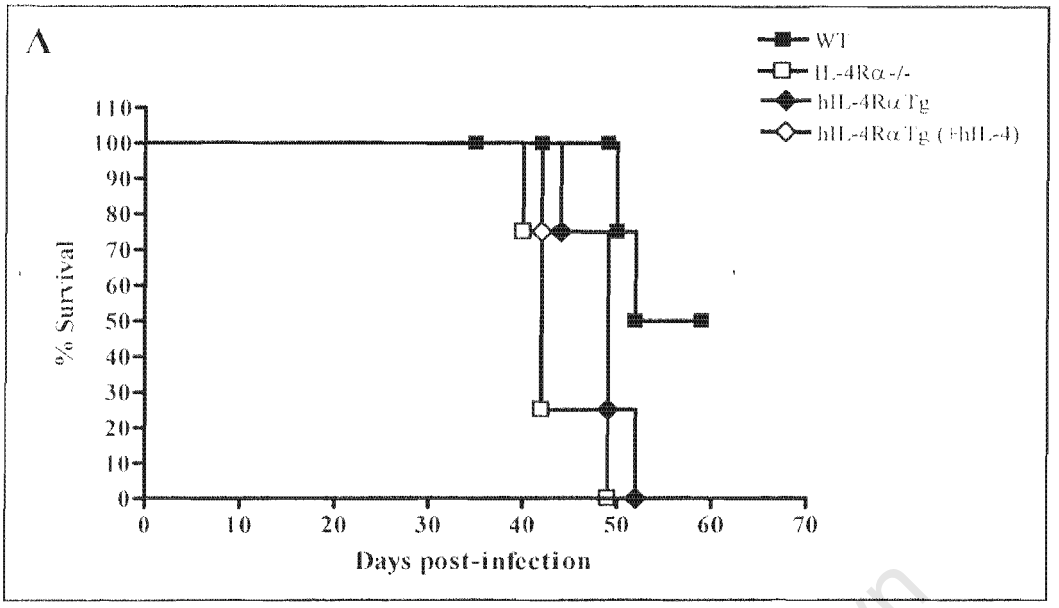

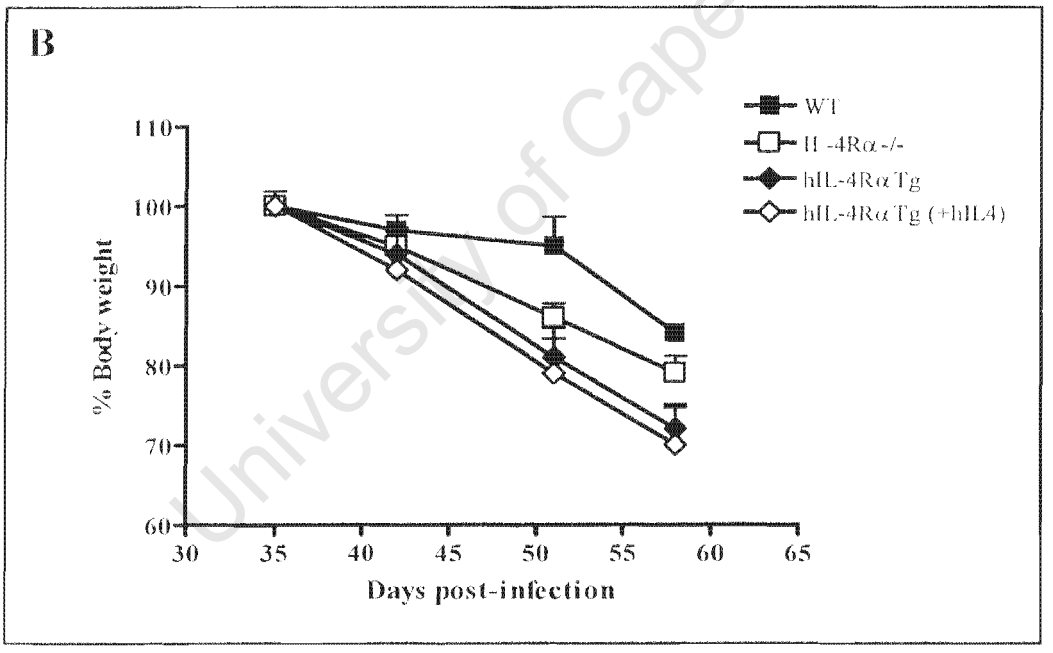

Figure 3.8

Mortality and morbidity rates in S. manson- infected mice.

Mice were percutaneously challenged with a dose of 75 *S. mansoni* cercariae and monitored for mortality (A) and morbidity (B) rates. The results are representative of 4 similar experiments (n =6- 8 mice/strain).

Similarly, treatment did not seem to have any significant effect on weight loss as there were no significant differences in body weight loss between the treated and non-treated transgenic mice as well as IL-4Rα$^{-/-}$ mice (Figure 3.8B). Accordingly, WT mice lost little weight over the course of infection, whereas the mutant strains experienced severe cachexia.

3.5 Death of hIL-4RαTg mice correlates with liver damage and severe gut pathology

To determine the cause of death in hIL-4RαTg mice a post-mortem analysis was made at termination of the study. Macroscopic examination of infected mice revealed a severe multi-organ pathology that involved liver degeneration, spleen atrophy, and marked swollen small intestines that was hemorrhagic and oedematous affecting the distal jejunum and ileum (Figure 3.9).

To asses the extent of hepatocellular damage, due to eggs trapped in the sinusoids, serum aspartate aminotrasferase (AST) was measured as an indicator of overall morbidity. hIL-4RαTg as well as IL-4Rα$^{-/-}$ mice produced 4-fold and 2-fold higher amounts of this enzyme than controls ($p<0.05$) respectively (Figure 3.10A). On the contrary, treatment of the transgenic strain with hIL-4 showed a decrease in the amounts of AST, although not significant (Figure 3.10A). Consequently, the mutant strains showed a severe abrogation of faecal egg excretion at week 7 post-infection On the contrary, there was a high rate of egg excretion in WT mice (Figure 3.10B).

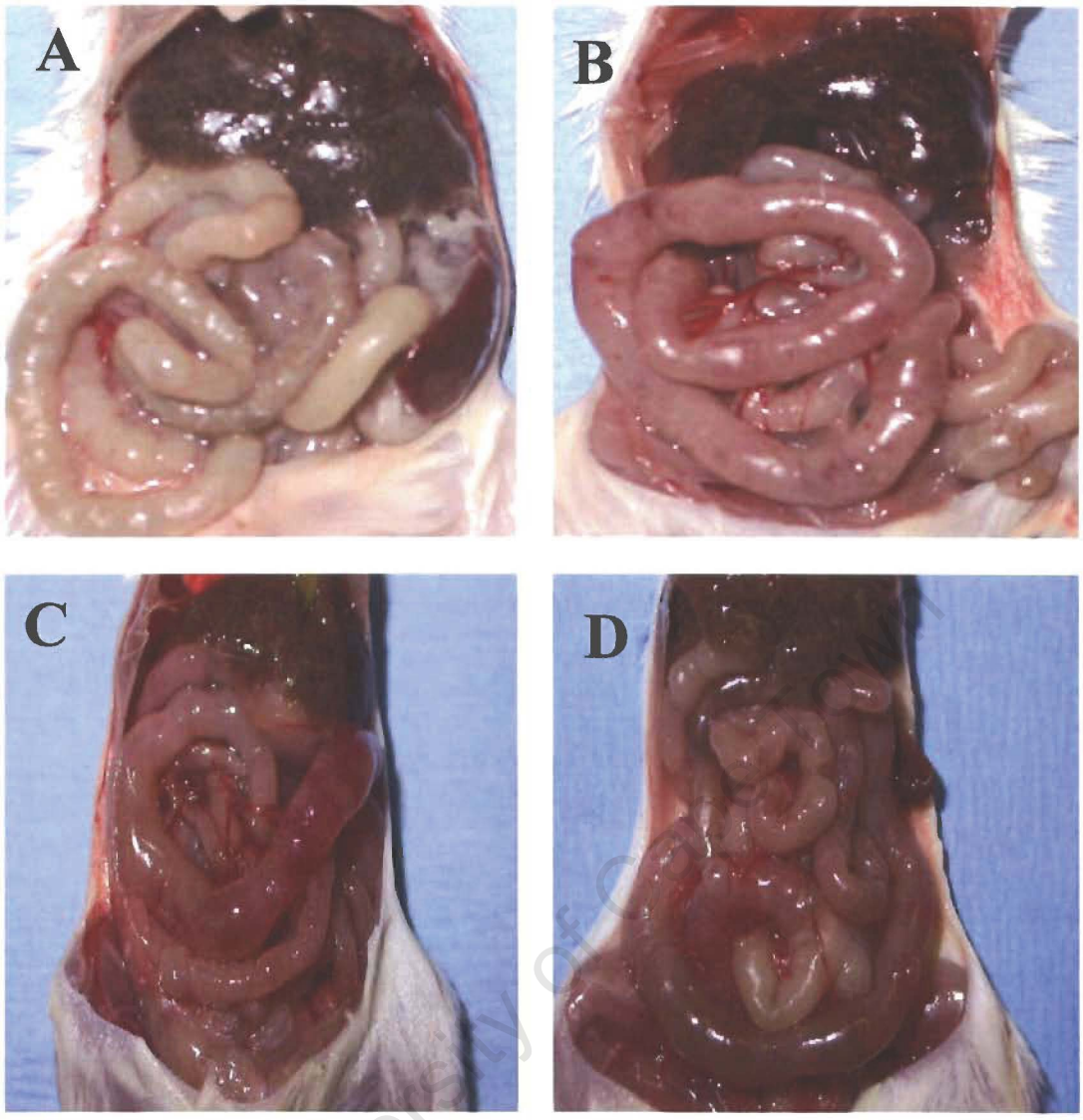

Figure 9

Excessive gut pathology in schistosome infected IL-4Rα$^{-/-}$ and hIL-4RαTg mice

Mice were infected with a dose of 75 *S. mansoni* cercariae and analyzed for pathology at termination of the experiment.

A- IL-4Rα$^{-/flox}$

B- IL-4Rα$^{-/-}$

C- hIL-4RαTg

D- hIL-4RαTg +100μg/ml hIL-4

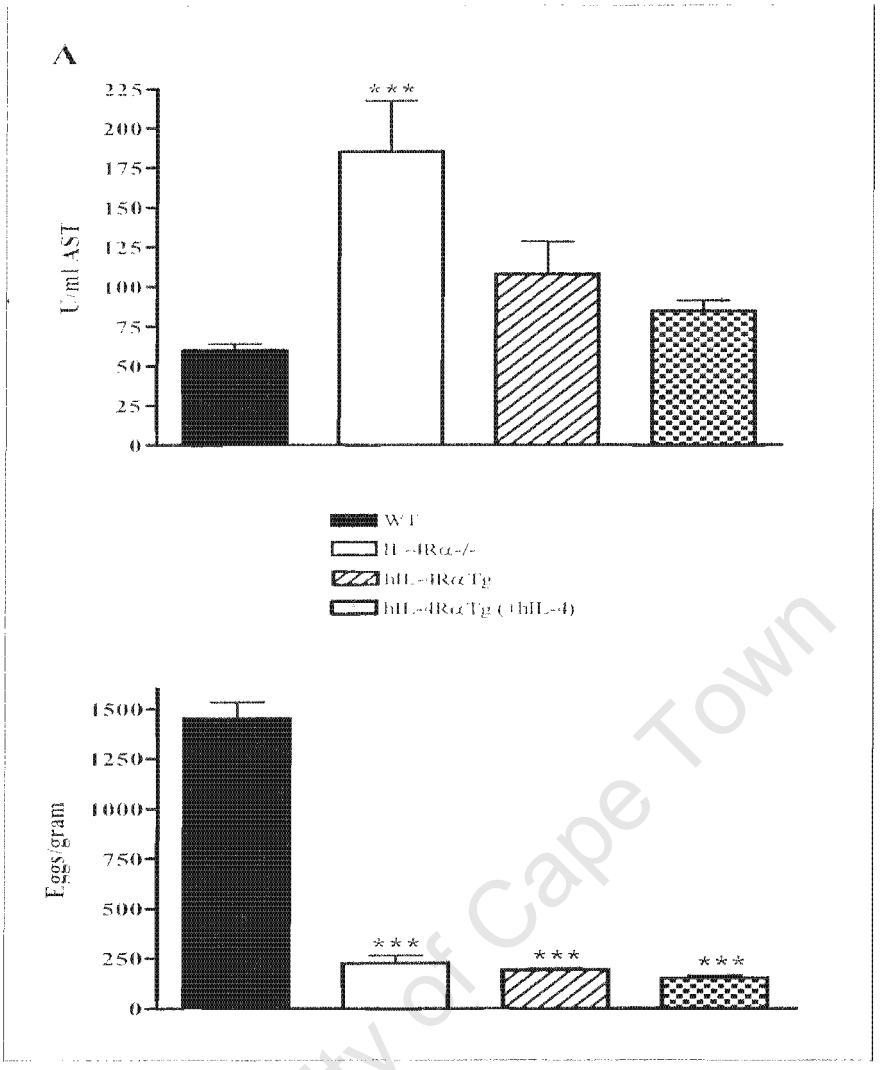

Figure 3.10

Hepatocellular damage and faecal egg outputs

Levels of aspartate amino-transaminase (AST), as an indicator of liver damage, were measured in sera of acutely infected mice (A). Faecal egg output (B) was determined from faecal samples at week 7.5 post-infection. Data are mean ± SD and are representative of four similar analyses. (**)= $p<0.001$ by ANOVA compared to IL-WT

3.6 Lung granuloma development is severely abrogated in hIL-4RαTg mice

It has previously been established that a protective immune response against *S. mansoni* egg-induced pathology is dependent on the host's ability to form granuloma that are well defined. Experiments were conducted to determine the role of lymphocyte specific interleukin IL-4 and IL-13 responsiveness during lung granuloma formation in WT, IL-4Rα$^{-/-}$, hIL-4RαTg, and hIL-4RαTg mice treated three times with 100μg/ml of human IL-4 (hIL-4RαTg + hIL-4). Groups of 12 -16 mice per strain mice were sensitized with live 5000 *S. mansoni* eggs intraperitoneally (i.p). Fourteen days post-sensitization all mice were intravenously challenged with 5000 live parasites eggs via the tail vein. Three to four mice from each group were killed at 7, 14, 21 and 28 days post challenge and lung granuloma development characterized by comparing granuloma sizes and cellular composition between the groups.

Results from four independent experiments showed no significant difference in pulmonary granuloma sizes between hIL-4RαTg mice (17.5μm^{2}x10^{-3} ± 10), and WT mice (21.56μm^{2}x10^{-3} ± 9.7) at day 7 post-challenge (Figure 3.11 and Figure 3.12). There was a significant abrogation in granuloma development at day 14 post-challenge in hIL-4RαTg mice (18μm^{2}x10^{-3} ± 9) and IL-4Rα$^{-/-}$ (21μm^{2}x10^{-3} ±9.7) compared to WT (40μm^{2}x10^{-3} ± 15) mice ($p<0.001$). The peak of granuloma development in WT and mutant mice was reached at day 21 with granulomas that developed in hIL-4RαTg mice (30μm^{2}x10^{-3} ± 9.4), and in IL-4Rα$^{-/-}$ mice (31μm^{2}x10^{-3} ± 12) significantly reduced compared to WT (93.2μm^{2}x10^{-3} ± 38)($p<0.001$). Similarly, granuloma sizes in hIL-4RαTg (the mutants was significantly abrogated at day 28 post-challenge compared to WT ($p<0.001$).

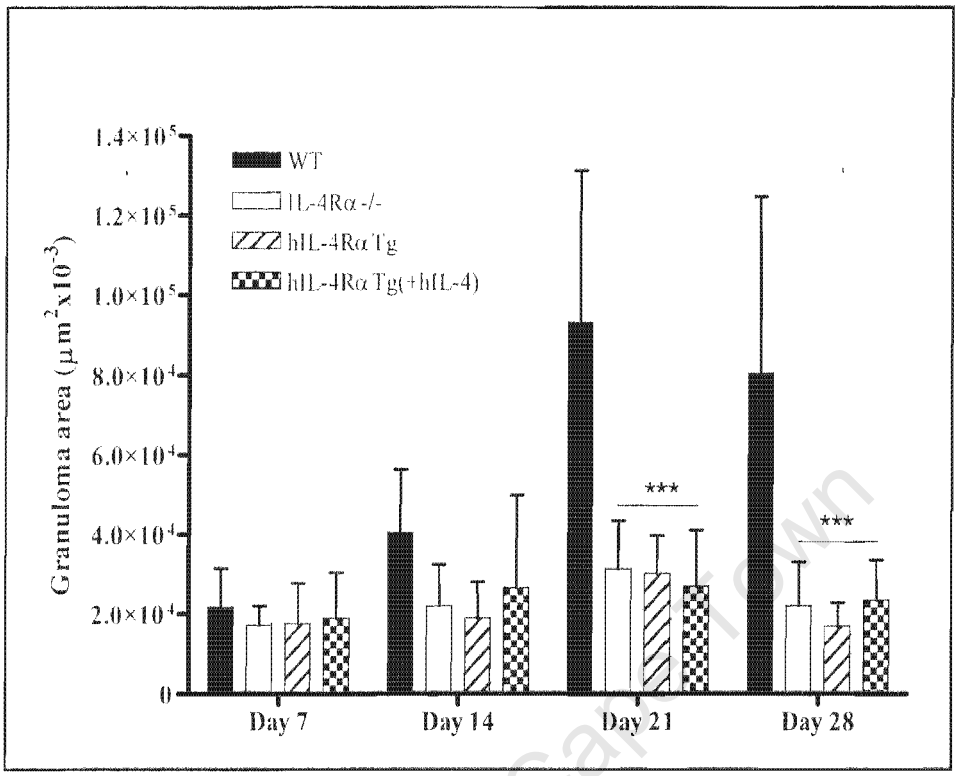

Figure 3.11

Pulmonary granuloma development in egg-challenged mice

Lungs were obtained from egg-challenged mice and processed for histology. Pulmonary granuloma sizes were determined from histological sections using computerized morphometry analysis program. An average of 50 granulomas per mouse was included in the analysis. Data are mean ± SD and are representative of four similar studies. *** $p<0.001$ by ANOVA compared to WT value

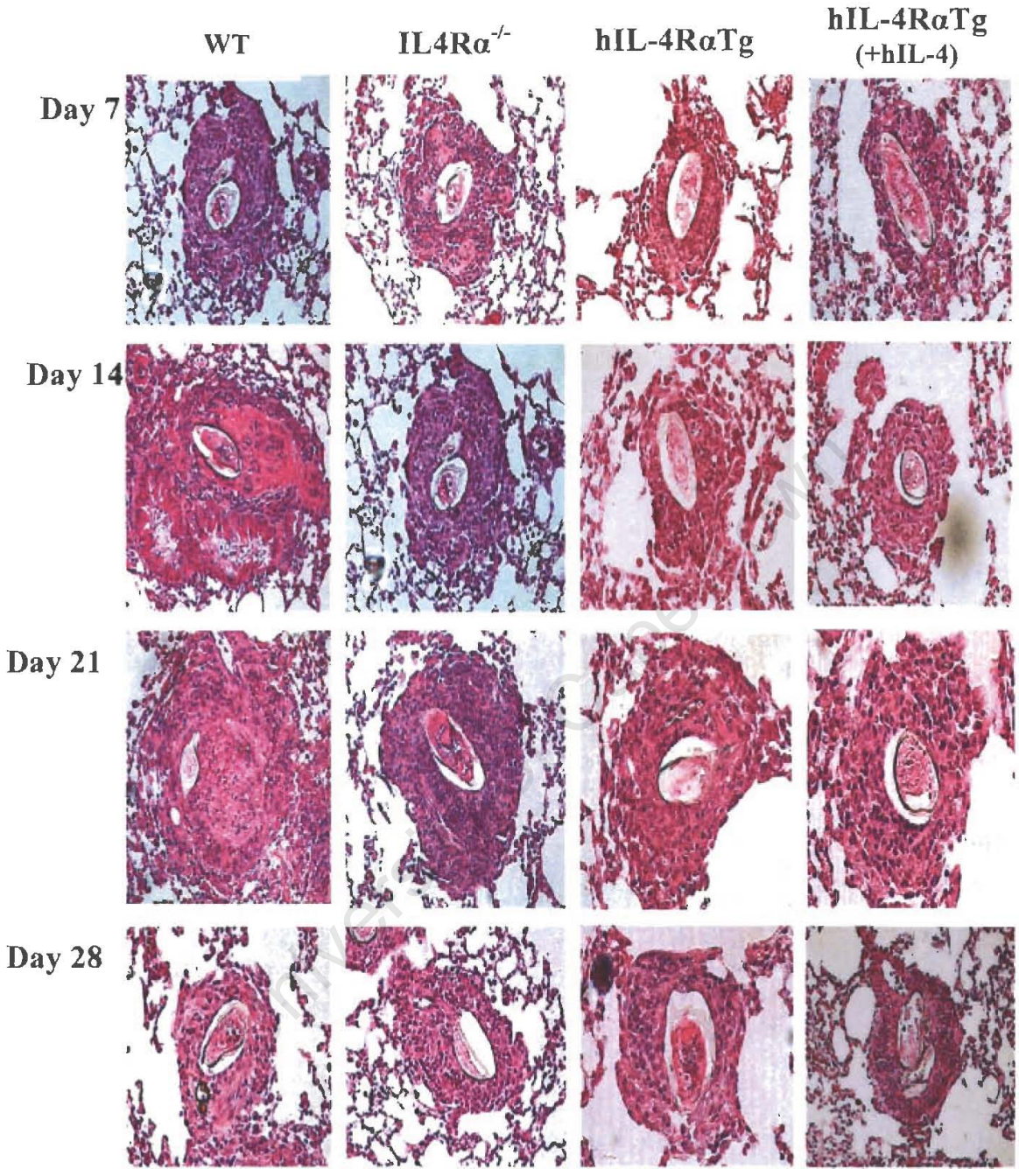

Figure 12

H&E staining of pulmonary granulomas in egg-challenged mice

Mice were sensitized with live eggs i.p and later challenged with live eggs i.v. Mice were sacrificed at day 7, 14, 21 and 28 and lungs removed. Paraffin embedded lungs were sectioned at 5μm and stained with H & E. sections are representative of 4 mice per strain at each time point. (magnification =200x)

Treatment of hIL-4RαTg mice with human IL-4 showed no significant effect on granuloma sizes between the treated ($18\mu m^2x10^{-3} \pm 11$) and non-treated ($17.5\mu m^2x10^{-3} \pm 10$) at day 7 post-challenge (Figure 3.12). Conversely, at day 14 post-challenge, granuloma sizes in treated hIL-4RαTg mice ($27\mu m^2x10^{-3}$ ±13) were significantly increased compared to their non-treated littermates ($18\mu m^2x10^{-3} \pm 9$)($p<0.001$). Similar to WT mice, granuloma sizes reached their peak at day 21 post-challenge in hIL-4RαTg mice. However, comparison of granuloma sizes between hIL-4 treated ($27\mu m^2x10^{-3} \pm 14$) and non-treated ($30\mu m^2x10^{-3} \pm 9.4$) hIL-4RαTg mice, showed no significant difference in granuloma sizes. Similarly at day 28 post-challenge, there was no significant differences in granuloma sizes of treated versus non-treated hIL-4RαTg mice (Figure 3.11 and 3.12).

To further characterize granuloma development in hIL-4RαTg mice, collagen deposition in the granuloma was quantitated from CAB-stained histological sections and acid-hydrolysed lung samples by measuring levels of hydroxyproline. WT, IL-4Rα$^{-/-}$ and hIL-4RαTg mice had similar levels of hydroxyproline at day 7 post-challenge. Conversely, at day 14 post-challenge, hydroxyproline levels were reduced in the mutant strains compared to WT controls (Figure 3.13 and Figure 3.14). Similarly, hydroxyproline levels in WT mice were significantly increased whilst they remained significantly reduced in the mutants at day 21 and 28 post-challenge ($p<0.001$). Quantitation of collagen content showed similar levels of hydroxyproline were produced at day 7, 14, and 21, by both the treated and non-treated hIL-4RαTg mice, although the levels were slightly higher in the treated mutants (Figure 3.13). Conversely, at day 28 post-challenge, hydroxyproline levels were significantly increased in hIL-4-treated hIL-4RαTg mice compared to their non-treated littermates ($p<0.05$).

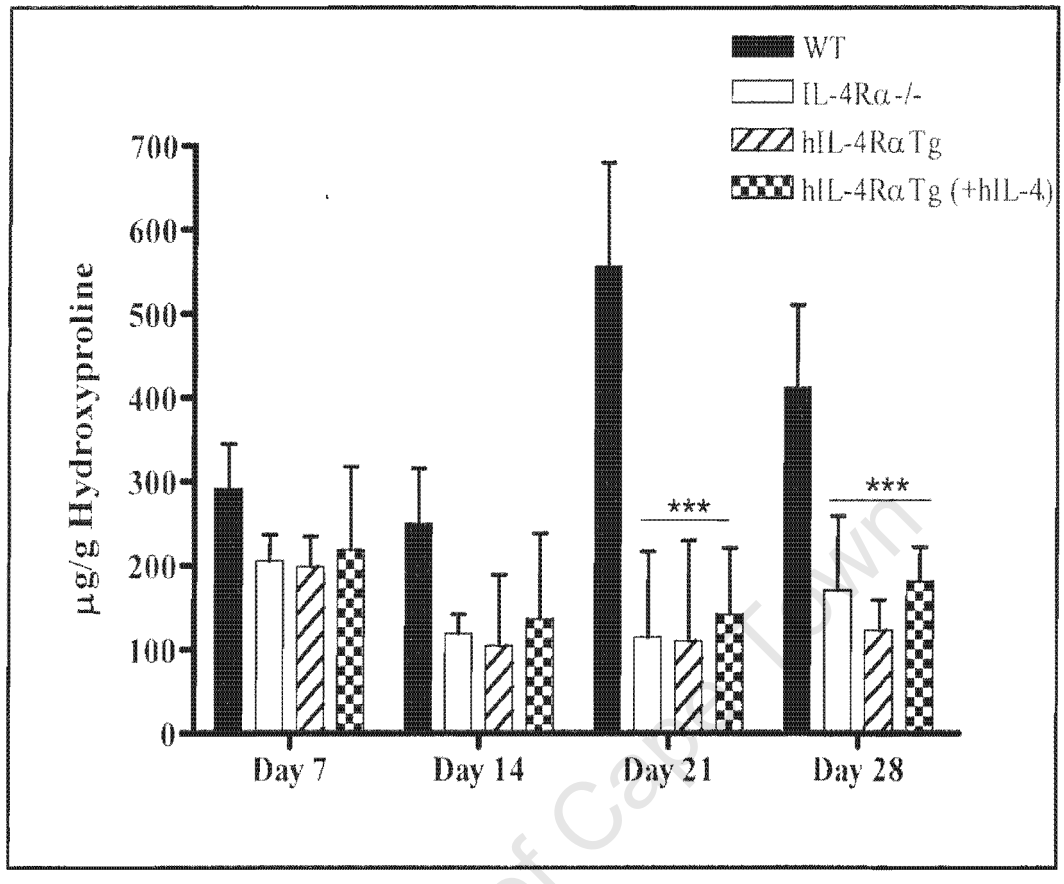

Figure 3.13

Hydroxyproline levels in the lungs of egg-challenged mice

Lungs were obtained from egg-challenged mice and processed for hydroxyproline assay. Hydroxyproline levels were measured from acid hydrolyzed lung sections at indicated time points. Data represents one of four similar experiments. (***) = $p<0.001$ by ANOVA compared to WT.

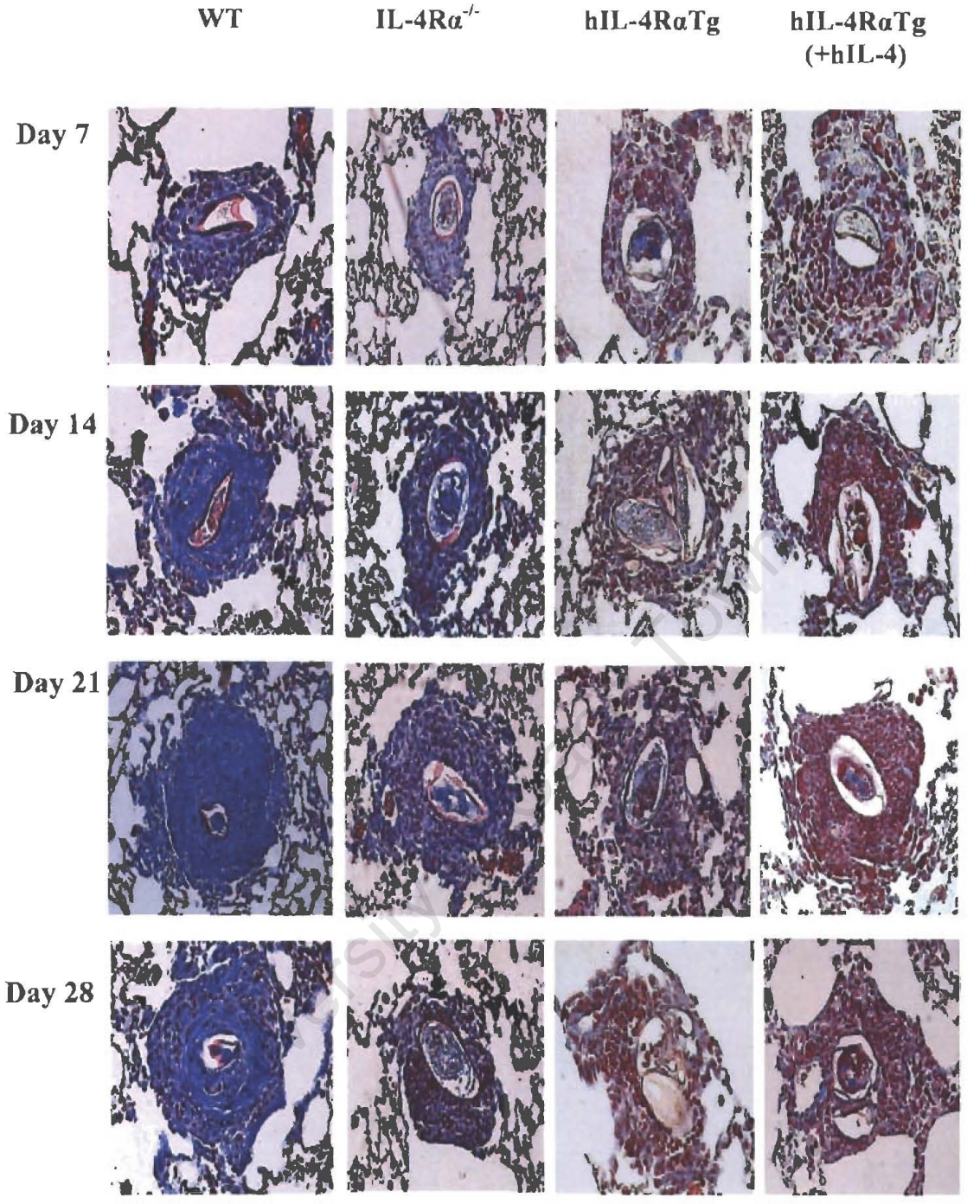

Figure 14

Collagen deposition in the lungs of hIL-4RαTg mice

Paraffin embedded tissue from sensitized, egg-challenged mice were sectioned and stained with CAB as described in Materials and Methods. Sections are representative of 3-4 mice per strain at each time point. (Magnification =200x).

3.7 Eosinophil recruitment is abrogated in granulomas of hIl-4RαTg mice

Closer examination of cellular recruitment in the resulting lung granulomas showed a complete abrogation of eosinophil recruitment per granuloma in the mutant strains on days 7 and 14 post-challenge (Table I) in comparison to WT mice ($p<0.001$). The peak number of granuloma eosinophils was observed at day 21 in WT mice. Similarly, the number of granuloma eosinophils in the mutant strains also peaked at day 21, with IL-4Rα$^{-/-}$ mice showing slightly higher numbers of eosinophils per granuloma compared to hIL-4RαTg mice, although the numbers were significantly lower compared to WT mice ($p<0.001$). There was, however, no difference in the number of granuloma eosinophils between the treated and non-treated hIL-4RαTg mice at days 7, 14 21 and 28 (Table I).

On the other hand, examination of PAS stained lung sections for mucus producing cells, showed no presence of PAS positive cells in the granuloma of gene deficient mice as compared to WT animals at all time points (Table I and Figure 3.15)($p<0.001$).

3.8 hIL-4RαTg mice develop T_H1/type1 immune response against *S. mansoni* egg deposition

Lung homogenates, mediastinal lymph nodes and splenocyte responses in WT, IL-4Rα$^{-/-}$as well as in hIL-4-treated and non-treated hIL-4RαTg mice were analyzed at each time point post-egg challenge for cytokine production. Four independent experiments show that analyzed cytokine levels in lung homogenates showed significantly impaired levels of T_H2 cytokines (IL-4, IL-5 and IL-13) and an enhanced production of the T_H1 cytokine, IFN-γ, in both IL-4Rα$^{-/-}$ and hIL-4RαTg mice at all four time points (Figure 3.16).

Table I

Reduced granuloma eosinophils and PAS positive cells in hIL-4RαTg mice

Eosinophils were counted from H & E stained lung sections using a light microscope under oil immersion at 100x magnification. 50 granulomas from each mouse were included in the analysis. Mucus producing (PAS positive) cells were quantified from lung sections stained with PAS using a light microscope at 100x magnification. Data represent the mean ± SD. The result represents one of four independent experiments. (***) = $p<0.001$ by ANOVA compared to WT

		IL-4Rα^{-} /flox	IL-4Rα$^{-/-}$	hIL-4RαTg	hIL-4RαTg (+hIL-4)
Day 7	**Eosinophils**	13 ±6.5	0.00 ± 0.00***	0.00 ± 0.00***	0.00 ± 0.00***
	PAS+ve	21 ± 17.85	0.00 ± 0.00***	0.00 ± 0.00***	0.00 ± 0.00***
Day 14	**Eosinophils**	28 ± 12.3	3 ± 1.87***	2 ± 1.12***	2 ± 1.01***
	PAS+ve	28 ± 13.25	0.00 ± 0.00***	0.00 ± 0.00***	0.00 ± 0.00***
Day 21	**Eosinophils**	37 ± 15.6	7 ± 5.2***	5 ± 3.6***	5 ± 3.3***
	PAS+ve	51 ± 11.95	0.00 ± 0.00***	0.00 ± 0.00***	0.00 ± 0.00***
Day 28	**Eosinophils**	24 ± 8.4	2 ± 1.03***	3 ± 2.1***	2 ± 1.2***
	PAS+ve	40 ± 9.68	0.00 ± 0.00***	0.00 ± 0.00***	0.00 ± 0.00***

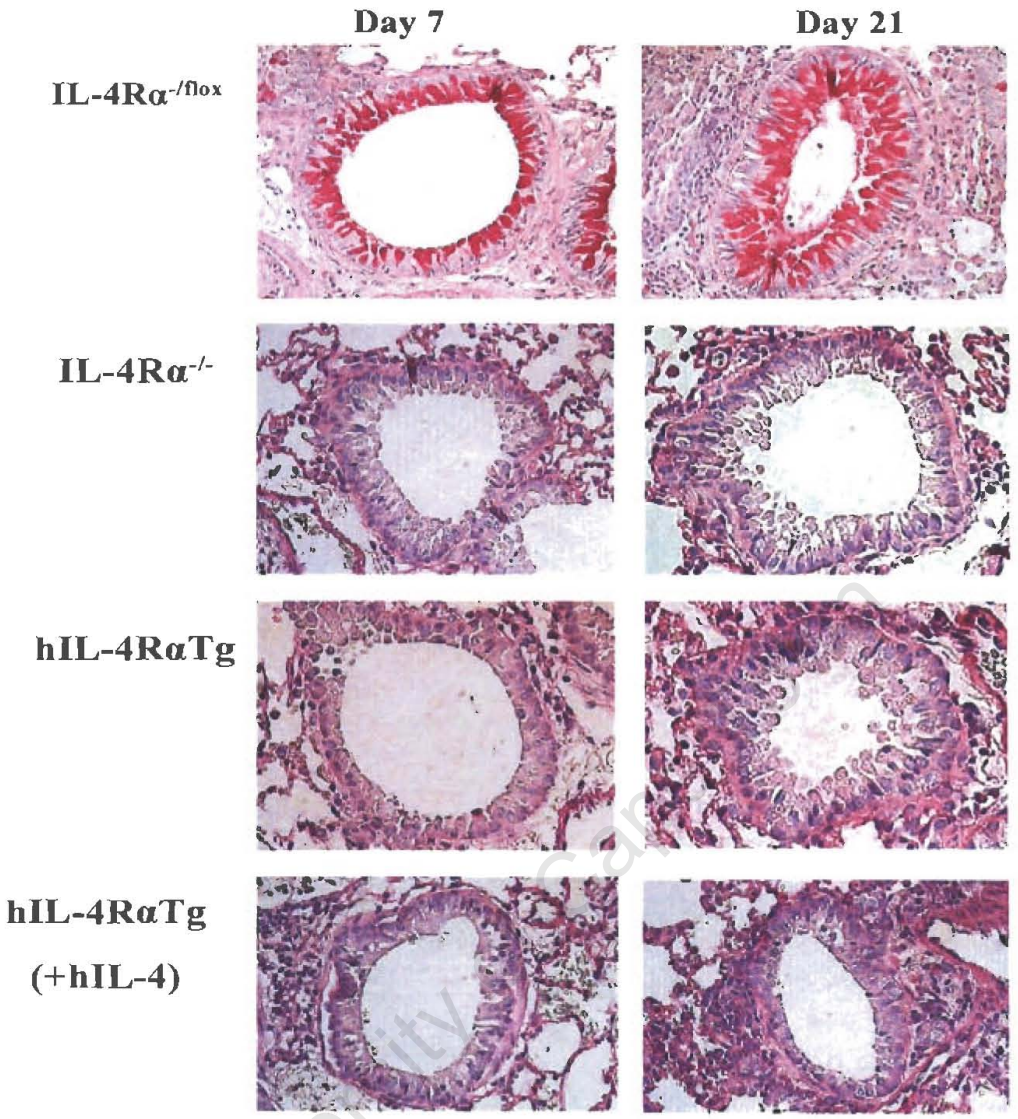

Figure 15

Absence of PAS positive cells staining in the lungs of egg-challenged hIL-4RαTg mice

Lung tissue from sensitized egg-challenged mice were removed, processed for histology and stained by PAS as described in Materials and Methods for PAS positive cells. Sections are representative of 4 mice per group at each indicated time points. (Magnification=200x)

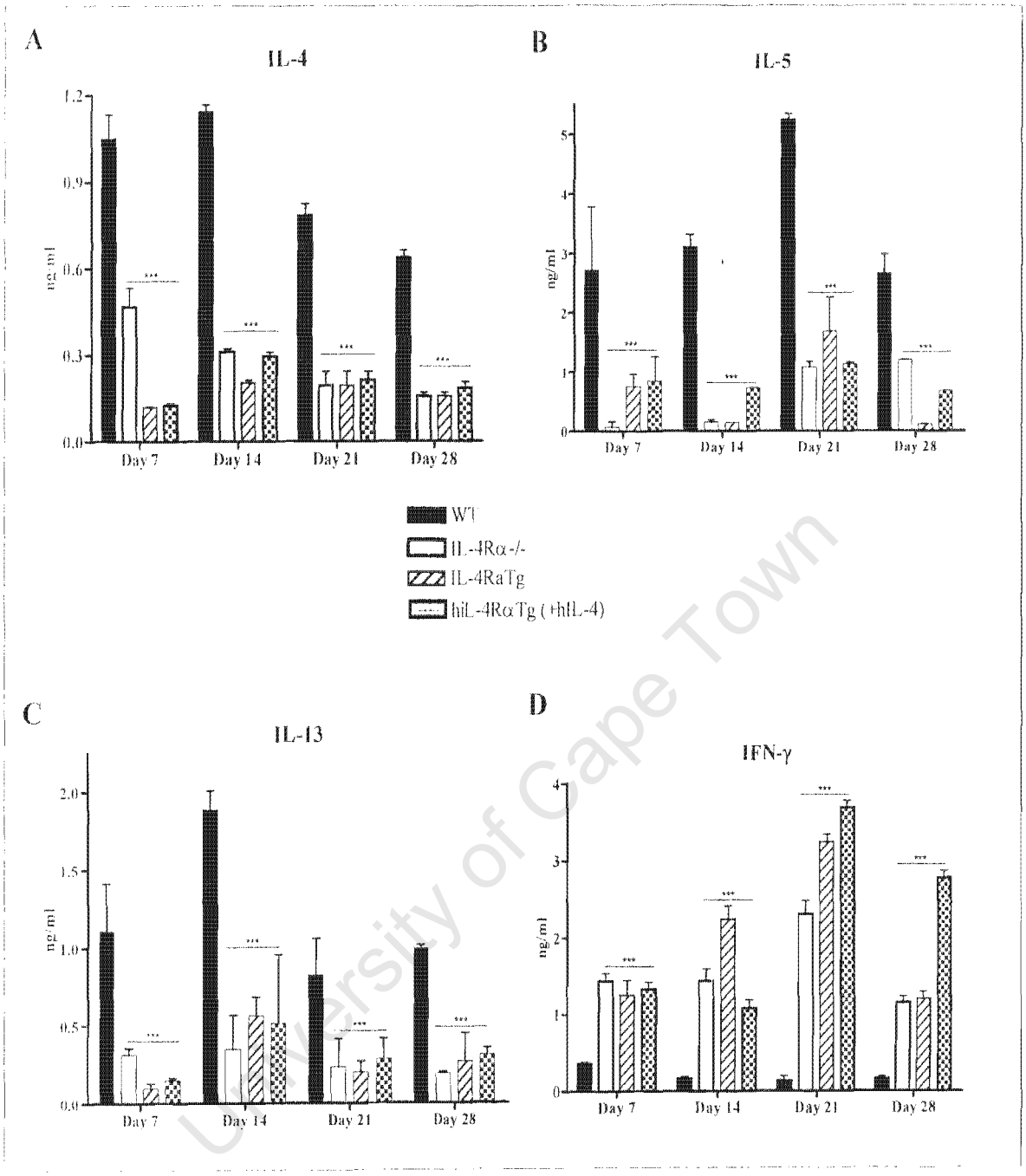

Figure 3.16

T_H1 and T_H2 cytokine profiles in lung homogenates of egg-challenged mice

Mice were injected with *S. mansoni* eggs 14 days after egg sensitization and T_H1 vs.T_H2 cytokine levels measured from lung tissue homogenates by ELISA. Each data point represents the average ± SD of triplicate lung homogenates samples. The results are a representative of one of four similar experiments. (***) = $p<0.001$ by ANOVA in comparison to WT value

Measurement of cytokines, IL-10 and TGF-β showed that IL-10 levels were similar between all groups on days 7 and 14, whereas TGF-β levels were significantly elevated in the mutant strains (Figure 3.17A& B). Peak production of IL-10 was observed on day 21 in WT mice, whilst TGF-β levels remained significantly lower ($p<0.05$). Treatment of hIL-4RαTg mice with hIL-4 did not have any significant effect in the production of IL-4, and IL-13 (Figure 3.16A-C), but elevated levels of IL-5 were observed on days 14 and 28 after treatment with hIL-4 (Figure 3.16B). Similarly, IFN-γ levels were also increased in treated animals on days 21 and 28. ELISA results from samples obtained from hIL-4 treated animals also showed significantly elevated levels of IL-10 ($p<0.001$) and TGF-β ($p<0.05$) on days 21 and 28 post-challenge in comparison to their non-treated littermates (Figure 3.17A & B).

Stimulation of mediastinal lymph nodes and splenocytes with the T cell mitogen anti-CD3 revealed a significantly impaired production of T_H2 cytokines (IL-4, IL-5 and IL-13) in IL-4Rα$^{-/-}$ and hIL-4RαTg strains in comparison to WT mice ($p<0.001$) (Figure 3.18 & Figure 3.19 A-C). Unlike the cytokine profiles in the lung homogenates of hIL-4RαTg mice, levels IL-4 and IL-13 were significantly increased by treatment of mice with hIL-4 ($p<0.05$) (Figure 18 and Figure 19 A&C). Analysis of T_H1 cytokines from anti-CD3 stimulated mediastinal LN (Figure 3.18D) and splenocytes (Figure 3.19D) culture supernatants showed elevated levels of IFN-γ in the mutant strains at all time points after egg-challenge compared to WT. Unlike in the lung homogenates, IFN-γ levels in the LN and spleen of hIL-4RαTg mice were not increased by treatment of these animals with hIL-4, on the contrary IFN-γ levels were significantly reduced ($p<0.05$) in splenocytes of treated mice at day 21 post-challenge compared to the non-treated mutants.

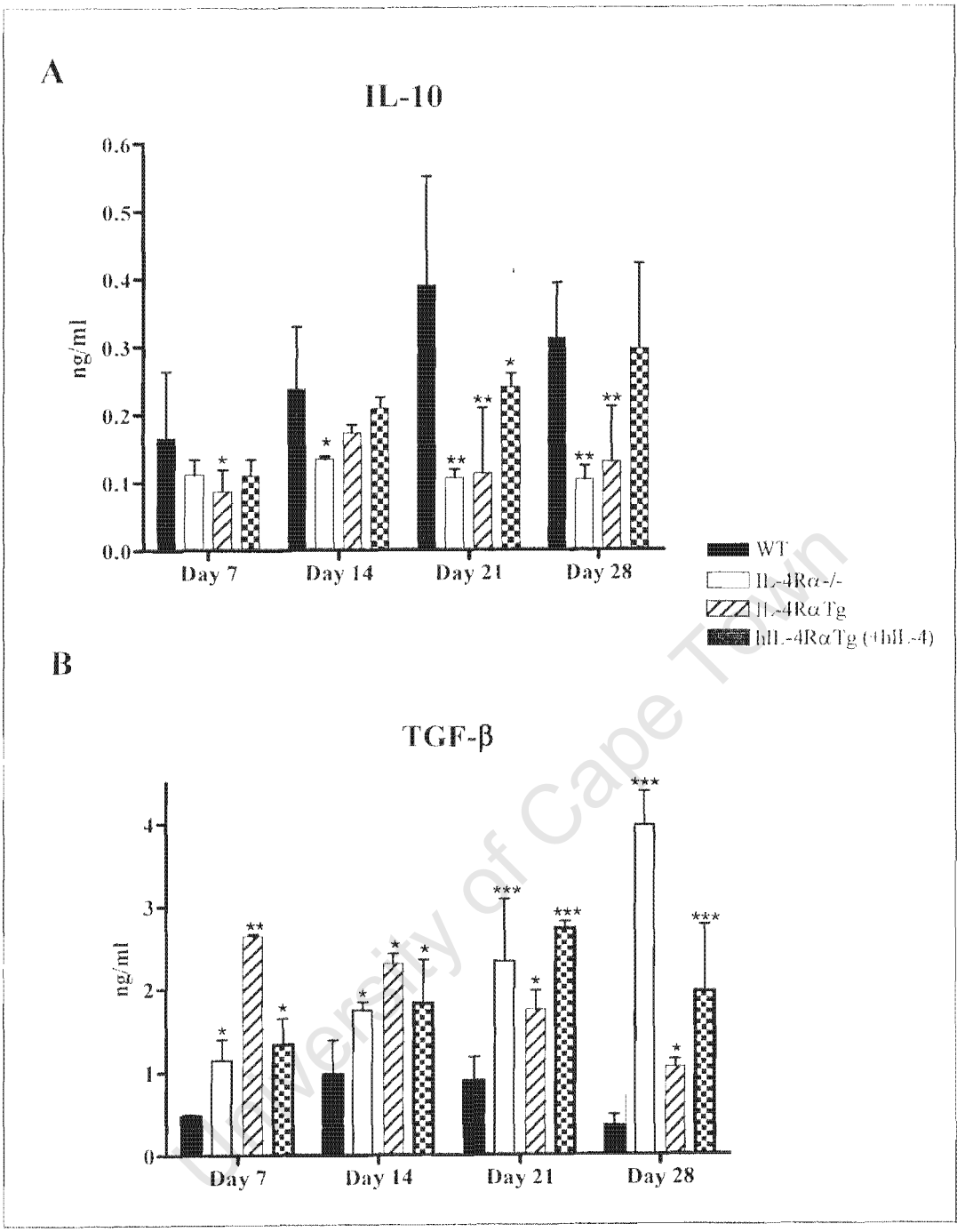

Figure 3.17

IL-10 and TGF-β levels in lung homogenates of sensitized egg-challenged mice

Mice were injected with schistosome eggs 14 days after egg sensitization and proinflammatory cytokine levels measured from lung tissue homogenates by ELISA. Each data point represents the average ± SD of triplicate lung homogenates samples. The results are representative of four independent experiments. (*) = $p<0.05$, (**) = $p<0.01$ and (***) = $p<0.001$ by ANOVA compared to WT

In contrast to IL-10 levels in the lung, mediastinal LN and splenocyte culture IL-10 levels were consistently higher in WT mice whereas TGF-β levels were low compared to mutant strains (Figure 3.20A &B). These data demonstrate that hIL-4RαTg mice, like IL-4Rα$^{-/-}$ mice develop an impaired T_H2 cytokine response against schistosome eggs.

Antibody responses were measured in the sera of egg-challenged mice at days 7, 14, 21, and 28 after egg-challenge. Measurements of the SEA-specific antibody response revealed a significant rise in IgG2a and IgG2b levels in IL-4Rα$^{-/-}$ as well as in both the treated and non-treated hIL-4RαTg mice from day 14 post-challenge (Figure 3.22 A & B). On the contrary, the levels of SEA-specific IgG1 and total IgE antibodies were significantly reduced in IL-4Rα$^{-/-}$ and hIL-4RαTg mice at all four time points compared to controls, which showed prominently type 2 antibody production (Figure 3.22C & D).

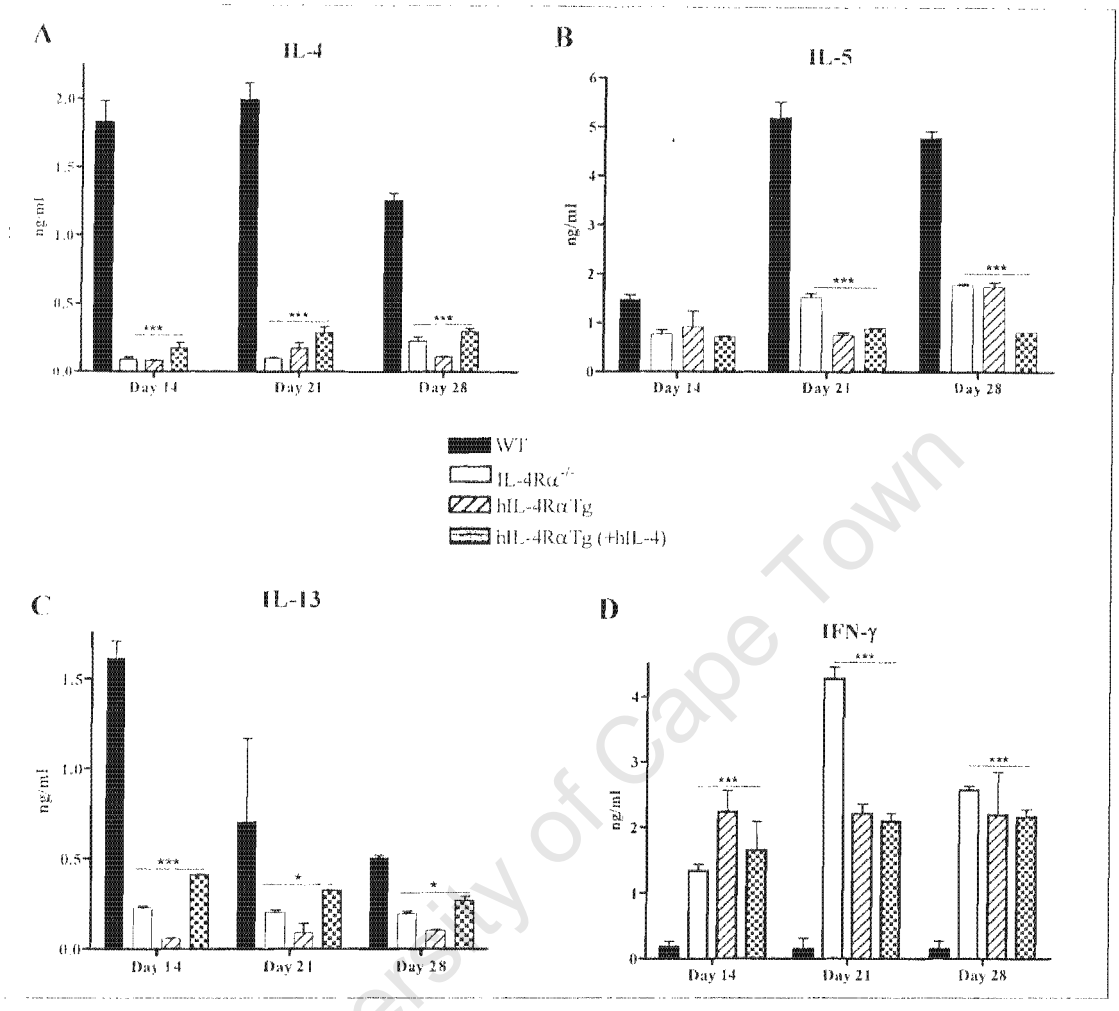

Figure 3.18

T_H1 and T_H2 cytokine levels in mediastinal lymph node of egg-challenged mice

T_H1 and T_H2 cytokine levels measured from anti-CD3 stimulated mediastinal lymph node culture supernatants by ELISA. Each data point represents the average ± SD of triplicate samples. The results are representative of four similar experiments. (*) = $p<0.05$ and (***) = $p<0.001$ by ANOVA in comparison to WT value

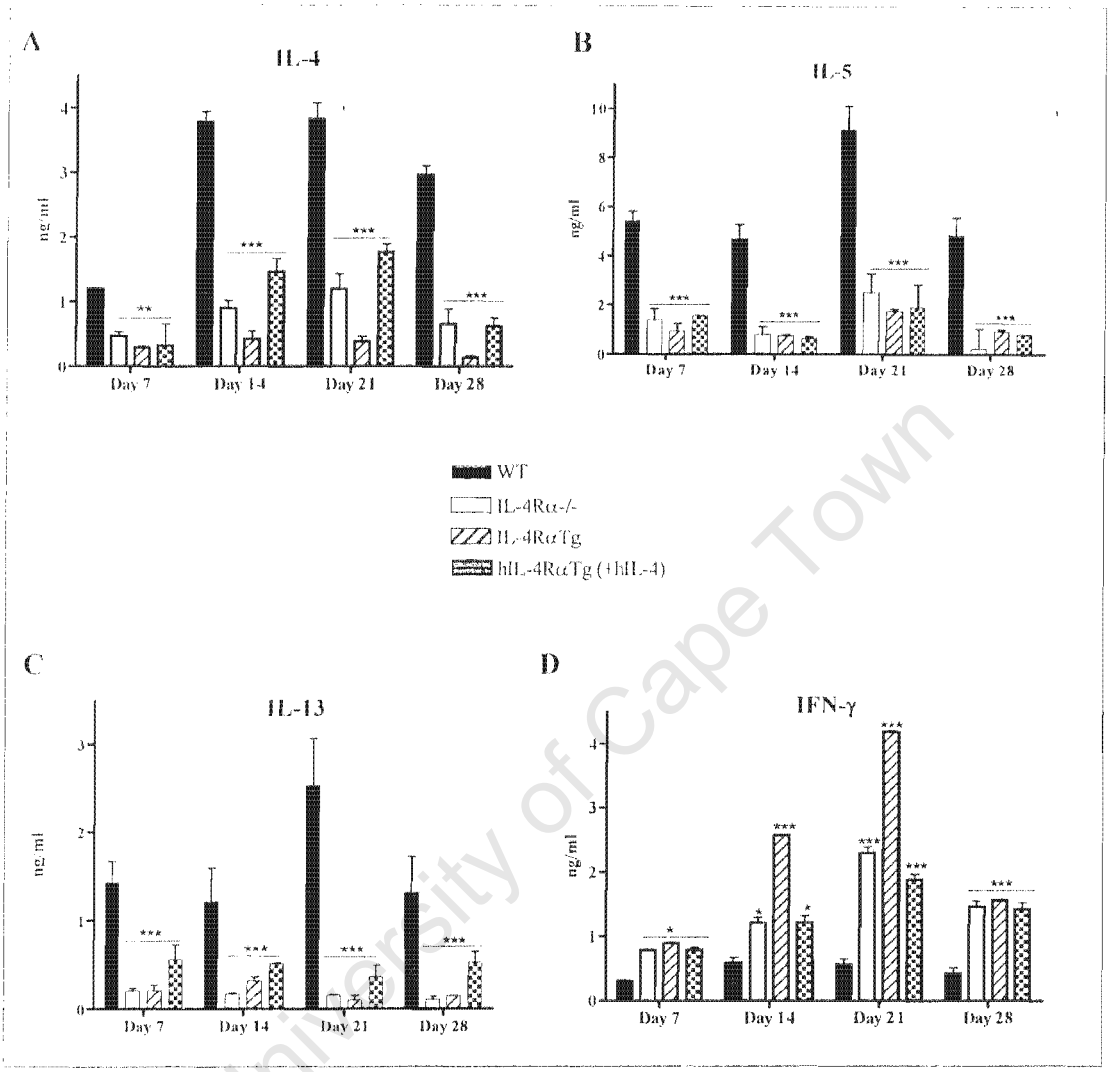

Figure 3.19

T_H1 and T_H2 cytokine levels in spleen cells of egg-challenged mice

T_H1 and T_H2 cytokine levels measured from anti-CD3 stimulated splenocyte culture supernatants by ELISA. Each data point represents the average ± SD of triplicate samples. The results are representative of four similar experiments. (*) = $p<0.05$ and (**) = $p<0.001$ by ANOVA in comparison to WT value.

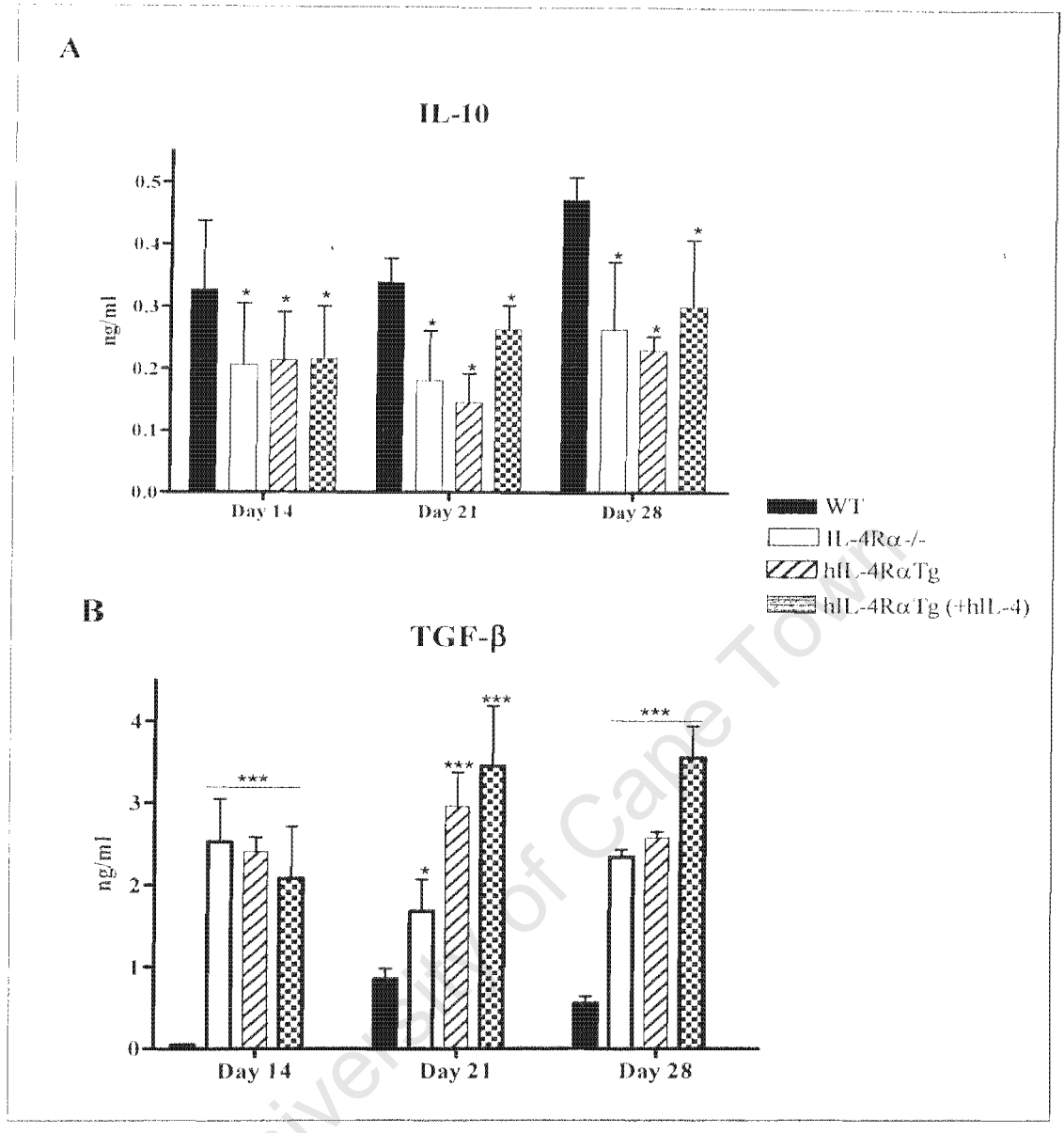

Figure 3.20

Elevated IL-10 and TGF-β levels in mediastinal lymph nodes of hIL-4 treated hIL4RαTg mice

Sensitized and egg-challenge mice injected with *S. mansoni* eggs 14 days after egg sensitization and cytokine levels measured from anti-CD3 stimulated mediastinal lymph node culture supernatants by ELISA. Each data point represents the average ± SD of triplicate samples. The results represent one of four similar experiments. (*) = $p<0.05$ and (**) = $p<0.001$ by ANOVA compared to WT value

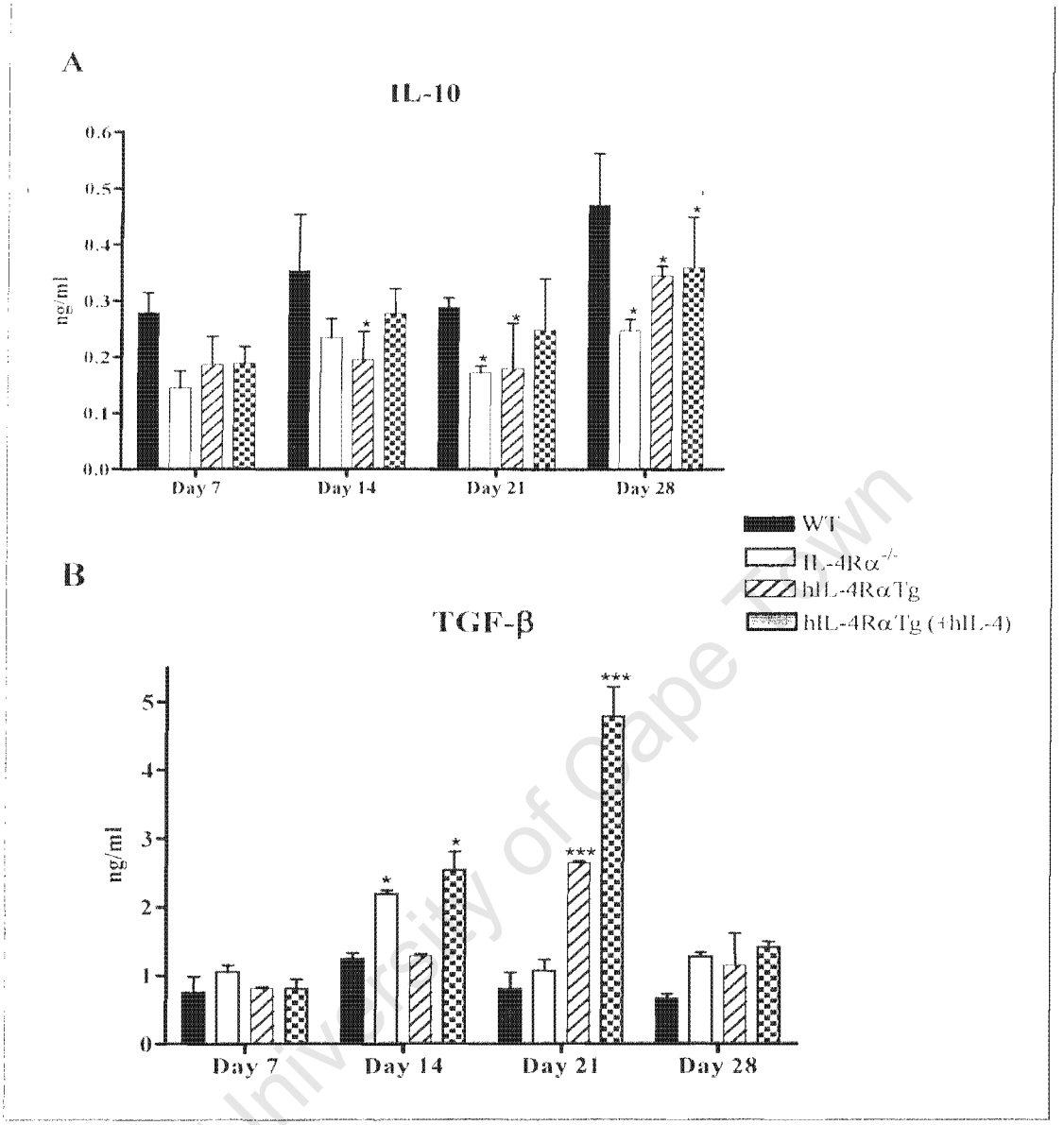

Figure 3.21

Elevated IL-10 and TGF-β levels in spleen cells hIL-4 treated hIL-4RαTg mice

Sensitized mice were injected with *S. mansoni* eggs 14 days after egg sensitization and cytokine levels were measured from anti-CD3 stimulated splenocytes culture supernatants by ELISA. Each data point represents the average ± SD of triplicate samples. The results represent one of four independent experiments. (*) = $p<0.05$ and (**) = $p<0.001$ by ANOVA in comparison to WT value

Human IL-4 treatment decreased the levels of both IgG2a and IgG2b in hIL-4RαTg mice (Figure 3.22A & B) at day 21 and day 28, but increased the levels of IgE significantly ($p<0.001$) from day 14 post-challenge. Similarly, IgG1 levels were increased after treatment but the levels were only significantly different ($p<0.05$) on day 28 post-challenge compared to their non-treated littermates, although the levels were still low compared to WT (Figure 3.22C &D). Collectively these data indicate that the immune response in hIL-4RαTg is similar to that in IL-4Rα$^{-/-}$ mice being predominantly type1. Similarly, exogenous hIL-4, although it can induce the production of IgE in naïve mice and increase levels of type 2 Abs in *S. mansoni* egg-challenged mice, it is not able to drive the immune response fully towards T_H2/type 2 immune response.

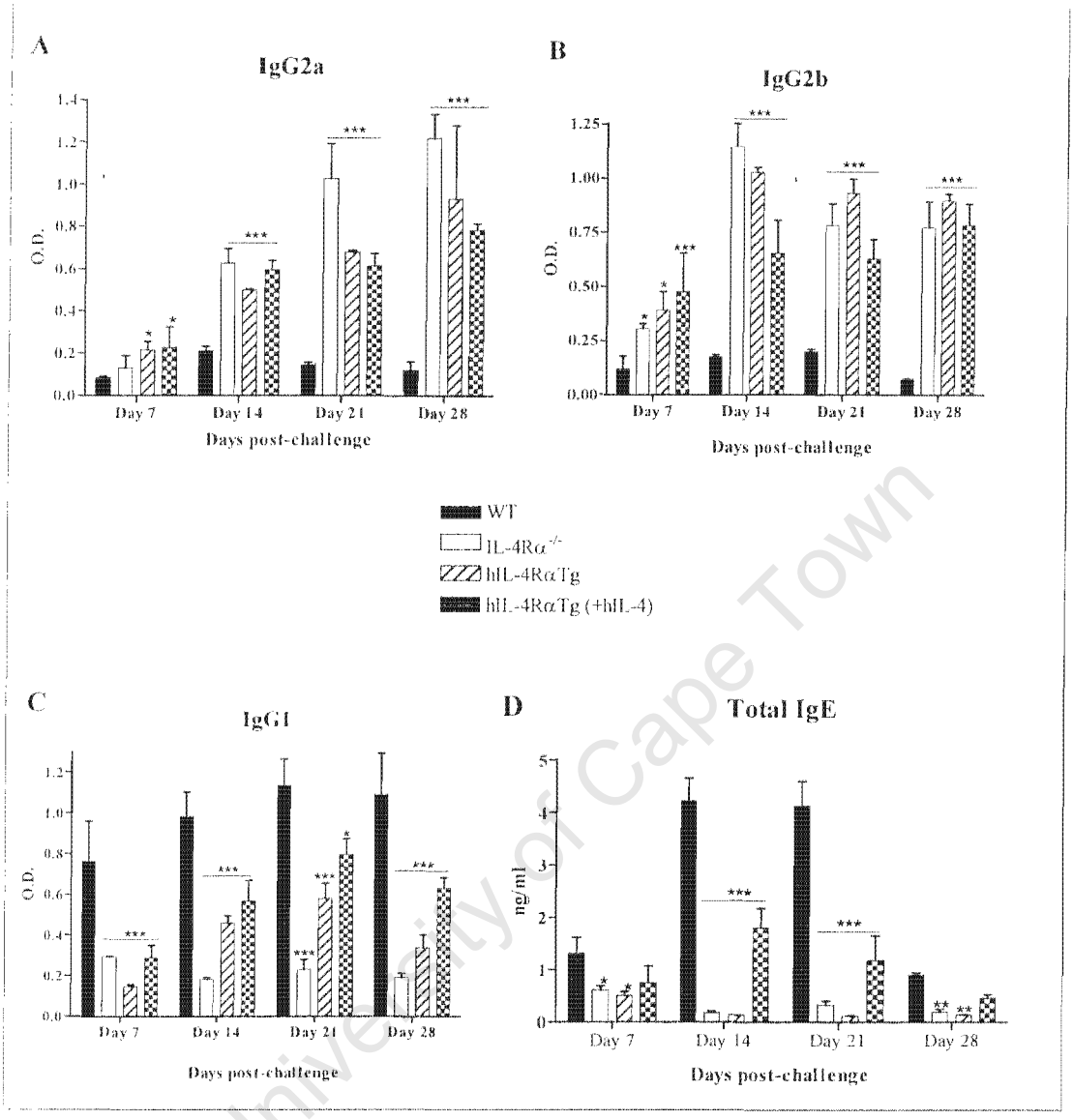

Figure 3.22

Antibody levels in sensitized egg-challenged mice

SEA-specific Type 1 (Panel A & B) vs. type 2 (Panel C & D) antibodies were analysed in the sera of egg-challenged mice ELISA at indicated time points. Panel D represents total serum IgE levels. Each data point represents the average ± SD of triplicate serum samples. The results are representative of four similar experiments. (*) = $p<0.05$, (**) = $p<0.01$ and (***) = $p<0.001$ by ANOVA in comparison to WT value

DISCUSSION

Human IL-4RαTg mice were generated to dissect the individual roles of IL-4R signalling and TCR signalling. This transgenic mouse model expresses the human IL-4Rα under the control of an intronic enhancer from the Ig H chain Eμ locus, to allow specific expression of the receptor only in lymphocytes (Seki et al., 2004). The chimeric IL-4R molecule composed of the hIL-4Rα chain and the mouse common γ-chain is responsive to hIL-4, therefore allowing the control of IL-4R signalling independent of endogenous IL-4. The study utilizing this mouse model revealed that IL-4 signalling was required at early stages of TCR-mediated T cell activation for lineage commitment to T_H2 (Seki et al., 2004).

Different protocols were explored in the current study to investigate the role of lymphocyte specific IL-4 and IL-13 responsiveness during *S. mansoni* infection with focus on the dependence on IL-4Rα signalling for granuloma development in hIL-4RαTg mice. Immunohistochemical staining of liver tissues indicated that the quality of granulomas in IL-4Rα$^{-/-}$ and hIL-4RαTg mice was significantly reduced compared to that of their WT littermates. Similarly, granulomas in these strains revealed a significant abrogation of eosinophil recruitment, thus further signifying the importance of mouse IL-4Rα signalling for full granuloma development and cellular recruitment. Failure to develop full granuloma formation was associated with an inability to control egg-induced pathology infection by the mutant strains. Human IL-4RαTg mice were unable to survive acute infection with *S. mansoni* and the severity of the disease was similar to IL-4Rα$^{-/-}$ mice. Compared to infected WT mice, hIL-4RαTg and IL-4Rα$^{-/-}$ mice presented with severe morbidity as infection progressed. Similar to findings by Brunet et al. (1997), this morbidity was characterized by cachexia, lethargy, and peri-orbital oedema (personal observation). The high susceptibility of hIL-4RαTg as well as IL-4Rα$^{-/-}$ mice to

infection demonstrates that there is an absolute dependence on IL-4 and IL-13 in mediating an effective protective immune response against *S. mansoni* infection. In the case of hIL-4RαTg mice, it might suggest that this response is non T cell dependent or cannot be mediated by signalling through the human chimeric form of the receptor. It has been suggested that during an infection with *S. mansoni* a response dominated by the production of T_H2 cytokines, like IL-4 and the suppressive cytokine IL-10, may play a crucial role in reducing the severity of acute disease and allowing survival (La Flamme et al., 2001). In contrast to WT mice, hIL-4RαTg and IL-4Rα$^{-/-}$ mice succumbed to infection and produced high levels of T_H1 cytokines in response to *S. mansoni* infection which is in accordance with reports that targeted deletion of the genes for IL-4, IL-4Rα or STAT-6 results in default T_H1 responses dominated by IFN-γ (Metwali et al., 2002; Patton et al., 2001).

Because adult schistosome worms live in the mesenteric veins, eggs either pass through the intestinal wall to be excreted or become lodged in the liver. In both sites the eggs induce granulomatous lesions (Brunet et al., 1997). Experiments were conducted to identify factors that could be correlated with mortality observed in IL-4Rα$^{-/-}$ and hIL-4RαTg mice. Compared to WT mice, the mucosal surface of the ileum of IL-4Rα$^{-/-}$ and hIL-4RαTg mice presented prominent red foci, which were not observed in WT, that were associated with reduced faecal egg output. This would suggest that since schistosome eggs naturally pass across the gut wall in order to enter the lumen, there is a greater potential for tissue destruction during the process. Our findings are similar to previous studies which showed that severe intestinal pathology is a characteristic of mouse strains in which IL-4 function (Brunet et al., 1997) or key immunological genes have been disrupted (Mombaerts et al., 1993; Sadlack et al., 1993; Shull et al., 1992). Indeed Fallon et al. have shown that in the absence of IL-4 (IL-4$^{-/-}$ of IL-4/IL-13$^{-/-}$mice), parasite eggs are not efficiently excreted and are trapped in the intestine, causing intestinal

inflammation leading to systemic LPS leakage which may exacerbate liver damage and ultimately results in death of the animal (Fallon et al., 2000).

In separate studies, mice were sensitized i.p with eggs to establish a polarized T_H2 response and then challenged i.v. with eggs at a later period to induce synchronized pulmonary granulomas. In these experiments, granulomatous inflammation was significantly abrogated but not totally ablated in hIL-4RαTg mice. Similarly, T_H2-like characteristics of synchronous pulmonary granuloma formation which include eosinophil infiltration and IgE production (McKenzie, 2000) were abolished or abrogated, respectively.

Egg induced pulmonary granuloma formation has been characterized as $CD4^+$ T-cell mediated delayed-type hypersensitivity reaction (Grzych et al., 1991; Mathew and Boros, 1986). Cytokine depletion studies, both in infected mice (Cheever et al., 1994) and in mice injected i.v. with schistosome eggs (Chensue et al., 1992; Wynn et al., 1993) have revealed an important role for IL-4 in driving the egg-induced T_H2-mediated inflammatory response, as well as the accompanying rise in IgE levels (Cheever et al., 1994). In addition Chiaramonte et al. (1999) have demonstrated that the host response to schistosome eggs is not totally dependent on IL-4, but other T_H2 cytokines like IL-13 serve as an important mediator of T_H2-mediated inflammation and also play a role in eliciting IgE responses triggered by schistosome eggs. Our findings also support this contention in that abrogation of granulomatous inflammation in hIL-4RαTg mice correlated with abrogation of T_H2 cytokine (IL-4 and IL-13) production after egg challenge.

Previous studies have established that IL-13 exhibits chemotactic activity for human eosinophils (Horie et al., 1997) and has a prominent role in fibrosis (Wynn, 2003). We therefore wanted to determine whether the altered granulomatous response in hIL-4RαTg mice was accompanied by changes in eosinophil accumulation and fibrosis. In contrast to WT mice, the number of eosinophils in hIL-4RαTg and IL-$4R\alpha^{-/-}$ mice were significantly decreased.

This lack of granuloma eosinophils may also explain lack of T_H2 cytokine production in these animals as activated eosinophils have been shown to be a major source of T_H2 cytokines in the granuloma milieu (Rumbley et al., 1999). Similarly, hydroxyproline levels, as an indicator of fibrosis, or collagen deposition, were significantly reduced in hIL-4RαTg mice and IL-4Rα$^{-/-}$ mice which also correlated with low levels of IL-13.

Evidence shows that IL-4 plays a major role in mediating pulmonary granuloma formation (Cheever et al., 1994), and parasite-induced IgE responses are believed to be almost entirely dependent upon IL-4 (Finkelman et al., 1988; Snapper et al., 1988). Total serum IgE, as well as SEA-specific IgG1, responses were significantly reduced in egg-injected hIL-4RαTg mice, further demonstrating the requirement for this cytokine in granuloma formation and IgE production. However, treatment of these animals with hIL-4 had a slight effect on IgE and IgG1. These findings support studies that showed that T_H2-like characteristics of synchronous pulmonary granuloma formation, including eosinophil infiltration and IgE production were significantly reduced in the absence of both IL-4 and IL-13 (Fallon et al., 2000). Indeed treatment of mice with hIL-4 did not have any effect on the immune response of egg-challenged mice which supports the contention that a hIL-4 signal was required at the early stages of TCR-mediated activation for lineage commitment to Th2 in hIL-4RαTg mice. (Seki et al., 2004). Secondly, Seki *et al.* have shown that the chimeric IL-4Rα molecule, composed of the hIL-4Rα chain and the mouse common γ-chain is only responsive to hIL-4, but not to endogenous mouse IL-4. Therefore it was not surprising that hIL-4RαTg mice were not able to mount a dominant type 2 immune response against schistosome eggs despite production of low levels of endogenous mouse IL-4. In their study Seki et al. (Seki et al., 2004) have established the time period for T cell differentiation, induced by hIL-4, to T_H2 lineage to be less than 36 hours after which period the frequency of differentiating cells declined. In our studies, a number of factors may be responsible for the observed phenotype. Firstly, during a live infection

with schistosome parasites each parasite stage elicit a different immune response in the host, which result in a mixed T_H1-T_H2 before egg-production (Pearce and MacDonald, 2002). Similarly, egg production which is a major stimulus responsible for T_H2 cytokine production is generally believed to start at week 5 post-infection. Given these factors, the time that we initiated treatment could have been inappropriate for the induction of a protective immune response or the dosage used was not optimal for eliciting the required protective immune response in the presence of pre-existing parasite antigens. On the other hand, in the synchronized pulmonary granuloma model, where there are no pre-existing worm responses and granuloma formation could be attained within a coordinated period, it is not known what influence egg-antigens have on treatment. It is clear from our studies though that although hIL-4 can induce IgE production in naïve mice, and increase levels of IgG1 and IgE in response to egg antigens, this type of response is not adequate to drive the immune response towards a full type 2 or for full granuloma development.

Discussion

This dissertation addressed the role of cell specific expression of IL-4Rα in egg pathology in *S. mansoni*-infected mice with a specific deletion of IL-4Rα on myeloid and lymphoid cell populations. This study utilized two experimental models of *S. mansoni*, the live infection model, and the lung model. In the live infection model mice were infected with live *S. mansoni* cercariae and most of the pathology is attributed to the animal's reaction to schistosome eggs which is maximal by the 8th week of infection. In the lung model, mice are intravenously injected with schistosome eggs which initiate synchronous granuloma formation in the lungs. The lung model allows study of the granuloma formation and cytokine production *in vivo* in naïve or egg-sensitized animals at defined periods after egg injection in the absence of pre-existing worm antigens (Cheever et al., 2002).

Studies in experimental murine models recognized that the adaptive immune response leading to immunopathology in schistosomiasis is principally mediated and orchestrated by MHC class II- restricted lymphocytes specific for schistosome egg antigen (Hernandez et al., 1997). After an infection, an initial pro-inflammatory CD4$^+$ T_H1-type polarized response predominates and continues into the period of oviposition at around 5 weeks post-infection, when granulomatous inflammation begins (Stadecker & Hernandez, 1998). The development of severe immunopathology is clearly attributed an inability to develop a T_H2 response to regulate the initial pro-inflammatory T_H1 response (Pearce & MacDonald, 2002). Overall, the $T_H1$to T_H2 switch is critical to prevent excessive host morbidity and promote enhanced survival; however, the absence of the various conversion mechanisms has dissimilar effects on the resulting immunopathology. Of greatest consequence is the lack of intact CD40-CD154 and B7-CD28 signalling as well as IL-4 (Stadecker et al., 2004) as their absences can result in lethal disease characterized by hepatic

inflammation with hepatocellular injury and necrosis (Brunet et al., 1997; Hernandez, Sharpe & Stadecker, 1999; MacDonald et al., 2002).

It has been postulated that, in addition to egg-specific $CD4^+$ lymphocytes, a population of non-T cell IL-4Rα$^+$ effector cells may be required in tissue pathology against schistosomiasis (Jankovic et al., 1999). However this premise has never been investigated. The current study addressed this hypothesis by utilizing mice with cell specific deletions of the IL-4Rα receptor. In the first set of experiments, the role of IL-4Rα expression was investigated during an acute *S. mansoni* infection whereas the second set of experiments determined the receptor's requirement for the extent of schistosome egg-induced lung inflammation and pathology. The first chapter of the results describes the generation, characterization and functional analyses of mice that lack the IL-4Rα chain selectively on macrophages and neutrophils, and further demonstrates what effect this deletion has in a disease model in which protection or pathology was dependent on type 2 immune responses. The findings of this study reveal an absolute dependence on IL-4/IL-13-activated alternative macrophages for surviving acute schistosomiasis. Mice with a specific deletion of IL-4Rα chain on myeloid cells succumbed to infection and suffered severe cachexia and endotoxemia despite the presence of a strong T_H2 immune response, suggesting that although necessary, T_H2 responses are not necessarily protective against an infection. The observation that myeloid specific deletion of IL-4Rα leads to increased classical macrophage activation further highlights IL-4/IL-13-activated alternative macrophages as crucial for protection against infection. IL-4 and IL-13 inhibit nitric oxide production, enhance MHC class II antigen and macrophage mannose receptor (Gordon et al., 1995), indicating that they are able to participate in antigen presentation and efficient uptake of selected pathogens. However, the present study shows that these cytokines were not able to inhibit nitric oxide production nor enhance macrophage mannose receptor, suggesting that during an infection with *S.*

mansoni in LysM^{Cre}IL-4Rα$^{-/flox}$ mice their functional capacity in these two processes is impaired.

We addressed the requirement of T cell specific IL-4Rα signalling for the extent of granulomatous pathology and egg-induced fibrosis. We concluded that T cell-independent specific IL-4Rα expression is required for prevention of lethal T_H1 gut pathology through promotion of alternative macrophage activation, and control of CD^+CD25^+ T regulatory cells. Similarly it was determined that mice with a specific deletion of the IL-4Rα on $CD4^+$T cells developed granulomas that were larger and more fibrotic than in wild type controls suggesting that $CD4^+$T cell independent IL-4Rα expression is required for liver or lung granuloma development.

Furthermore it was determined that granuloma development in hIL-4RαTg mice was significantly abrogated. This was associated with elevated levels of T_H1/type-1 immune responses in the lung and the draining lymph nodes. Failure of hIL-4RαTg mice to develop T_H2/type 2 immune responses or develop full pulmonary granulomas may be related to their IL-4Rα expression. IL-4 and IL-13 mediate their effects via the type 2 IL-4R complex system comprised of IL-4Rα and IL-13Rα1, with IL-4 and IL-13 both utilizing the IL-4Rα chain for signal transduction (Nelms et al., 1999). In addition to binding the signalling type 2 receptor, IL-13 binds the high affinity IL-13Rα2 which is expressed in various tissues and exists as a soluble receptor in the urine and serum of mice (Donaldson et al., 1998; Zhang et al., 1997). Andrews *et al.* have shown that transfected cells expressing human IL-4Rα or human IL-13Rα1 alone were unable to respond or signal to IL-13 (Andrews et al., 2001). This suggested that IL-13Rα could not combine with the endogenous murine IL-4Rα to generate a functional IL-13Rα. However, cells transfected with both human IL-4Rα and IL-4Rα1 responded to IL-13 indicating that the heterodimeric interaction between IL-4Rα and IL-13Rα1 is species specific. This study confirmed an earlier study which showed that IL-13 and IL-4 were able to

activate STAT-6 in cells expressing both IL-4Rα and IL-13Rα1, while no activation was observed in cells expressing either one of the other alone (Miloux et al., 1997). Because hIL-4RαTg mice only express human IL-4Rα, this might suggest that an additional human IL-13Rα1 may be needed to generate a functional IL-13R to allow IL-4 and IL-13 activated signalling in the mouse.

Conclusion

This dissertation provides new/or more insight concerning the role of IL-4/IL-13 responsive myeloid and lymphoid cells in parasitic helminth infection. Although it is has been previously shown that T_H2 lymphocytes play a major role in the immunopathology induced by *S. mansoni* infection, data presented here reveals the role of IL-4/IL-13-activated alternative macrophages as crucial downstream effector cells responsible for protection conferred by T_H2 cytokines, and provides a cellular model to explain the beneficial role of T_H2 cytokines during schistosomiasis. This would suggest that the destructive potential of *S. mansoni* egg induced inflammation is not only dependent on T_H2 responses but may be counterbalanced by alternatively activated macrophages, thus allowing preservation of intestine, liver and lung functions.

In addition, TGF-β producing $CD4^+CD25^+$ regulatory T cells might also contribute to protect against lethal gut pathology in an IL-4Rα dependent manner. This would be achieved by balancing the potentially fatal T_H1-driven egg responses in the gut and promoting passage of faecal eggs. However the the non-T cell, IL-4Rα expressing cell that controls entry and /or expansion of regulatory T cells in granuloma tissue is still unknown and further studies are required to study this phenomenon. Current data demonstrate the role of IL-4Rα in the behaviour of regulatory T cells *in vivo* and thus provide insight for the design of therapies that limit or promote the presence of regulatory T cells during anti-tumour or anti-parasite responses. However, our data still does not fully explain why Lck^{Cre}IL-$4R\alpha^{-/flox}$ mice survive infection better than WT controls and this result requires further investigation.

Finally hIL-4RαTg mice succumbed to infection at with similar kinetics as IL-$4R\alpha^{-/-}$ mice and failed to develop full hepatic or pulmonary granulomas. This was associated with elevated levels of T_H1-type-1 immune responses, which were not altered by treatment with hIL-4. Two possible scenarios may explain

this discrepancy. Firstly it is possible that the dosage of hIL-4 used in treatment studies was inadequate or secondly, there was no signalling through the chimeric human receptor. Because IL-4Rα and IL-13Rα1 are species-specific and both are required to generate a functional IL-13Rα, in hIL-4RαTg mice the generation of a functional receptor was not possible. The generation and characterization of the hIL-4RαTg mice should be revisited with probable changes which may include in addition to the hIL-4Rα, a functional hIL-13Rα1.

REFERENCES

Akbari, O., DeKruyff, R.H., Umetsu, D.T. 2001. Pulmonary dendritic cells producing IL-10 mediate tolerance induced by respiratory exposure to antigen. *Nat Immunol* **2:**725-31

Arai, N., Nomura, D., Villaret, D., DeWaal Malefijt, R., Seiki, M., Yoshida, M., Minoshima, S., Fukuyama, R., Maekawa, M., Kudoh, J., et al. 1989. Complete nucleotide sequence of the chromosomal gene for human IL-4 and its expression. *J Immunol* **142:**274-82

Araujo, M.I., de Jesus, A.R., Bacellar, O., Sabin, E., Pearce, E., Carvalho, E.M. 1996. Evidence of a T helper type 2 activation in human schistosomiasis. *Eur J Immunol* **26:**1399-403

Asahi, H., Hernandez, H.J., Stadecker, M.J. 1999a. A novel 62-kilodalton egg antigen from Schistosoma mansoni induces a potent CD4(+) T helper cell response in the C57BL/6 mouse. *Infect Immun* **67:**1729-35

Asahi, H., Osman, A., Cook, R.M., LoVerde, P.T., Stadecker, M.J. 2000. Schistosoma mansoni phosphoenolpyruvate carboxykinase, a novel egg antigen: immunological properties of the recombinant protein and identification of a T-cell epitope. *Infect Immun* **68:**3385-93

Asahi, H., Stadecker, M.J. 2003. Analysis of egg antigens inducing hepatic lesions in schistosome infection. *Parasitol Int* **52:**361-7

Atochina, O., Daly-Engel, T., Piskorska, D., McGuire, E., Harn, D. 2001. A schistosome-expressed immunomodulatory glycoconjugate expands peritoneal Gr1(+) macrophages that suppress naive CD4(+) T cell proliferation via an IFN-gamma and nitric oxide-dependent mechanism. *J Immunol* **167:**4293-4303

Bazan, J.F. 1990. Structural design and molecular evolution of a cytokine receptor superfamily. *Proc Natl Acad Sci U S A* **87:**6934-6938

Biedermann, T., Mailhammer, R., Mai, A., Sander, C., Ogilvie, A., Brombacher, F., Maier, K., Levine, A.D., Rocken, M. 2001. Reversal of established delayed type hypersensitivity reactions following therapy with IL-4 or antigen-specific Th2 cells. *Eur J Immunol* **31:**1582-91

Bergman, I., Loxley, R. 1963. Two improved and simplified methods for the spectrophotometric determination of hydroxyproline. . *Anal. Chem* **35:**1–5

Bergman, I., Loxley, R. 1969. Lung tissue hydrolysates: studies of the optimum conditions for the spectrophotometric determination of hydroxyproline. *Analyst* **94:**575-84

Boros, D.L. 1989. Immunopathology of Schistosoma mansoni infection. *Clin Microbiol Rev* **2:**250-69

Boros, D.L. 1999. T helper cell populations, cytokine dynamics, and pathology of the schistosome egg granuloma. *Microbes Infect* **1:**511-6

Boulay, J.L., Paul, W.E. 1992. The interleukin-4 family of lymphokines. *Curr Opin Immunol* **4:**294-8

Brombacher, F. 2000. The role of interleukin-13 in infectious diseases and allergy. *Bioessays* **22:**646-56

Brombacher, F., Kastelein, R.A., Alber, G. 2003. Novel IL-12 family members shed light on the orchestration of Th1 responses. *Trends Immunol* **24:**207-12

Brown, K.D., Zurawski, S.M., Mosmann, T.R., Zurawski, G. 1989. A family of small inducible proteins secreted by leukocytes are members of a new superfamily that includes leukocyte and fibroblast-derived inflammatory agents, growth factors, and indicators of various activation processes. *J Immunol* **142:**679-87

Brunet, L.R., Finkelman, F.D., Cheever, A.W., Kopf, M.A., Pearce, E.J. 1997. IL-4 protects against TNF-alpha-mediated cachexia and death during acute schistosomiasis. *J Immunol* **159:**777-85

Brunet, L.R., Kopf, M.A., Pearce, E.J. 1999. Schistosoma mansoni: IL-4 is necessary for concomitant immunity in mice. *J Parasitol* **85:**734-6

Butterworth, A.E., Curry, A.J., Dunne, D.W., Fulford, A.J., Kimani, G., Kariuki, H.C., Klumpp, R., Koech, D., Mbugua, G., Ouma, J.H. 1994a. Immunity and morbidity in human schistosomiasis mansoni. *Trop Geogr Med* **46:**197-208

Butterworth, A.E., Curry, A.J., Dunne, D.W., Fulford, A.J., Kimani, G., Kariuki, H.C., Klumpp, R., Koech, D., Mbugua, G., Ouma, J.H., et al. 1994b. Immunity and morbidity in human schistosomiasis mansoni. *Trop Geogr Med* **46:**197-208

Cai, Y., Langley, J.G., Smith, D.J., Boros, D.L. 1996. A cloned major Schistosoma mansoni egg antigen with homologies to small heat shock proteins elicits Th1 responsiveness. *Infect Immun* **64:**1750-5

Chatterjee, S., De Man, J., Van Marck, E. 2001. Somatostatin and intestinal schistosomiasis: therapeutic and neuropathological implications in host-parasite interactions. *Trop Med Int Health* **6:**1008-15

Cheever, A.W., Finkelman, F.D., Caspar, P., Heiny, S., Macedonia, J.G., Sher, A. 1992. Treatment with anti-IL-2 antibodies reduces hepatic pathology and eosinophilia in Schistosoma mansoni-infected mice while selectively inhibiting T cell IL-5 production. *J Immunol* **148:**3244-8

Cheever, A.W., Hoffmann, K.F., Wynn, T.A. 2000. Immunopathology of schistosomiasis mansoni in mice and men. *Immunol Today* **21:**465-6

Chensue, S.W., Terebuh, P.D., Warmington, K.S., Hershey, S.D., Evanoff, H.L., Kunkel, S.L., Higashi, G.I. 1992. Role of IL-4 and IFN-gamma in Schistosoma mansoni egg-induced hypersensitivity granuloma formation. Orchestration, relative contribution, and relationship to macrophage function. *J Immunol* **148:**900-6

Chiaramonte, M.G., Donaldson, D.D., Cheever, A.W., Wynn, T.A. 1999a. An IL-13 inhibitor blocks the development of hepatic fibrosis during a T-helper type 2-dominated inflammatory response. *J Clin Invest* **104:**777-85

Chiaramonte, M.G., Schopf, L.R., Neben, T.Y., Cheever, A.W., Donaldson, D.D., Wynn, T.A. 1999b. IL-13 is a key regulatory cytokine for Th2 cell-mediated pulmonary granuloma formation and IgE responses induced by Schistosoma mansoni eggs. *J Immunol* **162:**920-30

Chitsulo, L., Engels, D., Montresor, A., Savioli, L. 2000. The global status of schistomomiasis and its control. *Acta Trop* **77:**41-45

Chomarat, P., Banchereau, J. 1998. Interleukin-4 and interleukin-13: their similarities and discrepancies. *Int Rev Immunol* **17:**1-52

Clausen, B.E., Burkhardt, C., Reith, W., Renkawitz, R., Forster, I. 1999. Conditional gene targeting in macrophages and granulocytes using LysMcre mice. *Transgenic Res* **8:**265-77

Coligan, J.E., Kriusbeek, A.M., Shievach, E.M., Warren, S. 1991. Current Protocols in Immunology. **1-4**

Colley, D.G., LoVerde, P.T., Savioli, L. 2001. Medical helminthology in the 21st century. *Science* **293:**1437-1438

Corraliza, I.M., Campo, M.L., Soler, G., Modolell, M. 1994. Determination of arginase activity in macrophages: a micromethod. *J Immunol Methods* **174:**231

Damian, R.T. 1987. The exploitation of host immune responses by parasites. *J Parasitol* **73:**3-13

de Jesus, A.R., Silva, A., Santana, L.B., Magalhaes, A., de Jesus, A.A., de Almeida, R.P., Rego, M.A., Burattini, M.N., Pearce, E.J., Carvalho, E.M. 2002. Clinical and immunologic evaluation of 31 patients with acute schistosomiasis mansoni. *J Infect Dis* **185:**98-105

de Vries, J.E. 1998. The role of IL-13 and its receptor in allergy and inflammatory responses. *J Allergy Clin Immunol* **102:**165-9

Dessein, A.J., Hillaire, D., Elwali, N.E., Marquet, S., Mohamed-Ali, Q., Mirghani, A., Henri, S., Abdelhameed, A.A., Saeed, O.K., Magzoub, M.M., Abel, L. 1999. Severe hepatic fibrosis in Schistosoma mansoni infection is controlled by a major locus that is closely linked to the interferon-gamma receptor gene. *Am J Hum Genet* **65:**709-21

Doenhoff, M.J. 1997. A role for granulomatous inflammation in the transmission of infectious disease: schistosomiasis and tuberculosis. *Parasitology* **115 Suppl:**S113-25

Doherty, T.M., Kastelein, R., Menon, S., Andrade, S., Coffman, R.L. 1993. Modulation of murine macrophage function by IL-13. *J Immunol* **151:**7151-60

Donaldson, D.D., Whitters, M.J., Fitz, L.J., Neben, T.Y., Finnerty, H., Henderson, S.L., O'Hara, R.M., Jr., Beier, D.R., Turner, K.J., Wood, C.R., Collins, M. 1998. The murine IL-13 receptor alpha 2: molecular cloning, characterization, and comparison with murine IL-13 receptor alpha 1. *J Immunol* **161:**2317-24

Dunne, D.W., Butterworth, A.E., Fulford, A.J., Kariuki, H.C., Langley, J.G., Ouma, J.H., Capron, A., Pierce, R.J., Sturrock, R.F. 1992a. Immunity after treatment of human schistosomiasis: association between IgE antibodies to adult worm antigens and resistance to reinfection. *Eur J Immunol* **22:**1483-94

Dunne, D.W., Butterworth, A.E., Fulford, A.J., Ouma, J.H., Sturrock, R.F. 1992b. Human IgE responses to Schistosoma mansoni and resistance to reinfection. *Mem Inst Oswaldo Cruz* **87 Suppl 4:**99-103

Dunne, D.W., Pearce, E.J. 1999. Immunology of hepatosplenic schistosomiasis mansoni: a human perspective. *Microbes Infect* **1:**553-60

Eberl, M., al-Sherbiny, M., Hagan, P., Ljubojevic, S., Thomas, A.W., Wilson, R.A. 2002. A novel and sensitive method to monitor helminth infections by faecal sampling. *Acta Trop* **83:**183-7

Else, K.J., Finkelman, F.D. 1998. Intestinal nematode parasites, cytokines and effector mechanisms. *Int J Parasitol* **28:**1145-58

Emson, C.L., Bell, S.E., Jones, A., Wisden, W., McKenzie, A.N. 1998. Interleukin (IL)-4-independent induction of immunoglobulin (Ig) E, and pertubation of T cell development in transgenic mice expressing IL-13. *J Exp Med* **188**

Endo, T., Ogushi, F., Sone, S. 1996. LPS-dependent cyclooxygenase-2 induction in human monocytes is down-regulated by IL-13, but not by IFN-gamma. *J Immunol* **156:**2240-6

Falcone, F.H., Loke, P., Zang, X., MacDonald, A.S., Maizels, R.M., Allen, J.E. 2001. A Brugia malayi homolog of macrophage migration inhibitory factor reveals an important link between macrophages and eosinophil recruitment during nematode infection. *J Immunol* **167:**5348-5354

Fallon, P.G., Richardson, E.J., McKenzie, A.N., McKenzie, G.J. 2000. Schistosome infection of transgenic mice defines distinct and contrasting pathogenic roles for IL-4 and IL-13: Il-13 is a profibrotic agent. *J Immunol* **164:**2585

Fallon, P.G., Dunne, D.W. 1999. Tolerization of mice to Schistosoma mansoni egg antigens causes elevated type 1 and diminished type 2 cytokine responses and increased mortality in acute infection. *J Immunol* **162:**4122-32

Fearon, D.T., Locksley, R.M. 1996. The instructive role of innate immunity in the acquired immune response. *Science* **272:**50-3

Finkelman, F.D., Katona, I.M., Urban, J.F., Jr., Holmes, J., Ohara, J., Tung, A.S., Sample, J.V., Paul, W.E. 1988. IL-4 is required to generate and sustain in vivo IgE responses. *J Immunol* **141:**2335-41

Flores Villanueva, P.O., Harris, T.S., Ricklan, D.E., Stadecker, M.J. 1994a. Macrophages from schistosomal egg granulomas induce unresponsiveness in specific cloned Th-1 lymphocytes in vitro and down-regulate schistosomal granulomatous disease in vivo. *J Immunol* **152:**1847-55

Flores Villanueva, P.O., Reiser, H., Stadecker, M.J. 1994b. Regulation of T helper cell responses in experimental murine schistosomiasis by IL-10. Effect on expression of B7 and B7-2 costimulatory molecules by macrophages. *J Immunol* **153:**5190-9

Goerdt, S., Orfanos, C.E. 1999. Other functions, other genes: alternative activation of antigen-presenting cells. *Immunity* **10:**137-42

Gordon, S. 2003. Alternative activation of macrophages. *Nat Rev Immunol* **3:**23-35

Grzych, J.M., Pearce, E., Cheever, A., Caulada, Z.A., Caspar, P., Heiny, S., Lewis, F., Sher, A. 1991. Egg deposition is the major stimulus for the production of Th2 cytokines in murine schistosomiasis mansoni. *J Immunol* **146:**1322-7

Hagan, P. 1996. Immunity and morbidity in infection due to *Schistosoma haematobium*. *Am J Trop Med Hyg* **55:**116-120

Hagan P, Appleton CC, Coles GC, Kusel JR, LA., T.-T. 2004. Schistosomiasis control: keep taking the tablets. *Trends Parasitol* **20:**92-97

Hagan, P., Appleton, C.C., Coles, G.C., Kusel, J.R., Tchuem-Tchuente, L.A. 2004. Schistosomiasis control: keep taking the tablets. *Trends Parasitol* **20:**92-97

Harada, N., Yang, G., Miyajima, A., Howard, M. 1994. Identification of an essential region for growth signal transduction in the cytoplasmic domain of the human interleukin-4 receptor. *J Biol Chem* **267:**22752-22758

Herbert, D.R., Holscher, C., Mohrs, M., Arendse, B., Schwegmann, A., Radwanska, M., Leeto, M., Kirsch, R., Hall, P., Mossmann, H., Claussen, B., Forster, I., Brombacher, F. 2004. Alternative macrophage activation is essential for survival during schistosomiasis and downmodulates T helper 1 responses and immunopathology. *Immunity* **20:**623-35

Hernandez, H.J., Trzyna, W.C., Cordingley, J.S., Brodeur, P.H., Stadecker, M.J. 1997a. Differential antigen recognition by T cell populations from strains of mice developing polar forms of granulomatous inflammation in response to eggs of Schistosoma mansoni. *Eur J Immunol* **27:**666-70

Hernandez, H.J., Wang, Y., Tzellas, N., Stadecker, M.J. 1997b. Expression of class II, but not class I, major histocompatibility complex molecules is required for granuloma formation in infection with Schistosoma mansoni. *Eur J Immunol* **27:**1170-6

Hershey, G.K. 2003. IL-13 receptors and signaling pathways: an evolving web. *J Allergy Clin Immunol* **111:**677-90; quiz 691

Hesse, M., Modolell, M., La Flamme, A.C., Schito, M., Fuentes, J.M., Cheever, A.W., Pearce, E.J., Wynn, T.A. 2001a. Differential regulation of nitric oxide synthase-2 and arginase-1 by type 1/type 2 cytokines in vivo: granulomatous

pathology is shaped by the pattern of L-arginine metabolism. *J Immunol* **167**:6533-44

Hesse, M., Modolell, M., La Flamme, A.C., Schito, M., Fuentes, J.M., Cheever, A.W., Pearce, E.J., Wynn, T.A. 2001b. Differential regulation of nitric oxide synthase-2 and arginase-1 by type 1/type 2 cytokines in vivo: granulomatous pathology is shaped by the pattern of L-arginine metabolism. *J Immunol* **167**:6533-44

Hesse, M., Piccirillo, C.A., Belkaid, Y., Prufer, J., Mentink-Kane, M., Leusink, M., Cheever, A.W., Shevach, E.M., Wynn, T.A. 2004. The pathogenesis of schistosomiasis is controlled by cooperating IL-10-producing innate effector and regulatory T cells. *J Immunol* **172**:3157-66

Hoffmann, K.F., Caspar, P., Cheever, A.W., Wynn, T.A. 1998. IFN-gamma, IL-12, and TNF-alpha are required to maintain reduced liver pathology in mice vaccinated with Schistosoma mansoni eggs and IL-12. *J Immunol* **161**:4201-10

Hoffmann, K.F., James, S.L., Cheever, A.W., Wynn, T.A. 1999. Studies with double cytokine-deficient mice reveal that highly polarized Th1- and Th2-type cytokine and antibody responses contribute equally to vaccine-induced immunity to Schistosoma mansoni. *J Immunol* **163**:927-38

Hoffmann, K.F., Cheever, A.W., Wynn, T.A. 2000. IL-10 and the dangers of immune polarization: excessive type 1 and type 2 cytokine responses induce distinct forms of lethal immunopathology in murine schistosomiasis. *J Immunol* **164**:6406-16

Holmskov, U., Malhotra, R., Sim, R.B., Jensenius, J.C. 1994. Collectins: collagenous C-type lectins of the innate immune defense system. *Immunol Today* **15**:67-74

Horie, S., Okubo, Y., Hossain, M., Sato, E., Nomura, H., Koyama, S., Suzuki, J., Isobe, M., Sekiguchi, M. 1997. Interleukin-13 but not interleukin-4 prolongs eosinophil survival and induces eosinophil chemotaxis. *Intern Med* **36**:179-85

Ibelgauft, H. Cytokine Online Pathfinder Encyclopedia. Phillippine Universities Library. www.copewithcytokines.de

Iellem, A., Mariani, M., Lang, R., Recalde, H., Panina-Bordignon, P., Sinigaglia, F., D'Ambrosio, D. 2001. Unique chemotactic response profile and specific expression of chemokine receptors CCR4 and CCR8 by CD4(+)CD25(+) regulatory T cells. *J Exp Med* **194**:847-53

Jankovic, D., Kullberg, M.C., Noben-Trauth, N., Caspar, P., Ward, J.M., Cheever, A.W., Paul, W.E., Sher, A. 1999. Schistosome-infected IL-4 receptor knockout (KO) mice, in contrast to IL-4 KO mice, fail to develop granulomatous pathology while maintaining the same lymphokine expression profile. *J Immunol* **163:**337-42

Jankovic, D., Kullberg, M.C., Noben-Trauth, N., Caspar, P., Paul, W.E., Sher, A. 2000. Single cell analysis reveals that IL-4 receptor/Stat6 signaling is not required for the in vivo or in vitro development of CD4+ lymphocytes with a Th2 cytokine profile. *J Immunol* **164:**3047-55

Jensen, P.L. 2000. The interleukin 13 receptor complex. *Stem Cells* **18:**61-2

Kaplan, M.H., Whitfield, J.R., Boros, D.L., Grusby, M.J. 1998. Th2 cells are required for the Schistosoma mansoni egg-induced granulomatous response. *J Immunol* **160:**1850-6

Karanja, D.M., Colley, D.G., Nahlen, B.L., Ouma, J.H., Secor, W.E. 1997. Studies on schistosomiasis in western Kenya: I. Evidence for immune-facilitated excretion of schistosome eggs from patients with Schistosoma mansoni and human immunodeficiency virus coinfections. *Am J Trop Med Hyg* **56:**515-21

Kawakami, K., Taguchi, J., Murata, T., Puri, R.K. 2001. The interleukin-13 receptor alpha2 chain: an essential component for binding and internalization but not for interleukin-13-induced signal transduction through the STAT6 pathway. *Blood* **97:**2673-9

Keegan, A.D., Nelms, K., White, M., Pierce, J.H., Paul, W.E. 1994. An IL-4 receptor region containing an insulin receptor motif is important for IL-4-mediated IRS-1 phosphorylation and cell growth. *Cell* **76:**811-820

Kelly-Welch, A.E., Hanson, E.M., Boothby, M.R., Keegan, A.D. 2003. Interleukin-4 and interleukin-13 signaling connections maps. *Science* **300:**1527-8

King, C.L. 2001. Transmission intensity and humna immune responses to lymphatic filiriasis. *Parasite Immunol* **23:**363-371

King, C.L., Malhotra, I., Mungai, P., Wamachi, A., Kioko, J., Ouma, J.H., Kazura, J.W. 1998. B cell sensitization to helminthic infection develops in utero in humans. *J Immunol* **160:**3578-84

Kopf, M., Le Gros, G., Bachmann, M., Lamers, M.C., Bluethmann, H., Kohler, G. 1993. Disruption of the murine IL-4 gene blocks Th2 cytokine responses. *Nature* **362:**245-8

Kurata, H., Lee, H.J., O'Garra, A., Arai, N. 1999. Ectopic expression of activated Stat6 induces the expression of Th2-specific cytokines and transcription factors in developing Th1 cells. *Immunity* **11:**677-88

La Flamme, A.C., Patton, E.A., Bauman, B., Pearce, E.J. 2001. IL-4 plays a crucial role in regulating oxidative damage in the liver during schistosomiasis. *J Immunol* **166:**1903-11

La Flamme, A.C., Patton, E.A., Pearce, E.J. 2001a. Role of gamma interferon in the pathogenesis of severe schistosomiasis in interleukin-4-deficient mice. *Infect Immun* **69:**7445-52

Lee, C. G., R. J. Homer, et al. 2001. Interleukin-13 induces tissue fibrosis by selectively stimulating and activating transforming growth factor beta(1). J Exp Med **194**(6): 809-21.

Leonard, W.J., Lin, J.X. 2000. Cytokine receptor signaling pathways. *J Allergy Clin Immunol* **105:**877-88

Linehan, S.A., Coulson, P.S., Wilson, R.A., Mountford, A.P., Brombacher, F., Martinez-Pomares, L., Gordon, S. 2003. IL-4 receptor signaling is required for mannose receptor expression by macrophages recruited to granulomata but not resident cells in mice infected with Schistosoma mansoni. *Lab Invest* **83:**1223-31

Loke, P., MacDonald, A.S., Robb, A., Maizels, R.M., Allen, J.E. 2000. Alternatively activated macrophages induced by nematode infection inhibit proliferation via cell-to-cell contact. *Eur J Immunol* **30:**2669-2678

Luttmann, W., Knoechel, B., Foerster, M., Matthys, H., Virchow, J.C., Jr., Kroegel, C. 1996. Activation of human eosinophils by IL-13. Induction of CD69 surface antigen, its relationship to messenger RNA expression, and promotion of cellular viability. *J Immunol* **157:**1678-83

MacDonald, A.S., Araujo, M.I., Pearce, E.J. 2002. Immunology of parasitic helminth infections. *Infect Immun* **70:**427-33

Mahanty, S., Ravichandran, M., Raman, U., Jayaraman, K., Kumaraswami, V., Nutman, T.B. 1997. Regulation of parasite antigen-driven immune responses by interleukin-10 (IL-10) and IL-12 in lymphatic filariasis. *Infect Immun* **65:**1742-1747

Maizels, R.M., Bundy, D.A.P., Selkirk, M.E., Smith, D.F., Anderson, R.M. 1993. Immunological modulation and evasion by helminth parasites in human populations. *Nature* **365:**797-805

Mantovani, A., Sozzani, S., Locati, M., Allavena, P., Sica, A. 2002. Macrophage polarization: tumor-associated macrophages as a paradigm for polarized M2 mononuclear phagocytes. *Trends Immunol* **23:**549-55

Mathew, R.C., Boros, D.L. 1986. Anti-L3T4 antibody treatment suppresses hepatic granuloma formation and abrogates antigen-induced interleukin-2 production in Schistosoma mansoni infection. *Infect Immun* **54:**820-6

McInnes, A., Rennick, D.M. 1988. Interleukin 4 induces cultured monocytes/macrophages to form giant multinucleated cells. *J Exp Med* **167:**598-611

McKee, A. S. and E. J. Pearce (2004). $CD25^{+}CD4^{+}$ cells contribute to Th2 polarization during helminth infection by suppressing Th1 response development. *Journal of Immunology* **173**: 1224-1231.

McKenzie, A.N. 2000. Regulation of T helper type 2 cell immunity by interleukin-4 and interleukin-13. *Pharmacol Ther* **88:**143-51

McKenzie, G.J., Bancroft, A., Grencis, R.K., McKenzie, A.N. 1998a. A distinct role for interleukin-13 in Th2-cell-mediated immune responses. *Curr Biol* **8:**339-42

McKenzie, G.J., Emson, C.L., Bell, S.E., Anderson, S., Fallon, P., Zurawski, G., Murray, R., Grencis, R., McKenzie, A.N. 1998b. Impaired development of Th2 cells in IL-13-deficient mice. *Immunity* **9:**423-32

Metwali, A., Elliott, D., Blum, A.M., Li, J., Sandor, M., Lynch, R., Noben-Trauth, N., Weinstock, J.V. 1996. The granulomatous response in murine Schistosomiasis mansoni does not switch to Th1 in IL-4-deficient C57BL/6 mice. *J Immunol* **157:**4546-53

Minty, A., Chalon, P., Derocq, J.M., Dumont, X., Guillemot, J.C., Kaghad, M., Labit, C., Leplatois, P., Liauzun, P., Miloux, B., et al. 1993. Interleukin-13 is a new human lymphokine regulating inflammatory and immune responses. *Nature* **362:**248-50

Mohamed-Ali, Q., Elwali, N.E., Abdelhameed, A.A., Mergani, A., Rahoud, S., Elagib, K.E., Saeed, O.K., Abel, L., Magzoub, M.M., Dessein, A.J. 1999. Susceptibility to periportal (Symmers) fibrosis in human schistosoma mansoni

infections: evidence that intensity and duration of infection, gender, and inherited factors are critical in disease progression. *J Infect Dis* **180:**1298-306

Mombaerts, P., Mizoguchi, E., Grusby, M.J., Glimcher, L.H., Bhan, A.K., Tonegawa, S. 1993. Spontaneous development of inflammatory bowel disease in T cell receptor mutant mice. *Cell* **75:**274-82

Montenegro, S.M., Miranda, P., Mahanty, S., Abath, F.G., Teixeira, K.M., Coutinho, E.M., Brinkman, J., Goncalves, L., Domingues, L.A., Domingues, A.L., Sher, A., Wynn, T.A. 1999. Cytokine production in acute versus chronic human Schistosomiasis mansoni: the cross-regulatory role of interferon-gamma and interleukin-10 in the responses of peripheral blood mononuclear cells and splenocytes to parasite antigens. *J Infect Dis* **179:**1502-14

Montesano, M.A., Colley, D.G., Willard, M.T., Freeman, G.L., Jr., Secor, W.E. 2002. Idiotypes expressed early in experimental Schistosoma mansoni infections predict clinical outcomes of chronic disease. *J Exp Med* **195:**1223-8

Mohrs, M., Ledermann, B., Kohler, G., Dorfmuller, A., Gessner, A., Brombacher, F. 1999. Differences between IL-4- and IL-4 receptor alpha-deficient mice in chronic leishmaniasis reveal a protective role for IL-13 receptor signaling. *J Immunol* **162:**7302-8

Munder, M., Eichmann, K., Modolell, M. 1998. Alternative metabolic states in murine macrophages reflected by the nitric oxide synthase/arginase balance: competitive regulation by CD4+ T cells correlates with Th1/Th2 phenotype. *J Immunol* **160:**5347-54

Murata, T., Husain, S.R., Mohri, H., Puri, R.K. 1998. Two different IL-13 receptor chains are expressed in normal human skin fibroblasts, and IL-4 and IL-13 mediate signal transduction through a common pathway. *Int Immunol* **10:**1103-10

Nakagawa, R., Naka, T., Tsutsui, H., Fujimoto, M., Kimura, A., Abe, T., Seki, E., Sato, S., Takeuchi, O., Takeda, K., Akira, S., Yamanishi, K., Kawase, I., Nakanishi, K., Kishimoto, T. 2002. SOCS-1 participates in negative regulation of LPS responses. *Immunity* **17:**677-87

Nelms, K., Keegan, A.D., Zamorano, J., Ryan, J.J., Paul, W.E. 1999. The IL-4R receptor: Signaling mechanisms and biological functions. *Annu Rev Immunol* **17:**701-738

Noben-Trauth, N., Paul, W.E., Sacks, D.L. 1999. IL-4- and IL-4 receptor-deficient BALB/c mice reveal differences in susceptibility to Leishmania major parasite substrains. *J Immunol* **162:**6132-40

Noben-Trauth, N., Shultz, L.D., Brombacher, F., Urban, J.F., Jr., Gu, H., Paul, W.E. 1997. An interleukin 4 (IL-4)-independent pathway for CD4+ T cell IL-4 production is revealed in IL-4 receptor-deficient mice. *Proc Natl Acad Sci U S A* **94:**10838-43

Noelle, R., Krammer, P.H., Ohara, J., Uhr, J.W., Vitetta, E.S. 1984. Increased expression of Ia antigens on resting B cells: an additional role for B-cell growth factor. *Proc Natl Acad Sci U S A* **81:**6149-53

Ohara, J., Paul, W.E. 1988. Up-regulation of interleukin 4/B-cell stimulatory factor 1 receptor expression. *Proc Natl Acad Sci U S A* **85:**8221-5

Patton, E.A., Brunet, L.R., La Flamme, A.C., Pedras-Vasconcelos, J., Kopf, M., Pearce, E.J. 2001. Severe schistosomiasis in the absence of interleukin-4 (IL-4) is IL-12 independent. *Infect Immun* **69:**589-92

Patton, E.A., La Flamme, A.C., Pedras-Vasoncelos, J.A., Pearce, E.J. 2002. Central role for interleukin-4 in regulating nitric oxide-mediated inhibition of T-cell proliferation and gamma interferon production in schistosomiasis. *Infect Immun* **70:**177-84

Paul, W.E. 1991. Interleukin-4: a prototypic immunoregulatory lymphokine. *Blood* **77:**1859-70

Paul, W.E., Ohara, J. 1987. B-cell stimulatory factor-1/interleukin 4. *Annu Rev Immunol* **5:**429-59

Pearce, E.J., Caspar, P., Grzych, J.M., Lewis, F.A., Sher, A. 1991. Downregulation of Th1 cytokine production accompanies induction of Th2 responses by a parasitic helminth, Schistosoma mansoni. *J Exp Med* **173:**159-66

Pearce, E.J., Cheever, A., Leonard, S., Covalesky, M., Fernandez-Botran, R., Kohler, G., Kopf, M. 1996. Schistosoma mansoni in IL-4-deficient mice. *Int Immunol* **8:**435-44

Pearce, E.J., MacDonald, A.S. 2002. The immunobiology of schistosomiasis. *Nat Rev Immunol* **2:**499-511

Pearce, E.J., Kane, C.M., Sun, J., J, J.T., McKee, A.S., Cervi, L. 2004. Th2 response polarization during infection with the helminth parasite Schistosoma mansoni. *Immunol Rev* **201:**117-26

Pearce, E.J., MacDonald, A.S. 2002. The immunobiology of schistosomiasis. *Nat Rev Immunol* **2:**499-511

Pope, S.M., Brandt, E.B., Mishra, A., Hogan, S.P., Zimmermann, N., Matthaei, K.I., Foster, P.S., Rothenberg, M.E. 2001. IL-13 induces eosinophil recruitment into the lung by an IL-5- and eotaxin-dependent mechanism. *J Allergy Clin Immunol* **108:**594-601

Phillips, S.M., Colley, D.G. 1978. Immunologic aspects of host responses to schistosomiasis: resistance, immunopathology, and eosinophil involvement. *Prog Allergy* **24:**49-182

Pruss, A., Kay, D., Fewtrell, L., Bartram, J. 2002. Estimating the burden of disease from water, sanitation, and hygiene at a global level. *Environ Health Perspect* **110:**537-42

Rihet, P., Demeure, C.E., Bourgois, A., Prata, A., Dessein, A.J., Satti, M.Z., Lind, P., Vennervald, B.J., Sulaiman, S.M., Daffalla, A.A., Ghalib, H.W., Naus, C.W., Booth, M., Jones, F.M., Kemijumbi, J., Kariuki, C.H., Ouma, J.H., Kabatereine, N.B., Dunne, D.W., Gryseels, B., Stelma, F.F., Talla, I., van Dam, G.J., Polman, K., Sow, S., Diaw, M., Sturrock, R.F., Doehring-Schwerdtfeger, E., Kardorff, R., et al. 1991. Evidence for an association between human resistance to Schistosoma mansoni and high anti-larval IgE levels. *Eur J Immunol* **21:**2679-86

Roitt, I., Brostoff, J., Male, D. 2002. Immunology. Mosby, Spain

Rumbley, C.A., Sugaya, H., Zekavat, S.A., El Refaei, M., Perrin, P.J., Phillips, S.M. 1999. Activated eosinophils are the major source of Th2-associated cytokines in the schistosome granuloma. *J Immunol* **162:**1003-9

Sadlack, B., Merz, H., Schorle, H., Schimpl, A., Feller, A.C., Horak, I. 1993. Ulcerative colitis-like disease in mice with a disrupted interleukin-2 gene. *Cell* **75:**253-61

Shull, M.M., Ormsby, I., Kier, A.B., Pawlowski, S., Diebold, R.J., Yin, M., Allen, R., Sidman, C., Proetzel, G., Calvin, D., et al. 1992. Targeted disruption of the mouse transforming growth factor-beta 1 gene results in multifocal inflammatory disease. *Nature* **359:**693-9

Snapper, C.M., Finkelman, F.D., Paul, W.E. 1988. Differential regulation of IgG1 and IgE synthesis by interleukin 4. *J Exp Med* **167:**183-96

Ruth, J.H., Warmington, K.S., Shang, X., Lincoln, P., Evanoff, H., Kunkel, S.L., Chensue, S.W. 2000. Interleukin 4 and 13 participation in mycobacterial (type-1) and schistosomal (type-2) antigen-elicited pulmonary granuloma formation: multiparameter analysis of cellular recruitment, chemokine expression and cytokine networks. *Cytokine* **12:**432-44

Schmidt, G.D., Roberts, L.S. 1989. Foundations of Parasitology. Times/Mirror Mosby College Publishing, St.Louis

Schopf, L.R., Hoffmann, K.F., Cheever, A.W., Urban, J.F., Jr., Wynn, T.A. 2002. IL-10 is critical for host resistance and survival during gastrointestinal helminth infection. *J Immunol* **168:**2383-92

Seki, N., Miyazaki, M., Suzuki, W., Hayashi, K., Arima, K., Myburgh, E., Izuhara, K., Brombacher, F., Kubo, M. 2004. IL-4-induced GATA-3 expression is a time-restricted instruction switch for Th2 cell differentiation. *J Immunol* **172:**6158-66

Seldin, D.C., Leder, P. 1994. Mutational analysis of a critical signaling domain of the human interleukin 4 receptor. *Proc Natl Acad Sci U S A* **91:**2140-2144

Stadecker, M.J., Hernandez, H.J. 1998. The immune response and immunopathology in infection with Schistosoma mansoni: a key role of major egg antigen Sm-p40. *Parasite Immunol* **20:**217-21

Stadecker, M.J. 1999. The development of granulomas in schistosomiasis: genetic backgrounds, regulatory pathways, and specific egg antigen responses that influence the magnitude of disease. *Microbes Infect* **1:**505-10

Stadecker, M.J., Kamisato, J.K., Chikunguwo, S.M. 1990. Induction of T helper cell unresponsiveness to antigen by macrophages from schistosomal egg granulomas. A basis for immunomodulation in schistosomiasis? *J Immunol* **145:**2697-700

Stahl, P.D. 1992. The mannose receptor and other macrophage lectins. *Curr Opin Immunol* **4:**49-52

Stites, S.P., Terr, A.I., Parslow, T.G. 1993. Medical Immunology. Appleton & Lange, Stamford, Connecticut

Stumpo, R., Kauer, M., Martin, S., Kolb, H. 2003. IL-10 induces gene expression in macrophages: partial overlap with IL-5 but not with IL-4 induced genes. *Cytokine* **24:**46-56

Takeda, Y., Kishimoto, T. 1997. STAT6: its role in interleukin 4-mediated biological functions. *J Mol Med* **75:**317-326

Thompson, C.B. 1995. New insights into V(D)J recombination and its role in the evolution of the immune system. *Immunity* **3:**531-9

Tielens, A.G., Van der Meer, P., van den Heuvel, J.M., van den Bergh, S.G. 1991. The enigmatic presence of all gluconeogenic enzymes in Schistosoma mansoni adults. *Parasitology* **102 Pt 2:**267-76

Ulevitch, R.J., Tobias, P.S. 1995. Receptor-dependent mechanisms of cell stimulation by bacterial endotoxin. *Annu Rev Immunol* **13:**437-57

Urban, J.F., Jr., Noben-Trauth, N., Donaldson, D.D., Madden, K.B., Morris, S.C., Collins, M., Finkelman, F.D. 1998. IL-13, IL-4Ralpha, and Stat6 are required for the expulsion of the gastrointestinal nematode parasite Nippostrongylus brasiliensis. *Immunity* **8:**255-64

Vella, A.T., E. J. Pearce. 1992. CD4+Th2 response induced by Schistosoma mansoni eggs develops rapidly, through an early, transient, Th0 like stage. *J Immunol* **148:**2283

Williams, D.L., Asahi, H., Botkin, D.J., Stadecker, M.J. 2001. Schistosome infection stimulates host CD4(+) T helper cell and B-cell responses against a novel egg antigen, thioredoxin peroxidase. *Infect Immun* **69:**1134-41

Williams, M.E., Montenegro, S., Domingues, A.L., Wynn, T.A., Teixeira, K., Mahanty, S., Coutinho, A., Sher, A. 1994. Leukocytes of patients with Schistosoma mansoni respond with a Th2 pattern of cytokine production to mitogen or egg antigens but with a Th0 pattern to worm antigens. *J Infect Dis* **170:**946-54

Wills-Karp, M., Luyimbazi, J., Xu, X., Schofield, B., Neben, T.Y., Karp, C.L., Donaldson, D.D. 1998. Interleukin-13: central mediator of allergic asthma. *Science* **282:**2258-61

Wynn, T.A., Eltoum, I., Cheever, A.W., Lewis, F.A., Gause, W.C., Sher, A. 1993. Analysis of cytokine mRNA expression during primary granuloma formation induced by eggs of Schistosoma mansoni. *J Immunol* **151:**1430-40

Wynn, T.A., Eltoum, I., Oswald, I.P., Cheever, A.W., Sher, A. 1994. Endogenous interleukin 12 (IL-12) regulates granuloma formation induced by eggs of Schistosoma mansoni and exogenous IL-12 both inhibits and prophylactically immunizes against egg pathology. *J Exp Med* **179:**1551-61

Wynn, T.A., Morawetz, R., Scharton-Kersten, T., Hieny, S., Morse, H.C., 3rd, Kuhn, R., Muller, W., Cheever, A.W., Sher, A. 1997. Analysis of granuloma formation in double cytokine-deficient mice reveals a central role for IL-10 in polarizing both T helper cell 1- and T helper cell 2-type cytokine responses in vivo. *J Immunol* **159:**5014-23

Wynn, T.A. 2003. IL-13 effector functions. *Annu Rev Immunol* **21:**425-56

Wynn, T.A., Thompson, R.W., Cheever, A.W., Mentink-Kane, M.M. 2004. Immunopathogenesis of schistosomiasis. *Immunol Rev* **201:**156-67

Zheng, W. and R. A. Flavell (1997). "The transcription factor GATA-3 is necessary and sufficient for Th2 cytokine gene expression in CD4 T cells." Cell **89**(4): 587-96.

Zurawski, G., de Vries, J.E. 1994. Interleukin 13, an interleukin 4-like cytokine that acts on monocytes and B cells, but not on T cells. *Immunol Today* **15:**19-26